Bone Morphogenetic Protein Signalling in Adult Lung Epithelial Cells

Emer Louise Molloy
B.Sc. (Hons)

A thesis submitted to
The National University of Ireland, Maynooth
for the degree of

Doctor of Philosophy

Department of Biology
National University of Ireland
Maynooth

NUI MAYNOOTH
Ollscoil na hÉireann Má Nuad

Oct 2008

Research Supervisor: Dr. Shirley O'Dea

Abbreviations

α-SMA	Alpha smooth muscle actin
μM	Micrometer
1 Kb	Kilobase
100 bp	100 base pair
18S	18 ribosomal strand
28S	28 ribosomal strand
ActR	Activin receptor
AEC	Airway epithelial cell
Alk	Activin receptor-like kinase
APC	Adenomatous polyposis coli
APS	Ammonium persulphate
AQP5	Aquaporin 5
AR	Allergic rhinitis
ATCC	American type culture collection
BADJ	Bronchoalveolar duct junction
BAMBI	BMP associated membrane bound inhibitor
BASC	Bronchial alveolar stem cell
BEAS	Bronchial epithelial airway cells
BME	B-mercaptoethanol
BMP	Bone morphogenetic protein
BMPR	Bone morphogenetic protein receptor
BOOP	Bronchiolitis obliterans organizing pneumonia
BrdU	5-bromo-2'-deoxyuridine
BRE	BMP responsive element
BSA	Bovine serum albumin
CBFA1	Core-binding factor 1
CBP	CREB binding protein
CC10	Clara cell 10
CCND1	Cyclin D1

CCSP	Clara cell secretory protein
CDMP2	Cartilage-derived morphogenetic protein 2
cDNA	Complementary DNA
CKO	Conditional knockout
CM	Conditioned medium
COPD	Chronic obstructive pulmonary disease
CT	Cycle threshold
DAB	3, 3'-diaminobenzidine
DAPI	4',6-diamidino-2-phenylindole
DEPC	DiethylenePyrocarbonate
DMEM	Dulbecco's Modified Eagle Medium
DMSO	Dimethylsulphoxide
dnAlk6	Dominant negative Alk6
dNTP	Deoxynucleoside triphosphate
Dpp	Decapentaplegic
DSFM	Defined serum-free medium
DTT	Dithiothreitol
E 9.5	Embryonic day 9.5
E12/E47	Enhancer binding proteins E12/E47
EBAO	Ethidium bromide acridine orange
ECACC	European collection of cell cultures
ECL	Enhanced chemiluminescence
ECM	Extracellular matrix
ECP	Eosinophil cationic protein
Ecsit	Evolutionarily conserved signalling intermediate in Toll Pathways
ED50	Effective dose
EDN	Eosinophil-derived neurotoxin
EDTA	Ethylene diamino tetraacetic acid
EGF	Epidermal growth factor
EGFR	Epidermal growth factor receptor

EMT	Epithelial-mesenchymal transition
EPO	Eosinophil peroxidase
ER	Endoplasmic reticulum
ERK	Extracellular signal related kinase
ETS	E26 transforming retrovirus oncogene
Evi-1/ZF	Ecotropic viral integration site 1/zinc finger
FAP	Focal adhesion proteins
FBS	Fetal bovine serum
Fc	Fragment crystallizable region
FGF	Fibroblast growth factor
FHA	Forkhead associated
FOP	Fibrodysplasia ossificans progressiva
FSP1	Fibroblast specific protein 1
G0	Gap 0
G1	Gap 1
G2	Gap 2
GAPDH	Glyceraldehyde 3-phosphate dehydrogenase
GDF	Growth differentiation factor
GH	Growth hormone
HC	Hydrocortisone
HDAC	Histone deacetylase
HGF/SF	Hepatocyte growth factor/scatter factor
HLH	Helix-loop-helix
HRP	Horse radish peroxidase
ICAM	Intracellular adhesion molecule
Id	Inhibitor of differentiation
IgE	Immunoglobulin E
IL-1	Interleukin 1
IL-5R	Interleukin 5 receptor
INF-γ	Interferon gamma
IPF	Idiopathic pulmonary fibrosis

IRAK	Interleukin 1 receptor associated kinase
I-Smad	Inhibitory-Smad
IκB	Inhibitor of κB
JNK	Jun N-terminal kinase
JP	Juvenile Polyposis
K5	Cytokeratin 5
kDa	Kilo-dalton
LEF1/Tcf	Lymphoid enhancer factor 1
M	Mitosis
MADH4	Mad homology 4
MAEC	Murine airway epithelial cell
MAPK	Mitogen activated protein kinase
MBP	Major basic protein
MEKK1	MEK kinase 1
MET	Mesenchymal-epithelial transition
MFI	Mean fluorescent intensity
MgCl2	Magnesium
MH1	Mad homology 1
MH2	Mad homology 2
MMP2	Matrix metalloprotease 2
MTS	inner salt or tetrazolium salt
MYC	Myelocytomatosis viral oncogene
NaCl	Sodium chloride
N-Cor	Nuclear receptor corepressor
NEB	Neuroendocrine body
NES	Nuclear export sequence
NFκB	Nuclear factor κB
ng/ml	Nanogram per mililitre
NGF	Neuronal growth factor
NHBE	Normal human bronchial epithelial
NLS	Nuclear localisation sequence

nm	Nanometre
NRT	No reverse transcriptase
NSCLC	Non small cell lung carcinoma
NSO	Mouse myeloma cell line
O/N	Overnight
OAZ	Olf-1/EBF associated zinc finger
OD	Optical density
OE	Olfactory epithelium
OP1	Osteogenic protein 1
OR	Odorant receptors
OSN	Olfactory sensory neurons
OVA	Ovalbumin
p21/CDKN1A	Cyclin-dependent kinase inhibitor 1A
P5	Post-natal day 5
PAR	Perrenial allergic rhinitis
PBS	Phosphate buffered saline
PCNA	Proliferating cell nuclear antigen
PCR	Polymerase chain reaction
P-D axis	Proximal-distal axis
PDGF	Platelet derived growth factor
PI	Propidium iodide
QPCR	Quantitative Polymerase chain reaction
RA	Retinoic acid
RANTES	Regulated upon Activation, Normal T-cell Expressed and Secreted
R-Smad	Receptor-Smad
RTK	Receptor tyrosine kinase
RT-PCR	Reverse transcriptase Polymerase chain reaction
S	Synthesis of DNA
S1	Site 1
S2	Site 2

SAP49	Schizosaccharomyces pombe RNA-binding protein 49
SAR	Seasonal allergic rhinitis
SA-β-gal	Senescence-associated β-galactosidase
SBE	Smad binding element
SDS	Sodium dodecyl sulphate
SER	Smooth endoplasmic reticulum
SIP1	Smad interacting protein 1
Smad	Mothers against decapentaplegic homolog
Smurf1	Smad ubiquitination factor 1
SNAI1	Snail1
SNIP	Smad nuclear interacting factor
SP-C	Surfactant protein C
Stat	Signal Transducers and Activators of Transcription
SV-40	Simian virus 40
TAB1	TGF-β activated kinase 1 binding protein
TAE	Tris-acetate-EDTA
TAK1	TGF-β activated kinase 1
TBS	Tris buffered saline
TGF-β	Transforming growth factor-β
TGF-βR	Transforming growth factor- β receptor
TLR	Toll-like receptor
Tlx-2	T-cell leukemia homeobox 2
TNF-α	Tumor necrosis factor-α
TRAF6	Tumor necrosis factor (TNF) receptor-associated factor 6
Tsg	Twisted gastrulation
TTF	Thyroid transcription factor
U /ml	Units per mililitre
UV	Ultraviolet

VCAM	Vascular cell adhesion molecule
XIAP	X-linked inhibitor of apoptosis protein
YY1	Ying Yang 1
ZEB1	Zinc finger E-box binding homeobox 1
ZEB2	Zinc finger E-box binding homeobox 2
ZO-1	Zonula occludens-1

Acknowledgements

I would like to thank my supervisor Shirley O'Dea for all her help, reassurance and unwavering positivity over the last three years. To everyone who I've had the pleasure of working with (and socialising with the odd time ;-)), Joanne, Ciara, Jennifer, James, Áine, Bernadette, Karen and Deirdre. Special thanks to Aine for all her help and experstise in everything and to Deirdre for all her help with the animal work. Also heartfelt thanks to all my colleagues in the Institute of Immunology (especially the coffee-roomers!) for all the chat over the last three years.

Special thanks to my family, my sister Elaine and my brother Paul and especially my parents, Eamonn and Marena, for all their support both emotional and financial! Thanks so much to Rachel and Nicola for all their support and understanding and for being great friends. Most of all I would like to thank Dave who I couldn't imagine doing anything without. Thank-you so much for everything, for all your support, thoughtfulness, encouragement and all the laughs which have made the last four years the best ever.

Thesis Title: Bone Morphogenetic Protein (BMP) Signalling in Adult Lung Epithelial Cells

Summary

Bone morphogenetic protein (BMP) signalling is essential for correct lung development where it mediates lung branching morphogenesis. In the adult lung, the BMP pathway is activated during airway inflammation. However, a role for activated BMP signalling has not yet been elucidated. The aims of this project were to identify a role for BMP signalling in adult airway epithelial cells (AECs) and to further investigate BMP signalling during airway inflammation. AECs used included the transformed bronchial cell line, BEAS-2B, the adenocarcinoma-derived cell line, A549, and normal primary murine airway epithelial cells (MAECs). BMP2 and BMP4 inhibited E-cadherin expression in BEAS-2B cells. In addition, BMP4 induced an epithelial-mesenchymal transition (EMT) in BEAS-2B where cells acquired a mesenchymal phenotype including fibroblast-like morphology and increased mesenchymal gene expression. Investigation of BMP4-mediated signalling in A549 cells revealed hydrocortisone (HC) as a determining factor where in the presence of HC A549 cells adopted a senescent-like phenotype and in the absence of HC cells underwent an EMT-like change in phenotype in the response to BMP4. Further analysis of BMP4-mediated effects in normal primary MAECs revealed downregulation of E-cadherin expression and a concurrent increase in expression of the transcriptional repressor of E-cadherin, Snail1. To further investigate the involvement of BMP signalling in airway inflammation, BMP pathway components were assessed in nasal biopsies from individuals with allergic rhinitis (AR). In AR nasal biopsies, the BMP pathway was found to be modulated with the apparent relocalisation of the BMP receptor, BMPR-IA, to the nucleus of airway epithelial cells. Furthermore, this nuclear localisation was recapitulated in normal primary MAECs co-cultured with eosinophils or stimulated with eosinophil cationic proteins. These data further implicate BMP signalling in the pathogenesis of lung inflammation where activated BMP signalling may be involved in remodelling processes.

1.0 INTRODUCTION

1.1. Lung biology

1.1.1. Lung Development

The lung comprises the largest epithelial surface in the body and functions as the interface between the body and the external environment where it warms, conditions and purifies inhaled air before mediating gas exchange with the circulating blood system. Importantly, the airway epithelium also serves as a barrier where it protects the host body from invading pathogens. Lung development can be separated into four complex processes namely branching morphogenesis, alveolarisation, angiogenesis and vasculogenesis (Shi et al., 2007). Lung formation begins with a protrusion, termed the laryngotracheal groove, from the primitive esophagus. This laryngotracheal groove, or the primitive trachea, splits into two primary buds which represent nascent bronchi (Fig. 1.1). These main bronchi begin an asymmetrical pattern of branching morphogenesis which continues for a total of 23 generations (Fig. 1.1). Following complete branching morphogenesis the process of alveolarisation is initiated and continues postnatally (Fig. 1.1). The overall structure of the lung in humans is a bilobed left and a trilobed right lung. The processes of branching morphogenesis in mice are similar. However, the murine adult lung consists of a unilobar left and a quadrilobed right lung. The process of alveolarisation also differs between human and murine lung development, in humans it is relatively advanced by birth whereas in the mouse it is initiated postnatally (Warburton et al., 2000) (Fig. 1.2).

Lung development has been divided into four chronological stages termed the pseudoglandular stage (mouse E9.5-16-6; human 17-16 wks) where the bronchial and respiratory tree develop; the canalicular stage (mouse E16.6-17.4; human 16-24 wks) where the terminal sacs develop and vascularisation initiates; the terminal sac stage (mouse E17.4 to postnatal day 5 (P5); human 24-36 wks) during which the number of terminal sacs and vascularisation increases and type I and type II pneumocytes

differentiate and lastly the alveolar stage (mouse P5-P30; human 36 wks – 7 yrs) where the terminal sacs develop into mature alveoli (Shi et al., 2007) (Fig. 1.2).

Growth factor signalling is essential for lung development. Growth factors can originate from either the endoderm or the adjacent mesoderm and complex interactions between these signalling molecules regulate lung morphogenesis. Fibroblast growth factor (FGF) signalling has been identified as one of the critical signals during lung development. FGF10 initiates formation of the laryngotracheal groove and mediates subsequent lung branching. Furthermore, FGF7 participates in Type II alveolar cell differentiation. TGF-β mediated signalling is thought to inhibit lung branching through both suppression of N-myc (a proto-oncogene involved in lung branching) and through the production of extracellular matrix production surrounding the airways. Null mutation of TGF-β3 results in immature pulmonary epithelial, mesenchymal and vascular cells, a phenotype which is lethal shortly after birth. EGF stimulates branching morphogenesis. Null mutations in the EGF receptor (EGFR) leads to a 50% reduction in the level of distal airway branching. PDGF null mutation results in a failure in alveolar septation (final step in alveolarisation) and postnatal lethality from emphysema (Bostrom et al., 1996). In addition, BMP4 is critical for lung development. BMP4 coordinates with FGF10 in the lung to correctly mediate lung branching morphogenesis. BMP signalling during lung development will be discussed in section 1.2.3.

The instruction of lung morphogenesis and cell lineage determination is under tight transcriptional control through the action of transcription factors including the thyroid transcription factor, TTF-1, pou, hox, and Id transcription factors. In addition, glucocorticoid and retinoic acid receptor signalling are critical for correct lung development (Warburton et al., 2000).

1.1.2. Lung Architecture: The Proximal-Distal (P-D) Axis

In the adult lung the airways as they extend from the nasal cavity to the alveolar region is termed the proximal-distal (P-D) axis. Cells located along the P-D axis have specialized functions according to their proximity to the external environment and their involvement in gas exchange.

1.1.2.1. Nasal epithelium

In addition to its role as an olfactory organ, the nasal passage is responsible for a diverse range of functions such as purifying, humidifying and warming inhaled air as well as detoxifying many hazardous agents before they come in contact with the more sensitive tissue of the lower airways. The nasal epithelium is composed of four distinct regions each with their own function and cellular composition so called the olfactory, squamated, transitional and respiratory epithelium. The olfactory epithelium (OE) is localised dorsally to the remaining epithelium. It is largely composed of olfactory sensory neuronal (OSN) cells interspersed between supporting cells and basal cells. The OSN cells are highly ciliated and contain odorant receptors (OR). The extent to which the nasal cavity is composed of olfactory epithelium accounts for a species level of smell. Fifty percentage of the nasal epithelium in rodents consists of olfactory epithelium whereas this is less than three percent in humans (Harkema et al., 2006). The most proximal area of the nasal tract in covered with squamated epithelium consisting of lightly keratinized, stratified squamous epithelial cells and basal cells. The squamated epithelium is followed by the transitional epithelium which consists of non-ciliated cuboidal or columnar cells as well as basal cells and in addition, mucous secreting goblet cells. This epithelial layer is usually 1-2 cells thick. The respiratory epithelium covers the remaining nasal epithelium as it extents towards the trachea. The respiratory epithelium is a pseudostratified ciliated layer consisting of six distinct cells types in the rat namely mucous, ciliated, cuboidal, non-ciliated columnar, brush and basal (Harkema et al., 2006). Specific cell types within these populations have metabolic capabilities with the expression of a number of enzymes involved in

xenobiotic metabolism including aldehyde dehydrogenase, cytochrome P450 and glutathione S-transferases (Harkema et al., 2006).

The nasal epithelium is covered by a layer of mucous commonly referred to as the 'mucous blanket'. This layer is comprised of two layers the gel phase and the sol phase. The gel-like properties of the gel phase depends primarily on its content of mucins (Rose, 1992). Ciliated cells are responsible for dragging this protective layer by mucociliary action toward the posterior nasopharynx where it is then swallowed. Loss of cilia action can lead to chronic inflammation of the upper airways but in addition, leaves the lower airways increasingly susceptible to infection.

1.1.2.2. **Conducting Airways**

The conducting airways consist of the trachea, primary bronchi, small bronchi and bronchioles. Similar to the nasal epithelium the function of the conducting airways involves filtering and conditioning inhaled air, metabolism of reactive chemicals and clearance of deposited materials. However, by virtue of the increased surface area, the lower airways are increasing susceptible to invasion from potential pathogens and subsequent inflammation and epithelial damage. In the mouse trachea and primary bronchi, the epithelium is pseudostratified and composed of columnar ciliated cells and clara-like cells. Clara-like cells are similar to Clara cells in structure and in their secretion of CCSP (Clara cell secretory protein). However, clara-like cells have been shown to secrete proteins unique to this cell type and respond differently to a number of stimuli (Stripp and Reynolds, 2006). In addition, neuroendocrine cells are present which can be found singly or in clusters termed neuroepithelial bodies (NEBs). Mucosal cells in the proximal airway are restricted to a few mucosal glands. A distinguishing feature of the trachea and primary bronchi is the presence of relatively unspecialized basal cells which are positive for both Keratin 14 (K14) and K5.

The small bronchi and bronchioles are lined by a simple epithelium composed mainly of Clara cells and ciliated cells. There are increased numbers of NE cells compared to the trachea and main bronchi in this region. Mucosal glands are found and contain

both serous and mucosal cell types. Importantly, basal cells are not detected in the lower or distal conducting airways.

1.1.2.3. **Alveolar region**

The most distal region of the lung is specialized for gas exchange and is organized into a complex system of alveoli. Each alveolar unit is apposed with blood vessels and it is here where the circulating blood is oxygenated. The alveoli are lined with Type1 and Type 2 alveolar epithelial cells (AEC1 and AEC2). Type I pneumocytes are regarded as terminally differentiated and possess the thin-walls required for gas exchange. Type II pneumocytes are cuboidal cells recognizable by their secretory granules which contain surfactant material such as surfactant protein C (SP-C or Sftpc).

1.1.3. **Lung Stem Cells and Repair**

Repair in adult tissue can be mediated by resident stem cells which possess relatively undifferentiated functions during homeostasis, reside in specific niches and can proliferate in response to injury and give rise to other cell types. In the lung these stem cells have been identified following injury to airway epithelial cells. Two commonly used injury models include naphthalene injury to Clara cells and bleomycin injury to type I alveolar cells.

Following naphthalene injury specific stem cells have been identified. Basal cells respond to injury in the nasal epithelium and the trachea (Rawlins and Hogan, 2006). A subset of Clara cells, termed variant Clara cells ($Clara^{V}$), can repopulate the proximal airways following naphthalene injury. Clara cells are specifically killed on account of their production of cytochrome P450 enzymes which metabolize naphthalene into it toxic metabolites. $Clara^{V}$ cells are not affected by naphthalene because they do not express the enzyme CYP2F2, a member of the cytochrome P450 family. A similar subset of cells termed bronchioalveolar stem cells (BASCs) were identified in the more distal airway. These are likely to be the same as $Clara^{V}$ cells.

However, their involvement during *in vivo* repair has yet to be demonstrated. In addition to Clara^{V} cells, ciliated cells have been shown to respond following naphthalene injury to repair the epithelium (Park et al., 2005). However, the overall data surrounding this is contentious. In summary, injury models have identified basal cells as the tissue specific stem cell of the nasal and trachea and Clara^{V} cells and BASCs as the tissue specific stem cell of conducting airways.

1.1.3.1. **Clara cells**

Aside from resident stem cells, certain differentiated lung epithelial cells can retain the ability to proliferate in response to injury and give rise to other cell types. These differentiated cells include alveolar Type II AECs which following bleomycin injury to alveolar Type I AECs can give rise to both Type I and Type II AECs. Similarly, Clara cells in the proximal airways have been shown to retain the ability to proliferate and differentiate into both Clara cells and ciliated cell types.

Clara cells are non ciliated, cuboidal cells which contain abundant smooth endoplasmic reticulum (SER) and secretory granules. Clara cells secrete a variety of nonmucinous proteins including surfactant A and D, proteolytic enzymes, antimicrobial peptides and a number of growth factors, chemokines and cytokines. For this reason these cells contribute to the hypophase layer of bronchoalveolar fluid and are important mediators of the immune response. Clara cell secretory protein, CCSP (also known as Scgb1a1, CC10 or CCA), constitutes 40% of the secreted proteins produced by Clara cells. CCSP -/- deficient mice demonstrate alterations in Clara cell structure and airway lining fluid composition and have increased susceptibility to oxidant gases as well as increased cellular damage in response to ozone (Stripp and Reynolds, 2006). Because of these alterations in response to damage in mice lacking CCSP, Clara cells and the secretory proteins they produce are regarded as important mediators of lung homeostasis and protection against lung damage. In addition to their secretory role, Clara cells are the principal detoxifying cell of the airway epithelium. Clara cells are rich in both SER and mitochondria. They are the principal site for

expression of cytochrome P450 monooxygenase, an enzyme involved in xenobiotic metabolism of compounds such as formaldehyde, chlorine and naphthalene.

Therefore Clara cells are multifunctional. They carry out the specialized functions critical for normal lung homeostasis but in addition, represent the reparative cell lineage of the bronchial epithelium.

1.2. Bone Morphogenetic Protein (BMP) signalling

BMP signalling is critical during embryogenesis where it mediates early tissue patterning (Kishigami and Mishina, 2005). During *Xenopus, Zebrafish and Drosophila* development BMPs have been identified as ventralising factors where BMP2 and BMP4 have the ability to drive mesodermal (notochord and muscle) and ectodermal (brain) cells towards a ventral mesoderm fate (blood and skin) (Nakayama et al., 2000). In the mouse, BMP signalling is necessary for correct mesoderm formation (Winnier et al., 1995). This critical role of BMP signalling during embryogenesis has been exemplified in a number of knockout studies which result in embryonic lethality (Gazzerro and Canalis, 2006). During organogenesis BMP signalling is essential for correct formation of almost all tissues and organs including the skeleton, limbs, heart and lungs. In the adult, BMP signalling is activated during chronic inflammation and BMP pathway components have been found upregulated, lost or mutated in cancer (discussed in section 1.2.4). A role for BMP signalling during cancer and inflammation is currently unknown.

1.2.1. BMP Pathway: Signal transduction

1.2.1.1. Ligands

BMPs are members of the TGF-β superfamily of secreted polypeptide growth factors. The TGF-β superfamily is comprised of three sub-groups: the TGF-βs, the activins, and the BMPs. BMPs mediate a diverse range of biological processes involved in embryogenesis and organogenesis including proliferation, differentiation and apoptosis through complex regulation of the signal transduction and cross-talk between other critical signalling pathways. In 1965, the activity of BMPs was first identified from their ability to induce ectopic bone formation when injected subcutaneously into rodents (Urist, 1965). The specific proteins responsible for this bone induction were identified with the purification and sequencing of BMP3 and cloning of BMP2 and BMP4 (Wozney et al., 1988, Luyten et al., 1989). Now more

than 20 BMP-related proteins have been identified across a number of species including Drosophila, Xenopus, Mouse and human (Fig. 1.3). BMPs have been classified into three subgroups based on structure and function. Group 1 (BMP2/4 group), contains BMP2, BMP4 and the *drosophila decapentaplegic* (*dpp*) gene product. Group 2 (OP1 group), consists of BMP5, BMP6, BMP7 (OP1), BMP8 (OP2) and the *drosophila gbb-60A* gene product. Group 3 (GDF5 group), contains the last subset of BMP ligands including growth differentiation factor 5 (GDF5 or cartilage-derived morphogenetic protein 1, CDMP1), GDF6 (CDMP2 or BMP13) and GDF7 (BMP12) (Miyazono et al., 2005). BMP1 is classed apart from other BMP ligands as it does not act in BMP signalling and functions as a metalloprotease (Hopkins et al., 2007). BMP ligands are synthesized as large precursor pro-proteins which are subsequently cleaved and secreted from the cell in their biologically active form.

1.2.1.2. **Receptors**

BMPs elicit their biological function through binding to serine/threonine receptors on the surface membrane. Members of the BMP family utilize two distinct types of receptors namely Type I and Type II. BMP ligands can bind to three Type I receptors, BMPR-IA (Alk3), BMPR-IB (Alk6) and activin receptor-like kinase (Alk2) and three Type II receptors, BMP type II receptor (BMPR-II), activin type II receptor (ActR-II) and activin type IIB receptors (ActR-IIB). However, binding affinities of ActR-II and ActR-IIB are higher for activins than for BMPs (Yamashita et al., 1995). Type II receptors possesses constitutively active kinase domains and upon ligand binding, phosphorylate the type I receptor at Gly-Ser (GS) sites within the intracellular domain leading to type I receptor activation (Fig. 1.4). Therefore, a type II receptor and a type I receptor are necessary for BMP signal transduction. Among the three type I receptors, BMPR-IA and BMPR-IB have the highest level of sequence homology. BMPR-IA and BMPR-IB bind group 1 BMP ligands namely BMP2 and BMP4. Alk2 and BMPR-IB can bind group 2 BMP ligands where group 3 BMP ligands bind to BMPR-IB. In addition, a co-receptor for BMP signalling, DRAGON, was shown to potentiate BMP signalling through its direct interaction with BMP ligands and receptors (Samad et al., 2005).

The mechanisms involving ligand-receptor binding have been extensively characterised for TGF-β specific signalling and for many years it had been presumed BMP signals were transduced via similar mechanisms. However, distinct modes of ligand-induced BMP pathway activation have recently been described. TGF-β ligands display a high affinity for type II receptors. In this way, TGF-β ligands initially bind a type II TGF-β receptor. This event allows the subsequent recruitment of the type I receptor, forming the stable complex consisting of two receptors of each type where each pair is connected via the ligand dimer (Feng and Derynck, 2005). Differences between TGF-β and BMP ligand-receptor binding have been highlighted in a number of studies. These studies have focused on the mode of BMP2 binding to BMPR-IA and BMPR-IB and the type II receptor, BMPR-II, using coimmunoprecipitation techniques and immunofluorescence analysis of receptor complexes formed on live cells (Gilboa et al., 2000, Nohe et al., 2001). In contrast to TGF-β ligands, BMP2 cannot bind to BMPR-II in the absence of a type I receptor (Gilboa et al., 2000). In addition, BMP receptors, both type II and type I, have been identified as preformed homomeric (RIA-RIA, RIB-RIB, RII-RII) and heteromeric (RIA-RIB, RIA-RII, RIB-RII) receptor complexes and are rarely found expressed as single receptors on the cell surface (Gilboa et al., 2000). BMP2 can bind to all of the above receptor complexes except for the BMPR-II homomeric complex (RII-RII). Therefore, BMP2 has two options in order to initiate signal transduction. BMP2 can bind to the preformed heteromeric receptor complexes which consist of a Type I and a Type II receptor (RIA-RII, RIB-RII) or can bind with high affinity to a type I receptor homomeric complex (RIA-RIA, RIB-RIB) and subsequently recruit a type II receptor. Nohe et al., characterised these two modes of ligand binding and demonstrated that while BMP2 binding to heteromeric preformed complexes (RIA-RII, RIB-RII) activated the canonical Smad signalling pathway, BMP2-induced receptor complexes initiated signalling via the Smad independent P38 MAPK pathway (Nohe et al., 2001) (Fig. 1.4). TGF-β ligands can also activate both the MAPK pathway and the canonical Smad pathway. However it has not been shown whether this is achieved through differential ligand-receptor binding.

Non-canonical BMP-MAPK signalling involves BMP activation of the TGF-β activated kinase (TAK1) which is a member of the MAPK family of signalling proteins. TAK1 associates with the TAK1 binding protein (TAB1). XIAP was identified as possible link between BMP receptors and the TAK1-TAB1 complex. TAK1 in the nucleus promotes activation of p38 MAPK and Jun-N terminal kinase (JNK) (Von Bubnoff and Cho, 2001, Herpin and Cunningham, 2007) (Fig. 1.4). This form of signal transduction was demonstrated in a number of studies during development and in adult cells. TAK1 overexpression in *Xenopus* was shown to mimic BMPs ventralising effects (Shibuya et al., 1998). In addition, BMP2 has been shown to increase TAK1 expression and activate p38 MAPK during BMP2-induced apoptosis and neuronal differentiation (Kimura et al., 2000, Iwasaki et al., 1999).

1.2.1.3. **Smad intracellular signalling proteins**

Canonical BMP signal transduction is mediated via the intracellular family of Smad proteins. Smads have been subdivided into three groups based on their structure and function. Smads involved in signal transduction are termed receptor Smads or R-Smads and are so called from their direct association with the intracellular domain of the type I receptor. R-Smad2 and 3 respond to TGF-β pathway activation where R-Smad1, 5 and 8 preferentially mediate BMP signal transduction. The second group consists of the co-Smad, Smad4, so called from its ability to mediate both TGF-β and BMP signals. The third group consists of Smad6 and Smad7 or inhibitory Smads (I-Smads) which have been demonstrated to inhibit TGF-β and BMP signals through a number of mechanisms (discussed in section 1.2.2.3). Consistent with their different functions each set of Smads have distinct structural organization. R-Smads share two highly conserved regions, an N-terminal MH1 domain (Mad homology 1) and a C-terminal MH2 domain (Mad homology 2) separated by a less conserved linker region. The MH1 domain for all Smads, except for Smad2, confers a weak affinity for DNA binding whereas the MH2 domain facilitates protein-protein interactions with Smads, transcriptional coactivators, or corepressors. In addition, R-Smads possess a phosphorylation motif SSXS of which two distinct serine residues are phosphorylated by the type I receptor. The L45 loop present in the type I receptor mediates this

phosphorylation through its interaction with the L3 loop present on the R-Smad (Feng and Derynck 1997, Lo et al., 1998). Smad4, or co-Smad, similar to the R-Smads possess an MH1 and MH2 domain however lacks a SSXS phosphorylation motif and therefore is not phosphorylated by the type I receptor.

Following R-Smad phosphorylation by the type I receptor the Smad protein undergoes a conformational alteration resulting in its release from the intracellular receptor compartment. The R-Smad is then free to bind with the co-Smad and it is this complex which can enter the nucleus and mediate gene transcription (Fig. 1.4). Binding of the R-Smad to Smad4 can involve the formation of heterotrimers where two R-Smads bind one Smad4 or as heterodimer (a single R-Smad binding the Smad4 protein) (Chacko et al., 2001). The possibility of either one or two R-Smads combining with the co-Smad increases the diversity of the signal transduction.

R-Smad proteins and Smad4 all contain nuclear localisation signals which permit nuclear translocation (Xiao et al., 2001). R-Smads possess weak intrinsic DNA binding ability. While in the nucleus the activated Smad protein can form a weak association with a Smad-binding element (SBE) but this is not sufficient to regulate transcription. It is through the interaction between the Smad proteins and transcription factors, including DNA binding partners and coactivators, or corepressors, that directly regulate gene transcription. In this way, activated Smad proteins in the nucleus bind to SBEs upstream of the promoter regions and recruit distinct transcription factors associated with that gene and thus increase their binding affinity (Shi and Massagué, 2003, Feng et al., 2000, Qing et al., 2000).

1.2.1.4. **Coactivators and corepressors**

Smads interact with a diverse range of DNA binding transcription factors as well as coactivators and corepressors. DNA binding partners include Hoxc-8, estrogen receptor, CBFA1/Runx2/AML, GATA4, 5, 6, GliΔC-ter, OAZ, YY1, β-catenin, LEF1/Tcf and NCID. In addition, a number of Smad interacting coactivators and

corepressors have been identified including CBP/p300, GCN5, ZEB1, Evi-1 (ZF), SNIP (FHA), Tob and ZEB2/SIP1 (Feng and Derynck, 2005) (Fig. 1.4).

1.2.2. **BMP Pathway: Regulation**

The range of diverse processes mediated by BMP signalling implicates a need for tight regulation. In this way, the pathway is controlled by extracellular and intracellular factors that function at different levels to regulate BMP signal transduction.

1.2.2.1. **Ligands**

BMP ligands are produced as large inactive pre-cursor proteins and following proteolytic cleavage an active BMP dimer is released from the cell. The proprotein convertase, furin, has been shown to cleave BMP ligands at the multibasic motif, R-S-K-R. Cleavage at this site adjacent to the mature ligand to yields the active C-terminal mature dimer (Aono et al., 1995). More recently it has been shown that the *Drosophila* BMP homolog *dpp*, BMP2 and BMP4 possess two cleavage sites. This is not the same for other BMPs ligands such as BMP7 which lacks a second cleavage site. BMP4 cleavage initially takes place the optimal furin motif (-RSKR-) this is followed by cleavage at a minimal furin motif (-RSKR-) upstream within the prodomain. Cleavage at one or both of these sites has been implicated in regulating the bioactivity of the BMP4 ligand (Nakayama et al., 2000). Cui et al., demonstrated failure to cleave at the second site (S2) restricts the range over which BMP4 can signal whereas cleavage at both sites enhances BMP4 diffusion *in vivo* (Cui et al., 2001).

In addition to regulation of BMP ligands by proteolytic cleavage their activity is modulated by a number of extracellular binding proteins which disrupt ligand-receptor interactions. These include noggin, the chordin family, twisted gastrulation (Tsg) and the Dan family of secreted peptides, of which gremlin has been the most characterised. These factors all bind BMP ligands outside the cell thus masking receptor binding epitopes and preventing ligand-receptor binding (Fig. 1.4). They are specific for BMP

ligands and do not bind other members of the TGF-β superfamily. All of these BMP binding partners bind BMP2 and BMP4, in addition, noggin, chordin and gremlin can bind BMP7 where noggin can also bind BMP6, GDF5 and GDF6 (Gazzerro and Canalis, 2006). Their expression is often induced in response to BMP signalling and therefore these extracellular BMP antagonists commonly function as part of a negative feedback loop to decrease cellular exposure to BMPs. The processes involving BMP ligand inhibition are complex. For example, chordin bound to BMP is a substrate for BMP1, the metalloprotease, which can cleave chordin and release the bound BMP ligand (Fig. 1.4). The complexity of regulation mediated by these extracellular inhibitors is further exemplified by the action of twisted gastrulation (Tsg), a 23.5kDa secreted glycoprotein. Tsg can both inhibit as well as promote BMP activity. As an antagonist, Tsg can bind BMP-chordin inactive complexes further inhibiting the release of the bound ligand. While in an opposing role, Tsg can associate with BMP1 and aid in the cleavage of chordin and subsequent release of the BMP ligand into the extracellular space. Null mutations in these antagonists are embryonic lethal, in particular gremlin knockout mice exhibited defects in lung airways (Gazzerro and Canalis, 2006). Similarly, mutations in the genes encoding for or misexpression of a number of these antagonists has disease implications. For example, missense mutations in the noggin coding sequence have been identified in the diseases proximal symphalangism and multiple synostosis syndrome involving multiple joint fusion (Gong et al., 1999, Marcelino et al., 2001). Similarly, gremlin is overexpressed during idiopathic pulmonary fibrosis (Koli et al., 2006).

1.2.2.2. **Receptors**

In addition to the level of extracellular regulation, the pseudoreceptor BAMBI (BMP and Activin Membrane Bound Inhibitor), serves to dampen TGF-β family signal transduction (Onichtchouk et al., 1999) (Fig, 1.4). While the extracellular domain of BAMBI resembles that of other TGF-β type I receptors it lacks the intracellular kinase domain. Stable association of BAMBI with other type I receptors prevent the formation of active receptor complexes and can block TGF-β, activin and BMP signalling. Studies have shown the expression of BAMBI coincides with the

expression of BMP ligands during embryogenesis. Furthermore, in *Xenopus* BAMBI is induced by BMP4 (Karaulanov et al., 2004). This is in keeping with the extracellular inhibitors where the balance between pathway activation and inhibition is under tight control. The human BAMBI homologue, BAMBI/NMA, is elevated in human colorectal and hepatocellular carcinomas and when over expressed in a colorectal tumor cell line, cells were not responsive TGF-β signalling. This raised the possibility of BAMBI acting as a proto-oncogene, allowing tumor cells to escape the anti-mitogenic activities of TGF-β signalling (Sekiya et al., 2004). However, contrary to this, the *nma* gene was downregulated in metastatic melanoma indicating possible tumor suppressor activity (Degen et al., 1996). Of note, the study found no expression of *nma* in the lung.

1.2.2.3. **Smads**

In the cytoplasm, a variety of regulatory mechanisms exist which target the Smad intracellular signalling proteins. The first form of regulation involves the limited availability of the co-Smad, Smad4, for the signal transduction of both BMP and TGF-β signals. This stable Smad4 pool means BMP and TGF-β signal transduction directly compete for Smad4. In this way, increased BMP signalling can serve to negatively regulated TGF-β signalling and vice versa.

As previously mentioned the third subset of Smad proteins includes the inhibitory Smads, or I-Smads, Smad6 and Smad7. Smad6 and Smad7 can inhibit the activation of R-Smads. Smad6 can also inhibit BMP-MAPK signalling (Kimura et al., 2000) (Fig. 1.4). While both Smad6 and Smad7 possess the protein binding MH2 domain, a MH1 (DNA binding) domain had only been identified in Smad7 (Hanyu et al., 2001). Smad6 can inhibit both BMP and TGF-β signalling while Smad7 is more effective in inhibiting the TGF-β pathway specifically. The most common mode of action by I-Smads involves binding to the intracellular domain of the type I receptor through their MH2 domain and thus blocking R-Smad recruitment and subsequent activation. Moreover, Smad6 specifically inhibits BMP signalling, through its association with Smad1 again via the MH2 protein binding domain thus sequestering Smad1 via

inactive Smad1:Smad6 complexes (Hata et al., 1998). Interestingly, Smad6 and Smad7 are rapidly induced in response to BMP and TGF-β signals.

In addition to the inhibitory Smads, a splice variant of Smad8 (Smad8B) was identified in various human tissue including placenta, kidney, brain and heart (Nishita et al., 1999). Smad8B shares sequence homology with Smad8, however, Smad8B lacks a portion encoding 47 amino acids including the SSXS phosphorylation site (Nishita et al., 1999). Smad8B can associate with both Smad8 and Smad4. In cells overexpressing Alk2 (receptor shown to phosphorylated Smad8), Smad8 was phosphorylated and translocated to the nucleus where Smad8B remained in the cytoplasm (Nishita et al., 1999). In this way, Smad8B can antagonize BMP signalling in one of two ways, by binding to Smad8 and forming inactive Smad8:Smad8B complexes or binding to Smad4 and thus inhibiting the activated Smad8 from binding Smad4 and translocating to the nucleus (Fig. 1.4).

The Smad ubiquitin regulatory factor 1 (Smurf 1) was identified as an important intracellular negative regulator of BMP signalling (Fig. 1.4). Smurf1 is a member of the Hect (Homologues to E6-associated protein C terminus) class of E3 ubiquitin ligases (Zhu et al., 1999). Overexpression of Smurf1 negatively regulates BMP signalling through its action of Smad1 and Smad5 poly-ubiquitination and subsequent degradation via the proteasome. In the presence of Smurf1, the half life of Smad1 was reduced from 6hr to 2 hr (Zhu et al., 1999). Smurf1 is not induced in response to BMP pathway activity and therefore does not serve to "switch off" BMP pathway activation but rather modulates the cells proficiency in transducing BMP signals (Nakayama et al., 2000). In addition, Smurf1 in association with Smad7 can lead to degradation of TGF-β type I receptors (Ebisawa et al., 2001).

In addition to the I-Smads and Smurf1, a number of other Smad interacting factors have been identified and shown to inhibit TGF-β and BMP signalling. Among these negative regulators are Ski, SnoN and Tob. Ski and SnoN are highly conserved members of the ski family of protooncoproteins (Liu et al. 2001). They have the

ability to inhibit both TGF-β and BMP signalling through there direct interaction with Smad1, 2, 3, 4, and 5 (Fig. 1.4). Both ski and SnoN inhibit Smad-mediated transcription through the recruitment of the histone deacetylase, HDAC via the transcription factor N-CoR resulting in the repression of transcription of Smad target genes or via stabilization of Smad complexes with DNA and thus preventing the access of newly activated Smads to the Smad binding element (Von Bubnoff and Cho, 2001, Gazzerro and Canalis, 2006) (Fig. 1.4). In addition, Ski/SnoN can interfere with Smad binding to the coactivator CBP/p300 (Von Bubnoff and Cho, 2001) (Fig. 1.4). These inhibitory effects were demonstrated during *Xenopus* development where Ski inhibition of Smad1/4 induced neuronal development consistent with an opposition in BMP-mediated ventralisation (Lou, 2003).

Tob was found to negatively regulate BMP signalling (Fig. 1.4). Tob knockout mice exhibited increased bone mass with enhanced proliferation of osteoblasts in response to BMP2 (Yoshida et al., 2000). Tob, similar to ski and SnoN, directly binds R-Smad-Smad4 complexes and inhibits transcription (Yoshida et al., 2003). However, in addition, Tob has been shown to directly interact with I-Smads and type I BMP receptors at the plasma membrane and inhibit BMP signal transduction (Yoshida et al., 2003).

1.2.2.4. **Targets**

A number of BMP target genes have been identified. In *Drosophila*, *Dpp* (BMP2/4 homologue) mediates gene expression of *tinman*, *Ultrabithorax* (*Ubx*) *labial* and *spalt optomotor* (*omb*) *vestigial* among others including *Dpp* itself (Raftery and Sutherland, 1999). In *Xenopus,* through analysis of genes with an identical expression pattern to BMP4, a BMP4 synexpression group, direct targets of BMP/Smad signalling was identified. These target genes contained BMP-responsive elements (BREs) in addition to SBEs and Smad-cofactor binding motifs in their promoter and included *bambi*, *smad7*, *vent1* and *2*, *tlx2* and msx genes (Karaulanov et al., 2004). An extensive array of BMP target genes have been identified during bone development (Miyazono et al., 2005). In particular, 215 BMP2 responsive genes were identified in a study of BMP2-

induced bone formation in mouse quadriceps (Clancy et al., 2003). These genes included a number of transcription factors *Id1*, *2*, *4* (discussed below), *Runx2*, *Stat1*, Slug/*Snail2* and *Nfkbia*. Bone formation involves remodeling encompassing a precise balance between bone formation by osteoblasts and bone resorbtion by osteoclasts (Clancy et al., 2003). Additional genes regulated by BMP2 reflected these processes with a number of collagens and matrix metalloproteases identified (Clancy et al., 2003). Another study investigated genes modulated in response to BMP2 in osteoprogenitor cells (C2C12) (De Jong et al., 2004). Gene rapidly induced in response to BMP2 included *Smad6*, *Smad7*, *OASIS*, *Prx2* and *TIEG* (De Jong et al., 2004). Other BMP target genes include *Osteopontin* (Hullinger et al., 2001).

Members of the Id (inhibitor of differentiation or inhibitor of DNA binding) family of transcription factors, Id1, 2 and 3, were identified as targets of BMP/Smad signalling (Hollnagel et al., 1999). Id family members are negative regulators of basic helix-loop-helix (bHLH) transcription factors. They function through binding to HLH transcription family members and preventing them from binding to promoter E boxes thus inhibiting transcription of genes involved in differentiation. In this way, Id proteins are positive regulators of cell proliferation (Perk et al., 2005). Id proteins are commonly targeted by oncogenic pathways and their expression is elevated in cancer (Perk et al., 2005).

1.2.2.5. **Inter-pathway crosstalk**

BMP signalling can interact with other pathways either in a synergistic or antagonistic fashion (Fig. 1.5). FGF can inhibit BMP signalling during osteoblast differentiation, neural development and lung morphogenesis (discussed in section 1.2.3) (von Bubnoff and Cho, 2001, Weaver et al., 2000). FGF and other growth factors, such as EGF and HGF, activate their respective receptor tyrosine kinases (RTKs) which subsequently activates ERK (extracellular signal regulated kinase), a member of the mitogen-activated protein kinases (MAPK) (Von Bubnoff and Cho, 2001). The linker regions of Smad1, 5 and 8 contain four MAPK phosphorylation sites (PXSP motifs) (Derynck and Zhang, 2003). It has been demonstrated that activated MAPK signalling, through

FGF activation of ERK, can phosphorylate the linker region of Smad1 and thus target the protein for ubiquitination and subsequent degradation mediated by Smurf1 (Sapkota et al., 2007). In addition, phosphorylation at the MAPK sites prohibits binding of nucleoporin, Nup214, and prevents nuclear accumulation following Smad1 activation (Sapkota et al., 2007).

The Toll-like receptor (TLR) signalling family plays a key role in innate immunity (Aderem and Ulevitch, 2000). In brief, TLR pathway signal transduction begins with TLR activation and subsequent recruitment of the adapter protein MyD88. MyD88 binds to the TLR and subsequently recruits and interacts with a death domain within the serine threonine kinase IRAK (Interleukin 1 receptor associated kinase). Phosphorylated IRAK then interacts with TRAF6 (Tumor necrosis factor (TNF) receptor-associated factor 6) at which point there can be one of two outcomes. Firstly, the IRAK: TRAF6 complex can interact with TAK1 ultimately leading to the phosphorylation of IκB (inhibitor of κB) by IKK (inhibitor of κB kinase) causing IκB to become ubiquitinated and subsequently degraded. As a result NF-κB is no longer sequestered by IκB and is free to translocate to the nucleus to mediate TLR specific gene expression (Aderem and Ulevitch, 2000). Alternatively, the IRAK: TRAF6 complex can interact with the Toll-like intermediate Ecsit through interaction with MEKK1 (MEK kinase 1) which leads to activation of MAPK kinase, JNK and p38 (Moustakas and Heldin, 2003).

Xiao et al. demonstrated Ecsit as an essential component of both Toll and BMP signalling pathways (Xiao et al., 2003) (Fig. 1.5). Ecsit was shown to interact with Smad4 constitutively while interacting with the Smad1/Smad4 complex following BMP pathway activation to mediate transcription of the BMP target gene, *tlx2*. Furthermore, targeted null mutation of *Ecsit* resulted in abrogation of both Ecsit and BMP signalling with inhibition of BMP target gene expression (Xiao et al., 2003). In addition, abrogation of Ecsit was embryonic lethal with a phenotype which closely resembled that of the BMPR-IA null mutant (Xiao et al., 2003, Eblaghie et al., 2006). Ecsit may function as a cofactor for Smad proteins in BMP signal transduction (Xiao

et al., 2003). BMP-MAPK signalling may also communicate with TLR signalling through the activated TAK1-TAB1 complex to mediate inflammatory gene expression (Herpin and Cunningham, 2007).

BMP signalling communicates with other pathways including the Ca2+/Calmodulin, Wnt, JAK/STAT, TGF-β/activin and Notch signalling (Herpin and Cunningham, 2007, von Bubnoff and Cho, 2001). From these studies it is clear BMP signalling does not function alone but instead operates as a key component in a signalling network enabling BMP activity to induce pleiotropic effects during embryogenesis, organogenesis and repair in adult tissue.

1.2.3. **BMP Signalling During Lung Development**

BMP signalling is critical for embryogenesis. BMP4 knock-out mice die before embryonic day 10 (E10) with failure in mesoderm initiation (Winnier et al., 1995). Null mutations in BMPR-IA have resulted in similar early embryonic lethality (Mishina et al., 2002). BMP signalling in the lung cannot be assessed in these knockout mice due to death before the onset of lung development (E9.5) (Winnier et al., 1995). Therefore, several other approaches have been used to study BMP signalling during lung development. *Bmp4-LacZ* (LacZ inserted into *BMP4* locus) reporter mice as well as *in situ* hybridization have been used to assess the temporal and spatial expression pattern of BMP pathway components. Targeted misexpression of BMP4 has been achieved through the overexpression of BMP pathway inhibitors and dominant negative receptors under the control of the SP-C promoter. SP-C (surfactant protein C) is a lung specific gene expressed in the distal epithelium from E10.5 and therefore transgenes under the control of the SP-C promoter are expressed during the pseudoglandular stage of lung development (E9.5-16.6) where lung branching has initiated (Warburton et al., 2000). Finally, using the cre-lox system, transgenic animals expressing SP-C-Cre or doxycycline (Dox) inducible SP-C-Cre have been used to specifically delete BMPR-IA following the initiation of lung

morphogenesis and during late lung development, respectively (Eblaghie et al., 2005, Sun et al. 2008).

BMP4 is expressed at high levels in the distal tips of developing lung buds and weakly in the proximal airways (Bellusci et al., 1996) (Fig. 1.6). Evidence from aberrant BMP signalling has demonstrated a critical role for BMP4 during lung branching morphogenesis. The current hypotheses surrounding this role implicates BMP4 as a positive regulator of lung branching by promoting epithelial cell proliferation, inhibiting apoptosis and maintaining distal epithelial progenitor cells in a de-differentiated state as the lung branch extends (Fig. 1.6). The restricted expression of BMP4 in the distal tip creates a signalling gradient whereby cells located at the branch tip are exposed to high levels of BMP4 while cells located further from the lung branch tip receive little or no BMP signal. As a result cells located distally, at the lung branch tip, are maintained in an undifferentiated proliferative state and the epithelial cells further back along the lung branch, in the absence of BMP4 signals, undergo a programme of proximal cell differentiation (Fig. 1.6). In this way BMP4 mediates the extension of the lung branch. BMP signalling remains active during late lung development during which time the terminal sacs develop (E16.6-17.4), alveolar type I and type II cells differentiate (E17.4-P5) and mature alveoli are formed (P5-30) (Alejandre-Alcázar et al., 2007). Using the inducible Cre-lox system, BMPR-IA (Alk3) was abrogated in late lung development (E17.5 conditional knockout (CKO)). Mice were born but died shortly afterwards from respiratory distress (Sun et al., 2008). Together these data demonstrate BMP4 as an important mediator of lung branching morphogenesis by maintaining the distal progenitor cells in a dedifferentiated state and promoting proliferation. In addition, during late lung development BMP signalling remains active implicating this pathway as a mediator of distal lung differentiation.

The majority of studies which have focused on BMP signalling during lung development support the above hypothesis. Weaver et al. through overexpression of both Noggin (BMP ligand antagonist) and a dominant negative form of the BMP receptor, BMPR-IB (dnAlk6), under the control of the SP-C promoter inhibited BMP

signalling in distal epithelial cells from E10.5. Both approaches displayed a similar lung phenotype with lungs which were fifty percent reduced in size. In addition, a reduction in the presence of distal cell types with a concurrent increase in proximal cell types was observed at the lung periphery (Weaver et al., 1999). Eblaghie et al., using the Cre-lox system deleted BMPR-IA (Alk3) at the onset of SP-C expression (E10.5). Abnormalities in the lung architecture were visible from E16.5 and all pups which were born died from severe respiratory distress. Epithelial cell proliferation was reduced and increased apoptosis was detected. Serial sectioning through the mutant lungs revealed an absence in smaller distal airways consistent with an inhibition of stereotypic branching morphogenesis. In addition, and the most likely cause of the post-natal lethality, in place of correctly formed terminal sacs was the presence of large fluid filled spaces. Consistent with a role for BMP signalling in inhibiting proximal cell differentiation, CC10 expression, a peripheral cell marker retained by Clara cells, was aberrantly expressed in the periphery of the lungs (Eblaghie et al., 2005).

Sun et al., characterised a similar phenotype when BMPR-IA was conditionally deleted at ~ E7.5-12.5 (BMPR-IA Conditional Knockout (CKO)) (Sun et al., 2008). The study reported a more dramatic inhibition in lung branching in the BMPR-IA-CKO mice compared to Eblaghie et al. However, an abnormal lung phenotype consistent with previous studies was observed with large fluid filled sacs in place of terminal buds, columnar cells aberrantly localised distally in the lung and a decrease in distal lung markers SP-C and AQ5. In another set of experiments, BMPR-IA expression was inhibited at E17.5 by means of the doxycycline induced BMPR-IA-CKO. Loss of BMPR-IA at E17.5 did not significantly alter lung architecture. However despite this, animals died postnatally from respiratory distress. Molecular analysis of these mice (BMPR-IA-CKO at E17.5) revealed a dramatic decrease in distal cell differentiation markers, SP-C and AQ5. Consistent with previous studies apoptosis was significantly increased. However, in contrast to studies where BMPR-IA was abrogated at an earlier time point, proliferation was also increased. Lastly,

when BMPR-IA expression was abrogated postnatally (P1-Alk3/BMPR-IA CKO) no abnormal lung phenotype was observed.

These studies collectively show BMP signalling during early lung development is required for correct lung branching mediated by epithelial cell proliferation and a concurrent inhibition of apoptosis. In addition, BMP signals maintain distal progenitor cells and inhibit proximal cell differentiation. During late lung development, BMP signalling is required for the establishment and maintenance of the distal lung phenotype. This role for BMP signalling in late lung development is likely to involve inhibition of distal cell proliferation while continuing to prevent apoptosis. The molecular mechanisms which control this switch from BMP-mediated distal cell proliferation to the initiation of distal cell differentiation are not known. Abrogation of BMPR-IA did not affect postnatal lung development (Sun et al., 2008) despite active BMP signalling at this time (Alejandre-Alcázar et al., 2007). This suggests that maintenance of the distal lung phenotype postnatally may be mediated through other BMP receptors.

The studies outlined above support the hypothesis of BMP signalling as a positive regulator of airway branching. However, not all experimental data support this model. Bellusci et al., developed a transgenic line where BMP4 under the SP-C promoter resulted in aberrant BMP4 expression in a larger domain of the distal epithelium than normal (Bellusci et al., 1996). In these animals a reduction in lung branching was reported (Bellusci et al., 1996). However, similar abnormal distal lung development was also reported with a reduction in type II pneumocytes and increased fluid filled sacs indicative of abnormal terminal sac development. The study indicated that a finely tuned level of BMP4 expression is required for correct lung development (Bellusci et al., 1996). In the absence of mesenchyme BMP4 inhibited outgrowth of lung branches *in vitro* (Weaver et al., 2000). Furthermore, Bragg et al., demonstrated BMP4 promoted lung branching and increase cell proliferation in the presence of mesenchyme but BMP4 did not stimulate lung branching when restricted to the

epithelium (Bragg et al., 2001). This indicated BMP signalling requires signals arising from the mesenchyme to positively mediate lung branching.

BMP signalling cooperates with both FGF to mediate correct lung development. FGF10 expression in the mesenchyme is required for lung bud initiation and subsequent induction of BMP4 in the endoderm. However, BMP signalling can inhibit FGF10-mediated lateral outgrowth. *In vivo*, a critical interplay between FGF and BMP is proposed. BMP4 expression in the distal tip inhibits FGF signalling and therefore lateral outgrowth does not occur and the lung bud extends. As the BMP4 stimulus diminishes along the extended lung branch FGF signalling is no longer inhibited and lateral branching occurs. In this way, signalling from both the endoderm (BMP) and the mesenchyme (FGF) are required for correct lung branching (Weaver et al., 1999). Communication between BMP and FGF signalling can, in part, explain the lung phenotype reported by Bellusci et al., where BMP4 overexpression reduced overall lung size (Bellusci et al., 1996). It is likely the aberrant expression of BMP4 inhibited FGF signalling along a broader domain and thus inhibited FGF-mediated lateral outgrowth.

In conclusion, carefully regulated BMP4-mediated signalling is critical for lung branching morphogenesis and establishment of the distal lung phenotype. This role in lung development is elicited though complex epithelial-mesenchymal interactions between BMP4 expressed in the endoderm of the developing lung branch and growth factors such as FGF10 originating from the adjacent mesenchyme.

1.2.4. **BMP Signalling During Disease**

BMP signalling is a positive regulator of proliferation and a negative regulator of apoptosis during lung development. In addition, BMP signalling, via suppression of Wnt signalling, can inhibit differentiation and promote stem cell self renewal (Varga and Wrana, 2005). However, BMP signalling can also induce apoptosis in the

developing limb and promote neuronal differentiation in certain stem cell lineages (Robert et al., 2007, Bailey et al., 2007). This role for BMP signalling in regulating cell proliferation and differentiation implicates BMP signalling as a target in cancer. The following section will describe BMP signalling in cancer. More recently, BMP signalling has been implicated during inflammatory processes in a number of tissue types and this will be outlined below.

1.2.4.1. **Cancer**

BMP ligands and receptors have been found upregulated in a variety of cancer types including prostate, oral, colon and breast (Bailey et al., 2007). BMP2 expression corresponded to metastatic potential in human breast cancer cells (Bailey et al., 2007). In oestrogen receptor-positive breast cancer, high tumor grade, proliferation and poor prognosis was associated with strong expression of BMPR-IB (Helms et al., 2005). Moreover, expression of a dominant negative form of BMPR-II in human breast cancer cell became resistant to BMP2-induced Smad phosphorylation and exhibited reduced proliferation (Pouliot et al., 2003). Smad4 knockdown in MDA-MB-231 breast cancer cells reduced bone metastasis by 75% and increased survival after intracardial injection into nude mice (Deckers et al., 2006).

BMP4, BMPR-IA and BMPR-IB mRNA have recently been shown to be elevated in colorectal cancer (Bailey et al., 2007). Moreover overexpression of BMP4 in human colon cancer cells (HCT116 cells) protected cells from apoptosis and increased their migratory potential (Deng et al., 2007b, Deng et al., 2007a). Juvenile polyposis can predispose an individual to colorectal and gastric cancer (Chow and Macrae, 2005). Juvenile polyps are characterised by normal epithelium and a lamina propria markedly expanded by dilated glands, abundant stroma and an inflammatory infiltrate (Howe et al., 2007). Germline mutations in both *Smad4* (*MADH4*) and *BMPR-IA* genes have been identified in patients with juvenile polyposis (JP) (Howe et al., 2007). In addition, BMPs have been reported overexpressed in malignant melanoma (Rothhammer et al., 2005) and their expression in osteosarcomas has been correlated with tumor proliferation and metastasis (Yoshikawa et al., 2004).

BMP2, but not BMP4, is highly overexpressed in non small cell lung carcinomas (NSCLCs) (Langenfeld et al., 2003). Furthermore, BMP2 can stimulate angiogenesis of tumors derived from A549 cells (adenocarcinoma derived lung cancer cell line) injected into nude mice (Langenfeld and Langenfeld, 2004). However, in contrast this pro-proliferative role for BMP2 in lung cancer, BMP3b and BMP6 were shown to be epigenetically silenced in NSCLC indicating a tumor suppressor role for BMP signalling mediate by these ligands (Kraunz et al., 2005). Similarly, BMP4 was shown to inhibit A549 cell proliferation and reduce tumor growth and metastasis *in vivo* (Buckley et al., 2004).

The functional significance of increased BMP signalling in cancer has not been elucidated to date. It is likely to relate to aberrant expression of BMP target genes involved in proliferation and inhibition of differentiation such as the Id transcription factors. Id proteins are widely expressed in cancer and have been associated with invasiveness and angiogenesis (Perk et al., 2005).

1.2.4.2. **Inflammation**

In contrast to BMP signalling in cancer, BMP involvement during inflammation has received little attention to date. Inflammation occurs as part of the host defense against infection. However, sustained or aberrant inflammation can cause damage to the local tissue. For this reason, the processes of inflammation, injury and repair operate in close association to ultimately protect the body against potential pathogens and regain tissue homeostasis. The pathways involved in the inflammatory processes and repair in many adult tissue types have not been clearly defined. However, a widely accepted hypothesis involves the reactivation of developmentally relevant pathways to repair damage in the adult tissue. BMP signalling is a critical developmental pathway and for this reason is likely to be recapitulated during injury in the adult.

BMP signalling is necessary for correct joint morphogenesis with null mutations in several BMP pathway components resulting in severe defects in joint patterning

(Settle et al., 2003). In addition, mutations in the BMP antagonist Noggin leads to defects in joint formation (Gong et al., 1999, Marcelino et al., 2001). BMP3, 4, 7 and CDMP1 have been shown to stimulate proteoglycan synthesis *in vitro*. Similarily, conditional BMPR-IA knockout mice had reduced proteoglycan and collagen type II expression in joints. These functions indicated a role for BMP signalling in the homeostasis of articular cartilage and the joint. Furthermore, BMP7 expression and protein synthesis was enhanced by the pro-inflammatory cytokine IL-1 (Lories and Luyten, 2005). Rheumatoid arthritis (RA) is a chronic systemic inflammatory disease that primarily affects the synovial joints (Lories and Luyten, 2005). BMP2, 6 and 7 are elevated in patients with RA compared to non-inflammatory controls. It is likely the critical role for BMP in joint morphogenesis is recapitulated in normal joint homeostasis and disease to stimulate remodeling following injury.

BMP signalling is active during kidney organogenesis. However, only BMP7 is absolutely required for proper formation of the kidney (Simic and Vukicevic, 2005). *In vitro*, BMP7 can promote survival of explanted metanephric mesenchyme by inhibiting apoptosis and maintaining cells in an undifferentiated state, processes which closely mimic BMP4 in the lung. BMP7 is critical for kidney homeostasis and has ability to ameliorate several forms of kidney disease. A number of mouse models are used to study both acute and chronic renal injury. They include the ischemic/reperfusion insult model whereby blood flow to the kidney is prevented and subsequent oxygen deprivation results in tubular epithelial cell apoptosis, necrosis and immune cell infiltration culminating in renal failure. Following ischemic acute renal injury, BMP7 can inhibit apoptosis and reduce ICAM expression thus reducing accumulation of neutrophils. In animal models of acute toxic kidney injury, BMP7 has been shown to reduce the severity of the damage. This has been shown in both mercury chloride- and cisplatinum-induced nephrotoxcity. In mice, these chemicals cause kidney damage largely through their induction of reactice oxygen species. BMP7 has been shown to protect the kidney function following administration of mercury chloride and cisplatinum leading to the proposed role of BMP7 as a free radical scavenger. Kidney fibrosis is associated with end-stage renal disease (ESRD).

A well established model involving tissue fibrosis is that of nephrotoxic serum (NTS) nephritis. In this model injury is induced from the administration of heterologous antibodies against glomerular basement membrane (GBM). Following binding of the anti-GBM antibodies in the kidney and subsequent host antibody response against the heterologous antibodies, immune complexes are formed resulting in chronic renal fibrosis. BMP7 has been shown to reduce chronic fibrosis and improve survival following NTS administration. BMP7 reduced the accumulation of extracellular matrix proteins while sustaining the expression of tissue degrading enzymes such as the matrix metalloprotease, MMP2. In addition, BMP7 repressed the expression of proinflammatory genes thus reducing immune cell recruitment and subsequent activation of local fibroblasts. In this way, BMP7 appeared to have opposing roles in extracellular deposition when compared to BMP2 and BMP4 in joint homeostasis. Taken together, BMP7, a critical mediator of kidney development, appears to be reactivated during renal disease to protect against injury (Simic and Vukicevic, 2005).

Considering the pivotal role of BMP signalling during lung development, BMP signals are likely to be reactivated during injury to repair lung damage and maintain lung homeostasis. BMP signalling is required for all stages of lung development (Alejandre-Alcázar et al., 2007). In bronchopulmonary dysplasia, a disease where alveolar development is arrested from high exposure to O_2 (hyperoxia), BMP signalling is impaired (Alejandre-Alcázar et al., 2006). It is not known what level of BMP activity, if any, exists at any time in the quiescent lung. However, BMP pathway expression has been reported in the airway epithelium of large conducting airways at P28 (post natal day 28) in mice indicating BMP signalling may be required for homeostasis of the developed lung (Alejandre-Alcázar et al., 2007).

Rosendahl et al., provided the first report of activated BMP signalling during OVA-induced airway inflammation. The OVA (ovalbumin) model of allergic inflammation involves sensitization of mice to OVA by means of an intraperitoneal injection followed by repeated exposure to inhaled OVA to elicit an allergic response. This experimental model resembles the acute inflammatory response that occurs following

exposure to high-dose antigens such as pollen (Rosendahl et al., 2002). The study assessed the activation of BMP signalling via immunohistochemical and western blot analysis of BMP pathway components in airway epithelial cells and whole lung, respectively. The study found ubiquitous expression of Smad1 in the epithelial cells of normal non-allergic airways but only detected the phosphorylated form in the airways of challenged mice. BMP Type I receptors were expressed in the epithelial cells of normal airways and were visibly increased in response to OVA challenge. Healthy lungs contained high levels of mature BMP2 and BMP5 and moderate levels of BMP4, 6 and 7 (Rosendahl et al., 2002). BMP2 and BMP6 were increased following OVA challenge. In contrast, a reduction in the level of mature BMP4 and BMP5 expression was detected. However, BMP4 and BMP5 proprotein were increased in the allergic animals. No induction of BMP7, either the mature ligand or the pro-protein, was detected. The constitutive expression of Smad1, BMP receptors and ligands in the lungs of healthy animals strongly suggests BMP signalling is involved in lung homeostasis. BMP7 has been linked to anti-inflammatory processes in the kidney whereas BMP2 and BMP6, through interaction with pro-inflammatory signals, are involved in ECM deposition in the joint and skin (Lories and Luyten, 2005, Stelnicki et al. 1998, Kaiser et al., 1998). BMP7 was not induced following OVA-challenge and moreover was significantly downregulated at the mRNA level. In contrast, BMP2 and BMP6 were significantly elevated at the mRNA and protein level. Taken together, this study implicated BMP signalling in the pathogenesis of allergic inflammation where the activated pathway may contribute to pro-inflammatory processes and ECM deposition *in vivo*.

Kariyawasam et al., demonstrated activated BMP signalling in human patients with mild asthma. Immunohistochemistry was used to assess BMP pathway expression in the airways of non-allergic individuals and individuals with mild asthma at baseline as well as 24 hours and 7 days after inhalational allergen challenge. BMP type I receptors BMPR-IA (Alk3), BMPR-IB (Alk6) and BMPR-II were expressed on the epithelial cells in airways of normal non-allergic individuals. A reduction in receptor expression (BMPR-IB, BMPR-II) in the airways of individuals with mild asthma was reported

when compared to non-allergic individuals. Similarly, phosphorylated Smad1 and 5 (p-Smad1/5) was detected in the cytoplasm of the airway epithelial cells of normal airways where the level of p-Smad1/5 appeared reduced in allergic airways. However, following allergen challenge the pathway appeared activated in allergic individuals. Increased expression of BMP type I receptors was detected as was an increase in p-Smad1/5 expression. Both BMPR-IA (Alk3) and BMPR-II remained unaltered following allergen challenge. This level of pathway activation was seen at 24hrs post-challenge and was sustained up to 7 days post challenge. BMP2, 4 and 7 were detected in the normal airway and no alteration in the level of expression was seen in asthmatic individuals at baseline. Following allergen challenge no change in BMP2 and BMP4 was detected. In contrast, BMP7 expression by epithelial cells was significantly increased. In addition, infiltrating eosinophils were positive for BMP7 protein. Upregulation of BMP7 led the authors to hypothesize BMP signalling may serve to reduce inflammation in the surrounding tissue. Taken together, BMP pathway components are expressed in normal airways and this level of expression appeared reduced in individuals with mild asthma. Whether this reduced BMP activity in the airways predisposes an individual to asthma or whether it is as a result of the disease is not known. Nonetheless, the BMP pathway was activated in allergic individuals in response to allergen challenge suggesting BMP signalling is activated during inflammation in human airways (Kariyawasam et al., 2008).

In conclusion, there is evidence to suggest a BMP pathway is expressed in normal airways highlighting a possible role for BMP signalling during normal lung homeostasis. BMP signalling is activated during inflammation the outcome of which is currently unknown and is likely to rely on a number of factors including the particular ligand which mediates the response.

1.3. Epithelial-Mesenchymal Transition (EMT)

Epithelial to mesenchymal transition (EMT) involves a number of processes which enable cellular movement. EMT occurs during vertebrate embryogenesis to disperse cells and in the adult to mediate wound repair. However, aberrant EMT has been correlated to tumor metastasis and fibrosis. In this section the process of EMT will be discussed including changes in cell phenotype and the role of BMP signalling during EMT in development and disease.

1.3.1. Changes in Cell Phenotype associated with EMT

Epithelial cells function as physical barriers between the internal body cavity and the external environment. Epithelial cells are uniform in shape and form layers or sheets usually one cell thick. They possess apical to basal polarity and are fixed in position via a range of adhesion systems connecting cells to each other and to the underlying substratum. Conversely, mesenchymal cells are not uniform in structure. They possess weak or no intercellular adhesion which facilitates migration through extracellular matrix (ECM). In place of apical-basal polarity mesenchymal cells have front-back or leading-trailing edge polarity. Where epithelial cells can move as a sheet, mesenchymal cells move individually. The process of epithelial-mesenchymal transition (EMT) has been studied in a number of contexts including developmental EMTs, *in vitro* experimentation involving a variety cell types and EMT-inducing factors and during cancer metastasis (Kalluri and Neilson, 2003). From these studies common phenotypic changes have been identified including loss of cell-cell adhesion, actin reorganization, alterations in morphology, loss of epithelial related genes, increased expression of mesenchymal genes, increased migratory capacity, resistance to apoptosis and decreased mitosis (Lee et al., 2006, Kalluri and Neilson, 2003).

A hallmark of EMT involves the disruption of cell-cell adhesion. Epithelial cells possess a number of adhesion junctions such as tight junctions, desmosomal junctions,

adherens junction proteins and gap junctions (Cavallaro and Christofori, 2004) which confer stability to the epithelium as well as mediate juxtacrine signalling. Tight junctions include the transmembrane claudins, occludins and scaffold protein ZO1 which associates with the actin cytoskeleton (Zavadil and Böttinger, 2005). They are located in the most apical region between the epithelial cells and prevent movement of molecules over 0.18 kDa between cells (Olver et al., 1981). Desmosomes mediate cell-cell adhesion through desmocolin and desmoglein cadherin molecules. Desmosomes are responsible for connecting cell-cell adhesion proteins to the cytoskeletal keratin fibers (Zavadil and Böttinger, 2005).

Zonula adherens junctions are the best characterised and consist of classical cadherin molecules (Ivanov et al., 2001) (Fig. 1.7). Classical cadherin molecules include E-(epithelial), N-(neuronal), P-(placental), R-(Retinal), VE-(vascular endothelial) cadherin expressed by epithelial, neuronal, myoepithelial, retinal and endothelial cells respectively (Ivanov et al., 2001). Classical cadherins are transmembrane glycoproteins consisting of five extracellular domains which mediate Ca^{2+}-dependent homophilic cell-cell adhesion (Ivanov et al., 2001). The intracellular domain of classical cadherins is associated with cytoplasmic proteins called catenins of which α- and β-catenin are the two major components. β-catenin can bind directly to the intracellular domain of the cadherin protein via conserved sequences termed *armadillo* repeats (Ivanov et al., 2001). α-catenin binds to β-catenin and to the actin cytoskeleton. This interaction with the actin cytoskeleton stabilizes the adhesive complex. γ-catenin or plakoglobin, a protein homologous to β-catenin, can substitute for β-catenin in the cadherin-catenin complex. However, in β-catenin null embryos, γ-catenin failed to substitute for β-catenin and so a role for this catenin protein is not yet fully understood (Ivanov et al., 2001). Cadherins cannot mediate correct cell-cell adhesion in the absence of the cytoplasmic catenin proteins.

Disassembly of the E-cadherin-mediated adherens junction is regarded as a hallmark of EMT. Moreover, the use of anti-E-cadherin antibodies or low calcium conditions can disrupt E-cadherin expression leading to the induction of EMT. In this way, E-

cadherin is regarded as the caretaker of the epithelial phenotype. A number of mechanisms can inhibit E-cadherin expression. At the transcriptional level an array of transcriptional repressors of E-cadherin have been identified including Snail1, Snail2/Slug, Snail3, Zeb1/δEF1/Zfhx1a, ZEB2/SIP1/Zfhx1b, E47, mITF2 and Twist (Batlle et al., 2000, Bolos et al., 2003, Cano et al., 2000, Comijn et al., 2001, Peinado et al., 2004a, Peinado et al., 2004b, Shih et al., 2005, Yang et al., 2004). The common method of repression among these factors involves binding of e-boxes within the E-cadherin promoter preventing transcription of the E-cadherin gene. In addition to transcriptional repression, epigenetic silencing of the E-cadherin gene via hypermethylation of the promoter CpG islands can also lead to loss of E-cadherin expression (Ribeiro-Filho et al., 2002). However, while transcriptional inhibition of E-cadherin can result in weakening of the cell adherens junction, inhibition of membrane associated E-cadherin is necessary for complete loss of cell-cell adhesion.

E-cadherin within the cell membrane is not fixed in position but instead is actively transported between the membrane and endocytic compartments to specifically regulate the level of cell-cell adhesion. Endocytosis of E-cadherin from the surface membrane can lead to an immediate recycling of the protein back to the surface, temporary sequestering of E-cadherin within the cell and/or subsequent degradation (Bryant and Stow, 2004). While temporary sequestering of E-cadherin within the cell facilitates cellular processes such as mitosis, E-cadherin degradation is likely to occur during EMT where a more permanent loss in E-cadherin expression in required. In summary, E-cadherin, an adhesion molecule essential for epithelial cell integrity, is downregulated during EMT and this is likely to involve concurrent inhibition at both the transcriptional and protein level.

EMT involves reorganization of the actin cytoskeleton. Epithelial cells are characterised by polarized cortical actin which is connected to the intracellular catenin component of the adherens junction and runs parallel to the membrane on the cytoplasmic side. Actin in this formation is responsible for giving an epithelial layer its rigidity. Loss of the epithelial apical-basal polarity occurs during EMT. This loss in

polarity involves a switch from cortical actin to actin stress fibers (Zavadil and Böttinger, 2005). Actin remodeling enables actin-myosin cell contraction and the formation of actin protrusions called lamellopodia which facilitates mesenchymal cell migration (Zavadil and Böttinger, 2005). In addition to alterations in the actin cytoskeleton, acquisition of a mesenchymal phenotype is generally associated with a scattered or fibroblast-like change in morphology.

EMT involves alteration in protein expression termed the EMT proteome (Kalluri and Neilson, 2003). Proteins attenuated mainly involve adhesion proteins such as E-cadherin, desmoplakin and ZO-1 and/or epithelial specific cytoskeletal proteins, cytokeratins. In addition, EMT is associated with the acquisition of a number of mesenchymal genes including ECM proteins, fibronectin and collagen as well as mesenchymal cytoskeletal proteins, vimentin and α-SMA. FSP1 (fibroblast specific protein 1) or S100/A4 has recently been recognized as a marker of 'transitioning' epithelial cells undergoing EMT (Okada et al., 1997). Similarly, during kidney fibrosis in mice, FSP1 positive fibroblasts were shown to have arisen from the surrounding epithelium (Iwano et al., 2002). The acquisition of mesenchymal proteins has been correlated with increased expression of Snail transcription factors involved in repression of E-cadherin (see above), Snail1 and SIP1, implicating them in the induction of mesenchymal genes as well as inhibition of the epithelial phenotype (Kalluri and Neilson, 2003).

During EMT cells must detach from the substratum below in order to fully migrate away from the local area. The integrin family of transmembrane proteins is expressed on epithelial cells and bind to extracellular matrix proteins such as collagen and fibronectin. Antibody mediated disruption of integrin expression results in cell-substratum disassociation as well as cell-cell detachment (Savagner et al., 2001) highlighting the role for this family of proteins in epithelial cell integrity. Matrix metalloproteases (MMPs) have been implicated in the disruption of the cell-substratum adhesion system (Savagner et al., 2001). In addition, MMPs mediate degradation of the ECM to facilitate mesenchymal cell movement. In this way, EMT

is associated with alterations in integrin expression, increased expression of MMPs and increased migration and invasiveness of the EMT transitioning cell.

These alterations associated with EMT are not a strict set of guidelines and in many cases the proteins acquired or lost is highly dependent on context, cell type and EMT-inducing factors involved.

1.3.2. **Growth Factors involved in EMT**

Receptor tyrosine kinases (RTKs), RTK ligands, TGF-β and TGF-βR, integrins cooperate to mediate EMT in a number of cell types (Thiery, 2003). RTKs and their ligands include hepatocyte growth factor (HGF) or scatter factor and receptor c-met, FGF and FGFR and EGF and EGFR (Strutz et al., 2001). HGF/SF is secreted by fibroblasts and can disrupt cell-cell adhesion in epithelial cells *in vitro* and stimulates cell migration during wound healing *in vivo* (Nusrat et al., 1994). Activated FGF signalling via the PI3K-AKT pathway can induce Snail inhibition of E-cadherin (Katoh and Katoh, 2006). In addition, EGF in PMC42 (breast cancer) cells can decrease E-cadherin expression and increase vimentin production (Lee et al., 2006). Most importantly, TGF- β has been consistently described as an inducer of EMT in a number of cell types including mammary cells, epidermal keratinocytes, airway epithelial cells, kidney tubular epithelial cells and lens epithelial cells (Valcourt et al., 2005, Willis et al., 2005, Kasai et al., 2005, Forino et al., 2006, De Longh et al., 2005). The EMT process initiated by HGH/SF, EGF, FGF has been referred to as 'cell scattering' where removal of the EMT inducing factor leads to a reversal of the mesenchymal phenotype by the process termed mesenchymal-epithelial transition (MET). Conversely, 'true' EMT has been characterised as an irreversible change in cell phenotype reportedly driven by TGF-β and the Ras superfamily (see below). This differentiation between 'true EMT' and 'cell scatter' has been disputed (Thompson and Newgreen, 2005). This is due to the fact that EMT which was first recognized during development was reversible by the process of mesenchymal-epithelial

transition (MET). For this reason, it seems counterintuitive to regard irreversibility as a defining characteristic of EMT in the adult.

EMT is under the control of the Ras superfamily of small GTPases. This family signal through MAP kinases and are key in the shaping of the mesenchymal phenotype through their involvement in protein trafficking, actin cytoskeletal integrity and remodeling, proliferation, differentiation, cell adhesion and cell migration (Hall et al., 1993, Michiels and Collard, 1999). Three of the best studied small GTPases are Rho, Rac and Cdc42. These proteins mediate re-organization of the actin cytoskeleton and the formation of lamellopodia and filopodia (Nobes and Hall, 1995). Communication between TGF-β and the Ras downstream mediators Raf/MAPK and PIsK-PK3/Akt is essential for the induction of EMT (Janda et al., 2002). Raf can induce TGF-β secretion which maintains the mesenchymal phenotype where PIsK-PK3/Akt signalling inhibits TGF-β induced apoptosis (Janda et al., 2002). EMT mediated by TGF-β can converge with other signalling cascades including ERK MAPK, p38 MAPK, Jagged/Notch and NF-κB in a number of cell types (Zavadil and Böttinger, 2005).

In addition to its role as a member of the adherens junction complex, β-catenin is a transducer and transcriptional activator of Wnt signals and its activation has been regarded as a marker for EMT. Canonical Wnt signals are transduced through the frizzled family of receptors and the LRP5/LRP6 coreceptor (Katoh and Katoh, 2006). β-catenin within the cell is secured within the adherens junction complex and any unbound cytoplasmic β-catenin is degraded in the proteosome initiated by GSK3β phosphorylation. Following Wnt pathway activation, cytoplasmic β-catenin is released from GSK3β, stabilized and free to translocate to the nucleus. Nuclear translocation of β-catenin leads to apoptosis. However, nuclear translocation of β-catenin in association with the LEF1/Tcf family of transcription factors and can directly bind to the number of gene promoters including FGF20, MYC and CCND1 and has been implicated in the induction of EMT (Katoh and Katoh, 2006). Stabilized β-catenin in the presence of LEF-1 is sufficient to drive EMT in human epithelial colon carcinoma

cells (DLD1) (Kim et al., 2002). Furthermore, β-catenin/LEF1 nuclear translocation has been reported in a number of normal epithelial cells undergoing EMT. APC prevents β-catenin transcription though exporting β-catenin from the nucleus. Mutations in APC and activation of Wnt signalling have been reported in colorectal cancer (Segditsas and Tomlinson, 2006).

1.3.3. BMP Signalling and EMT in Early Development

During embryogenesis the first cells formed adopt an epithelial phenotype with the development of tight junctions, adherens junctions and the formation of apical-basal polarity (Shook and Keller, 2003). In this way, epithelial cells provide mechanical stability to the developing embryo as well as serving as a barrier from the external environment allowing the formation of a physiologically controlled internal cavity. Primary EMT is an essential part of embryogenesis and involves the ingression of epithelial cells from the primary epithelium into the internal cavity (Shook and Keller, 2003). These newly formed mesenchymal cells with their ability to move in three dimensions can mediate organ formation. Similarly, at the correct time, location and in response to the correct signals the mesenchymal cell can undergo the reverse process of mesenchymal-epithelial transition (MET) to form secondary epithelia. It is this interplay between EMT and MET transitions which allows the formation of the three germ layers and organization of the adult into epithelial, mesenchymal and endothelial cell types.

BMP signalling is critical in a variety of developmental processes which encompass EMT aspects of morphogenesis (Chen et al., 2004). BMP signalling is essential for gastrulation the process whereby the primitive epithelial cells or epiblasts give rise to the first region of mesenchymal tissue termed the primitive streak (Kishigami and Mishina, 2005). Similarly, BMP4 is required for mesoderm formation in the mouse (Winnier et al., 1995). BMP4 induces EMT during neural crest formation via upregulation of Snail2 (Sakai et al., 2006). Inactivation of either BMPR-IA or BMP2 inhibits EMT during heart formation in the developing mouse embryo (Okagawa et

al., 2007, Song et al., 2006, Ma et al., 2005). Similarly in the heart, BMP2 mediates EMT through Twist inhibition of VE-cadherin (Ma et al., 2005). In summary, the molecular mechanisms underlying EMT during development have remained largely unknown. BMP signalling is highly expressed at sites undergoing EMT in the developing embryo and abrogation of this signalling inhibits mesenchymal cell formation. This implicates EMT as a fundamental outcome of BMP signalling.

1.3.4. BMP Signalling and EMT in Disease

Alterations in cell phenotype associated with EMT including loss in cell-cell contact and increased invasiveness parallel changes associated with tumor metastases. Differentiated tumors express E-cadherin and loss of E-cadherin has been inversely correlated to increased tumor invasiveness. The transcriptional repressor of E-cadherin, Snail, is expressed in poorly differentiated breast carcinoma tissue and in lymph node positive tumors and its expression has been correlated with loss of E-cadherin in breast carcinoma and oral squamous-cell carcinoma (Thiery, 2002). Therefore the hallmark of EMT, loss of E-cadherin expression, facilitates tumor de-differentiation which correlates with increased tumor grade and poor patient survival. A role for BMP signalling during cancer has not been elucidated. While it is likely the elevated BMP signalling during cancer may mediate proliferation it is also likely BMP-mediated EMT may promote cancer metastasis. However, there is no experimental data to support this.

EMT has been implicated during fibrosis in the kidney and may contribute to fibrosis of the lung and the liver. During renal fibrosis is has been demonstrated that approximately 14-15% of fibroblasts arise from the bone marrow, 50% arise from local proliferation and about 36% of new fibroblasts come from local EMT (Iwano et al., 2002). TGF-β signalling has been implicated in fibrosis of the heart, kidney and lung (Zeisberg et al., 2007, Zeisberg et al., 2003, Allen and Spiteri, 2002). Evidence surrounding the role of BMP signalling during EMT in the adult has been contradictory. BMP7 was the first BMP ligand to be implicated during fibrosis when it

was shown to inhibit TGF-β1-induced EMT in the kidney (Zeisberg et al., 2003). BMP7 can also reverse cardiac fibrosis through inhibition of TGF-β1-induced endothelial-mesenchymal transition (EndMT) (Zeisberg et al., 2007). Similarly, idiopathic pulmonary fibrosis (IPF) has been associated with increased TGF-β expression and increased Gremlin expression. Gremlin, a BMP antagonist, specifically inhibits BMP2, BMP4 and BMP7 and this increased expression during lung fibrosis further implicates BMP signalling as an anti-fibrotic signalling pathway in adult organs.

In 2007, a number of papers were published implicating BMP4 as an inducer of EMT in mammary, ovarian and pancreatic cell types (Montesano, 2007, Thériault et al., 2007, Hamada et al., 2007). BMP4 was shown to induce disassociation of cell-cell adhesion and increase migration of mammary cells *in vitro* (Montesano, 2007). Inhibition of the MAPK signalling pathway mediators in particular p38 MAPK inhibited this BMP4-induced invasive phenotype. Thériault et al. demonstrated the induction of EMT in primary ovarian cells treated with BMP4 or in cells which overexpressed BMPR-IA (Alk3: BMP specific receptor). These cells exhibited acquisition of an irregular mesenchymal shaped morphology, actin reorganization and the upregulation of a number of mesenchymal markers including a number of integrins, focal adhesion proteins (FAPs) and extracellular matrix (ECM) proteins (Thériault et al., 2007). This newly acquired mesenchymal phenotype was associated with a repression of the epithelial phenotype with a loss in E-cadherin expression and a concurrent increase in the expression of E-cadherin transcriptional repressors, Snail1 (formerly Snail) and Snail2 (formerly Slug) (Thériault et al., 2007). BMP4 also increased ovarian cell migration. These changes corresponded to increased Ras signalling with BMP4-induced increased activity of Rac1, Rho and Cdc42 Rho GTPases (Thériault et al., 2007).

Hamada et al. demonstrated a similar induction of EMT in a pancreatic cell line in response to BMP4 (Hamada et al., 2007). In the study, cells cultured with BMP4 exhibited loose cell-cell contact and a fibroblast-like appearance. E-cadherin protein

expression was inhibited and vimentin was increased. Cytoplasmic β-catenin was observed consistent with a disruption in correct adherens junction localisation. The study identified the *Xenopus* BMP target, MSX2, as the downstream target of BMP4-mediated signalling and MSX2 expression was essential in the induction of EMT. In addition, it was demonstrated both canonical (Smad) and non-canonical (ERK, P38 MAPK) BMP signalling was activated following BMP4 stimulation and that both pathways were involved in BMP4-mediated EMT in pancreatic cells (Hamada et al., 2007).

In summary, BMP4-mediated signalling has been implicated as an inducer of EMT *in vitro* in a number of adult cell types. This is in contest with a previously recognized role for BMP7-mediated signalling in the inhibition of TGF-β-induced EMT *in vivo* during renal fibrosis. *In vivo* evidence for a role for BMP4-mediated signalling during fibrosis has not yet been provided. Nonetheless, BMP signalling is involved in EMT during development. The BMP pathway is activated during inflammation the outcome of which is unknown. BMP-mediated EMT during inflammatory disease may promote repair following injury or may exasperate inflammation by causing fibrosis of the inflamed tissue. Further experimental evidence is required to identify whether BMP4-mediated EMT occurs *in vivo* in the adult and if so, the outcome of such an event.

1.4. Allergic Rhinitis (AR)

Allergic rhinitis (AR) is a chronic inflammatory disease of the upper airways. The prevalence of AR has increased over the last decade with up to 25% of the worlds population affected (Sibbald, 1993, Aberg et al., 1996). AR and asthma often occur together in a patient. Individuals who suffer from asthma often have AR and AR sufferers have increased susceptibility to asthma (Jeffery and Haahtela, 2006). Asthma and AR are characterised by similar inflammatory processes but display obvious dissimilarities in the level of remodeling associated with the disease. In this section the inflammatory processes in response to allergy during AR will be outlined including the critical role of the eosinophil and the occurrence of remodeling following inflammation of the upper airways.

1.4.1. Pathological Features of AR

Allergic rhinitis (AR) occurs following IgE-mediated recognition of an allergen in the nose. AR is characterised by two phases, the initial sensitisation phase, involving recognition of an allergen through IgE-mediated mast cell interaction, and the clinical phase, involving manifestation of disease symptoms (Salib et al., 2003a). These symptoms can be further sub-divided into an early and late phase response. The early phase, which occurs minutes after allergen exposure, is characterised by rhinorrhoea, nasal obstruction, itching and sneezing. These reactions arise from mast cell degranulation or exocytosis releasing histamine, tryptase, leukotrienes and prostaglandin D_2 (Togias et al., 2000). Histamine can bind to its receptors (H_1 and H_4) and activate nerve cells, as well as directly affect blood vessels by causing plasma exudation and congestion (Togias et al., 2000). Leukotrienes have strong effects on blood vessels and are potent inducers of nasal congestion (Salib et al., 2003a). In addition, mast cells release chemotactic mediators which promote the recruitment of lymphocytes, eosinophils and basophils (Galli et al., 2008). This local recruitment and activation of leukocytes contribute to the development of late phase reactions.

The late phase often occurs 2-6 hr after allergen exposure and peaks after 6-9 hr. It involves persistence of the disease symptoms. This stage is characterised by an influx of basophils, eosinophils and T_{H2} lymphocytes as well as sustained activation of resident mast cells. Basophils have similar functions to mast cells and predominate over mast cells during the late phase reaction. In addition to IgE-mediated recognition of allergen and histamine release, basophils contribute to the late phase through their secretion of pro-inflammatory cytokines IL-4 and IL-8 (Pawankar et al., 2007). T_{H2} lymphocytes recruited during the late phase produce IL-4 and IL-5 which potentiate the inflammatory response as well as mediate cellular changes such as vasodilation (Galli et al., 2008).

1.4.2. **Role of Eosinophils**

Eosinophils are the predominant effector cells of the late phase response during allergic rhinitis despite comprising less than 5% of the circulating immune cells in non-allergic individuals (Kariyawasam and Robinson, 2007). There primary role is said to have evolved from protection against parasitic helminthic infection and there involvement during diseases such as asthma, allergic rhinitis and dermatitis is a so called atopic or 'out of place' reaction to otherwise harmless environmental agents (Galli et al., 2008). Eosinophils are bilobed granulocytes which contain four primary cationic proteins namely, major basic protein (MBP), eosinophil cationic protein (ECP), eosinophil-derived neurotoxin (EDN), and eosinophil peroxidase (EPO) which they use to mediate their cytotoxic effects (Walsh, 2001). Eosinophils are trafficked from the bone marrow to sites of inflammation in response to IL-5 and a number of chemokines namely RANTES (Regulated upon Activation, Normal T-cell Expressed and Secreted), macrophage/monocyte chemotactic protein 4 and the eosinophil-specific chemokine, eotaxin. Eotaxin can be produced by mast cells, alveolar macrophages, eosinophils, airway smooth muscle cells and vascular endothelial cells with the highest level of eotaxin produced by epithelial cells (Trivedi and Lloyd, 2007). Eosinophils can upregulate adhesion molecules such as ICAM and VCAM on

the surface of the epithelial cells to facilitate eosinophil infiltration (Wong et al., 2006). Eosinophils which have crossed the epithelial barrier release their toxic granules causing epithelial cell injury, loosening cell-cell adhesion and resulting in epithelial cell shedding into the airway lumen (Trautmann et al., 2002).

Prolonged or repeated exposure to allergen leads to chronic inflammation involving sustained innate and adaptive cellular infiltrate as well as structural changes in the surrounding tissue termed remodeling.

1.4.3. **Remodeling**

Remodeling involves a number of irreversible changes to the local architecture and cellular composition as a result of chronic inflammation. Eosinophils have an important role in airway remodeling. This was evident in a transgenic mouse line in which the eosinophil lineage had been ablated and no evidence of remodeling was observed following OVA-induced airway inflammation (Humbles et al., 2004). A number of mechanisms involved in eosinophil-mediated remodeling have been suggested. Eosinophils are the predominant source of TGF-β1 during inflammation. TGF-β1 has been shown to mediate myofibroblast transformation and subsequent ECM deposition, two processes central to airway remodeling (Kariyawasam and Robinson, 2007). Similarly, eosinophil cationic proteins can stimulate epithelial cells to release factors involved in remodeling such as TGF-β1, platelet-derived growth factor (PDGF)-β, epidermal growth factors receptor (EGFR), metalloprotease (MMP)-9, fibronectin and tenascin (Pégorier et al., 2006).

Changes associated with remodeling include epithelial shedding, myofibroblast activity, submucosal collagen deposition, mast cell and eosinophil infiltration, mucus gland hypertrophy, increased airway smooth muscle and airway wall thickness (Wilson and Bamford, 2001). Remodeling during allergic rhinitis, has received little attention to date and the data which has been generated, regarding the level of structural changes, has been contradictory. In contrast, remodeling has been well

characterised in asthma and is related to the severity of the disease. During AR it is unclear to what extent the epithelium of the upper airways is damaged where epithelial shedding as well as that of an intact epithelium has been reported (Salib and Howarth, 2003). Alterations in cellular composition during AR have also provided contradictory results. However, increased goblet and ciliated cell types as well as epithelial cell metaplasia have been observed following pollen exposure and throughout the year in both seasonal (SAR: AR in response to seasonal allergens such as pollen) and perennial AR (PAR: AR in response to perennial allergens such as dust mite), respectively. Basement membrane thickening occurs as a result of increased collagen deposition and can be linked to myofibroblast transformation and elevated local TGF-β expression. Data regarding collagen deposition during AR has not provided a clear answer as to the extent of deposition but increased TGF-β activity has been consistently reported during AR suggesting profibrotic pathways are active in the nasal epithelium of AR individuals. TGF-β has been shown to induce myofibroblast transformation during inflammation leading to tissue fibrosis. However, it is possible this increased fibroblast activity may also arise from local EMT. In this way pathways involved during EMT may have a pivotal role during remodelling following inflammation.

In healthy subjects the respiratory epithelium of the nose and bronchi are comparable. Furthermore, isolated human nasal and bronchial epithelial cells are morphologically identical and respond similarly to cytokine stimulation (McDougall et al., 2008). Similarly, the inflammatory response to allergy in both upper and lower airways can be characterised by analogous immune cell infiltration and cytokine expression. However, during chronic inflammation the structural changes are notably different. A number of possible explanations have been proposed for these differences in remodeling. One such explanation has been the embryological origin of the nose and bronchi which arise from the nasal placode and laryngotracheal groove, respectively (Bousquet et al., 2004). It has been suggested that fetal genes expressed during development which may be incorrectly silenced in the adult may predispose an individual to asthma. In this way, the persistence of fetal genes which may differ

between upper and lower airways may be involved in the differential response to inflammatory stimuli. No data has been generated to date which supports this hypothesis. The upper airways do not contain underlying smooth muscle cells as seen in the trachea and the lower conducting airways. Smooth muscle cell contraction causes airway narrowing or bronchoconstriction a potentially fatal reaction during asthma to proinflammatory stimuli. Bronchoconstriction can stimulate the epithelium to release TGF-β increasing the profibrogenic environment of the lower airways in asthma which may lead to increased ECM deposition (Bousquet et al., 2004).

In a study investigating collagen expression in the nasal airway during AR the authors reported no difference in the level of collagen between normal and AR individuals but did observed significantly elevated levels of collagen expression in the 'normal' nose compared to that seen in the lower airways (Braunstahl et al., 2003). It was suggested that a certain level of remodeling may occur in the 'normal' nose on account of its increased exposure to environmental stimuli compared to the lower airways. In this way remodeling as a result of inflammatory processes may be more difficult to ascertain.

Taken together the data from these studies suggests remodeling during AR is less extensive compared to the structural changes observed in the lower airways seen in asthma. This difference in the level of remodelling may be attributed to, recapitulation of different signalling pathways active during development, dissimilarities in cellular composition such as smooth muscle cells present in the lower airways or a basal level of tissue remodeling which exists in the upper airways, not in the lower airways, on account of an increased exposure to environmental stimuli. Nonetheless, certain features of remodelling have been described during AR such a goblet cell hyperplasia, eosinophil infiltration, epithelial cell shedding and collagen deposition. AR is also associated within increased TGF- β pathway activity, a known pro-fibrotic pathway. A role for BMP signalling during AR has not been previously investigated. We hypothesise BMP may be involved in remodelling processes during inflammation and may be activated during AR.

1.5. Experimental Aims

BMP4 is essential for correct lung morphogenesis where it promotes lung branching through its inhibition of airway epithelial cell differentiation as the lung branch extents. During alveolarisation, the BMP pathway remains active where it is thought to mediate differentiation of the distal cell types. A role for BMP signalling in the adult lung is unknown. However, the BMP pathway is reactivated in the mouse OVA model of allergic inflammation suggesting BMP signalling may function in the pathogenesis of disease in the adult lung. There remains a widely accepted concept that developmentally relevant pathways may be reinitiated following injury to stimulate repair of the adult tissue. We hypothesise reactivated BMP signalling in adult airway epithelial cells (AECs) may serve to regulate airway cell differentiation during repair. Therefore, data regarding a role for BMP signalling in AECs is of great importance and has prompted a number of experimental questions which will be addressed in this study.

The first objective aimed to determine whether adult AECs express a BMP pathway and whether this pathway can be activated *in vitro* in response to BMP2 and BMP4 stimulation. For these experiments the transformed human bronchiolar cell line, BEAS-2B and the widely used adenocarcinoma-derived cell line, A549 will be used. Since BEAS-2B cells are transformed and A549 cells derived from cancer, they are likely to behave differently to normal lung cells. For this reason, our experiments are to also include normal primary airway epithelial cells isolated from mouse (MAECs). These experiments will include both immunofluorescence and western blot analysis of BMP pathway components in cells cultured in the presence of BMP2 and BMP4.

The second objective aimed to characterise the effect of activated BMP signalling on airway epithelial cell (AEC) differentiation. A previous study reported the induction of senescence in the adenocarcinoma cell line, A549, in response to BMP4. For this reason the induction of a senescence phenotype will be investigated in BEAS-2B and

A549 cells in response to both BMP2 and BMP4. This will involve the analysis of senescence associated β-galactosidase (SA-β-gal) expression as well as analysis of morphology and proliferation in response to either ligand following six days of treatment.

During lung branching morphogenesis BMP4 can inhibit proximal airway epithelial cell differentiation. We hypothesised reactivated BMP signalling in the adult lung be involved in inhibiting the epithelial phenotype in order to initiate repair. To investigate this further the effect of activated BMP signalling on the epithelial phenotype will be characterised. These experiments will involve characterisation of adherens junction complex in BEAS-2B cells which have been cultured in the presence of BMP2 and BMP4. More specifically, the effect of BMP4 on the epithelial specific marker, E-cadherin, will be investigated in BEAS-2B cells, A549 cells and MAECs. E-cadherin is commonly regarded as the 'caretaker' of the epithelial phenotype with loss of E-cadherin expression being sufficient to promote loss of epithelial characteristics and gain of mesenchymal characteristics, a complex process commonly referred to as epithelial-mesenchymal transition (EMT). EMT is an essential process during embryogenesis and more recently has been linked to repair in adult tissue and disease such as cancer and fibrosis. A specific objective will be to investigate the induction of EMT in BEAS-2B cells in response to BMP4.

Finally, another primary aim of this research is to investigate BMP signalling in human allergic rhinitis (AR). Specifically, human nasal biopsy sections from both normal individuals and individuals with allergic rhinitis (AR) will be immunolocalised for BMP pathway components. The specific aim of this work is to determine whether a BMP pathway is expressed in normal human upper airways and to investigate any pathway modulation which may occur during inflammation of the upper airways. Further to this, the effect of eosinophils on the expression and localisation of the BMP receptor, BMPR-IA, will be investigated in AECs using a co-culture system. In addition, AECs will be stimulated with eosinophil-derived proteins and the effect on BMPR-IA localisation assessed.

Together the aims of this research are to provide novel data surrounding a role of activated BMP signalling in AECs and to further investigate the involvement of BMP signalling in the pathogenesis of allergic inflammation.

2.0 MATERIAL AND METHODS

2.1. Materials

2.1.1. Reagents

Product	Company	Address
1 Kb DNA Ladder	Invitrogen	Paisley, UK
100 bp Ladder	Promega	Madison, WI, USA
Acridine Orange	Sigma	Dublin, Ireland
Agarose	Sigma	Dublin, Ireland
Ammonium Persulphate	Sigma	Dublin, Ireland
B-mercaptoethanol	Sigma	Dublin, Ireland
Bio-Rad Protein Assay Reagent	Bio-Rad	Herts, UK
Bis-Acrylamide	Bio-Rad	Herts, UK
Blocking Serum	Sigma	Dublin, Ireland
BMP2	R&D Systems	Oxon, UK
BMP4	R&D Systems	Oxon, UK
Bovine Serum Albumin (30% v/v)	Sigma	Dublin, Ireland
Bovine Serum Albumin	Sigma	Dublin, Ireland
α-CD16 immunomagnetic beads	Miltenyi Biotech	Surrey, UK
Cell Titer 96® AQueous One Solution Cell proliferation Assay	Promega, Promega Corp	Madison, WI, US

Chloroform	Sigma	Dublin, Ireland
Complete Mini Protease Inhibitor Cocktail	Roche Diagnostics	Dublin, Ireland
Cryovial	Nalge Nunc	USA
DAPI	Sigma	Dublin, Ireland
DEPC	Sigma	Dublin, Ireland
DMEM: Hams/F12	Gibco	Paisley, UK
DNase I	Roche Diagnostics	Dublin, Ireland
DMSO	Sigma	Dublin, Ireland
DNase (RT-PCR)	Invitrogen	Paisley, UK
dNTP (Set of dATP, dCTP, dGTP, dTTP)	Invitrogen	Paisley, UK
Enhanced Chemiluminescence Kit	Amersham	Buckinghamshire, UK
Epidermal growth factor	R&D Systems	Oxon, UK
Ethanol (100%)	Sigma	Dublin, Ireland
Ethylene diamine tetra acetic acid (EDTA)	Sigma	Dublin, Ireland
Ethidium Bromide	Sigma	Dublin, Ireland
Farramount Aqueous Mounting Medium	DAKO	Galway, Ireland
Fibronectin	Sigma	Dublin, Ireland
Ficoll	Amersham Pharmacia	St. Albans, UK

	Biotech	
Foetal Calf Serum	Gibco	Paisley, UK
Formaldehyde 37% v/v	Sigma	Dublin, Ireland
Gycine	Reidel-deHaen	Hanover, Germany
Heparin	Leo Laboratories,	Princes Risborough, UK
Hydrocortisone	Sigma	Dublin, Ireland
ImaGene Green C_{12}FDG	Invitrogen	Paisley, UK
LacZ detection kit		
Insulin-transferin-selenium	Gibco	Paisley, UK
Isopropanol	Sigma	Dublin, Ireland
L-Glutamine	Gibco	Paisley, UK
Marvel (non fat dried milk)	Dunnes Stores	Maynooth, Ireland
Methanol	Sigma	Dublin, Ireland
MOPS Buffer	Chemicon	Hampshire, UK
Nitrocellulose Membrane	Amersham	Buckinghamshire, UK
Oligo (12-18) dT Primers	Invitrogen	Paisley, UK
Penicillin-Streptomycin	Gibco	Paisley, UK
Pentabarbitone, Euthanal	Rhône Mérieux	Ireland
Phosphate Buffered Saline	Sigma	Dublin, Ireland
Propidium Iodide	Sigma	Dublin, Ireland
Poly-Acryl Carrier	MRC	Cincinnati, OH, USA
Qiashredder	Qiagen	West Sussex, UK
Retinoic Acid	Sigma	Dublin, Ireland

RNase OUT	Invitrogen	Paisley, UK
RNA Ladder	Sigma	Dublin, Ireland
RNA Loading Buffer	Sigma	Dublin, Ireland
RPMI – 1640	Sigma	Dublin, Ireland
Sodium dodecyl sulphate	Sigma	Dublin, Ireland
SeeBlue Protein Molecular Weight Ladder	Invitrogen	Paisley, UK
Sodium Chloride (NaCl)	BDH	Lennox, Dublin
Speedy-Diff	Clin-Tech	Guildford, UK
Sterilin	Barloworld Scientific	Staffordshire, UK
SYBR Green two step PCR Kit	Qiagen	West Sussex, UK
Taq Ploymerase –Go Taq Flexi	Promega	Madison, WI, USA
TEMED	Sigma	Dublin, Ireland
2X TGS Running Buffer	Invitrogen	Paisley, UK
10X TGS Running Buffer	Bio-Rad	Herts, UK
Tissue Culture Plate Inserts	Greiner Bio-One	Gloucestershire, UK
Transblot Filter Paper	Bio-Rad	Herts, UK
Trypan blue	Sigma	Poole, UK
Tris	BDH	Lennox, Dublin
TriZol	Invitrogen	Paisley, UK
Trypsin (Clara isolation)	Sigma	Dublin, Ireland

Trypsin-EDTA	Gibco	Paisley, UK
Tween	Sigma	Dublin, Ireland

2.1.2. Instrumentation

Instrument	Company	Address
Densitometer	BioRad	Herts, UK
DNA Engine Opticon	MJ Research	Waltham, MA, USA
FACScan Flow Cytometer	BD Bioscience	Oxford, UK
Olympus IX81 Fluorescence microscope	Mason Technologies	Dublin, Ireland
Olympus CK40 light microscope	Olympus	Germany
Olympus CAMEDIA Digital Camera C-310 Zoom	Olympus	Germany
QuantityOne Software	BioRad	Herts, UK
Spectrophotmeter – Biometra Gene Ray	Mason Technologies	Dublin, Ireland
Tecan Plate Reader	Unitech	Dublin, Ireland
Thermal Cycler – PTC-100	MJ Research	Waltham, MA, USA
Thermal Gradient Cycler – G-Storm	Mason Technologies	Dublin, Ireland
Trans-Blot SD Semi Dry Transfer Cell	BioRad	Herts, UK
UV Microscope	Nikon	Surrey, UK
Western Blotting Electrophoresis Rig	BioRad	Herts, UK

2.1.3. **Primers**

Gene	Species	Sequence	Product (bp)	Annealing Temp (°C)	$MgCl^2$ (mM)
BMPR-IA	Hu	F: 5'- ATGACCAGGGAGAAACCACA -3' R: 5'- ATTCTATTGTCCGGCGTAGC -3'	105	55	1.5
BMPR-IB	Hu	F: 5'- ACTCAAGGCAAACCAGCAAT -3' R: 5'- TCTGTTCAAGCTCTCGTCCA -3'	204	58	1.5
BMPR-II	Hu	F: 5'- GCCCGCTTTATAGTTGGAGA -3' R: 5'- AGCAAGACGGCAAGCGATTA -3'	144	55& 58	1.5
Smad1	Hu	F: 5'- GCTTACCTGCCTCCTGAAGA -3' R: 5'- GCATATACCTCCCCTCCAAC -3'	359	55 & 58	1.5
Smad5	Hu	F: 5'- CCAACCCAACAACACTCCTT -3' R: 5'- GGCTCTTCATAGGCAACAGG -3'	270	55&58	1.5
Smad7	Hu	F: 5'- TCCAGATACCCGATGGATTT -3' R: 5'- GGGCCAGATAATTCGTTCC -3'	94	55	1.5
Smad4	Hu	F: 5'- AGGACAGCAGCAGAATGGAT -3' R: 5'- TGGTGGTGAGGCAAATTAGG -3'	114	55&58	1.5
BMP4	Hu	F: 5'- TACATGCGGGATCTTTACCG -3' R: 5'- ATGTTCTTCGTGGTGGAAGC -3'	132	55	1.5
BMP6	Hu	F: 5'- TCTTACAGGAGCATCAGCACA -3' R:5'-GGTCTTGGAAACTCACATACAGC-3'	435	53	1.5
Id1	Hu/Mse	F: 5'- GCAAAGTGAGCAAGGTGGAG -3' R: 5'- ATCGTCGGCTGGAACACAT -3'	191	55&58	1.5/2.5
TGF-β1	Hu	F: 5'- CAACAATTCCTGGCGATACC -3' R: 5'- CTAAGGCGAAAGCCCTCAAT -3'	135	55	2.5
TGF-β2	Hu	F: 5'- TGGCACCTCCACATATACCA -3' R: 5'- CTAAAGCAATAGGCCGCATC -3'	171	55	2.5
COL1A1 Set 1	Hu/Mk	F: 5'- GTGCTACTGGTTTCCCTGGT -3' R: 5'- ACCTTTGCCACCTTCTTTG -3'	110	55	1.5
COL1A1 Set 2	Hu	F: 5'- CTGGTGCTAAAGGTGCCAAT -3' R: 5'- CTCCTCGCTTTCCTTCCTCT -3'	231	55&58	1.5/2.5
COL1A2 Set 1	Hu/Mk	F: 5'- CCGAACTGGAGAAGTAGGTG -3' R: 5'- AGGGAGACCCAGAATACCAG -3'	142	55	1.5
COL1A2 Set 2	Hu	F: 5'- GAAAACATCCCAGCCAAGAA -3' R: 5'- GCCAGTCTCCTCATCCATGT -3'	228	55&58	1.5/2.5
Vimentin Set 1	Hu/Mk	F: 5'- AACCTGACCGAGGACATCATG -3' R: 5'- TTCTCGGCTTCCTCTCTCTGAA -3'	74	55	1.5

Vimentin Set 2	Hu	F: 5’- CGAAAACACCCTGCAATCTT -3' R: 5’- GTGAGGTCAGGCTTGGAAAC -3'	201	55&58	1.5/2.5
α-SMA	Hu/Mse	F: 5’- ACTACTGCCGAGCGTGAGAT -3' R: 5’- ATAGGTGGTTTCGTGGATGC -3'	234	55&58	1.5/2.5
N-cadherin	Hu/Mk	F: 5’- TGTTTTGGACCGAGAATCAC -3' R: 5’- TAACACTTGAGGGGCATTGT -3'	148	5	1.5
Desmin	Hu/Mk	F: 5’- AACCTTCTCTGCCCTCAACT -3' R: 5’- GATCATCACCGTCTTCTTGG -3'	82	55	1.5
Fibronectin	Hu/Mk	F: 5’- GGAAAAGGAGAATGGACCTG -3' R: 5’- CTTCTCCCAGGCAAGTACAA -3'	139	55	1.3
K18	Hu/Mk	F: 5’- GGAGCACTTGGAGAAGAAGG -3' R: 5’- GGGCATTGTCCACAGTATTT -3'	107	55	1.3
SNAI1	Hu/Mk	F: 5’- CCAGAGTTTACCTTCCAGCA -3' R: 5’- CAGAGTCCCAGATGAGCATT -3'	112	58	2.5
SNAI2	Hu	F: 5’- CCTGGTCAAGAAGCATTTCA -3' R: 5’- CCTTGGAGGAGGTGTCAGAT -3'	278	55&58	1.5/2.5
SNAI3	Hu	F: 5’- ACACAGGGGAGAAGCCCTAT -3' R: 5’- ACATGCGGGAGAAGGTCT -3'	141	58	1.5
Twist	Hu/Mk	F: 5’- CTTCTCGGTCTGGAGGATG -3' R: 5’- TCCATTTTCTCCTTCTCTGG -3'	126	55	1.5
ZEB1	Hu/Mk	F: 5’- CACCCTTGAAAGTGATCCAG -3' R: 5’- TCTTCCGCATTTTCTTTTTG -3'	129	55	1.5
GAPDH	Hu/Mse	F: 5’- CTGCACCACCAACTGCTTAG -3' R: 5’- CCAGGAAATGAGCTTGACAAA -3'	487	55&58	1.5/2.5
E-cadherin	Hu/Mse	F: 5'- GGCTGGACCGAGAGAGTT -3' R: 5'- CTGCTTGGCCTCAAAATCC -3'	350	58	1.5
Snai1	Mse	F: 5'- CACACTGGTGAGAAGCCATT -3' R: 5'- GACTCTTGGTGCTTGTGGAG -3'	167	55&58	1.5/2.5

2.1.4. **Antibodies**

Antibody/Clone	Isotype	IF	WB	Company
E-cadherin/36	IgG2a	1/200	1/2000	BDB
N-cadherin/32	IgG1	1/200	1/2000	BDB
α-catenin/5	IgG1	1/50	1/250	BDB
β-catenin/14	IgG1	1/200	1/500	BDB
γ-catenin/15	IgG2a	1/200	1/1000	BDB
K18/CY-90	Mse IgG1	1/800	1/30,000	Sigma
Actin/20-33	Rb IgG	1/100	1/2000	Sigma
BMPR-IA/H-60	Rb poly IgG	1/20	1/200	S/C
BMPR-IB/N-17	Gt poly IgG	1/200	ND	S/C
BMPR-II	Gt IgG	1/20	1/100	R&D
Smad5/D-20	Gt poly IgG	1/50	1/100	S/C
Smad8/A-17	Gt poly IgG	1/50	ND	S/C
p-Smad1/5/8	Rb poly IgG	1/50	1/1000	C/S
Smad4/B-8	Mse IgG1	1/100	1/100	S/C

2.2. Tissue Culture

2.2.1. Cell Lines

The human bronchial SV-40 transformed cell line, BEAS-2B, was obtained from the American Type Culture Collection (ATCC). The human adenocarcinoma cell line, A549, was obtained from the European collection of cell cultures (ECACC). Cells were routinely cultured in culture medium consisting of a 1:1 mixture of DMEM: Hams-F12 medium supplemented with 5 % fetal bovine serum and 2 mM L-glutamine. Cells were maintained at 37 ºC in a humidified atmosphere of 5 % CO_2. Experiments were carried out within five passages.

2.2.2. Sub-culture

Cell lines were sub-cultured upon reaching 80 %-100 % confluency. Culture medium was removed from the flask and cells were rinsed with 5 ml PBS. 0.5 % trypsin-EDTA solution was added to the flask and incubated at 37 ºC until the cells had detached (not exceeding 20 min). At this point, an equal volume of serum-containing medium was added to the flask and the entire contents were transferred to a 30 ml sterilin and centrifuged at 259 x g for 5 min in a bench-top centrifuge. The supernatant was discarded and the pellet was resuspended in fresh culture medium. Cells were used to either re-seed the tissue culture flask or for experimental set up.

2.2.3. Cell Freezing

Cells were periodically frozen and stored in liquid nitrogen to maintain cell stocks. Cells at 50-70 % confluency were suitable for freezing (i.e. they were in the log phase of growth and actively dividing). Freezing medium consisting of a 9:1 ratio of FBS: DMSO was first prepared and protected from light. Cells were trypsinised as described above and the resulting pellet was resuspended in 500 µl FBS. Dropwise 500 µl freezing medium was added to the cell suspension using a Pasteur pipette and the entire volume (1 ml) was then transferred to a cryovial and stored on ice. Cryovials

were initially placed at -70 ºC for no longer then two weeks before being transferred to liquid nitrogen for long term storage.

2.2.4. Cell Thawing

DMSO can enter living cells and quickly freezes thus preventing crystal formation within the cell at reducing temperatures. However, at room temperature this chemical is toxic to cells. Culture medium (1:1 DMEM/F12, 5 % FBS, 2 mM L-Glutamine) was prepared initially and 10 ml was added to a sterilin prior to thawing of cells. The cryovial was removed from liquid nitrogen and kept on ice. Cells were thawed by placing cryovial in a 37 ºC water bath. On thawing cells were quickly transferred to the sterilin containing 10 ml culture medium (1:1 DMEM/F12, 5 % FBS, 2 mM L-Glutamine) and spun at 259 x g for 5 min. Pellet was resuspended in culture media and entire volume was transferred to a tissue culture flask and placed in a 37 °C incubator humidified with 5 % CO_2. Culture medium was changed 8 – 17 hrs later to remove any secreted DMSO.

2.2.5. Cell Counting

Cells were trypsinised, spun at 259 x g and re-suspended in an appropriate volume of culture medium. A haemocytometer was used onto which a glass coverslip was affixed by applying gentle pressure. Newton's rings were observed to ensure the correct depth between haemocytometer and coverslip. Approximately 10 µl of the cell suspension was allowed flow between the haemocytometer and the coverslip by capillary action to fill the upper chamber. Cells contained within each of the four 16 corner squares were counted and an average obtained. This count was representative of the total number of cells x 10^4 per ml of the original cell suspension. In order to assess cell viability, cells were stained with Ethidium Bromide Acridine Orange (EBAO) (0.025 mM Ethidium Bromide, 0.027 Acridine Orange) at a 1:1 ratio of cell suspension to EBAO solution. The EBAO stained cell suspension was counted by similar means as described above using a UV microscope. Viable cells were labeled with the cell

permeable Acridine orange and fluoresced green under UV light. Non viable cells were labeled with Ethidium bromide and so emitted an orange fluorescence.

2.2.6. Fibronectin Coating

Fibronectin (FN) coating was performed aseptically in a laminar flow hood. Fibronectin was reconstituted in dH_20 to a stock concentration of 1 mg/ml, aliquoted and stored at -20 °C. The FN stock solution was subsequently diluted to a working concentration of 50 µg/ml with HAMS/F12 basal medium. FN working solution was added to the wells to be coated. The FN coated plates were wrapped with parafilm and incubated at 4 °C overnight. The FN solution was removed and the plates were either used immediately or stored at -20 °C for future use.

2.2.7. Isolation of Primary Murine Epithelial Cells / Clara Cells

Primary murine airway epithelial cells (MAECs) were isolated from female C3/HEN mice. This MAEC population had previously been charcterised and found to be > 80% enriched for Clara cells (Mc Bride et al., 2000). However, these cells will be referred to as MAECs from here on in. Briefly, mice were sacrificed by intraperitoneal injection of pentabarbitone. Lungs were perfused with saline to remove blood cells. The lungs were then excised from the body cavity. The lungs were filled intratracheally with pre-warmed trypsin solution (30 mg trypsin in 10ml Ca/Mg+ solution; 0.9 % NaCl, 0.15 M KCL, 0.11 M $CaCl_2$, 0.15 M $MgSO_4$, 0.10 M phosphate buffer pH 7.4, 0.20 M Hepes) and incubated for 15 min at 37 ºC. The lungs were then chopped roughly for 2-3 min with a curved scissors and the trypsin was deactivated with the addition of FBS. The lung tissue was transferred to a 50 ml tube and a DNase I solution (6.25 mg DNase in 25 ml Ca/Mg- solution; 0.9 % NaCl, 0.15 M KCL, 0.10 M phosphate buffer pH 7.4, 0.20 M Hepes) was added and shook by hand (quite vigorously) for 4 min after which it was filter through a 100 µm nylon filter and subsequently a 40 µm nylon filter. The crude cell suspension was then centrifuged twice at 30 x g for 6 min in a bench top centrifuge, resuspending the pellet with additional a DNase II solution (2.5 mg DNase in 50 ml Ca/Mg- solution; 0.9 % NaCl,

0.15 M KCL, 0.10 M phosphate buffer pH 7.4, 0.20 M Hepes) following the first spin. The resulting pellet was then resuspended in Differential Attachment Medium (1:1 M199: Hams/F12, 2mM L-glutamine, 100 U/ml Penicillin/Streptomycin) and incubated on a non-tissue culture grade petri dish for 1 hr at 37 ºC. Blood cells will adhere to the petri dish during this incubation period. The cell suspension was then collected from the petri dish and subsequently centrifuged at 120 x g for 5 min. The resulting pellet contained the isolated airway epithelial cells which are enriched for Clara cells (Mc Bride et al., 2004). MAECs are isolated in clumps so obtaining a cell count using a haemocytometer is not feasible. To overcome this, an aliquot of cells was taken prior to seeding and using the reagent from the Cell Titer 96® AQueous One Solution Cell proliferation Assay an absorbance value was obtained. This absorbance value (OD) corresponded to the number of living cells in the cell suspension. Cells were seeded at the same OD in each experiment onto fibronectin coated glass chamber slides, 96-well, 24-well or 6-well plates in plating medium (DMEM, 5% FBS, 2 mM L-glutamine, 100 U/ml Penicillin/Streptomycin) and allowed to adhere O/N.

2.3. BMP Stimulation

2.3.1. Reconstitution of recombinant BMP2 and BMP4

Human BMP2 and BMP4 recombinant protein was purchased from R&D systems. One ml Hams/F12 basal medium was added to 10 µg recombinant protein to yield a 10 µg/ml stock concentration. This stock was aliquoted and stored at -20 ºC.

2.3.2. Reconstitution of Retinoic Acid (RA)

Retinoic acid (RA) in a glass vial was transferred to a bijous prior to reconstitution. 3 ml 333 µl DMSO was added to 100 mg RA yielding a 30 mg/ml solution equivalent to 0.1 M RA. This solution was aliquoted into 100 µl and 5 µl aliquots and stored at -80 ºC.

Prior to use an aliquot was removed from the -80 ºC freezer and kept on ice. For 10^{-6} M RA, a 1/100,000 dilution was required. A 1/10 dilution in DMSO (1µl 0.1M RA into 9µl DMSO) was made initially upon thawing. 1 µl of this RA solution was added to 10 ml medium. The remaining RA was discarded.

2.3.3. BMP stimulation of BEAS-2B and A549 Cell Lines

2.3.3.1. Experimental outline for day 6 analysis of BMP effect on BEAS-2B and A549 cells

Cells were trypsinised and counted as described above in Section 2.2.2 and 2.2.5, respectively. For day 6 analysis cells were seeded at a low density of 2 x 10^3/cm^2. After overnight attachment in culture medium (1:1 DMEM:F12, 5 % FBS, 2 mM L-Glutamine), cells were rinsed once with Hams-F12 basal medium and defined serum-free medium (DSFM) (1:1 Hams-F12:M199, 2mM L-glutamine, 100 U/ml penicillin, 100 µg/ml streptomycin, 100 U/ml insulin-transferin-selenium, 100 ng/ml hydrocortisone and 10 ng/ml epidermal growth factor containing 100 ng/ml BMP2 or 100ng/ml BMP4 was added. A549 cells were cultured in the same medium as described above except for BMP experiments A549 cells were cultured in either DSF medium containing hydrocortisone (+HC) or DSF medium with hydrocortisone omitted (-HC).

2.3.3.2. Experimental outline for 20 min, 2 hr and 17 hr analysis of BMP pathway activation in BEAS-2B and A549 cells

Cells were seeded at a higher density for the short timecourse pathway activation experiments. Cells were trypsinised and counted as described in Section 2.2.2 and 2.2.5, respectively. Cells were seeded at 2 x 10^4/well in a chamber slide or 1.6 x 10^4/cm^2 in either a 24-well or 6-well plate in culture medium (1:1 DMEM/F12, 5 % FBS, 2 mM L-Glutamine). The following day the medium was changed to DSF medium (1:1 Hams-F12:M199, 2 mM L-glutamine, 100 U/ml penicillin, 100 µg/ml streptomycin, 100 U/ml insulin-transferin-selenium, 100 ng/ml hydrocortisone and 10 ng/ml epidermal growth factor). Cells were cultured in DSFM for an overnight period

before the addition of BMP. It was thought this would allow any pathway activity, which may have occurred from BMPs present in the serum-containing culture medium, to subside. The next day, the DSFM was removed and replaced with fresh DSFM alone or containing 100 ng/ml BMP2 or BMP4.

2.3.4. BMP stimulation of Primary Murine Airway Epithelial Cells

2.3.4.1. Experimental outline for day 3-6 analysis of BMP effect on MAECs

MAECs were isolated as described above in Section 2.2.7. MAECs were seeded in plating medium (DMEM, 5% FBS, 2 mM L-glutamine, 100 U/ml Penicillin/Streptomycin) at either 0.1 OD/chamber slide well or 0.25 OD/cm^2 in a 24-well or 6-well plate. For analysis of EMT morphology and E-cadherin expression in response to BMP4, MAECs were cultured in either defined serum-free medium (DSFM) (1:1 Hams-F12:M199, 2mM L-glutamine, 100 U/ml penicillin, 100 µg/ml streptomycin, 100 U/ml insulin-transferin-selenium, 100 ng/ml hydrocortisone and 10 ng/ml epidermal growth factor) or conditioned medium (CM) from BEAS-2B cells cultured in DSFM for 6 days. Conditioned medium (CM) was re-supplemented with 2mM L-glutamine, 100 U/ml penicillin, 100 µg/ml streptomycin, 100 U/ml insulin-transferin-selenium, 100 ng/ml hydrocortisone and 10 ng/ml epidermal growth factor. Retinoic acid (RA) was added to both DSFM and CM for MAEC culture at a concentration of 10^{-6} M, 10^{-5} M or 33^{-9} M to assess the effect of RA on MAECs (data not shown). However, for analysis of E-cadherin expression in BMP4-treated MAECs, RA was omitted from the DSFM and CM.

2.3.4.2. Experimental outline for 20 min, 2 hr and 17 hr analysis of BMP pathway activation in MAECs

MAECs were isolated as described above in Section 2.2.7. MAECs were seeded in plating medium (DMEM, 5% FBS, 2 mM L-glutamine, 100 U/ml Penicillin/Streptomycin) at 0.1 OD/chamber slide well for immunofluorescence analysis of BMP pathway activation. The following day cells were rinsed once with Hams/F12 basal medium and defined serum-free medium (DSFM) (1:1 Hams-

F12:M199, 2mM L-glutamine, 100 U/ml penicillin, 100 µg/ml streptomycin, 100 U/ml insulin-transferin-selenium, 100 ng/ml hydrocortisone and 10 ng/ml epidermal growth factor) was added. MAECs were cultured in DSFM for an additional O/N period. The next day, the DSFM was changed and fresh DSFM was added alone (DSFM) or containing 100 ng/ml BMP2 (+BMP2) or 100 ng/ml BMP4 (+BMP4). MAECs were cultured for 20 min, 2 hr and 17 hr after which time they were methanol fixed as described in Section 2.10.1.

2.4. Eosinophil Co-culture and Protein Treatment

2.4.1. Isolation of Eosinophils and Granule Proteins

Eosinophils were isolated by Samir Sedky Gendy in the Department of Medicine, Royal College of Surgeons in Ireland, Beaumont Hospital, Ireland. Eosinophils were prepared from 45 ml of peripheral blood drawn from healthy human volunteers. After phlebotomy, 15 ml of blood was added to 25 ml PBS to which 100 units of heparin had been added and 30 ml of this blood/PBS mixture was then layered over 23 ml Ficoll (1.077+/-0.001 g/ml) and centrifuged at 720 x g for 20 min at room temperature. The upper layer of serum and mononuclear cells was discarded and the pellet containing granulocytes and erythrocytes were subjected to hypotonic lysis. The granulocytes were then resuspended in MACS buffer (PBS with 2 mM EDTA and 0.5% bovine serum albumin) with anti-CD16 immunomagnetic beads and passed through a magnetic separation column. The eluted eosinophils were collected, resuspended in differentiation medium and their viability and purity were determined by Trypan Blue and Speedy-Diff staining. Only populations of eosinophils > 98% pure and > 95% viable were used in co-culture experiments. Purified eosinophil proteins were a gift from Dr. G. Gleich, prepared as previously described (Gleich et al., 1973).

2.4.2. Eosinophil Co-culture

MAECs were isolated as described in Section 2.2.7 and seeded at 0.1 OD on to fibronectin coated (50 µg/ml) 24-well transwell inserts (300 µl/insert) in plating medium (DMEM, 5% FBS, 2 mM L-glutamine, 100 U/ml Penicillin/Streptomycin). The following day MAECs were rinsed once with PBS and the medium was changed to DSF medium. In the 24 well plate, medium only (DMEM containing 2mM L-glutamine, 100 U/ml penicillin, 100 µg/ml streptomycin) (Untreated) or medium (DMEM containing 2mM L-glutamine, 100 U/ml penicillin, 100 µg/ml streptomycin) containing eosinophils (+Eos) to a final concentration of 3×10^5 was added. MAECs were cultured with eosinophils for 20 min, 2 hr and 17 hr after which time the insert was removed, rinsed three times with PBS and methanol fixed as described in Section 2.10.1.

2.4.3. Eosinophil Protein Treatment

MAECs were isolated and seeded on to fibronectin coated 8-well chamber slides at 0.1 OD/chamber slide well. The next day the medium was changed to DSF medium 5-6 hr prior to eosinophil protein stimulation. The medium was changed again and either fresh DSF medium was added or DSF medium containing either 0.5 µg/ml or 5 µg/ml EDN, EPO or MBP (Stock concentrations; EDN (eosinophil-derived neurotoxin) 1 mg/ml, EPO (eosinophil peroxidase) 2.4 mg/ml, MBP (major basic protein) 1.1 mg/ml). MAECs were cultured for 2 hr, 17 hr or 48 hr at which time they were rinsed three times with PBS and methanol fixed as described in Section 2.10.1.

2.5. Proliferation

2.5.1. Cell Counts

Following BMP treatment cell number and viability was determined by EBAO staining. Supernatant was removed and placed in a 1.5 ml eppendorf followed by

trypsinised cells and spun at 10,000 x g. The pellet was resuspended in an appropriate volume. Immediately prior to cell counting either an equal volume of EBAO was added directly to the cell suspension or 10 µl was removed to a separate tube and combined with 10 µl EBAO. Cells were counted on a haemocytometer as described in section 2.2.5 on a UV microscope.

2.5.2. MTS Assay

Cell metabolic activity was determined using the CellTiter Aqueous One Solution Cell proliferation Assay. This kit was used for quantification of MAECs. Briefly, 100 µl aliquot of MAEC cell suspension was removed and combined with 20 µl MTS reagent in a 96-well plate. As a medium only control, 100 µl plating medium plus 20 µl MTS reagent was included. MTS is converted to formazan by dehydrogenase enzymatic activity which absorbs light at 490 nm. This absorbance value reflects the number of metabolically active cells. Cells were incubated for 1 hr at 37 ºC and absorbance at 450 nm was determined on a Biometra Gene Ray Spectrophotometer.

2.6. Acquisition of Bright Field Images

Phase contrast images were captured on an Olympus CK40 light microscope using an Olympus CAMEDIA Digital Camera C-310 Zoom.

2.7. RNA Isolation

2.7.1. RNA Harvest

Medium was removed from cells and 1 ml TriZol was added directly into the well and incubated for 5 min at room temperature. The TriZol solution was then transferred to a 1.5 ml eppendorf. To maximize the quantity of isolated RNA, 5 µl poly-acyrl carrier was added to 1 ml TriZol. The RNA isolation was carried out directly from this point or alternatively, samples were stored at – 20 ºC for up to one month.

2.7.2. RNA Isolation

Samples stored at – 20 ºC were allowed to thaw. Phase separation was performed by adding 200 µl chloroform to each sample and shaking the solution vigorously for 15 sec. The samples were incubated at room temperature for 3 min and subsequently centrifuged at 4 ºC at 13,800 x g for 15 min. The mixture separates into a lower, red phenol phase, a white interphase (DNA) and an upper aqueous phase containing the RNA. This aqueous phase was transferred to a fresh 1.5 ml eppendorf taking care not to disturb the DNA interphase layer. RNA was precipitated with the addition of 500 µl isopropanol. The solution was mixed by inversion. This was allowed sit for 12 min at room temperature and subsequently centrifuged at 4 ºC at 13,800 x g for 8 min. RNA was visible as a gelatinous pellet from this point. The supernatant was removed entirely and the RNA pellet was washed twice in 1 ml 75 % ethanol by vortexing and subsequently centrifuged at 4 ºC at 9,000 x g for 5 min. After the second centrifugation step, the supernatant was removed entirely and the pellet was allowed to air dry for 2-3 min. The RNA pellet was then resuspended in DEPC by gentle pipetting. The RNA was kept on ice for use in cDNA synthesis or stored at -80 ºC.

2.7.3. RNA Quantification

RNA samples were diluted 1:50 in RNA: DEPC water (2µl RNA into 98µl DEPC). Absorbance at 230 nm, 260 nm and 280 nm was determined using a spectrophotometer. Absorbance at 260 nm was used to calculate RNA concentration using the following equation: OD 260 nm x 40 x dilution (50) factor/1000 where the resulting value represents microgram RNA per microlitre DEPC (µg/µl).

2.8. RT-PCR

2.8.1. cDNA Synthesis

Initially RNA samples were DNase treated to remove any possible contaminating DNA which may have occurred during the RNA isolation procedure. As a control, to

ensure all DNA had been degraded, up to three random RNA samples was prepared in duplicate during the DNase step with one sample in each set not receiving any cDNA synthesis reagents. These controls were referred to as a **N**o **R**everse **T**ranscriptase controls or NRT controls. These samples received an equal volume of DEPC water in place of reagents. For DNase treatment, RNA (500 ng – 1 µg) was added to a 0.5 ml eppendorf containing 1 µl 10x DNase buffer and 1 µl DNase enzyme and DEPC water. The final volume in the tube was 10 µl. This was incubated at room temperature for 22 min. The DNase enzyme was deactivated with the addition of 1 µl EDTA and subsequent incubation at 65 ºC for 10 min.

For cDNA synthesis, 1 µl Oligo $dT_{(12\text{-}18)}$ primers and 1 µl 10 mM dNTPs was added to each sample (except NRT samples) and incubated at 70 ºC for 5 min. The samples were placed on ice for at least 1 min and the following reagents were added to each tube (except NRT): 4 µl 5X First Strand Buffer, 2 µl DTT, 1 µl RNaseOut and 1 µl Superscript III (200 units). Reverse transcription was performed for 1 hr at 50 ºC followed by 10 min at 75 ºC which stops the reaction. cDNA was stored at 4 ºC for immediate use or at -20 ºC for up to one month. PCR products were visualised on ethidium bromide stained gels and semi-quantified using the QuantityOne software (BioRad). Values obtained were normalised using housekeeping gene, GAPDH.

2.8.2. **Primer Design**

Gene sequences were obtained from the NCBI *Entrez Nucleotide* database (http://www.ncbi.nlm.nih.gov/sites/entrez). Primers were designed for RT-PCR using the Primer3' software from the Whitehead Institute for Biomedical Research (http://frodo.wi.mit.edu/cgi-bin/primer3/primer3_www.cgi).

2.8.3. **Polymerase Chain Reaction**

Reagents used in PCR reaction are described below:

		(Final Conc.)
5µl	5 X Go Taq Flexi PCR Buffer	
1.5-2.5µl	25mM $MgCl_2$	1.5 mM - 2.5 mM
4µl	1.25 mM dNTP mix	200 µM each dNTP
0.5µl	Forward Primer	300 nM
0.5µl	Reverse Primer	300 nM
0.125µl	Go Taq Flexi Polymerase (5U/µl)	
0.5µl	cDNA	
to 25µl	DEPC-treated water	

PCR mastermix was prepared on ice. Samples were immediately transferred to a thermal cycler. Initially samples were heated to 95 ºC for 5 min to denature DNA. The generic PCR cycle consisted of 95 ºC for 45 sec, followed by 45 sec at a specific annealing temperature and extension at 72 ºC for 1 min. The correct annealing temperature and $MgCl_2$ concentration was determined for each primer set (see Primer list in Section 2.1.3). Samples underwent a final extension step for 10 min at 72 ºC before cooling to 4 ºC. PCR programmes routinely involved 30 cycles. The number of cycles was reduced to 25 in the event of a strong product signal.

2.8.4. **Electrophoresis**

A 1.5 % w/v agarose gel was made up by dissolving 1.5 g agarose in 100 ml TAE buffer (40 mM Tris, 0.35 % v/v Acetic Acid, 0.5 mM EDTA). Ethidium bromide was added at a 0.003 % v/v of a 10 mg/ml ethidium bromide solution to visualise the DNA. The gel was cast and allowed to solidify for 30 min. 10 µl -20 µl PCR product was electrophoresed for 20 min at 200 volts. A 1 Kb Ladder or 100 bp (depending on product size) was run adjacent to samples to verify correct product size. Gels were

visualised under UV light. An image of the gel was captured and saved for subsequent densitometric analysis.

2.9. Real Time Quantitative PCR

2.9.1. RNA Gel

In order to confirm RNA integrity an RNA gel was run. This allows visualization of 18 S and 28 S ribosomal RNA components which should appear as intact and distinct bands. Degraded RNA samples would appear as a smear on the RNA gel. The RNA gel was made up by dissolving 1.5 g agarose in 108 ml DEPC-treated water. The gel was heated to 60 ºC in a water bath before the addition of 15 ml MOPS buffer and 27 ml 37 % v/v formaldehyde. Gel was cast and allowed to set for 30 min. Gel was prepared and run in a chemical fume hood. The RNA samples were thawed on ice and a minimum of 0.5 µg (minimum necessary to visualise) was transferred to a 0.5 ml eppendorf. An equal volume of RNA loading buffer was added. The RNA samples were denatured with 10 min incubation at 60 ºC and place on ice before loading. A RNA ladder was run adjacent to samples. This was prepared by adding 3 µl ladder to 2 µl RNA loading buffer, 3 µl DEPC and 1 µl potassium acetate. Samples were loaded and the gel was electrophoresed for 90 min at 100 volts. The gel was visualised under UV light.

2.9.2. Real Time Quantitative PCR

Real time analysis of E-cadherin expression in murine airway epithelial cells (MAECs) was carried out. A standard curve approach was used. The standard curve for both E-cadherin and GAPDH was made from pooled MAECs samples. Dilutions of MAEC cDNA were made up: 1/10, 1/100, 1/1,000 and 1/10,000. Standards were run in duplicate while samples were run in triplicate. The relative quantity of amplified product was calculated based on the cycle threshold (CT). The average and standard deviation of triplicates were obtained. The CT values obtained for GAPDH

were subtracted from their respective E-cadherin values. Normalised E-cadherin CT values were represented as $2^{-\Delta\Delta CT}$. Values obtained from BMP-treated cells were then represented as fold compared to untreated cells.

Samples were set up in 8-well PCR strips. Primers were added to a concentration of 400 nM. To each well, 10µl SYBR Green was added and 1µl cDNA. Samples were made up to 20µl with DEPC-treated water and immediately transferred to a DNA Engine Opticon. An initial denaturation step of 10 min at 95 ºC was carried out, followed by 40 cycles of 95 ºC for 45 sec, annealing at 58 ºC for 45 sec and extension for 1 min at 72 ºC.

2.10. Immunofluorescence

2.10.1. Methanol Fixation

At given time points, cells were methanol fixed for analysis of protein expression and localisation by immunofluorescence. Medium was removed and cells were rinsed with PBS three times. Ice cold methanol was added to wells and cells were placed at -20 ºC for 5 min. Methanol was removed and cells were allowed air dry for approximately 15-20 min. Following air dry, cells were stored at -20 ºC or used immediately. Methanol waste was kept and disposed of separately.

2.10.2. Indirect Immunofluorescence on Cells

Cells were removed from -20 ºC and allowed to reach room temperature for 5min. Following this, cells were equilibrated for an additional 5 min at room temperature in 1X Tris-Buffered Saline (TBS: 0.01M-Tris, 0.15M-Nacl, pH 7.5). To block non-specific binding sites (such as FC receptors) cells were incubated with 20 % normal serum diluted in TBS for 30 min at room temperature. Primary antibodies were diluted in TBS and incubated either for 2 hr at 37 ºC or overnight at 4 ºC. Cells on chamber slides or in 24-well plates were placed on moistened tissue in order to ensure they remained humidified during the primary incubation. Following incubation with the

primary antibody, cells were washed with TBS containing 0.1% v/v Tween-20 three times in 10 min. Alexa 488 fluorescent secondary antibodies were diluted in 20 % normal serum (same as that used for blocking step) and incubated for 30 min at room temperature. Cells were washed again following incubation with secondary antibody. Cells were counterstained using DAPI nuclear stain for 5 min at room temperature. Cells were mounted in faramount aqueous mounting medium and coverslip. Fluorescently tagged antigens were examined using an Olympus IX81 fluorescent microscope where camera and microscope settings (exposure time, brightness and light intensity) were kept constant across treatments for each antibody examined. Cells omitting primary antibody were included as a control for secondary antibody binding (Ab Cntrl) or cells incubated with an irrelevant IgG as a control for non-specific primary antibody binding (Isotype Cntrl). Controls were included with every immunofluorescence experiment.

2.10.3. **Indirect Immunofluorescence on Tissue**

Paraffin-embedded human nasal epithelial and lung tissue sections were de-waxed in xylene for 5 min in a chemical fume hood. The sections were then rehydrated in an ethanol series through to H_2O involving 2 min in 90 % ethanol, 2 min in 75 % ethanol, 2 min in 75 % ethanol and 2 min in H_2O. Antigen retrieval was performed by boiling the sections in a citric acid solution for 15 min (3 X 5 min, releasing steam following each 5 min). Sections were cooled by bringing the citric acid solution up to room temperature with the addition of cold water and subsequently samples were allowed to further cool on the bench for 2-3 min. Tissue sections were encircled using a wax marker as close to the tissue sections as possible to minimize volume of antibody required. Immunofluorescence protocol from this point was the same as described above. Briefly, tissue sections were blocked with 20 % normal serum and primary antibodies were incubated overnight at 4 ºC in TBS. Incubation with appropriate Alexa488 secondary antibodies was carried out for 30 min at room temperature in 20 % serum. Nuclei were counterstained using DAPI. All antibodies used are outlined in Section 2.1.4.

2.10.4. **Sequential Double Immunofluorescence on Cells**

For double immunofluorescence it was important to consider the species in which the two primary antibodies were raised to ensure compatibility. In addition, instead of 20 % normal serum, 1 % BSA diluted in TBS was used as a blocking solution and also as the diluent for both primary and secondary antibodies. Cells (methanol fixed, stored at -20 ºC) were allowed to come up to room temperature for 5 min and subsequently equilibrated in TBS for 5 min. Cells were blocked in 1 % BSA for 30 min at room temperature. Following this, cells were incubated in optimally diluted primary antibody (primary antibody # 1) in 1 % BSA for an overnight period at 4 ºC. Cells were washed three times by pipetting with TBS containing 0.1 % v/v Tween-20. Subsequently, cells were incubated with an Alexa488 secondary antibody diluted in 1 % BSA for 30 min at room temperature. It is recommended to use the Alexa488 (Green) secondary antibodies as the first secondary antibody on account of their increased stability when compared to the Alexa568 (Red) secondary antibodies. Following the secondary antibody # 1 incubation, cells were washed three times in ten minutes in TBS containing 0.1% v/v Tween-20. Cells were subsequently re-blocked in 1% BSA for 30 min at room temperature. Cells were then incubated in the second primary antibody solution (primary antibody # 2) for either 2 hr at 37 ºC or overnight at 4 ºC. Cells were subsequently washed as described previous and incubated with an Alexa568 secondary antibody (secondary antibody # 2) for 1 hr at room temperature. Cells were washed for a last time and incubated with DAPI nuclear counterstain for 5 min at room temperature. Cells were mounted under a coverslip in the faramount aqueous mounting solution and viewed using the Olympus IX81 fluorescent microscope.

2.11. Western Blot Analysis

2.11.1. Protein Harvest

For protein harvest, cells were scraped in chilled phosphate buffered saline (PBS) and centrifuged twice at 12,000 x g (1.5 ml eppendorf in a microfuge) or 800 x g (30 ml sterilin in a benchtop centrifuge). The resulting pellet was resuspended in chilled PBS and spun again. The supernatant was removed entirely and the pellet was resuspended in RIPA buffer (150 mM-NaCl, 1.0%-IgepalCA-630, 0.5%-sodium deoxycholate, 0.1% v/v-SDS, 50mM Tris, pH 8.0) supplemented with 1X Complete Mini Protease Inhibitor Cocktail. Samples were passed through a Qiashredder to break up bound DNA and protein. This was done by pipetting the lysed cell solution into a Qiashredder which was spun at 12,000 x g for 5 min at 4 ºC. The eluate was collected and stored at -80 ºC.

2.11.2. Bradford Quantification

Protein concentration was determined using the BioRad protein assay, based on the Bradford method. Bovine serum albumin (BSA) was used to prepare a standard curve ranging from 0.2 – 1.4 µg/µl (w/v). Samples and standards were assayed in duplicate. Samples were diluted 1/10 and 4 µl of either standard or diluted sample was incubated with 200 µl BioRad reagent in a 96-well plate for 5 min. Absorbance was read at 620 nm. Protein concentration was calculated using the standard curve generated.

2.11.3. Sample Preparation

Following quantification samples were prepared for protein separation via polyacrylamide gel electrophoresis (PAGE). 10 µg of protein was combined with an equal volume of loading buffer containing β-mercaptoethanol (BME) (25µl BME to 500µl 2X loading buffer). The samples were the boiled for 5 min at 95 ºC. β-

mercaptoethanol reduced disulfide bonds and subsequent boiling at 95 ºC denatured the protein. Samples were collected by brief centrifugation and placed on ice.

2.11.4. Sodium Dodecyl Sulphate – Polyacrylamide Gel Electrophoresis (SDS-PAGE)

A 10 % polyacrylamide resolving gel was routinely used for protein separation (section 2.11.5). Temed and APS (made fresh before use) were added last, in that order, just before gel was poured. The resolving gel was poured and allowed to polymerise for 30 min. Following this, distilled water was pipetted on top to ensure the resolving gel polymerised evenly. The quantities outlined in Section 2.11.5 were sufficient to pour two resolving gels with approximately 1 ml remaining. After the 30 min had elapsed the 1 ml remaining in the sterilin was checked to have completely polymerised. Subsequently, a 4 % stacking gel was prepared in the same way outlined in Section 2.11.5. After the addition of the stacking gel, well combs were placed between the glass plates. The stacking gel was allowed polymerise for 45 min. Gels were used immediately or stored overnight at 4 ºC

Protein samples were prepared as described in Section 2.11.3. A protein ladder was run adjacent to the protein samples. Two forms of molecular weight protein ladder were used, a colorimetric SeeBlue ladder which was used to track the migration of the proteins through the gel and a MagicMark ladder which was visible on the developed film and used for confirmation of correct protein size. Samples were electrophoresed in 1X TGS buffer (240 mM-Tris, 1.92 M-Glycine, 1% w/v-SDS, pH 8.3) at 130 volts for 75-85 min.

2.11.5. **SDS-PAGE Gels**

	Resolving Gel			Stacking Gel
	8 %	10 %	12 %	4%
30 % Acrylamide Bis	2.7 ml	3.3 ml	4.0 ml	1.3 ml
Distilled H20	4.7 ml	4.1 ml	3.4 ml	6.1 ml
1.5 M Tris-HCL, pH8.8	2.5 ml	2.5 ml	2.5 ml	
0.5 M Tris-HCL, pH8.8				2.5 ml
10 % SDS	100 µl	100 µl	100 µl	100 µl
10 % Ammonium Persulphate	50 µl	50 µl	50 µl	50 µl
Temed	9 µl	9 µl	9 µl	9 µl

2.11.6. **Semi-Dry Transfer**

After separation of the proteins by electrophoresis, the protein was transferred electrophoretically from the gel to the nitrocellulose membrane by semi dry transfer. While the gel was running, Towbin's transfer buffer was prepared (25 mM Tris, 192 mM glycine, 20% v/v methanol). The pH of this buffer was confirmed to be between 8.3 and 8.5 pH and was not adjusted. After electrophoresis, the stacking gel was removed and the gel was scored to ensure correct orientation. Two sheets of blot paper (extra thick), a nitrocellulose membrane (cut to size) and the gel were equilibrated in Towbin buffer for 5, 10 and 15 min, respectively. The blot paper, nitrocellulose membrane, gel and second sheet of blot paper were placed on the Trans-Blot SD Semi Dry transfer cell in that order. Protein was electrophoretically transferred from the gel to the membrane at 25 volts for 45 min. The colorimetric SeeBlue ladder was observed on the nitrocellulose membrane and served as a transfer control.

2.11.7. **Immunoblotting**

The nitrocellulose membrane, or blot, was initially incubated in blocking buffer for 1 hr. All incubations were carried out on a rocking platform. Primary antibodies were incubated either at room temperature or overnight. Following primary incubation any unbound antibody was removed by washing the blot in TBS containing 0.1% Tween-20. Generally washes involved three buffer changes in ten minutes. However, for antibodies which had high background staining this was increased up to nine buffer changes in 45 min. The blot was then incubated with the relevant horseradish peroxidase-labeled (HRP labeled) secondary antibodies for 1 hr at room temperature. The blot was washed as before in TBS containing 0.1% Tween-20. Visualisation of protein was performed with the detection of immunolabeled protein using the enhanced chemiluminescence (ECL) western blotting detection reagents, as per manufacturer's instructions. The blots were placed protein side up between two acetates in an x-ray film cassette. Blots were autoradiographed in a dark room under

safe light illumination using the Hyperfilm^{TM}ECL. Film was developed, fixed and analysed for protein signal.

2.12. Flow Cytometry

2.12.1. Cell Preparation and Fixation

For cell cycle analysis both adherent cells and cells contained in the supernatant were included. The supernatant from a confluent T-25 tissue culture flask was poured into a 15 ml tube. The cells were trypsinised as described in section 2.2.2 and combined with the supernatant and the entire cell suspension was centrifuged at 800 x g for 5 min. The resulting pellet was washed in chilled PBS and centrifuged as before. The supernatant was then removed leaving a small volume of liquid into which the pellet was resuspended. At this point, 1 ml ice cold 75 % v/v ethanol was added dropwise to the resuspended pellet while vortexing. Cells were stored at -20 ºC. For propidium iodide staining, cells were kept at -20 ºC for at least one week to ensure best resolution.

2.12.2. Propidium Iodide Staining

Cells were fixed in 70 % ethanol as described in Section 2.12.1. Prior to analysis, cells were rinsed in PBS containing 1 % FBS and centrifuged at 800 x g for 5 min. The pellet was re-suspended in 500 µl propidium iodide staining solution (40 µg/ml propidium iodide (PI), 100 µg/ml RNaseA, in PBS). Cells were incubated for 30 min at 37 ºC and analysed using a FACScan Flow Cytometer using Cell Quest software.

2.12.3. Quantification of β-Galactosidase Expression

Senescence associated β-galactosidase (SA- β-gal) activity was determined using the ImaGene Green C_{12}FDG LacZ detection kit according to manufacturer's instructions. Cells were cultured up to day 6 in 24-well plates. This kit contains two reagents necessary for the detection of SA- β-gal. Chloroquine inhibits endogenous β-gal by raising lysosomal pH. C_{12}FDG, a fluorogenic substrate for β-gal emits a green

fluorescence in the presence of SA-β-gal activity. Untreated and BMP4-treated BEAS-2B and A549 cells were analysed for SA-β-gal activity. Four treatment groups were set up: 1) Medium only, as a negative control; 2) Chloroquine only, as a control for any adverse effects this chemical may have on the cells; 3) Chloroquine and C_{12}FDG combined, permitting the detection of SA- β-gal only; 4) C_{12}FDG, permitting the detection of SA- β-gal and endogenous β-gal.

Cells were incubated for 90 min with 300 μM chloroquine in fresh phenol-free culture medium (Phenol free 1:1 DMEM/F12, 5 % FBS, 2 mM L-Glutamine) to inhibit endogenous β-galactosidase activity. After washing with PBS, cells were incubated for 30 min with 33 μM C_{12}FDG, a fluorogenic substrate of β-galactosidase. After two washes with PBS, cells were trypsinisation with the addition of 200 μl trypsin into each well. The trypsin was deactivated with the addition of 200 μl phenol-free culture medium (Phenol free 1:1 DMEM/F12, 5 % FBS, 2 mM L-Glutamine). Samples were kept on ice, protected from light and fluorescence was quantified immediately using a FACScan Flow Cytometer.

3.0 BMP2- and BMP4-mediated Signalling in the Transformed Bronchial Airway Cell Line - BEAS-2B

3.1. Introduction

BMPs are multi-functional growth factors which regulate processes such as morphogenesis, apoptosis and differentiation in a variety of cell types both during development and in adult tissue (Chen et al., 2004). In the developing lung, BMP4 is critical for lung branching morphogenesis where it serves to promote proliferation of distal progenitor cells as the lung branch extends. BMP signalling has been shown to be reactivated during OVA-induced airway inflammation in the mouse. In addition, in human patients with asthma the BMP pathway is activated following allergen challenge. These studies highlight a role for BMP signalling in the adult lung and furthermore in the pathogenesis of airway disease. However, a role for activated BMP signalling in adult lung epithelial cells (AECs) remains unknown.

To investigate the function of BMP signalling in AECs we used the BEAS-2B cell line. The BEAS-2B cell line was originally derived from normal human bronchial epithelial (NHBE) cells which were transformed with an adenovirus 12-SV40 hybrid virus (Reddel et al., 1988). Initial characterisation revealed that BEAS-2B cells retained characteristic epithelial cell morphology, expressed desmosomes and tight junctions and were keratin positive (Reddel et al., 1988). BEAS-2B cells were shown to be non-tumorigenic when injected into athymic nude mice and possessed the ability to repopulate denuded rat trachea that was subcutaneously (s.c.) grafted onto athymic mice (Reddel et al., 1988). Therefore, BEAS-2B cells are a transformed cell line which has retained characteristics of normal differentiated epithelial cells.

BEAS-2B cells were cultured in the presence of 100 ng/ml BMP2 and BMP4 for six days under serum-free culture conditions. BMP pathway expression in BEAS-2B cells alone and in response to either BMP2 or BMP4 was determined. BMP4-mediated signalling during lung development regulates proliferation of distal airway progenitor cells. For this reason, the effect of BMP2 and BMP4 on BEAS-2B cell proliferation was investigated. BMP signalling during development is active in tissues under going epithelial-mesenchymal transition (EMT) and may be involved in these processes.

Similarly, BMP4 during lung branching morphogenesis inhibits proximal airway cell differentiation. For this reason, the effect of BMP signalling on BEAS-2B cell differentiation was investigated with the assessment of a range of differentiation markers including the epithelial cell marker, E-cadherin. The aims of these experiments were to investigate alterations in BEAS-2B cell proliferation and differentiation in response to activated BMP2- and BMP4-mediated signalling.

3.1.1. Actin as a suitable housekeeper protein for BMP2 and BMP4 experiments

Actin expression was assessed by western blotting in BEAS-2B cells treated with BMP2 and BMP4 for 6 days and normalised to GAPDH (Fig. 3.1). No significant alteration in actin expression was detected in BEAS-2B cells in response to BMP2 or BMP4 treatment (Fig. 3.1). Actin was therefore deemed a suitable housekeeper protein for subsequent BMP experiments.

3.1.2. Western blot analysis of BMP pathway activation in BEAS-2B cells following 20 min and 2 hr BMP2 and BMP4 stimulation

It had not been previously demonstrated whether BEAS-2B cells express a BMP signalling pathway or whether these cells are responsive to BMP stimulation. BMPR-IA, BMPR-II, phosphorylated Smad1/5/8 and Smad4 were all detected in untreated BEAS-2B cells grown in control serum-free medium (Fig. 3.7). The level of expression of BMPR-IA, phosphorylated Smad1/5/8 and Smad4 was determined at 20 min and 2 hr following stimulation with 100 ng/ml BMP2 and BMP4.

In response to BMP2, BMPR-IA was significantly reduced after 20 min stimulation (Fig. 3.2) (BMPR-IA visible as double bands). There was no significant change in BMPR-IA expression at 2 hr (Fig. 3.2). At 20 min, a 40 % increase in p-Smad1/5/8 expression occurred in response to BMP2 compared to untreated cells (Fig. 3.2 B). At 2 hr this increased level of expression was sustained and found to be significantly higher than untreated cells (Fig. 3.2 B). Smad4 expression did appear reduced in BMP2-treated cells at 20 min but the change in expression compared to untreated cells was not found to be statistically significant (Fig. 3.2 B). At 2 hr, Smad4 levels were comparable between untreated and BMP2-treated cells (Fig. 3.2 B).

BMPR-IA, phosphorylated Smad1/5/8 (p-Smad1/5/8) and Smad4 expression was determined at 20 min and 2 hr following stimulation with 100 ng/ml BMP4 (Fig. 3.3). No significant change in BMPR-IA expression was observed following 20 min or 2 hr

BMP4 treatment (Fig. 3.3). A three-fold increase in p-Smad1/5/8 levels was detected at 20 min following BMP4 stimulation (Fig. 3.3 B). At 2 hr a two-fold increase in p-Smad1/5/8 expression remained in BMP4-treated cells (Fig. 3.3 B). Smad4 expression was not modulated in BMP4-treated cells following 20 min and 2 hr BMP4 stimulation (Fig. 3.3).

3.1.3. Immunofluorescence analysis of BMP pathway activation in BEAS-2B cells following 20 min, 2 hr and 17 hr BMP2 and BMP4 stimulation

20 min

The localisation and relative expression of BMP pathway components was assessed by immunofluorescence in BEAS-2B cells following 20 min BMP2 or BMP4 treatment. In response to BMP2 no change in the level of expression or localisation of BMPR-IA was apparent (Fig. 3.4 a, b). BMPR-II expression appeared upregulated in response to BMP2 (Fig. 3.4 b, f). An increase in nuclear translocation of p-Smad1/5/8 and Smad4 was apparent indicating BMP pathway activation in response to BMP2 (Fig. 3.4 c, g and d, h, respectively).

In response to BMP4, BMPR-IA expression did not appear modulated at 20 min (Fig. 3.4 a, i). In contrast, BMPR-II expression appeared upregulated following BMP4 treatment (Fig. 3.4 b, j). A marked increase in cytoplasmic p-Smad1/5/8 was observed following 20 min BMP4 treatment with some nuclear translocation evident (Fig. 3.4 c, k). Nuclear translocation of Smad4 in BMP4-treated cells was also observed (Fig. 3.4 d, l).

2 hr

BMP pathway expression was assessed following 2 hr BMP2 and BMP4 stimulation. In untreated BEAS-2B cells cultured in serum-free medium alone, alterations in pathway expression were evident compared to 20 min. BMPR-IA expression appeared reduced in untreated cells while BMPR-II was increased (Fig. 3.5 a, b compared to Fig. 3.4 a, b). Interestingly nuclear translocation of p-smad1/5/8 was evident in

untreated cells at this time point (Fig. 3.5 c). In addition, weak nuclear accumulation of Smad4 was evident (Fig. 3.5 d). This suggests a level of pathway modulation which may occur in BEAS-2B cells in serum-free medium in the absence of exogenous BMP stimulation. In response to 2 hr BMP2 stimulation an increase in BMPR-IA was observed (Fig. 3.5 e). However, BMPR-IA did not appear localised throughout the cell but instead was expressed in aggregates either inside the cell or on the cell membrane. Similar aggregates were seen on BMPR-II immunolocalised cells (Fig. 3.5 f). These may represent condensed areas of receptor expression which can occur following ligand binding and preceding receptor endocytosis (Zwaagstra et al., 1999). Nuclear translocation of p-Smad1/5/8 was apparent (Fig. 3.5 g). In addition nuclear Smad4 was apparent (Fig. 3.5 h). However, compared to 20 min, the level of nuclear Smad4 appeared reduced at this time point in BMP2-treated cells (Fig. 3.4 h).

Similar changes were seen in pathway components following 2 hr BMP4 treatment. BMPR-IA expression was increased on BMP4-treated cells (Fig. 3.5 a, i). BMPR-II expression was comparable between untreated and BMP4-treated cells (Fig. 3.5 b, j). P-Smad1/5/8 localisation was predominantly nuclear in BMP4-treated cells at 2 hr (Fig. 3.5 k). In addition and in contrast to BMP2-treated cells, nuclear Smad4 was evident in BMP4-treated cells at this timepoint (Fig. 3.5 l).

As previously mentioned, the presence of nuclear p-Smad1/5/8 in untreated BEAS-2B cells indicates pathway activation in the absence of exogenous BMP stimulation. However, the presence of predominantly nuclear p-Smad1/5/8 and increased nuclear Smad4 in BMP4-treated cells indicates this pathway activation is potentiated following BMP4 stimulation.

17 hr

BMP pathway expression was further investigated at 17 hr following BMP2 and BMP4 stimulation. At this time point the level of pathway expression in untreated cells was comparable to that observed at 2 hr (Fig. 3.6 a-d compared to Fig. 3.5 a-d). In response to BMP2 stimulation a dramatic increase in BMPR-IA expression was

observed (Fig. 3.6 e). In contrast, no change in BMPR-II expression was evident (Fig. 3.6 f). In addition, an increase in nuclear accumulation of p-Smad1/5/8 was evident with BMP2 (Fig. 3.6 g). However, no nuclear Smad4 was observed at 17 hr in BMP2-treated cells (Fig. 3.6 h).

In response to BMP4, BMPR-IA expression was unaltered at 17 hr when compared to untreated cells (Fig. 3.6 i). BMPR-II expression appeared slightly reduced in BMP4-treated cells at 17 hr (Fig. 3.6 j). Nuclear translocation of p-Smad1/5/8 was apparent in untreated cells (Fig. 3.6 c). However, p-Smad1/5/8 was predominantly localised to the nuclei in BMP4-treated cells (Fig. 3.6 k). Smad4 nuclear translocation was evident in BMP4-treated cells with no evidence of Smad4 nuclear translocation in untreated cells at 17 hr (Fig. 3.6 l).

In summary, a BMP pathway is expressed by BEAS-2B cells and can be activated *in vitro* by BMP2 and BMP4 stimulation as determined by both western blot analysis of protein expression (20 min and 2 hr) and immunofluorescence analysis of protein localisation (20 min, 2 hr and 17 hr). While BMP2 and BMP4 both activated BMP signalling differences in the effects on receptors and Smad proteins were apparent. BMP2 stimulation resulted in modulation of BMPR-IA with the apparent downregulation of BMPR-IA following 20 min ligand stimulation. In contrast, BMPR-IA remained largely unaltered in response to BMP4. BMP2 induced phosphorylation of Smad1/5/8 as well as nuclear translocation of these activated proteins. In addition, Smad4 nuclear translocation was also detected in response to BMP2. Increased levels of p-Smad1/5/8 and nuclear translocation of both p-Smad1/5/8 and Smad4 were also apparent in response to BMP4. However, in contrast to BMP2, this nuclear translocation of p-Smad1/5/8 and Smad4 was sustained up to 17 hr post stimulation in BMP4-treated cells.

3.1.4. Western blot analysis of BMP pathway activation in BEAS-2B cells at day 6 following BMP2 and BMP4 stimulation

As described above, the BMP pathway was activated following 20 min and 2 hr BMP2 and BMP4 stimulation. Next, BEAS-2B cells were grown to confluency (day 6) at which time they were characterised for changes in response to BMP2 and BMP4. The level of pathway activation at day 6 was assessed in BMP2-treated cells (Fig. 3.7). Western blot analysis revealed a reduction in BMPR-IA expression at day 6. No change in BMPR-II expression was observed. At day 6, the level of p-Smad1/5/8 expression in BMP2-treated cells was comparable with untreated cells. Similarly, no alteration in the level of Smad4 was observed in BMP2-treated cells at this time point. BMP4-treated cells were also assessed for expression of BMPR-IA, BMPR-II, p-Smad1/5/8 and Smad4 at day 6 (Fig. 3.8). While BMPR-IA, BMPR-II and Smad4 levels were comparable between untreated and BMP4-treated cells (Fig. 3.8), increased levels of p-Smad1/5/8 expression were sustained at this time point (Fig. 3.8 B).

3.1.5. Immunofluorescence analysis of BMP pathway activation in BEAS-2B cells at day 6 following BMP2 and BMP4 stimulation

Immunofluorescence analysis was carried out for BMP pathway components in BMP2- and BMP4-treated cells at day 6. The level of expression and localisation of BMPR-IA, BMPR-II, p-Smad1/5/8 and Smad4 did not appear altered in BMP2-treated cells compared to untreated cells in serum-free medium (Fig. 3.9 a-h). In contrast, a marked difference in pathway expression was observed between untreated and BMP4-treated cells. BMPR-IA expression appeared increased in BMP4-treated cells (Fig. 3.9 i). However, BMPR-II expression was comparable to untreated cells (Fig. 3.9 j). Interestingly, p-Smad1/5/8 expression was detected in the nuclei of untreated cells (Fig. 3.9 c). However, increased cytoplasmic expression in addition to nuclear translocation was observed in response to BMP4 (Fig. 3.9 k). Smad4 nuclear translocation was also apparent in BMP4-treated cells not seen in untreated (Fig. 3.9 d, l). In addition to active BMP

signalling, BMP4-treated cells looked morphologically different to untreated cells at day 6 with cells which appeared elongated and fibroblast-like. BMP4-induced morphology will be discussed in section 3.1.7.

In summary, while both BMP2 and BMP4 had the ability to activate the canonical BMP-Smad signalling pathway in BEAS-2B cells this pathway activation appeared to be sustained only in BMP4-treated cells at day 6.

3.1.6. Analysis of senescence features in BMP2- and BMP4-treated BEAS-2B cells

We have shown BEAS-2B cells possess the canonical BMP signalling pathway and are responsive to BMP stimuli. To date, there has been little published data focusing on BMP signalling and its effect on lung epithelial cells. However, a previous study had demonstrated the induction of a senescent phenotype in A549 cells (lung adenocarcinoma-derived cell line) in response to 100 ng/ml BMP4 in 1 % serum-containing medium. In the study, A549 cells cultured with BMP4 acquired an enlarged, flattened, senescent-like phenotype and had increased senescence-associated β-galactosidase (SA-β-gal) activity (Buckley et al., 2004). In the present study, BMP4 induced a fibroblast-like morphology rather than a senescent-like morphology. Nonetheless, the induction of senescence in both BMP2- and BMP4-treated BEAS-2B cells was assessed at day 6. Senescence associated β-galactosidase (SA-β-gal) is commonly used as a marker of senescence (Dimri et al., 1995). Untreated BEAS-2B cells were on average 74 % positive for SA-β-gal at day 6 under serum-free conditions (Fig. 3.10 A). However, a reduction in the number of cells positive for SA-β-gal following BMP2 and BMP4 treatment was observed with 70 % and 57 % SA-β-gal-positive cells detected at day 6, respectively (Fig. 3.10 A). In addition, the level of expression of SA-β-gal, as determined by the mean fluorescence intensity (MFI), was significantly reduced in BMP2- and BMP4-treated cells (Fig. 3.10 B). The onset of cellular senescence is commonly associated with a halt in the cell cycle and accumulation of cells at S, G2/M and G0 phases (Masterson et al., 2007). Cell cycle progression was

assessed in BMP2- and BMP4-treated cells by propidium iodide staining of DNA. No significant alteration in cell cycle profile was observed with either treatment when compared to untreated cells at day 6 (Fig. 3.10 C). Taken together, we conclude that neither BMP2 nor BMP4 induce senescence in BEAS-2B cells under these conditions.

3.1.7. BEAS-2B cell morphology and proliferation in BMP2- and BMP4-treated cells

The BEAS-2B cell line was originally derived from normal bronchial epithelium (Reddel et al., 1998). BEAS-2B cells displayed characteristic epithelial cobblestone morphology. BEAS-2B cells were assessed over 6 days (day 1-6) for changes in morphology in response to BMP2 (Fig. 3.11). At day 3, cells in serum-free medium alone cells appeared cobblestone in morphology where colonies had begun to form. Cells cultured in the presence of 100 ng/ml BMP2 did not exhibit any alteration in morphology at day 3 or up to day 6 (Fig. 3.11 A). Viability cell counts were carried out to determine whether BMP2 had an effect on BEAS-2B cell proliferation and/or cell viability. BMP2 had no significant effect on cell number or viability (data not shown) up to day 6 where 5.7 % and 4.7 % non-viable cells were detected in untreated and BMP2-treated cells, respectively (Fig. 3.11 B).

In contrast, alterations in BEAS-2B cell morphology were apparent in response to BMP4. At day 3, sub-confluent cells treated with 100 ng/ml BMP4 appeared angular in shape and had reduced cell-cell contact compared to untreated cells which had begun forming cobblestone colonies (Fig. 3.12 a, b). By day 6, BMP4-treated cells exhibited a spindle-shaped, fibroblast-like morphology (Fig. 3.12 c, d). When cells were re-fed at day 6 with serum-free medium containing 100 ng/ml BMP4, the morphology effect was even more pronounced at day 10 (Fig. 3.12 f). BMP4-treated cells which had the BMP4-containing medium removed and replaced with serum-free medium alone did exhibit fibroblast-like morphology at day 10 (Fig. 3.12 g). However, this morphology did appear reduced compared to their day 6 counterpart (Fig. 3.12 d). Similarly, when the medium on BMP4-treated cells was changed to serum containing

medium (SCM) at day 6, the fibroblast-like morphology was all but completely lost (Fig. 3.12 i). This suggests that removal of BMP4 and/or changing the local environment results in loss of this mesenchymal morphology.

Given the marked effect on cell morphology we investigated the effect on proliferation in BEAS-2B cells cultured with 100 ng/ml BMP4 (Fig. 3.13). After 6 days of culture, BMP4 induced a 48 % decrease in BEAS-2B cell number compared to untreated cells (Fig. 3.13). This reduction in cell number was not due to BMP4-induced toxicity with an average of 5.7% and 4.1% non-viable cells observed in untreated and BMP4-stimulated populations respectively (data not shown).

3.1.8. BMP4 increases BEAS-2B cell migration

A wound assay was carried out to analyse BEAS-2B cell motility in response to BMP4 (wound assay was performed by A Adams in Shirley O'Dea laboratory, Molloy et al., 2008) (Fig. 3.14). Untreated cells in serum-free medium alone migrated very slowly and the denuded area remained largely unchanged after 17 hrs. In contrast, cells cultured with 100 ng/ml BMP4 migrated to fill the wounded area. It is unlikely the area was repopulated by proliferating cells rather than migrating cells as proliferation was reduced in BMP4-treated cells compared to untreated controls (Fig. 3.13).

3.1.9. Western blot analysis of adherens junction and cytokeratin proteins in BEAS-2B cells at day 6 following BMP2 and BMP4 stimulation

Cells cultured with BMP4 acquired a fibroblast-like change in morphology and exhibited increased migration compared to untreated controls. We wished to investigate whether this apparent gain of a mesenchymal phenotype corresponded with a loss in epithelial cell markers. For this reason, we investigated the expression of the epithelial-related adherens junction proteins and the epithelial specific cytokeratins in BMP4-treated cells. The expression of adherens junction proteins, E-cadherin, N-

cadherin, α-, β- and γ-catenin as well as epithelial cell markers cytokeratin 8 and 18 were assessed in BMP2- and BMP4-treated BEAS-2B cells at day 6.

At day 6 E-cadherin expression was reduced by 30 % in BMP2-treated cells (Fig. 3.15). In contrast, N-cadherin expression was not modulated in response to BMP2 (Fig. 3.15). At day 6, no alteration in α-, β-, or γ-catenin expression was observed in BMP2-treated cells. Downregulation of E-cadherin represents an inhibition of the epithelial cell phenotype and is regarded as a hallmark for cells undergoing epithelial-mesenchymal transition (EMT). Although no effect on epithelial cell morphology was apparent under our cell culture conditions we investigated whether BMP2 had modulated the expression of epithelial cell markers cytokeratin 8 and 18. At day 6, no significant effect on cytokeratin expression was observed in BMP2-treated cells (Fig. 3.15).

Similarly, the expression of E-cadherin, N-cadherin, α-, β-, γ-catenin and cytokeratin 8 and 18 were examined in BMP4-treated cells at day 6 (Fig. 3.16). E-cadherin expression was almost completely abolished and was barely detectable by western blot at day 6. Similarly, N-cadherin expression was significantly reduced following BMP4 treatment. Expression of β- and γ-catenin was also significantly reduced in response to BMP4. No change in expression of α-catenin was detected. Interestingly, no alteration in the expression of cytokeratin 8 or 18 was detected in cells cultured with BMP4 at day 6 despite the apparent acquisition of a mesenchymal phenotype at this time point (Fig. 3.16).

3.1.10. Immunofluorescence analysis of adherens junction and cytokeratin proteins in BEAS-2B cells at day 6 following BMP2 and BMP4 stimulation

We examined the localisation of adherens junction proteins, E-cadherin, N-cadherin, α-, β- and γ-catenin, as well as the cytoskeletal proteins, cytokeratin 8 and actin, by immunofluorescence in BMP2- and BMP4-treated cells at day 6. Unexpectedly, E-cadherin was localised to the nuclei in untreated BEAS-2B cells (Fig. 3.17 a). This

localisation was not altered in response to BMP2 or BMP4 treatment (Fig. 3.17 h, o). N-cadherin was localised to the membrane in untreated BEAS-2B cells and appeared unchanged in response to BMP2 (Fig. 3.17 i). In contrast, N-cadherin did appear increasingly cytoplasmic in BMP4-treated cells (Fig. 3.17 p). α-catenin expression was apparent in the cytoplasm and at the membrane of untreated BEAS-2B cells and this localisation remained largely unchanged with BMP2 and BMP4 treatment (Fig. 3.17 j, q). Similarly, β-catenin which was localised to the membrane in BEAS-2B cells was not changed in BMP2-treated cells at day 6 (Fig. 3.17 d, k). However, in response to BMP4 β-catenin appeared localised to the cytoplasm (Fig. 3.17 r). γ-catenin expression appeared cytoplasmic in untreated BEAS-2B cells and while in some cases appeared increasingly membranous in BMP2-treated cells was largely unaltered in BMP4-treated cells (Fig. 3.17 e, l, s). Cytokeratin 8 localisation was comparable between untreated and BMP2- and BMP4-treated cells (Fig. 3.17 f, m, t). Polarised actin was observed in BEAS-2B cells. This polarised actin was not altered in BMP2-treated cells at day 6 but was lost in BMP4-treated cells (Fig. 3.17 g, n, u).

3.1.11. **Alterations in gene expression in response to BMP4**

To gain a better insight into the alterations at the molecular level in response to BMP4, changes in mRNA expression were assessed by both semi-quantitative PCR (RT-PCR) and quantitative PCR (QPCR) (RT-PCR was performed by EM Molloy and JC Masterson in Shirley O'Dea laboratory, QPCR was performed by A Adams and JB Moore in Shirley O'Dea laboratory, Molloy et al., 2008).

The expression of several mesenchymal markers typically expressed in EMT was examined by semi-quantitative PCR in BMP4-treated cells. Desmin and N-cadherin were significantly increased in BEAS-2B cells in response to BMP4 (Fig. 3.18). Expression of collagen 1A1 and 1A2, fibronectin and vimentin were also consistently increased (Fig. 3.18). In contrast, α-smooth muscle actin and cytokeratin 18 expression was not changed at the mRNA level (Fig. 3.18).

A broader view of changes in mRNA expression was assessed using ECM PCR array plates. From the 84 ECM-related genes examined, BMP4-treated cells displayed a significant decrease in 12 genes (Molloy et al., 2008) and significant increase in 13 genes (Molloy et al., 2008). From the PCR array cell adhesion molecules, ECM proteins and ECM-degrading enzymes were among the upregulated and downregulated cohorts of genes modulated. E-cadherin was downregulated 15-fold at the mRNA level. In addition, MMP2, collagen V1α1, collagen V1α2 and the tissue inhibitor of metalloproteases, TIMP2 were also found significantly inhibited in response to BMP4. VCAM, MMP16 and a number of collagens were among the genes upregulated in response to BMP4.

Of the genes altered on the PCR array, four genes were selected for independent validation including two upregulated genes, COL5A1 (collagen Vα1) and TGFBI (TGF-β-induced) and two downregulated genes, CDH1 (E-cadherin) and MMP2 (gelatinase A) (QPCR validation performed by JB Moore in Shirley O'Dea Laboratory, Molloy et al., 2008) (Fig. 3.19). QPCR was done using total RNA from three independent passages of BEAS-2B cells and using alternative primers to those used in the array experiments. Similar changes in gene expression were observed verifying the trends obtained on the PCR array (Fig. 3.19, Molloy et al., 2008).

3.1.12. Modulation of transcriptional repressors of E-cadherin in BMP4-treated cells

E-cadherin was inhibited at both the mRNA and protein level in response to BMP4. For this reason we looked at the expression of known transcriptional repressors of E-cadherin in BEAS-2B cells at day 6 (RT-PCR was performed by EM Molloy and JC Masterson in Shirley O'Dea laboratory, Molloy et al., 2008). The expression of SNAI1, SNAI2, SNAI3, ZEB1 and Twist were consistently increased in BMP4-treated cells at day 6 (Fig. 3.20).

3.2. Discussion

BMP signalling is activated during lung inflammation. However, a role for the activated BMP pathway had not previously been elucidated. In order to investigate the role of BMP signalling in adult lung cells, BEAS-2B cells were cultured in the presence of BMP2 and BMP4 for 6 days. Both ligands activated the canonical BMP-Smad signalling pathway *in vitro*. However, this pathway activity appeared to be only sustained in BMP4-treated cells by day 6. BMP2 and BMP4 inhibited E-cadherin expression. However, this inhibition was more pronounced in BMP4-treated cells and was associated with an induction of a fibroblast-like morphology. In addition, BMP4 significantly inhibited proliferation and upregulated a number of mesenchymal markers by day 6. These changes in cell phenotype are consistent with an epithelial-mesenchymal transition (EMT). Recently, similar studies have shown the induction of an EMT in response to BMP4 in ovarian, mammary and pancreatic cell types. This role suggests activated BMP4-mediated signalling during lung inflammation may contribute to fibrosis *in vivo*.

BMP2 and BMP4 are 86% homologous and have been reported to possess similar biological activity (Wozney et al., 1990). However, BMP2 appeared less potent in activating a canonical BMP signalling pathway in BEAS-2B cells and did not alter cell morphology and proliferation. One possible explanation may involve the system from which the recombinant protein was produced. In our study we used an E-coli-derived BMP2 recombinant protein and a NSO (mouse myeloma cell)-derived BMP4 recombinant protein from R&D systems. The difference between these two systems was highlighted in a report where an Id (BMP target gene) promoter-luciferase construct was used to assess the activity of different BMP ligands (Logeart-Avramoglou et al., 2006). In particular, the study highlighted the activity of a mammalian-derived compared to an E-coli-derived BMP2 recombinant protein. A ten-fold reduction in activity was detected with the E-coli derived BMP2 ligand. This difference in activity was reflected on the product datasheets with the ED_{50} value for induction of ALP (alkaline phosphatase) expression in the range of 10-30 ng/ml and

300-1000 ng/ml for BMP4 and BMP2, respectively. This reduction in activity with BMP2 can mostly likely be attributed to incomplete post-translational modification such as glycosylation by E-coli. Glycosylation is necessary for correct protein folding or to confer stability to secreted proteins (Brooks, 2004). This assumption was supported by a number of experiments carried out in our laboratory. Firstly, BEAS-2B cells cultured in the presence of an e-coli-derived BMP4 did not exhibit a fibroblast change in morphology. Secondly, the induction of a fibroblast-like morphology and inhibition of E-cadherin expression was recapitulated with an alternative HeLa-derived BMP4 (HeLa cell line derived from human cervical cancer) (data generated in lab). This strongly suggests the lack of BMP2-mediated effects on BEAS-2B cells could be attributed to the e-coli expression system from which recombinant BMP2 was derived.

However, R&D systems do manufacture a BMP2 recombinant protein in CHO (Chinese hamster ovary cells) cells. The ED_{50} value, of the CHO-derived BMP2, for the induction of ALP expression was lower than that reported for NSO-derived BMP4 with a range of 40-200 ng/ml compared to 10-30 ng/ml, respectively. This suggests BMP2 may have reduced activity compared to BMP4 despite the expression system from which the recombinant protein was derived. In a study where A549 cells were treated with BMP2, the authors report the activity of BMP2 as transient *in vitro* with little or no effect on cell proliferation following two days in culture (Langenfeld et al., 2006). Furthermore, in serum-free culture conditions BMP2 was less potent in activating a BMP signalling pathway compared to serum conditions. However in the study, the same BMP2 recombinant protein could elicit potent effects *in vivo*, where A549 cells co-injected with BMP2 exhibited increased proliferation and sustained BMP pathway activation. This indicated that local environment was critical for the potency of BMP2-mediated signalling. During development BMP2 is secreted from the cell and binds to the extracellular matrix in order to elicit a response (Suzawa et al., 1999). It is likely the serum-free culture conditions are sub-optimal for sustained BMP2 activity. Therefore, the reduced effects observed in response to BMP2 are

likely to be attributed to either the e-coli-derived ligand or the limited microenvironment provided by the serum-free culture conditions.

Despite reduced activity, BMP2 did activate a canonical BMP signalling pathway in BEAS-2B cells. Increased phosphorylation of receptor mediated Smads (R-Smads), Smad1, 5, and 8, was detected initially following BMP2 stimulation. In addition, nuclear translocation was observed at 20 min which was maintained up to 17 hr indicative of active signal transduction following BMP2 stimulation. Similarly, BMP4 increased levels of p-Smad1/4/8 and induced nuclear translocation of the activated proteins up to 17 hr post stimulation. Phosphorylation of either Smad1, 5, or 8 occurs following ligand binding and is the hallmark of activated BMP signalling. Nuclear translocation of p-Smad1, 5, or 8 occurs in conjunction with the co-Smad, Smad4. In BMP2-treated cells, while p-Smad1/5/8 was detected in the nuclei up to 17 hr, Smad4 did not remain in the nuclei for this duration with no nuclear p-Smad1/5/8 detected in the nuclei of BMP2-treated cells at 2 hr. R-Smads (Smad1, -5 and -8) and the co-Smad Smad4, both contain a nuclear localisation signal (NLS) and a nuclear export signal (NES) (Xiao et al., 2001). These sequences facilitate shuttling between the cytoplasm and the nucleus (Xiao et al., 2001). In our experiments, activated p-Smad1/5/8 appeared to reside in the nucleus in the absence of nuclear Smad4. This may reflect variation in the rate at which R-Smad proteins and Smad4 are exported from the nucleus. Smad4 nuclear translocation may be transient while p-Smad1/5/8 may reside in the nucleus to regulate gene expression. In contrast to BMP2, BMP4-mediated signalling resulted in nuclear translocation of both p-Smad1/5/8 and Smad4 up to 17 hr. We propose that nuclear translocation of both p-Smad1/5/8 and Smad4 together indicates sustained pathway activation in response to BMP4.

At day 6, canonical BMP pathway activity was sustained in BMP4- but not BMP2-treated cells (Fig. 3.9). No significant increase in p-Smad1/5/8 or Smad4 levels was detected in BMP2-treated cells. However, P-Smad1/5/8 was localised to the nuclei of BMP2-treated cells at day 6. P-Smad1/5/8 was also detected in the nuclei of untreated BEAS-2B cells at day 6. However, in both untreated and BMP2-treated cells this

nuclear p-Smad1/5/8 localisation was in the absence of Smad4 which was localised to the cytoplasm. This further indicates p-Smad1/5/8 may reside in the nucleus following initial nuclear translocation. It has previously been suggested that a mode of BMP pathway regulation may involve keeping the Smad protein bound to the DNA and thus inhibiting signal transduction by preventing a newly activated Smad protein from gaining access to the DNA binding elements. Therefore, it is possible the high level of nuclear p-Smad1/4/8 in untreated and BMP2-treated cells may represent a mode of BMP pathway inhibition. In contrast to cells stimulated with BMP2, increased p-Smad1/5/8 levels were sustained at day 6 following BMP4 stimulation. In addition, increased nuclear translocation of both p-Smad1/5/8 and Smad4 was detected, indicative of on going pathway activation. Sustained pathway activation for 6 days following stimulation with BMP4 strongly suggests BMP4 can induce autocrine signalling in BEAS-2B cells.

Smad4 was activated in response to BMP2 and BMP4 stimulation with nuclear translocation apparent. However, the level of expression was not significantly modulated in response to either ligand at 20 min, 2 hr or day 6. This indicates activated BMP signalling may not regulate levels of Smad4 within the cell. It has been proposed that a limited Smad4 pool may serve as a point of regulation to control the level of both TGF-β and BMP pathway activation within the cell at the same time (Nakayama et al., 2000).

BMP2 and BMP4 differentially regulated BMPR-IA expression where BMPR-II remained largely unaltered. BMPR-II expression at 20 min and 2 hr was not assessed by western blot in this study. However, immunofluorescence did reveal apparent induction of BMPR-II following 20 min BMP2 and BMP4 stimulation after which it remained largely unaltered in response to either ligand. Interestingly, BMPR-IA was significantly downregulated following 20 min BMP2 stimulation. TGF-β receptor internalisation and subsequent degradation following ligand binding has been previously reported (Zwaagstra et al., 1999). In the study, the BMP receptor complexes were visible as aggregates on the cell surface following ligand binding and

preceding receptor internalisation (Zwaagstra et al., 1999). Similar aggregates were visible on BMP2-treated cells at 2 hr (Fig. 3.5). In addition, BMPR-IA expression was significantly reduced in BMP2-treated cells at day 6. This is likely to reflect sustained receptor internalisation/degradation following ligand binding in the absence of additional extracellular BMP2. Receptor downregulation in response to ligand-receptor binding serves as a form of negative feedback to regulate the level of pathway activity. In contrast, no reduction in BMPR-IA expression was detected in response to BMP4 at 20 min, 2 hr or at day 6. BMP4-mediated receptor internalisation has been reported (Serrano De la Pena et al., 2005). However, in the disease fibrodysplasia ossificans progressive (FOP), a condition whereby skeletal muscle is progressively replaced with bone, misregulation of BMP4-mediated receptor internalisation led to a constitutively active BMP signalling pathway (Serrano De la Pena et al., 2005). The absence of BMP4-mediated BMPR-IA downregulation in BEAS-2B cells may be attributed, at least in part, to the sustained pathway activation observed following BMP4 stimulation.

In summary, canonical pathway activation was observed in response to BMP2 and BMP4. In contrast to BMP2, this pathway activation was sustained up to day 6 in BMP4-treated cells. Prolonged BMP pathway activation in BEAS-2B cells in response to BMP4 may be attributed to a number of factors including the increased activity of the BMP4 ligand, the possible induction of autocrine signalling by BMP4 or a lack of negative feedback signalling in BMP4-treated cells.

It had previously been reported that BMP4 induces senescence in A549 cells *in vitro* (Buckley et al., 1996). After establishing that BMP2 and BMP4 could activate BMP signalling in BEAS-2B cells we investigated whether there was any evidence of senescence following BMP2 and BMP4 stimulation for six days. Senescence associated β-galactosidase (SA-β-gal) expression was significantly reduced in both BMP2- and BMP4-treated cells which combined with a lack of senescent-like morphology conclusively demonstrates BMP2 and BMP4 do not induce senescence in BEAS-2B cells (Fig. 3.10).

BEAS-2B cells cultured in the presence of BMP4 undertook a mesenchymal change in morphology with an apparent loss in cell-cell contact. By day 6, BMP4-treated BEAS-2B cells appeared increasingly fibrotic compared to the characteristic epithelial morphology observed in untreated BEAS-2B cells (Fig. 3.12). This change in phenotype corresponded with an inhibition of proliferation at day 6. In contrast, BMP2 did not alter BEAS-2B morphology and no effect on proliferation was observed. BMP4-treated cells retained this fibroblast morphology for up to four days following removal of BMP4. However, cells did appear less fibrotic by day 10, following removal of the BMP4 stimulus, compared to their day 6 counterpart. Furthermore, BMP4-treated cells at day 6 when placed in serum-containing medium or re-seeded at both low and high density in serum containing medium (data not shown) exhibited almost complete loss of the BMP4-induced mesenchymal morphology (Fig. 3.12). This suggests that BMP4 or other growth factors contained in the culture medium at day 6 are required to maintain the mesenchymal phenotype. BMP4 significantly inhibited BEAS-2B cell proliferation. This supports previously described findings where the induction of a fibroblast-like alteration in morphology during EMT is accompanied by a decrease in mitosis (Janda et al., 2002).

BMP4-induced fibroblast morphology was associated with increased migration in BEAS-2B cells. During development, epithelial cells undergo EMT and disperse within the developing embryo to mediate organ formation. Similarly, during wound healing epithelial cells adjacent to the damaged area downregulate E-cadherin and migrate to protect the exposed area. Increased migration in response to BMP4 supports the acquisition of a mesenchymal phenotype. Under normal conditions, these EMT events are followed by the reverse process MET. MET mediates the formation of secondary epithelia during development or is involved in the restitution of an intact epithelium following injury. Upon removal of the BMP4 stimulus BEAS-2B cells regained their epithelial morphology. For this reason, BMP4-induced EMT is not likely to represent a permanent acquisition of a mesenchymal phenotype but rather a temporary repression of the epithelial phenotype in order to facilitate movement.

BMP2 and BMP4 both had the ability to inhibit E-cadherin expression (Fig. 3.15 and Fig. 3.16). BMP2-mediated inhibition of E-cadherin was not associated with a reduction in α-, β- or γ-catenin expression by day 6. This suggests E-cadherin downregulation may precede or occur in the absence of downregulated catenin expression. The induction of fibroblast-like morphology in response to BMP4 was associated with almost complete abrogation of E-cadherin expression at day 6. In addition and in contrast to BMP2, β- and γ-catenin were significantly downregulated. Similar to BMP2, no change in α-catenin was detected in response to BMP4 in BEAS-2B cells. Downregulation of E-cadherin is regarded as a hallmark during EMT and is widely accepted as the first step in repression of the epithelial phenotype. However, despite this inhibition in E-cadherin expression, the epithelial-specific cytokeratin proteins, cytokeratin 8 and 18, were not inhibited by day 6 in response to BMP2 or BMP4.

E-cadherin was found localised to the nuclei in BEAS-2B cells (Fig. 3.17). A role for nuclear E-cadherin has not yet been elucidated. However, nuclear E-cadherin has been reported in cancer including merkel cell carcinoma, epithelioid sarcoma, breast carcinoma and wilms tumor of the kidney suggesting a possible role in cell proliferation (Han et al., 2000, Saito et al., 2001, Sauer et al., 2001, Alami et al., 2003). In light of this, BMP2- and BMP4-mediated inhibition of E-cadherin expression in BEAS-2B cells does not appear to have implications for cell-cell adhesion. Nonetheless, these data implicate both BMP2 and BMP4 as negative regulators of E-cadherin expression.

Localisation of α-and γ-catenin remained largely unaltered in both BMP2- and BMP4-treated cells at day 6. However, a loss in β-catenin membrane localisation and increased cytoplasmic expression was observed in response to BMP4 in BEAS-2B cells. Free β-catenin in the cytoplasm is ubiquitinated and rapidly degraded. However, following Wnt pathway activation, β-catenin can translocate to the nucleus and mediate proliferation, apoptosis or, in the presence of LEF1/Tcf, can induce EMT (Liebner et al., 2004). β-catenin expression was reduced in BEAS-2B cells in response

to BMP4 suggesting the disruption of the adherens junction complex resulted in free β-catenin which was subsequently degraded. Nonetheless, BMP4-treated BEAS-2B cells did appear to adopt changes in cell phenotype associated with EMT suggesting nuclear translocation of β-catenin may not be required for EMT to occur. However, in light of the apparent lack of certain alterations associated with EMT such as reduced cytokeratin expression, it is possible activated Wnt signalling may be required for certain changes in cell phenotype associated with EMT.

Loss of polarised actin was observed in response to BMP4 in BEAS-2B cells. In addition to the altered actin localisation in BMP4-treated cells, actin appeared upregulated (Fig. 3.17). This was of considerable concern since actin had been chosen as the housekeeper protein to confirm equal loading for western blot analysis in BMP2- and BMP4-treated cells (Fig. 3.16 and Fig.3.17). Upregulation of actin in response to BMP4 would have lead to misleading data. To investigate whether actin was upregulated in response to BMP4 another housekeeping protein, GAPDH, was used as an equal loading control to compare levels of actin expression in untreated and BMP4-treated cells. By this means it was confirmed that actin was in fact not altered at the protein level in response to BMP4. At this point the question remained as to why actin appeared upregulated when assessed by immunofluorescence. Immunofluorescence is not a quantitative technique and is used largely to assess changes in localisation. It is probable that the polarised actin localisation in untreated cells resulted in concealed epitopes which became exposed following BMP4-induced loss in polarisation. This increased antigenicity of the actin protein following loss in polarisation may explain the apparent upregulation of actin within the cell. In summary, western blot analysis of actin expression using GAPDH as a housekeeping protein confirmed actin protein levels were unchanged following BMP4 treatment and thus validated the use of actin as a housekeeping protein for western blot analysis of BMP4-treated cells. The apparent increase in actin expression following immunofluorescence analysis is likely to be attributed to varying epitope availability between polarised actin in untreated cells and unpolarised actin in BMP4-treated cells.

Loss of membrane associated β-catenin indicative of adherens junction disassembly and actin reorganisation are key events during EMT and strongly implicate BMP4 as an inducer of EMT in adult lung cells.

In addition to inhibition at the protein level, E-cadherin was significantly inhibited at the mRNA level in BEAS-2B cells in response to BMP4 (Fig. 3.19, QPCR performed by JB Moore in Shirley O'Dea Laboratory). This inhibition corresponded to increased expression of a number of transcriptional repressors of E-cadherin including Snail1 and Snail2. Snail1 is expressed at stages of EMT during development and moreover, both Snail1 and Snail2 have been linked to breast cancer progression (Côme et al., 2004). Snail2 has previously been identified as a downstream target of BMP signalling (Clancy et al., 2003). While transcriptional repression of the E-cadherin gene is a well recognised form of inhibition, epigenetic mechanisms of E-cadherin inhibition such as hypermethylation of the CDH1 (E-cadherin gene) promoter have previously been reported. Hypermethylation of the E-cadherin promoter has been reported in poorly differentiated cancer such as gastric cancer (Graziano et al., 2003). However, transcriptional repression alone is unlikely to explain the dramatic reduction in E-cadherin protein following BMP4-treatment. E-cadherin can be cleaved by MMPs, including stromelysin and matrilysin, to produce a truncated form of the protein which can be secreted from the cell (Noë et al., 2001). In addition, E-cadherin is constantly trafficked between the membrane and endocytic vesicles in order to regulate the level of cell-cell adhesion in normal cells both during homeostasis and to facilitate proliferation. While E-cadherin within the cell can be re-routed to the cell membrane, endocytosis can lead to E-cadherin ubiquitination and subsequent degradation via the proteosome. Furthermore, during Ras and TGF-β-induced EMT in murine mammary epithelial cells the authors reported E-cadherin endocytosis after 48 hr. Following this, E-cadherin was ubiquitinated by the E3 ubiquitin ligase, Hakai, and trafficked to the proteosome and/or lysosome to be degraded (Janda et al., 2006). This mechanism of post-translational inhibition was suggested to precede transcriptional repression of the E-cadherin gene during EMT. Taken together, while transcriptional inhibition may

reduce levels of E-cadherin over time, post-translational inhibition is likely to mediate immediate loss of E-cadherin protein within the cell.

A number of mesenchymal-associated genes were upregulated in BMP4-treated BEAS-2B cells. Semi-quantitative PCR analysis revealed an increase in N-cadherin and desmin expression. These genes are expressed on neuronal and muscle cells, respectively and reflect a shift towards a mesenchymal fate in response to BMP4. A broader view of the phenotypic changes induced by BMP4 was obtained in the PCR array study (PCR array performed by A Adams and JB Moore in Shirley O'Dea Laboratory, Molloy et al., 2008) which revealed changes in the expression of genes encoding several ECM proteins and matrix degrading enzymes. Among the genes upregulated were a number of collagens including collagen 5A1, 12A1, 14A1 and 15A1. Increased TGF-β-induced (TGF-βI) was also upregulated. Increased collagen and TGF-β activity has been associated with tissue fibrosis *in vivo*. In addition, several other ECM proteins and matrix degrading enzymes were upregulated in BMP4-treated cells including thrombospondin 2, tenascin C, fibronectin, integrin β 2 and MMP7. These genes are modulated during the EMT process in development and tumour progression (Chagraoui et al., 2003, Maschler et al., 2004, Larue and Bellacosa, 2005). A number of genes which have previously been described upregulated during EMT were found downregulated in response to BMP4 such as MMP2. However, the changes associated with EMT are highly specific to the cell type, activation of additional signalling pathways and the time point within the EMT process. For example, MMP2 is expressed while neural cells undergo EMT but is rapidly degraded when they disperse (Duong and Erickson, 2004).

A previous study characterised the induction of EMT in response to BMP4 in human ovarian cancer cells (Thériault et al., 2007). In the study, Snail1 and Snail2 mRNA was upregulated within 1 hr following the addition of BMP4, where E-cadherin mRNA was significantly inhibited by day 2. In addition, ECM-related genes in BMP4-treated ovarian cells were assessed. A number of integrins were significantly upregulated by BMP4 in the study including integrin alpha1, 2, 4, 5, V and integrin β

1, 3. However, of these only integrin alpha 5 and integrin β 1, 3 were significantly modulated at day 6 while no alteration was observed in the remaining genes earlier than day 7. Similarly in the study, laminin and vitronectin were significantly upregulated however the level of upregulation was only detectable at day 7. This is interesting as all of the integrins examined in the present study, with the exception of integrin β 2, remained unaltered in response to BMP4 at day 6. In addition, no alteration in laminin (alpha 1-3, β 3 or gamma 1) or vitronectin was detected in our study in response to BMP4 by day 6. This suggests that while repression of the epithelial phenotype may occur rapidly in response to BMP4, the acquisition of a mesenchymal phenotype may occur at a later timepoint. This further highlights the specific temporal changes in gene expression during the EMT process.

N-cadherin was localised to the membrane in BEAS-2B cells. This was not surprising considering the mislocalisation of E-cadherin expression observed in these cells. N-cadherin localisation appeared increasingly cytoplasmic in BMP4-treated cells and the level of protein expression was reduced in response to BMP4 at day 6. N-cadherin or neuronal cadherin is found mainly expressed on mesenchymal cells and forms less stable cell-cell adhesion compared to the more robust adhesion mediated by E-cadherin (Chu et al., 2004). However, epithelial cells can express N-cadherin in place of E-cadherin through a process referred to as phenotypic switching. This process has been characterised in cancer where in the absence of E-cadherin, N-cadherin confers weak intercellular adhesion (Thiery, 2002). In this way, tumour cells which have switched to N-cadherin can adhere to other N-cadherin-positive cells such as myofibroblasts. This event is likely to facilitate tumour metastasis. During EMT in development, N-cadherin can be downregulated on cells which express it such as neural crest cells and somites (Thiery, 2002). Downregulation of N-cadherin in BMP4-treated cells suggests BMP signalling may have the ability to negatively regulate N-cadherin as well as E-cadherin and may function to regulate expression of both E- and N-cadherin within the cell. N-cadherin was upregulated at the mRNA level at the same time point (Fig. 3.18). While analysis of gene and protein expression at day 6 provides a ‘snap shot’ of the expression profile within the cell in response to

BMP4, it does not provide any information as to the sequence of events which preceded these changes in expression. We can propose upregulation of N-cadherin at the mRNA level may have occurred subsequent to reduction in expression at the protein level as a form of auto-regulation within the cell to prevent complete loss of cell-cell adhesion. The EMT process is therefore highly dependent on cell type where the phenotype of the transitioning cell will determine the level and/or directionality of changes in protein expression.

In summary, BMP4 induced an EMT-like transition in adult lung epithelial cells. Moreover both BMP2 and BMP4 could inhibit E-cadherin expression. BMP signalling is highly expressed at sites undergoing EMT during development suggesting BMP signalling may be involved in this process. These data suggest this critical role for BMP signalling is conserved in adult lung cells and can be reinitiated in response to BMP4. In addition, BMP4-treated cells acquired a mesenchymal phenotype with an increase in a number of collagens and matrix degrading enzymes. Some changes previously associated with EMT did not occur in BEAS-2B cells under our cell culture conditions for example there was no inhibition of the epithelial markers cytokeratin 8 or 18 expression. The processes involved in EMT have not been clearly defined and *in vitro* are likely to be sensitive to culture conditions including the presence of substrates and/or serum. In addition, the cell phenotype prior to the addition of the EMT-inducing factor is likely to affect the outcome. BEAS-2B cells expressed a number of mesenchymal genes under serum-free conditions and importantly expressed N-cadherin at the membrane. It is likely the extent to which the epithelial phenotype is repressed and a mesenchymal phenotype acquired will rely closely on cell type, cell culture conditions and the growth factors involved.

Nonetheless, BMP4-treated BEAS-2B cells did acquire mesenchymal-like characteristics including the upregulation at the mRNA level of the pro-fibrotic factors collagen and TGF-β-induced. TGF-β activity and subsequent collagen deposition are central to the remodelling processes which occur in asthma. BMP2 and BMP4 mediate remodelling during bone development and repair. Taken together, BMP-mediated

inhibition of E-cadherin suggests reactivated BMP signalling during inflammation may mediate repair of the damaged epithelium. However, sustained activation of BMP4-mediated signalling during inflammation may lead to remodelling and tissue fibrosis *in vivo*.

4.0 BMP2- and BMP4-mediated Signalling in the Alveolar Adenocarcinoma Cell Line - A459

4.1. Introduction

We have established that BMP4 induces an EMT-like response in BEAS-2B cells. In order to determine whether other lung cell lines responded similarly to BMPs we decided to examine the widely-used A549, alveolar-like, cell line. A549 cells were originally derived from a human alveolar cell carcinoma. These cells possess features of differentiated alveolar type II cells including the presence of inclusion bodies and surfactant production (Lieber et al., 1976, Vaporidi et al., 2005). A549 cells display membrane E-cadherin localisation indicative of a well differentiated epithelioid tumor. Therefore, A549 cells retain certain characteristics of differentiated lung epithelial cells.

Previous literature has identified differential effects in A549 cells in response to BMP2 and BMP4. A549 cells cultured with BMP2 exhibited increased proliferation *in vitro* and increased invasiveness *in vivo* (Langenfeld et al., 2003, Langenfeld et al., 2006). In contrast, a previous study investigating BMP4 effects on A549 cells reported an inhibition of proliferation and the onset of a senescence phenotype *in vitro* as well as reduced tumorgenicity of BMP4-treated A549 cells *in vivo* (Buckley et al., 2004).

In this chapter, A549 cells were cultured with 100 ng/ml BMP2 or BMP4 under serum-free culture conditions. The expression and activation of canonical Smad signalling in response to BMP4 was determined. BMP-treated A549 cells were assessed initially for changes in morphology, proliferation and senescence-associated β-galactosidase activity (SA-β-gal) at day 6. In addition, the induction of an EMT-like response in A549 cells in response to BMP4 was investigated. E-cadherin expression was assessed and PCR array analysis was performed (data generated by A Adams and JB Moore in O'Dea laboratory) to assess any alterations in ECM-related genes in response to BMP4. Differences between BEAS-2B and A549 cells were observed in response to BMP4. To investigate the differences seen, BMP pathway modulation in response to BMP4 was assessed in A459 and BEAS-2B cells.

4.1.1. BMP2- and BMP4-mediated effects on A549 cell morphology and proliferation

We have demonstrated the induction of an EMT-like response in BEAS-2B cells following BMP4 treatment (Molloy et al., 2008). To further investigate the potential of BMP signalling to act as a negative regulator of E-cadherin expression and an inducer of EMT in lung epithelial cells we cultured A549 lung epithelial cells in the presence of 100 ng/ml BMP2 and BMP4. As seen with BEAS-2B cells, BMP2 treatment did not significantly alter A549 morphology or proliferation (Fig. 4.1 A b). However, BMP4-treated A549 cells appeared enlarged by day 6 (Fig. 4.1 A c). This was in contrast to the BMP4 induced fibrotic phenotype observed with BEAS-2B cells under the same culture conditions (Fig. 3.12 d). This enlarged cell morphology was associated with a 70 % reduction in cell number at day 6 (Fig. 4.1 B). This reduction in cell number was not as a result of cell death with 4.7 %, 3.5 %, and 7.9 % non-viable cells in untreated, BMP2- and BMP4-treated cells, respectively.

4.1.2. Analysis of SA-β-gal expression in BMP2- and BMP4-treated A549 cells

BMP4 has previously been reported to induce senescence in A549 cells (Buckley et al., 2004). In the study, A549 cells were treated with 100 ng/ml BMP4 under low serum conditions (1 % FBS) where cells were re-fed with recombinant BMP4 every other day (Buckley et al., 2004). Increased SA-β-gal was detected following 17 days of BMP4 treatment (Buckley et al., 2004). In our experiments, A549 cells appeared enlarged at day 6 following an initial 100 ng/ml BMP4 stimulus. To further investigate whether this enlarged morphology did indeed reflect the onset of senescence, SA-β-gal expression was quantified (Fig. 4.2). The number of cells positive for SA-β-gal was consistent across treatments with 86.8 %, 87.4 % and 85.4 % of untreated, BMP2- and BMP4-treated cells expressing SA-β-gal respectively (Fig. 4.2 A). However, a 43 % increase in the level of SA-β-gal expression was detected in BMP4-treated cells. In

contrast, BMP2 induced a 20 % reduction in the level of SA-β-gal expression when compared to untreated cells (Fig. 4.2 B).

4.1.3. BMP2- and BMP4-mediated effects on A549 cell morphology and proliferation in the absence of hydrocortisone (-HC)

BMP2 and cortisol play opposing roles during bone marrow stem cell differentiation and in the maintenance of differentiated osteoblasts (Pereira et al., 2002, Centrella et al., 1997). Therefore, we examined the role of hydrocortisone (the synthetic form of cortisol), which was contained in our serum-free culture medium (section 2.2.7) used in our BMP experiments. In the absence of hydrocortisone (-HC) A549 cells in serum-free medium alone appeared more flattened and less uniform in shape (Fig. 4.3 A a) when compared to untreated cells in serum-free medium containing hydrocortisone (HC) (Fig. 4.3 A b). Interestingly, BMP4 did not appear to induce a senescent-like change in morphology when HC was omitted from the culture medium. Under these cell culture conditions, BMP4-treated cells appeared increasingly angular in shape and exhibited a loss in cell-cell contact (Fig. 4.3 A d). This change in morphology more closely resembled an EMT. BMP4 did induce a 40 % reduction in cell number by day 6 (Fig. 4.3 B). However, this inhibition of growth was not found to be statistically significant. Similar to the BMP2-mediated effect on A549 cells cultured in medium containing HC, BMP2 did not induce any alteration in A549 cell morphology or proliferation under these cell cultures conditions (Fig. 4.3).

4.1.4. Analysis of SA-β-gal expression in BMP2- and BMP4-treated A549 cells in the absence of hydrocortisone (-HC)

It appeared that in the absence of hydrocortisone (-HC), BMP4 no longer induced an increase in cell size or a significant reduction in cell number. For this reason we investigated the level of SA-β-gal expression in BMP4-treated cells in the absence of hydrocortisone (- HC). The number of cells positive for SA-β-gal was marginally higher in the absence of HC with 92 % of cells positive in untreated, BMP2- and BMP4-treated cells at day 6 (Fig. 4.4 A). Interestingly, where SA-β-gal expression was significantly elevated in response to BMP4 under HC-positive ($p=0.000001$) cell

culture conditions (Fig. 4.2 B), a less consistent upregulation was seen in BMP4-treated A549 cells in the absence of HC ($p=0.184093$) (Fig. 4.4 B). SA-β-gal expression was reduced in BMP2-treated cells in the absence of hydrocortisone (Fig. 4.4 B). However, in comparison to HC-positive cells this reduction was not found to be significant (Fig. 4.2 B).

4.1.5. Phosphorylated Smad1/5/8 and Smad4 expression in A549 cells following BMP4 stimulation

Because we were interested in the EMT effects of BMPs, subsequent experiments were carried out in serum-free culture medium omitting HC (-HC) and focused on BMP4. Pathway activation in response to BMP4 at day 3 and day 6 was assessed in A549 cells (Fig. 4.5). At day 3, nuclear phosphorylated Smad1/5/8 was detected in both A549 cells grown in serum-free medium alone and in serum-free medium containing 100 ng/ml BMP4 (Fig. 4.5 a, d). In addition, nuclear Smad4 was detected (Fig. 4.5 b, e). This nuclear accumulation of p-Smad1/5/8 and Smad4 was increased in BMP4-treated cells (Fig. 4.5 d, e). Nonetheless, BMP signalling was clearly active in untreated sub-confluent A549 cells at day 3 in the absence of exogenous BMP stimulation (Fig. 4.5 a, b). At day 6, p-Smad1/5/8 localisation was predominantly cytoplasmic with some weak nuclear translocation evident in untreated A549 cells (Fig. 4.5 g). However, this nuclear p-Smad1/5/8 was not co-localised with nuclear Smad4 (Fig. 4.5 h). In contrast, p-Smad1/5/8 localisation was predominantly nuclear in BMP4-treated cells at day 6 (Fig. 4.5 j). In addition, this nuclear p-Smad1/5/8 did co-localize with Smad4 in the majority of BMP4-treated A549 cells (Fig. 4.5 k). In summary, the BMP pathway was active in proliferating A549 cells cultured in serum-free culture medium. At day 6, a low level of nuclear p-Smad1/5/8 was visible in untreated confluent cells but appeared reduced compared to its day 3 counterpart. In contrast to untreated cells at day 6, A549 cells cultured in the presence of BMP4 exhibited sustained pathway activation with nuclear translocation of both p-Smad1/5/8 and Smad4 evident.

4.1.6. E-cadherin expression and localisation in BMP4-treated A549 cells

In the absence of hydrocortisone BMP4-treated A549 cells underwent changes in morphology consistent with an EMT such as a loss in cell-cell contact. For this reason we investigated whether E-cadherin was modulated in response to BMP4 under these cell culture conditions (Fig. 4.6). E-cadherin was assessed at the mRNA level in BMP4-treated A549 cells. E-cadherin was not reduced at the mRNA level but in fact was 2.4-fold increased compared to untreated A549 cells (Fig. 4.6, data also presented in Table 4.1). Despite the observed alteration in morphology, E-cadherin protein expression was not significantly reduced in A549 cells at day 6 (Fig. 4.6 B and C). Immunofluorescence revealed classic 'chickenwire' membrane E-cadherin localisation on untreated A549 cells. This membrane localisation was not apparent on BMP4-treated A549 cells lacking cell-cell contact. However, BMP4 did not appear to alter E-cadherin localisation between cells which were in direct cell-cell contact (Fig. 4.6 D).

4.1.7. Modulation of transcriptional repressors of E-cadherin in BMP4-treated A549 cells

E-cadherin was not modulated at the protein level and was found increased at the mRNA level in BMP4-treated A549 cells (Fig. 4.6). Inhibition of E-cadherin at the mRNA level in BMP4-treated BEAS-2B cells corresponded to increased expression of a number of transcriptional repressors of E-cadherin (Section 3.1.12). To gain an insight into whether E-cadherin was differentially regulated at the transcriptional level in response to BMP4 in A549 cells, a number of transcriptional repressors of E-cadherin were assessed (Fig. 4.7). Interestingly, SNAI1 and SNAI2 were upregulated in response to BMP4 at day 6 (Fig. 4.7 B). The level of upregulation was not statistically significant but was comparable to the increased levels detected in BEAS-2B cells following 6 days BMP4 treatment (Fig. 3.20). ZEB1 remained unchanged as assessed by semi-quantitative RT-PCR. In contrast to BEAS-2B cells, Twist was not detected in A549 cells cultured in medium alone or following BMP4 treatment at day 6 (Fig. 4.7 A).

4.1.8. Modulation of cytoskeletal and ECM-related genes in BMP4-treated A549 cells

Despite the lack of reduced E-cadherin expression following BMP4 treatment in A549 cells there did appear to be a loss in the characteristic epithelial morphology and gain of a mesenchymal phenotype. In light of this, the expression of a number of mesenchymal markers was assessed in A549 cells cultured in the presence of BMP4 for 6 days (Fig. 4.8). Similar to BEAS-2B cells desmin was significantly upregulated at day 6 (Fig. 4.8 B). In contrast, N-cadherin was not significantly altered. In addition, no change in the expression of fibronectin, vimentin, α-SMA or cytokeratin 18 was observed. In contrast to BEAS-2B cells, collagen Type 1A1 and 1A2 were not expressed by A549 cells under these cell culture conditions (Fig. 4.8 A).

In addition, PCR array analysis (performed by A Adams and JB Moore in Shirley O'Dea Laboratory) identified mesenchymal genes consistently upregulated in A549 cells in response to BMP4 (Table 4.1). These genes included a number of collagens, Collagen 5α1 (COL5A1), 6α2 (COL6A2), 16α1 (COL16A1) and 4α2 (COL4A2), the matrix metalloproteases, MMP2 and MMP10, the pro-fibrotic factor, TGF-β-induced (TGFBI) and extracellular matrix proteins, extracellular matrix protein 1 (ECM1) and vitronectin (VTN). Interestingly, many of the genes modulated in A549 cells in response to BMP4 were not among the genes changed in BMP4-treated BEAS-2B cells or were differentially altered to that seen in BEAS-2B cells (Table 4.1). Similarly, many of the genes modulated in BEAS-2B cells were either not detected (ND) or not changed (NC) in BMP4-treated A549 cells (Table 4.2)

Table 4.1 **Top 10 extracellular matrix-related genes regulated by BMP4 in A549 cells compared to BEAS-2B cells**

		A549 Cells		BEAS-2B Cells	
Gene Name	Symbol	P value	BMP4 /Untreated	P value	BMP4 /Untreated
Matrix metallopeptidase 2 (gelatinase A)	MMP2	0.0127	10.61	0.0001	-31.96
Transforming growth factor, beta-induced 68kDa	TGFBI	0.0123	7.22	0.0266	2.32
Collagen, type V, alpha 1	COL5A1	0.0255	7.04	0.0002	2.34
Contactin 1	CNTN1	0.0125	2.78	ND	ND
Collagen, type IV, alpha 2	COL4A2	0.0426	2.51	0.6513	-1.16
Cadherin 1, type 1, E-cadherin	CDH1	0.0275	2.41	0.0001	-15.15
Matrix metallopeptidase 10	MMP10	0.0782	2.33	ND	ND
Collagen, type VI, alpha 2	COL6A2	0.0242	2.26	0.0116	-2.42
Vitronectin	VTN	0.0332	2.20	0.7589	1.47
Extracellular matrix protein 1	ECM1	0.0206	2.17	0.2010	1.34
Collagen, type XVI, alpha 1	COL16A1	0.0105	1.96	0.3537	1.39
Selectin L	SELL	0.0377	1.86	ND	ND

Mean expression (Ct) values were calculated from n=3 arrays and fold difference between BMP4 and CTRL was calculated as $2\Delta\Delta C_t$. Fold changes less than 1 are expressed as the negative inverse. P values were calculated by Student's paired t-Test with a two-tailed distribution and significance established at $P<0.05$.

Table 4.2 **Top 10 extracellular matrix-related genes regulated by BMP4 in BEAS-2B cells compared to A549 cells**

		BEAS-2B Cells		A549 Cells	
Gene Name	Symbol	P value	BMP4 /Untreated	P value	BMP4 /Untreated
Vascular cell adhesion molecule 1	VCAM1	0.0014	13.48	ND	ND
Thrombospondin 2	THBS2	0.0001	9.17	ND	ND
C-type lectin domain family 3, member B (tetranectin)	CLEC3B	0.0007	8.82	ND	ND
Matrix metallopeptidase 16 (membrane-inserted)	MMP16	0.0000	7.05	ND	ND
Tenascin C (hexabrachion)	TNC	0.0015	5.51	NC	NC
Collagen, type V, alpha 1	COL5A1	0.0002	2.34	0.0255	7.04
Transforming growth factor, beta-induced, 68kDa	TGFBI	0.0266	2.32	0.0123	7.22
Catenin (cadherin-associated protein), delta 1	CTNND1	0.0458	-3.20	NC	NC
ADAM metallopeptidase w/thrombospondin type 1 motif, 8	ADAMTS8	0.0002	-4.12	ND	ND
Hyaluronan synthase 1	HAS1	0.0019	-4.77	NC	NC
Collagen, type VI, alpha 1	COL6A1	0.0011	-6.45	NC	NC
Cadherin 1, type 1, E-cadherin	CDH1	0.0001	-15.15	0.0275	2.41
Matrix metallopeptidase 2 (gelatinase A)	MMP2	0.0001	-31.96	0.0127	10.61

Mean expression (Ct) values were calculated from n=3 arrays and fold difference between BMP4 and CTRL was calculated as $2\Delta\Delta C_t$. Fold changes less than 1 are expressed as the negative inverse. P values were calculated by Student's paired t-Test with a two-tailed distribution and significance established at $P<0.05$.

In summary, A549 cells cultured in the presence of 100 ng/ml BMP4 undertook a mesenchymal change in morphology associated with increased desmin expression and upregulation of a number of mesenchymal-associated genes. However, despite an apparent upregulation in Snail1 and Snail2 no downregulation in E-cadherin was observed at the mRNA level or at the protein level following BMP4 treatment. In fact, E-cadherin was increased 2.4-fold at the mRNA level in A549 cells cultured with BMP4 at day 6 (Table 4.1). These BMP4-mediated effects on A549 cells were in contrast to those observed with BEAS-2B cells where upregulation of transcriptional repressors of E-cadherin corresponded to a 15-fold reduction in E-cadherin expression at the mRNA level (Table 4.1) and almost complete abrogation of E-cadherin at the protein level (Section 3.1.9).

4.1.9. Comparison of p-Smad1/5/8 levels in A549 and BEAS-2B cells in response to BMP4

BMP4 induced a marked decrease in E-cadherin mRNA and protein expression in BEAS-2B cells at day 6 (Section 3.1.9). In contrast, A459 cells cultured in the presence of BMP4 did not exhibit reduced E-cadherin protein expression and moreover had significantly elevated E-cadherin expression at the mRNA level at day 6. To gain an insight into whether the BMP pathway was differentially modulated in response to BMP4, phosphorylated Smad1/5/8 expression was assessed in BMP4-treated BEAS-2B cells and BMP4-treated A549 cells. BMP4 increased Smad1/5/8 phosphorylation in BEAS-2B cells after 20 min and 2 hr stimulation and this increase in p-Smad1/5/8 was sustained at day 6 (Section 3.1.4). The level of p-Smad1/5/8 in BEAS-2B and A549 cells in response to 100 ng/ml BMP4 stimulation was assessed at 20 min, 2 hr and day 6 (Fig. 4.9) (Note: BEAS-2B data at 20 min and 2 hr following BMP4 stimulation already presented in Fig. 3.3 A). Increased p-Smad1/5/8 expression was detected at 20 min, 2 hr and following 6 days BMP4 stimulation in both A549 and BEAS-2B cells (Fig. 4.9). However, at these time points the level of increased expression was not found to be significant in A549 cells (Fig. 4.9 B). This appeared to

be as a result of higher level of basal p-Smad1/5/8 expression in A459 cells in medium alone compared to BEAS-2B cells in medium alone (Fig. 4.9 B). At 20 min, 2 hr and day 6 an average increase in p-Smad1/5/8 expression of 46 %, 25 % and 10 % respectively was detected in A549 cells compared to BEAS-2B cells in serum-free medium alone (Fig. 4.9 B). However, across three experiments this increased expression was not found to be significant. Nonetheless, this increased level of p-Smad1/5/8 in the absence of exogenous BMP4 stimulation may explain the reduced induction of p-Smad1/5/8 expression in A549 cells in response to BMP4 compared to the statistically significant increase in p-Smad1/5/8 expression seen in BMP4-treated BEAS-2B cells.

4.1.10. BMP pathway mRNA expression in A549 and BEAS-2B cells at day 6

To identify whether the BMP pathway was differentially regulated in A549 cells compared to BEAS-2B cells, BMP pathway components were assessed in A549 and BEAS-2B cells cultured with 100 ng/ml BMP4 at day 6 by semi-quantitative RT-PCR (Fig. 4.10). No significant alteration was seen with BMPR-IA in either cell line in response to BMP4. However, there was a trend to suggest BMPR-IA may have been upregulated at the mRNA level in response to BMP4 in BEAS-2B cells (Fig. 4.10 B). BEAS-2B cells did not express BMPR-IB at the mRNA level under our cell culture conditions (Fig. 4.10). In contrast, BMPR-IB was detected in A549 cells and was significantly reduced in response to BMP4 (Fig. 4.10 B). BMPR-II was also significantly reduced in A549 cells at day 6 following BMP4 treatment. No significant modulation in BMPR-II at the mRNA level was detected in BEAS-2B cells at day 6 (Fig. 4.10). Smad1, 5, and 7 were not significantly changed in response to BMP4 at day 6 in either cell line. However, there was a trend to suggest Smad7 may have been upregulated in response to BMP4 in BEAS-2B cells (Fig. 4.10 B). BMP4 and BMP6 mRNA was significantly modulated in A549 cells in response to BMP4. A slight decrease in BMP4 mRNA was detected whereas BMP6 was significantly upregulated in A549 cells at day 6 (Fig. 4.10). Conversely, no effect on BMP4 or BMP6 mRNA

was detected in BEAS-2B cells in response to BMP4. However, there was a trend to suggest BMP6 may be downregulated in BEAS-2B cells at day 6 following BMP4 treatment (Fig. 4.10).

Id1 was significantly upregulated in BEAS-2B cells in response to BMP4. A similar increase was seen in A459 cells but was not found to be significant. Id1 was expressed at a relatively higher level in A549 cells compared to BEAS-2B cells (Fig. 4.10). This increased basal expression may explain the moderate upregulation in response to BMP4 stimulation compared to the dramatic increase in Id1 expression in BEAS-2B cells following BMP4 treatment (Fig. 4.10 B). Smad4 was not modulated in response to BMP4 at the mRNA level in either cell line (Fig. 4.10). TGF-β1 was upregulated in both BEAS-2B and A549 cells in response to BMP4 at day 6. However, this increase was only found to be significant in BEAS-2B cells (Fig. 4.10 B).

4.2. Discussion

We have previously identified an EMT-like response in BEAS-2B cells in response to BMP4. In order to determine whether other lung cell lines responded similarly to BMPs, we decided to examine the widely-used A549 cell line. It had previously been reported that BMP4 induced senescence in A549 cells (Buckley et al., 2004). In contrast, BMP2 had been shown to increase proliferation of A549 cells *in vitro* (Langenfeld et al., 2003, Langenfeld et al., 2006). However, both of these effects were dependent on the addition of serum in the culture medium. Our BEAS-2B BMP studies were carried out in serum-free medium. We therefore examined the effect of BMP2 and BMP4 on A549 cells in serum-free medium. Consistent with previous reports, BMP4 induced senescence in A549 cells under our cell culture conditions. At day 6, A549 morphology was enlarged following BMP4 treatment and a significant increase in SA-β-gal expression was detected (Figure 4.1 and Figure 4.2). In contrast, BMP2 under the same cell culture conditions did not appear to induce senescence in A549 cells. BMP2 had no significant effect on cell proliferation and SA-β-Gal was significantly reduced.

Interestingly, when hydrocortisone (HC) was omitted from the serum-free culture medium, the BMP4-induced senescence morphology was lost (Figure 4.3). Instead BMP4-treated A549 cells displayed a change in morphology which more closely resembled an EMT. Cells in the presence of BMP4 appeared more angular and there was a reduction in cell-cell contact. There was no significant induction of SA-β-gal under these cell conditions (Figure 4.4). The effect of BMP2 was similar when HC was present or absent. BMP2-induced cell morphology and proliferation was comparable to untreated cells while SA-β-gal expression remained reduced at day 6 in BMP2-treated cells compared to untreated.

BMPs are potent inducers of bone formation during development and in the adult (Chen et al., 2004). Excess cortisol (naturally occurring form of hydrocortisone) has been linked to bone loss and osteoporosis (Chiodini et al., 2008). Cortisol excess

inhibits bone formation, increases bone resorbtion and can affect a number of growth factors involved in bone metabolism. In addition, cortisol and BMP2 have opposing roles during stromal cell differentiation. BMP2 promotes an osteoblastic phenotype in pluripotent stromal cells whereas cortisol can mediate the differentiation of these cells into adipocytes (Pereira et al., 2002). Furthermore, glucocorticoid-induced stromal cell differentiation towards an adipocyte fate can occur at the expense of osteoblastic cell differentiation suggesting glucocorticoids such as cortisol may directly inhibit BMPs (Pereira et al., 2002). Similarly, BMP2 can oppose the inhibitory effects of cortisol on TGF-β activity in differentiated osteoblasts (Centrella et al., 1997). Taken together, BMPs and cortisol have opposing roles during bone development and bone homeostasis. We hypothesised hydrocortisone in our serum-free medium inhibited certain effects mediated by BMP4 in lung epithelial cells thus affecting the outcome of BMP4-mediated signalling.

Because we were interested in the EMT effects of BMPs, subsequent experiments were carried out in hydrocortisone free (-HC) medium. BMP pathway activation was assessed. Smad1//5/8 and Smad4 were activated in response to BMP4. Increased expression of p-Smad1/5/8 was detected in A549 cells following 20 min, 2 hr and 6 days BMP4 stimulation. In addition, increased nuclear accumulation of p-Smad1/5/8 and Smad4 was detected in BMP4-treated cells at day 3 and this was sustained up to day 6. Interestingly, nuclear p-Smad1/5/8 and Smad4 were detected in sub-confluent A549 cells at day 3 cultured in serum-free medium alone. This pathway activity had subsided in untreated cells upon reaching confluency at day 6 where some weak nuclear accumulation of p-Smad1/5/8 was visible with no detection of nuclear Smad4. This level of pathway activation in cells cultured in serum-free conditions in the absence of exogenous BMP indicates A549 cells are producing BMPs *in vitro*. Furthermore, pathway activity in sub-confluent cells which became reduced upon cells reaching confluency suggests BMP signalling is linked to A549 proliferation. Increased BMP signalling has been widely reported in cancer and is likely to promote proliferation of the tumorigenic cells. In addition, it is possible activated BMP

signalling during cancer may promote EMT of the epithelioid tumor leading to metastasis.

E-cadherin expression was upregulated 2.4-fold at the mRNA level in A549 cells. Despite this, the E-cadherin transcriptional repressors Snail1 and Snail2 were also upregulated at the mRNA level in A549 cells and the increased levels were comparable to that observed in BEAS-2B cells following BMP4 treatment (Figure 4.7). In contrast to BEAS-2B cells, Twist was not expressed by A549 cells under our cell culture conditions. The lack of E-cadherin downregulation at the mRNA level in A549 cells suggests Snail1 and Snail2 are not sufficient to inhibit E-cadherin expression or another mechanism is in place to counteract their inhibitory action.

At day 6, E-cadherin protein was not reduced in A549 cells in response to BMP4 as had occurred with BEAS-2B cells. Immunofluorescence analysis revealed classic 'chicken wire' E-cadherin and β-catenin (data not shown) localisation at day 6 in untreated A549 cells which remained largely unaltered in response to BMP4 at day 1, day 3 and day 6. However, an absence of membrane localisation was observed on BMP4-treated cells lacking cell-cell contact. E-cadherin can be endocytosed from the membrane to regulate adherens junction stability. This occurs under normal cell conditions to mediate processes such as mitosis and apoptosis. Following endocytosis, E-cadherin can be recycled to the membrane, temporally sequestered inside the cell and/or degraded (Bryant and Stow, 2004). Therefore, while E-cadherin is likely to be modulated in BMP4-treated cells lacking cell to cell contact in order to facilitate movement it may not involve degradation at the protein level or inhibition at the level of transcription.

Despite a lack of E-cadherin inhibition, regarded as the first step during the EMT process, BMP4-treated A459 cells did appear to adopt an increasingly mesenchymal morphology with an increase in angular shape and loss in cell-cell contact. For this reason, mesenchymal markers were assessed in BMP4-treated cells. Desmin was significantly upregulated in A549 cells (Figure 4.8) similar to that observed in BEAS-

2B cells (Figure 3.18). This upregulation in desmin expression indicates some mesenchymal genes may be upregulated in the absence of reduced E-cadherin expression. Collagen IA1 and IA2 were not detected in A549 cells nor were they induced following BMP4 treatment. Similarly, no alteration of vimentin, fibronectin, α-SMA or cytokeratin expression was observed. However, expression of these genes was also largely unaltered in BEAS-2B cells despite the loss in E-cadherin expression seen in these cells.

PCR array analysis of BMP4-treated A549 cells revealed a number of ECM-related genes modulated by BMP4 (QPCR performed by A Adams and JB Moore in Shirley O'Dea Laboratory). Upregulation of several collagens as well as extracellular matrix proteins, ECM1 and vitronectin were detected. Increased expression of these genes supports the acquisition of a mesenchymal phenotype in response to BMP4. In addition, increased expression of MMP2 and MMP10 was detected by day 6 indicating a possible increased migratory potential of A549 cells following BMP4 treatment. VCAM1, thrombospondin 2 and MMP16 were not detected in A549 cells whereas these genes were among the most highly upregulated genes in BMP4-treated BEAS-2B cells. Similarly, contactin 1 and selectin L were significantly upregulated in BMP4-treated A549 cells but conversely were not expressed by BEAS-2B cells in serum-free medium alone or following BMP4 treatment. Therefore, any EMT-like response is likely to be cell-type specific in terms of the genes which are altered and the extent to which they change.

Differences in BMP signalling between BEAS-2B and A549 cells may explain some of the differences in the BMP4 response observed between these two cell types. P-Smad1/5/8 was increased in A549 cells following BMP4 stimulation but the level of increased expression was not found to be significant (Figure 4.9). In contrast, a significant increase in p-Smad1/5/8 expression was detected in BEAS-2B cells following 20 min, 2 hr and 6 days BMP stimulation. P-Smad1/5/8 expression was compared between BEAS-2B and A549 cells. A549 cells appeared to express constitutively higher levels of p-Smad1/5/8 in cells cultured in serum-free medium

alone. This indicated a more quiescent BMP pathway in BEAS-2B cells in serum free medium when compared to A549 cells. In BEAS-2B cells, p-Smad1/5/8 expression increased dramatically following the addition of exogenous BMP4. A similar trend was observed with respect to Id1 expression. Id1, a member of the helix-loop-helix (HLH) family of transcription factors, is a well recognised target of BMP signalling. Id genes are not regarded as classical oncogenes. However, there expression is induced by a number of oncogenes including RAS, MYC and ETS. Elevated levels have been detected in a number of cancer types and are thought to directly contribute to the neoplastic transformation of a cell by their ability to inhibit differentiation, enhance proliferation and invasiveness (Perk et al., 2005). A549 cells expressed relatively higher levels of Id1 compared to BEAS-2B cells. Consequently, increased Id1 levels in A549 cells following BMP4 stimulation were not found to be significant. In contrast, Id1 was significantly upregulated in BEAS-2B cells in response to BMP4. Taken together these data indicate BMP signalling may be more active in A549 cells compared to BEAS-2B cells. As a result, A549 cells appeared less responsive to BMP4 stimulation *in vitro*.

Further investigation into BMP pathway expression by A549 and BEAS-2B cells revealed variations in BMP pathway modulation in response to BMP4 at day 6. Of particular interest was the lack in expression of BMPR-IB mRNA by BEAS-2B cells at day 6. In contrast, BMPR-IB was detected in A549 cells. In addition there was a trend to suggest BMPR-IA may be upregulated at the mRNA level in BEAS-2B cells where no modulation was apparent in A549 cells. This indicates BMP4-mediated signalling in A549 cells compared to BEAS-2B cells may involve the differential recruitment of BMP receptors. Interestingly, BMPR-IB and BMPR-II were significantly downregulated following BMP4 stimulation in A549 cells. Despite this reduction in receptor expression at the mRNA level the pathway was highly active as determined by p-Smad1/5/8 expression in A549 cells. These findings support other work generated in our laboratory which found that BMPR-IB mRNA and protein are reduced in lung adenocarcinoma while p-Smad and Smad4 mRNA and protein are elevated compared to normal lung cells. It is likely this reduction in receptor

expression may serve to deregulate BMP signalling resulting in constitutive pathway activation. In contrast to A549 cells Smad7 was upregulated following BMP4 treatment in BEAS-2B cells. This indicates negative feedback signalling active specifically in BEAS-2B cells and supports further the possible deregulated phenotype of BMP signalling in A549 cells.

Analysis of BMP4 and BMP6 mRNA also revealed variations in the expression profile between A549 and BEAS-2B cells. BMP4 mRNA was significantly reduced in BMP4-treated A549 cells where no modulation was detected in BMP4-treated BEAS-2B cells. BMP6 was significantly elevated in A549 cells but appeared reduced in BEAS-2B cells following BMP4 treatment. In breast cancer, BMP6 has been shown to induce E-cadherin expression by in inhibiting ZEB1 (transcriptional repressor of E-cadherin) from binding to the E-cadherin promoter (Yang et al., 2007). The study characterised the expression of BMP6 and ZEB1 in human breast cancer specimens and found an inverse relationship between BMP6/E-cadherin expression and ZEB1. ZEB1 expression was assessed in A549 cells at day 6 following BMP4 treatment but was not found to be changed (Figure 4.7). Nonetheless, it is tempting to hypothesise a similar mechanism occurs in lung cancer and increased BMP6 is indirectly responsible for increased E-cadherin expression in BMP4-treated A549 cells. This hypothesis was supported in BEAS-2B cells where inhibition of E-cadherin transcription correlated with increased ZEB1 and reduced BMP6 at the mRNA level.

It remains unclear however by what means the addition of exogenous BMP4 resulted in the opposing effects on E-cadherin seen in BEAS-2B and A459 cells. BMP4 treatment increased BMP6 at the mRNA level in A549 cells. No increase in BMP6 expression was seen in response to BMP4 in BEAS-2B cells at day 6. Therefore the increased levels of phosphorylated Smad1/5/8 expression in BMP4-treated A549 cells may be mediated through BMP6. In addition, BMP4 mRNA was significantly reduced in response to BMP4 in A459 cells at day 6. This indicates expression of BMP4 and BMP6 may be inversely related. It is likely the established pathway activity in A549 cells which may be mediated via BMP6 has resulted in cells which are less sensitive to

BMP4 stimulation. In contrast, BEAS-2B cells having a lower level of BMP pathway activity are increasingly responsive to BMP4 and as a result BMP4-mediated signalling predominates.

In summary, BMP4 induced differential effects in A549 cells in the presence and absence of hydrocortisone. In keeping with previous published literature, BMP4 did appear to induce senescence when A549 cells were cultured in the presence of hydrocortisone. However, an EMT-like change in morphology was apparent under hydrocortisone-free conditions in BMP4-treated A549 cells. This EMT-like change in morphology was associated with increased expression of a number of mesenchymal genes. However, despite this, E-cadherin was not downregulated at day 6. A possible explanation for this may be attributed to the significant upregulation of BMP6 at the mRNA level, a BMP ligand known to induce E-cadherin expression. Further investigation is required to determine whether BMP6 can in fact induce E-cadherin expression in lung epithelial cells. If so, overexpression of BMP6 may provide a possible mechanism to reverse the EMT process.

In addition these data provide a novel insight into crosstalk between glucocorticoid and BMP signalling in adult airway epithelial cells (AECs). Inhaled glucocorticoids remain the most effective treatment to reduce inflammation during asthma (Walsh, 2006). Glucocorticoids exert their anti-inflammatory effects via inhibition of immune cell recruitment, downregulation of inflammatory gene expression and by reducing the numbers of activated eosinophils, mast cells and T-cells. Our study has highlighted hydrocortisone (HC) as a determining factor in the outcome of activated BMP signalling in A549 lung epithelial cells. HC is the synthetic form of cortisol, a member of the glucocorticoid family of steroid hormones. In the presence of HC, BMP4 induced a senescent-like phenotype whereas in the absence of HC BMP4-treated A549 cells undertook a mesenchymal change in morphology associated with increased collagen expression. It is interesting to consider a similar interplay may occur *in vivo*. BMP can induce EMT in lung epithelial cells (Molloy et al., 2008) and the BMP pathway is activated during airway inflammation (Rosendahl et al., 2002). In addition,

TGF-β signalling is active during asthma. TGF-β1 is widely accepted as a prototypic inducer of EMT in a variety of cell types. Therefore, it is possible EMT may be involved in asthma pathology leading to a loss of epithelial barrier integrity, fibrosis and collagen deposition. In our study, BMP4 did not appear to induce a mesenchymal phenotype in BEAS-2B cells in the presence of HC. Instead, BMP4 induced a senescent phenotype in the presence of HC. No studies to date have characterised the senescent phenotype. However, data generated in our laboratory has shown that following BrdU-induced senescence in normal murine AECs (MAECs) the expression and localisation of the adherens junction complex, including E-cadherin, remained unaltered. These data suggest senescent AECs maintain epithelial integrity (data generated in Shirley O'Dea by Joanne C Masterson). Taken together, it is possible the induction of a senescent phenotype in response to BMP4 in the presence of HC may preserve epithelial barrier integrity *in vivo*. Whereas activated BMP-signalling in the absence of HC may promote EMT leading to exacerbation of inflammation. These data highlight a possible alternate means by which glucocorticoids may reduce inflammation in the asthmatic lung.

5.0 BMP4-mediated signalling in Primary Murine Airway Epithelial Cells

5.1. Introduction

We have previously characterised an EMT-like response in BEAS-2B cells cultured in the presence of BMP4 for six days. This was the first report of BMP4-induced EMT in bronchial lung epithelial cells. However, BEAS-2B cells are bronchiolar epithelial cells which have been transformed with SV-40 and therefore could behave differently to normal airway epithelial cells. We therefore investigated the ability of BMP4 to induce similar changes in normal primary murine airway epithelial cells (MAECs).

MAECs represent a population of primary airway epithelial cells that are >80% enriched for Clara cells (McBride et al., 2000). *In vivo*, Clara cells are involved in critical processes such as detoxifying harmful agents and surfactant production. In addition to their roles as differentiated airway epithelial cells, Clara cells retain to ability to proliferate in response to injury to give rise to both Clara and ciliated cell types. However, normal MAECs are difficult to isolate and culture successfully, are harvested in relatively low numbers (approximately 1.5 X 10^6 per mouse) and only survive approximately 7 days *in vitro*. Because of this, normal MAEC cultures are used by relatively few laboratories. The technique is well-established in the O'Dea laboratory (McBride et al., 2004).

The aims of this study were to examine whether MAECs express a BMP pathway and whether this pathway can be activated *in vitro* with exogenous BMP2 and BMP4 stimulation. In addition, MAECs were cultured in the presence of BMP4 in order to determine whether BMP4 can modulate MAEC morphology and downregulate E-cadherin consistent with an EMT.

5.1.1. BMP pathway expression in MAECs in the absence of exogenous BMP stimulation

It had not been previously demonstrated whether primary murine airway epithelial cells (MAECs) possess a BMP pathway. MAECs cultured in serum-free medium were assessed for BMP pathway expression. BMP receptors BMPR-IA, BMPR-IB and BMPR-II as well as the intracellular signalling molecules Smad5, Smad8 and Smad4 were examined by immunofluorescence. In addition, a p-Smad1/5/8 antibody was used which cross reacts with the phosphorylated form of Smad1, 5 and 8 to assess the activity of these molecules in MAECs.

Initially BMP pathway components were assessed in untreated MAECs cultured in defined serum-free medium (DSFM) for 20 min, 2 hr and 17 hr. BMPR-IA was localised to the cytoplasm of MAECs cultured in serum free medium (Fig. 5.1). BMPR-IA localisation and level of expression remained constant over the time course (Fig. 5.1 a-c). BMPR-IB, similar to BMPR-IA, did appear predominantly localised to the cytoplasm (Fig. 5.1). However, in MAECs membrane localisation of BMPR-IB was apparent at 20 min and 2 hr (Fig. 5.1 d, e). This apparent membrane localisation was not visible at 17 hrs (Fig. 5.1 f). BMPR-II was localised to the nuclei of untreated MAECs and this localisation did not appear to change over the time course (Fig. 5.1 g-i). Smad5 was expressed at low levels in untreated MAECs (Fig. 5.2 a, b) with a low level of nuclear localisation visible at 17 hr (Fig. 5.2 c). Smad8 was observed in the cytoplasm of untreated MAECs (Fig. 5.2). The level of expression appeared reduced at 17 hr compared to 2 hr and 20 min in untreated cells (Fig. 5.2 d-f). P-smad1/5/8 was predominantly localised to the nuclei of MAECs over the time course experiment (Fig. 5.2 g-i). Smad4 at 20 min was localised to the nuclei of MAECs (Fig. 5.2 j). At 2 hr and 17 hr, Smad4 was expressed predominantly in the cytoplasm of untreated cells (Fig. 5.2 j-l). The presence of phosphorylated Smad in the nuclei of MAECs cultured in serum free medium suggests BMP signalling is active in these cells.

5.1.2. BMP pathway activation in MAECs in response to BMP2 and BMP4 stimulation

In order to assess whether MAECs responds to BMP stimulation, MAECs were cultured in the presence of either 100 ng/ml BMP2 or BMP4 for 20 min, 2 hrs and 17 hrs.

The expression of BMPR-IA did not appear altered in response to BMP2 and BMP4 stimulation over the time course experiment (Fig. 5.3 A). Western blot analysis confirmed this antibody detects a protein at the correct size in mouse lung and MLE cell whole cell lysate (Fig. 5.3 B). Immunofluorescence analysis of BMPR-IA localisation in mouse airway revealed basolateral localisation of the receptor suggesting murine airway epithelial cells do express BMPR-IA *in vivo* (Fig. 5.3 C). BMPR-IB membrane localisation appeared reduced following BMP2 and BMP4 treatment at 20 min and 2 hr (Fig. 5.4 a-c, d-f, respectively). However, the levels of cytoplasmic expression did not appear altered over the time course (Fig. 5.4). BMP2 and BMP4 stimulation resulted in an apparent relocalisation of BMPR-II to the cytoplasm (Fig. 5.5 A). MAECs stimulated with BMP2 had increased cytoplasmic expression after 20 min (Fig. 5.5 A b). However, nuclear expression of the receptor remained after 17 hr BMP2 stimulation (Fig. 5.5 A h). Similarly, cells cultured in the presence of BMP4 had increased expression of BMPR-II in the cytoplasm at 20 min (Fig. 5.5 A c) which was further increased after 2 hr (Fig. 5.5 A f). After 17 hr of BMP4 stimulation little or no nuclear BMPR-II was observed (Fig. 5.5 A i). Confocal microscopy was used to assess nuclear localisation of BMPR-II and revealed distribution of BMPR-II throughout the nuclei in MAECs (Fig. 5.5 B).

Smad5 cytoplasmic expression was increased with BMP2 and BMP4 stimulation at 20 min, 2 hr and 17 hr (Fig. 5.6 A). Increased nuclear localisation was apparent at 17 hrs in BMP2-treated cells (Fig. 5.6 A h, denoted by arrows). Smad8 nuclear localisation was observed after 20 min BMP2 and BMP4 stimulation (Fig. 5.7 a-c). At 2 hr Smad8 expression levels were comparably between untreated and BMP2- and BMP4-treated

cells (Fig. 5.7 d-i). At 17 hr the level of Smad8 appeared elevated in BMP2-treated cells compared to untreated where virtually no Smad8 was visible (Fig. 5.7 g, h). Smad8 nuclear localisation was detected in BMP4-treated cells at 17 hr (Fig. 5.7 i). Following 20 min BMP2 and BMP4 stimulation similar levels of p-smad1/5/8 were localised to the nuclei in MAECs (Fig. 5.8 A). At 2 hrs an increase in cytoplasmic expression was apparent with BMP2 and BMP4 stimulation (Fig. 5.8 A e, f). At 17 hr p-Smad1/5/8 was localised to the nuclei in both BMP2- and BMP4-treated cells (Fig. 5.8 A h, i). This level of nuclear localisation was increased in BMP2- and BMP4-treated cells compared to untreated cells at the same time point (17 hr) (Fig. 5.8 g-i). P-Smad1/5/8 expression was also assessed by western blot in MAECs at day 3 in both untreated and BMP4-treated cells (Fig. 5.8 B and C). An increase in p-Smad1/5/8 levels was detected in response to both 50 ng/ml and 100 ng/ml BMP4 (Fig. 5.8 B). BMP4 at 100 ng/ml resulted in a significant increase in p-Smad1/5/8 expression (Fig. 5.8 C). Smad4 nuclear localisation was increased in BMP2- and BMP4-treated cells at 20 min (Fig. 5.9 A a-c) and this nuclear translocation was sustained at 2 hr and 17 hr (Fig. 5.9 A h, i).

5.1.3. **BMP4 effect on morphology at low and high seeding density**

MAECs in culture are sensitive to seeding density where a low seeding density may increase the onset of replicative senescence in culture. For this reason, cells were seeded at different densities to identify one which was optimal for subsequent BMP experiments. MAECs were seeded according to an absorbance value obtained using the Cell Titer 96® AQueous One Solution Cell proliferation Assay since these cells are isolated in clumps and cannot be counted. MAECs were seeded at 0.15 OD/cm^2, 0.2 OD/cm^2 and 0.25 OD/cm^2. Cells seeded at low density became enlarged by day 3 at which time multi-nucleation was evident suggesting these cells may be senescent in culture (Fig. 5.10 a). No evidence of senescent-like cells was observed when cells were seeded at the higher density of 0.25 OD/cm^2. At this density MAECs retained the characteristic epithelial cobblestone morphology (Fig. 5.10 c).

MAECs stimulated with BMP4 at 100 ng/ml at both a low (0.15 OD/cm^2) and high (0.25 OD/cm^2) seeding density (Fig. 5.10). Low density MAECs did change morphologically when cultured with 100 ng/ml BMP4 with elongated cells visible in culture which was not seen in untreated cells (Fig. 5.10 a, b). High density MAECs cultured with 100 ng/ml BMP4 had a more pronounced morphology change with cells which looked fibroblast in nature with loss of cell-cell contact apparent (Fig. 5.10 c, d). In some cases this morphology change did appear restricted to small sub populations. This high seeding density of 0.25 OD/cm^2 was used for subsequent experiments.

5.1.4. BMP4 effect on morphology in MAECs cultured in BEAS-2B conditioned media (CM)

Overall the change in morphology observed when MAECs were cultured with BMP4 was not as dramatic as seen previously with BMP4-treated BEAS-2B cells. MAECs were routinely cultured in defined serum-free medium (DSFM). However, EMT is a complex process likely to involve an array of growth factors. It is possible that BEAS-2B cells, which are immortalised, produce these factors while normal MAECs in the current culture conditions do not. Therefore, as an alternative to DSF medium, MAECs were cultured in conditioned medium from BEAS-2B cells which had been cultured in DSF medium for 6 days (CM).

MAECs cultured in CM medium alone appeared more angular compared to cells grown in dSF medium alone (Fig. 5.11 a, b). MAECs cultured in CM medium were treated with 100 ng/ml BMP4. Fibroblast-like cells were observed in CM medium at day 6 following BMP4 treatment (Fig. 5.11 d) similar to BMP4-treated cells in DSFM (Fig. 5.11 c). MAECs in CM medium did respond to BMP4 with increased p-Smad1/5/8 at day 3 in the presence of 100 ng/ml BMP4 (Fig. 5.12 A). However, despite an apparent morphology effect with MAECs cultured in CM medium, no increase in p-Smad1/5/8 levels were detected in MAECs in CM medium alone when compared to cells cultured in DSFM alone (Fig. 5.12 B).

5.1.5. E-cadherin localisation in response to BMP4 treatment

MAECs cultured in DSF and CM medium responded to BMP4 with increased p-Smad1/5/8 expression at day 3. There was an apparent morphology change in response to both 50 ng/ml and 100 ng/ml BMP4 under both sets of conditions. To determine whether this alteration in morphology corresponded to changes in E-cadherin, E-cadherin localisation was assessed by immunofluorescence in cells cultured in both DSFM (Fig. 5.13) and CM medium (Fig. 5.14) in response to 50 ng/ml BMP4 or 100 ng/ml BMP4 at day 2 and day 4.

5.1.5.1. Defined serum free medium (DSFM)

At day2, MAECs cultured in DSFM exhibited the characteristic 'chicken wire' E-cadherin staining at the cell membrane at points of cell-cell contact (Fig. 5.13 a). MAECs at low density appeared larger morphologically and had reduced 'chicken wire' E-cadherin localisation (Fig. 5.13 b). MAECs cultured in the presence of either 50 ng/ml or 100 ng/ml BMP4 did not appear to have altered E-cadherin expression on cells at high density (Fig. 5.13 c, e). However, cells at low density appeared to have reduced E-cadherin in response to 50 ng/ml and 100 ng/ml BMP4 treatment (Fig. 5.13 d, f). At day4, untreated MAECs (Fig. 5.13 g, h) appeared to have similar E-cadherin staining compared to day 2 (Fig. 5.13 a, b). At day 4, MAECs at high density cultured with either 50 ng/ml or 100 ng/ml BMP4 appeared more angular in morphology with a possible increase in cytoplasmic E-cadherin localisation (Fig. 5.13 i, k). MAECs at low density cultured in the presence of either 50 ng/ml or 100 ng/ml BMP4 had reduced E-cadherin expression apparent compared to untreated MAECs at a similar low cell density (Fig. 5.13 h, j, l).

5.1.5.2. Conditioned medium (CM)

At day 2 untreated MAECs in CM medium had a similar E-cadherin localisation (Fig. 5.14 a, b) compared to DSF medium at day 2 (Fig. 5.13 a, b). Cells cultured in the presence of 50 ng/ml and 100 ng/ml did not appear to have greatly altered E-cadherin

localisation on cells at high density (Fig. 5.14 c, e). However on cells al low density E-cadherin localisation appeared more cytoplasmic with both 50 ng/ml and 100 ng/ml BMP4 compared to untreated cells (Fig. 5.14 b, d, f). At day 4, similar 'chicken wire' expression was apparent on untreated MAECs at high density which did not appear altered by either 50 ng/ml or 100 ng/ml BMP4 treatment (Fig. 5.14 g, i, k). At day 4, E-cadherin expression appeared reduced on MAECs at low density (Fig. 5.14 h) compared to day 2 (Fig. 5.14 b). No further reduction in E-cadherin expression or altered localisation was seen in response to BMP4 on MAECs at low density at day 4 (Fig. 5.14 h, j, i).

5.1.6. **E-cadherin protein expression in response to BMP4 treatment**

Immunofluorescence analysis revealed reduced E-cadherin expression in BMP4-treated MAECs cultured in DSF medium which was most apparent in response to 100 ng/ml BMP4 at day 4. To further assess this reduction in E-cadherin expression, E-cadherin protein level was investigated in both DSFM and CM medium in response to 50 ng/ml and 100 ng/ml (DSFM only) BMP4 (Fig. 5.15). The E-cadherin antibody used in this study recognises both the full length E-cadherin (120 kDa) and a truncated form of the protein (33 kDa). This truncated form represents membrane-associated E-cadherin which has been cleaved. This can occur in a cell to regulate adherens junction stability. At day 3, E-cadherin was downregulated in response to 100 ng/ml BMP4. A similar downregulation was not seen with 50 ng/ml BMP4 in DSF medium or 100 ng/ml BMP4 in CM medium (Fig. 5.15). In addition, 100 ng/ml BMP4 also resulted in a significant inhibition in the level of truncated E-cadherin within the cell (Fig. 5.15). No change in the level of expression of the truncated isoform was seen in MAECs in response to 50 ng/ml BMP4 in DSF medium or 100 ng/ml BMP4 in CM medium (Fig. 5.15).

5.1.7. E-cadherin mRNA expression in response to BMP4 treatment

E-cadherin protein appeared downregulated in response to BMP4 at day 3 in MAECs cultured in serum-free medium (DFSM). In order to gain a better insight into whether this downregulation of E-cadherin had occurred at the transcriptional level, E-cadherin mRNA expression was assessed by quantitative PCR (QPCR) at day 2, day 4 and day 5 in MAECs cultured in the presence of 10, 50 or 100 ng/ml BMP4 in serum-free medium (DSFM) (Fig. 5.16 A). At day 2, E-cadherin mRNA expression was reduced in response to 10, 50 and 100 ng/ml BMP4 (Fig. 5.16 A). At day 4, E-cadherin inhibition was sustained. At day 5, MAECs cultured in the presence of 10 ng/ml BMP4 no longer exhibited a reduction in E-cadherin expression while E-cadherin mRNA remained reduced in MAECs in response to 50 and 100 ng/ml BMP4 at day 4 (Fig. 5.16 A).

5.1.8. Snail1 mRNA expression in response to BMP4 treatment

E-cadherin mRNA was reduced in response to BMP4. For this reason Snail1 mRNA, a transcriptional repressor of E-cadherin, was assessed by semi-quantitative PCR (RT-PCR). At day2, Snail1 expression was elevated in MAECs in response to 10, 50 and 100 ng/ml BMP4 (Fig. 5.16 B). This increase in Snail1 expression was only found to be significant in response to 100 ng/ml BMP4 (Fig. 5.16 B). At day 4 and day 5, the level of Snail1 expression in BMP4-treated MAECs appeared comparable to that detected in untreated MAECs (Fig. 5.16 B).

5.2. Discussion

While BMP2 does not appear to be expressed in the developing lung, abrogation or misexpression of BMP4 leads to abnormal lung development highlighting a pivotal role for this growth factor during lung morphogenesis (Bellusci et al., 1996, Weaver et al., 1999, Eblaghie et al., 2005). We have previously demonstrated an epithelial-mesenchymal transition (EMT) in BEAS-2B cells in response to BMP4 (Molloy et al., 2008). This effect combined with the known role of BMP4 in lung development led us to investigate the effect of BMP4-mediated signalling on normal murine airway epithelial cells (MAECs).

Initially we investigated the presence of a BMP signalling pathway in MAECs cultured in serum-free medium alone. Rosendahl et al., in a study of BMP signalling in the OVA mouse model had reported the presence of BMPR-IA and BMPR-IB in the cytoplasm of bronchial epithelial cells in mouse lungs (Rosendahl et al., 2002). BMPR-IA and BMPR-IB were expressed by MAECs and similar to Rosendahl et al., both receptors appeared predominantly localised to the cytoplasm. However, BMPR-IB expression at the cell membrane at points of cell-cell contact was observed. Over time this membrane localisation was reduced indicating possible receptor internalisation. BMPR-II was localised to the nuclei of MAECs and in some cells cytoplasmic localisation was observed. Nuclear translocation of growth factor receptors has been widely reported (Planque, 2006, discussed further in section 0). In addition, nuclear translocation of the TGF-β type I receptor has been reported (Zwaagstra at al., 2000) but whether type II receptors possess a similar function is currently unknown.

In addition to the BMP receptors the expression and localisation of the intracellular signalling molecules Smad5 and Smad8 was investigated. Smad5 and Smad8 were detected in the cytoplasm of MAECs cultured in serum free medium alone and in some cases nuclear translocation was apparent. MAECs therefore possess the BMP pathway components necessary to transduce BMP signals. In order to assess whether

BMP signalling is ongoing in untreated MAECs we investigated the expression and localisation of phosphorylated Smad1/5/8. Phosphorylation of the Smad signalling proteins and subsequent nuclear translocation is a hallmark of activated BMP signalling (Von Bubnoff and Cho, 2001). Interestingly, p-Smad1/5/8 expression was detected in untreated MAECs and appeared predominantly localised to the nuclei. Furthermore, this nuclear localisation appeared sustained over the time course experiment. This combined with the apparent alterations in localisation of BMPR-IB at the membrane of untreated MAECs and the occurrence of nuclear Smad5 provide strong evidence that BMP signalling is active in untreated MAECs and modulates over time in the absence of exogenous BMP stimulation. Smad4, known as the co-Smad, was also detected in the nuclei of MAECs at 20 min. Smad4 can transduce both TGF-β and BMP signals and therefore nuclear translocation can be indicative of active signalling in either pathway. However, with the apparent nuclear localisation of p-smad1/5/8 at the same time point, Smad4 nuclear translocation suggests active BMP signalling in MAECs.

During lung development BMP4 transcripts are expressed in the distal tips of the extending lung branches and in the mesenchyme surrounding the proximal airway (Weaver et al., 1999). BMP4 expression declines just before birth and little is known regarding the cell types which may express this ligand in the adult lung. Pathway activation in MAECs in the absence of serum indicates these cells can produce their own BMP ligands *in vitro* and possibly *in vivo* in the adult lung.

We hypothesise the BMP pathway is not actively signalling in healthy airways. This hypothesis was supported by Rosendahl et al., where BMP signalling was characterised in mouse lungs before and after OVA-induced inflammation. In their study BMP receptors were expressed by the bronchial epithelial cells in control mouse lungs. In addition, ubiquitous expression of Smad1 was detected in control animals. However, no phosphorylated form of the protein was observed. This suggests active BMP signalling is not required during homeostasis in healthy airways. However,

constitutive expression of the BMP pathway components suggests this pathway is equipped and in standby for an activation signal.

The BMP pathway is activated in response to allergen challenge in both murine and human airway epithelium (Rosendahl et al., 2001, Kariyawasam et al., 2008). However, the significance of this pathway activation has not been elucidated. The lung epithelium is the first point of contact with toxins and air borne pathogens and is a primary site for inflammation (Gómez and Prince, 2008). Inflammation results in damage to lung epithelial cells which must be repaired efficiently in order to prevent infiltration of potentially harmful agents (Takizawa, 2005). The processes encompassing lung injury and repair have been well characterised (Rawlins and Hogan, 2006). Figure 5.18 depicts the cells types which populate a healthy epithelial layer and the events which occur in response to injury. Chronic inflammation can result in epithelial cell shedding and exposure of the basement membrane (Fig. 5.18 B). At the onset of epithelial damage, cells which are adjacent to the damaged area must dedifferentiate, migrate and spread out to conceal the exposed epithelium (Fig. 5.18 B). Following this, cells undergo squamous metaplasia and subsequent proliferation which results in repopulation of the exposed area. Finally, cells initiate a programme of re-differentiation which continues until complete restoration of the pseudostratified mucociliary epithelium is achieved (Park et al., 2006, Puchelle et al., 2006). Clara cells have been identified as the principal reparative cell of the distal conducting airways where they can dedifferentiate and proliferate into both Clara cells and ciliated cell types following injury. Isolation of primary MAECs results in disruption of an intact epithelium. MAECs are subsequently seeded onto fibronectin. This loss in cell to cell contact combined with the presence of fibronectin resembles injury during inflammation. As a result MAECs *in vitro* are likely to resemble the squamated proliferating cells that exist during the repair process. BMP signalling is activated in MAECs in the absence of exogenous BMP. We propose BMP signalling is activated in the 'reparative' lung epithelial cells which are undergoing migration and proliferation in response to injury (Fig. 5.18 B).

In order to investigate whether the BMP signalling pathway in MAECs could respond to BMP stimulus *in vitro* MAECs were cultured in the presence of BMP2 and BMP4. BMPR-IA expression remained consistent in the presence of both BMP2 and BMP4. However, a reduction in membrane localisation of BMPR-IB was observed in response to BMP2 and BMP4. Ligand mediated internalisation of active receptor complexes has been reported and regulates pathway activation (Zwaagstra et al., 1999). The reduction in cells with apparent membrane localisation of BMPR-IB may represent receptor internalisation upon ligand binding. The downregulation of BMPR-IB at the membrane occurred in MAECs in medium alone. However, this process appeared to be accelerated with the addition of exogenous BMP2 and BMP4. BMPR-II was unexpectedly localised to the nuclei of MAECs. The addition of BMP2 and to a greater extent BMP4 resulted in the apparent relocalisation of BMPR-II to the cytoplasm. The significance of BMPR-II nuclear localisation and subsequent relocalisation in response to BMP4 is not known. Previous literature has highlighted a possible mitogenic role for receptor translocation (Planque, 2006). As previously mentioned, TGF-β Type I receptor nuclear translocation has previously been reported. However, no report to date has identified whether type II receptors possess similar functions. However, the TGF-β type II receptor has been shown to interact with cyclin B (Liu et al., 1999). The authors suggest this may occur through the cytoplasmic localisation of cyclin B rather than by means of TGF-β-RII nuclear translocation (Liu et al., 1999). Nonetheless, this interaction indicates type II receptors may also function in cell cycle control via direct binding to cell cycle mediators. Similarly, nuclear translocation of BMPR-II in MAECs may regulate proliferation which would support the 'reparative' phenotype of MAECs *in vitro*. BMP4-induced relocalisation may serve to potentiate BMP signalling by returning the receptor to the surface where it can reinitiate signal transduction.

Smad5 and Smad8 appeared upregulated following BMP2 and BMP4 stimulation (Figure 5.6). In addition, BMP4 appeared to induce Smad8 nuclear translocation. P-smad1/5/8 was predominantly localised to the nuclei of MAECs in medium alone and increased nuclear accumulation at 17 hr in BMP2- and BMP4-treated cells was

apparent. In addition, p-smad1/5/8 levels were increased by western blot following BMP4 stimulation. Nuclear translocation of p-smad1, -5, or -8 occurs in conjunction with the co-Smad, Smad4. Although nuclear localisation of Smad4 was detected in untreated MAECs at 20 min it was not sustained beyond this time point. In contrast, BMP2 and BMP4 stimulation resulted in nuclear Smad4 which appeared sustained over the time course experiment. The presence of both nuclear p-Smad1/5/8 and Smad4 in MAECs cultured in the presence of BMP2 and BMP4 suggests pathway activation which is ongoing in the cell. In contrast in untreated MAECs, the presence of nuclear p-Smad1/5/8 with the apparent cytoplasmic localisation of Smad4 may indicate pathway activation which occurred at an earlier time point such as 20 min where both p-Smad1/5/8 and Smad4 were localised to the nuclei in untreated MAECs (Figure 5.8). This highlights the importance of assessing the localisation of p-Smad1/5/8 and Smad4 together in order to fully determine the activation state of the cell. These data suggests BMP2 and BMP4 can potentiate ongoing pathway activation in MAECs *in vitro*.

BMP4 had the ability to inhibit E-cadherin mRNA and protein expression as well as modulate E-cadherin localisation at the cell membrane. This concurrent inhibition of membrane-associated E-cadherin as well as repression of the E-cadherin gene suggests BMP4 is a potent inhibitor of E-cadherin in normal airway epithelial cells. In addition, BMP4 reduced the expression of truncated E-cadherin in MAECs. Truncated E-cadherin results from cleavage of the full-length form of the protein. Elevated levels of truncated E-cadherin have been reported in the airway lumen during repair (Evans et al., 2002). The combined inhibition of full length E-cadherin and truncated E-cadherin supports transcriptional inhibition of the E-cadherin gene. However, it is also possible that the full-length membrane E-cadherin may have been cleaved in response to BMP4 and the truncated isoform released from the cell.

Transcriptional inhibition of E-cadherin corresponded to increased Snail1 expression at day 2. Interestingly, while E-cadherin inhibition at the mRNA level was detected up to day 5, the increased expression of Snail1 was not sustained later then day 2 (Figure

5.16). In cancer, it has been suggested that transcriptional repressors of E-cadherin with strong binding affinity for E-boxes in the promoter such as Snail may be expressed initially to rapidly repress transcription of the E-cadherin gene. In this way, Snail expression has been reported as transient where maintenance of the dedifferentiated phenotype is mediated by other E-cadherin repressors such as ZEB1 and E12/E47 (Bolos et al., 2003). It is possible that while Snail1 is induced initially to inhibit E-cadherin expression, other transcriptional repressors of E-cadherin are involved in the sustained repression of the E-cadherin gene in MAECs.

During bud extension BMP4, together with FGF and Wnt signalling, promotes proliferation of distal progenitor cells and maintains them in an undifferentiated state (Weaver et al., 1999, Eblaghie et al., 2005). As the lung branch extends, cells further away from the BMP4 stimulus initiate a program of proximal cell differentiation. A role for re-activated BMP signalling during inflammation in the adult lung has not been elucidated. BMP signalling was active in MAECs where it inhibited E-cadherin expression. We hypothesise active BMP signalling is present in the proliferating 'reparative' cells during lung injury (Fig. 5.18 B). Sustained BMP pathway activation in response to BMP ligands may result in maintaining these cells in an undifferentiated state by inhibiting the epithelial cell differentiation marker, E-cadherin.

BMP signalling is activated at sites undergoing EMT during development. Furthermore, abrogation of BMP signalling is embryonic lethal with a failure of early mesenchymal tissue to develop. During development downregulation of E-cadherin is mediated via simultaneous BMP and Wnt signalling. Wnt stabilisation of β-catenin facilitates β-catenin binding to LEF1. Subsequently LEF1 can enter the nucleus and negatively regulate E-cadherin expression (Jamora et al., 2003). BMP4 has been shown to induce LEF1 expression providing a possible mechanism through which BMP4 may inhibit E-cadherin gene expression (Kratochwil et al., 1996). In contrast, BMP6 and BMP7 have been shown to induce E-cadherin expression in breast cancer and kidney fibrosis, respectively (Yang et al., 2007, Zeisberg et al., 2003). However, BMP4 has been shown to downregulate E-cadherin in a number of adult cell types

such as pancreatic, ovarian and epithelial (Hamada et al., 2007, Theriault et al., 2007, Molloy et al., 2008). We have now demonstrated BMP4-induced downregulation of E-cadherin in primary MAECs and in addition in primary primate AECs (work ongoing in Shirley O'Dea laboratory). We hypothesise a primary role for BMP4-mediated signalling in adult tissue involves downregulation of E-cadherin expression.

During lung injury the exposed basement membrane is protected by neighbouring cells which migrate and proliferate in response to damage (Rawlins and Hogan, 2006) (Fig. 5.18 B). These processes resemble an EMT whereby the epithelial cell phenotype is repressed and the cell acquires mesenchymal traits. This migratory 'reparative' cell has been associated with vimentin expression (Buisson et al., 1996). Studies have shown different cells respond to injury depending on the location along the proximal-distal axis but little is known of the signalling pathways which mediate these processes (Rawlins and Hogan, 2006). Similarly, the pathways which control epithelial re-differentiation to restore an intact epithelium have yet to be clearly defined. It has been suggested that recapitulation of developmentally relevant pathways are likely to mediate repair. This is the case following naphthalene injury where transcription factors TTF-1, Foxj1, Foxa1 and Foxa2 as well as Sox family members Sox17 and Sox2 were upregulated in the squamated cells which had responded to injury and later in subsets of fully differentiated ciliated cells (Park et al., 2006). These proteins function during EMT in development and during lung morphogenesis (Lee et al., 2006, Warburton et al., 2000). We have shown BMP4 can downregulate E-cadherin in both BEAS-2B cells and primary MAECs. This repression of the epithelial cell phenotype is consistent with BMP4 mediated inhibition of epithelial differentiation during lung development (Weaver et al., 1999). E-cadherin downregulation is likely to be the first step during repair and may be initiated by reactivated BMP signalling to induce an EMT in the 'reparative' cells during injury.

The extent to which the epithelial cell phenotype was altered by BMP4 differed between BEAS-2B cells and MAECs in the conditions used. MAECs cultured in the presence of BMP4 exhibited a moderate change in morphology which was often

restricted to small subpopulations. In addition, E-cadherin was inhibited but not to the same extent as seen with BEAS-2B cells. BEAS-2B cells cultured in the presence of BMP4 for 6 days adopted a fibroblast-like morphology with loss of cell-cell contact which corresponded to a greater inhibition of E-cadherin at the mRNA and protein level. This E-cadherin profile is likely to represent an increasingly repressed epithelial cell phenotype in BEAS-2B cells in response to BMP4 (Molloy et al., 2008). Furthermore, MAECs cultured in conditioned medium (CM) from BEAS-2B cells did not downregulate E-cadherin in response to BMP4 (Fig. 5.15). It is important to note E-cadherin was also not inhibited in A549 cells in response to BMP4. Similar to MAECs, A549 cells possessed 'chicken wire' E-cadherin membrane localisation. In contrast, E-cadherin appeared localised to the nuclei in BEAS-2B cells. E-cadherin membrane localisation combined with robust E-cadherin expression in BMP4-treated cells suggests A549 cells more closely resemble normal MAECs. E-cadherin is commonly referred to as a 'safeguard' of the epithelial phenotype where loss of E-cadherin expression is sufficient to promote EMT. The occurrence of EMT *in vivo* would disrupt epithelial barrier integrity and may lead to inflammation, fibrosis and cancer. These deleterious effects implicate the need for tight control of E-cadherin expression and localisation. In this way, the level of E-cadherin stability observed in A549 cells and MAECs may more closely resemble the level of E-cadherin regulation *in vivo*. In other words E-cadherin inhibition in BMP4-treated BEAS-2B cells is unlikely to occur in normal cells to the same extent or at least not in response to a single stimulus.

We have hypothesised that reactivated BMP signalling during injury may initiate an EMT whereby E-cadherin is downregulated to facilitate migration of cells along the basement membrane. Sustained BMP signalling is likely to maintain these 'reparative' epithelial cells in an undifferentiated state and promote proliferation (Fig. 5.18 B). Inhibition of BMP pathway activation may be necessary to allow cells to undergo epithelial re-differentiation. In the event of misregulated BMP pathway activity these reparative cells may either in response to BMP4 or other pro-fibrotic factors such as TGF-β or both adopt an increasingly mesenchymal phenotype (Fig. 5.18 C). If cells,

which have undergone EMT *in vivo*, are capable of ECM deposition their epithelial to mesenchymal transition would further exacerbate damage. Furthermore epithelial cells undergoing mesenchymal differentiation could prevent complete repair of the epithelium (Fig. 5.18 C). Therefore, while BMP signalling may be reactivated to mediate epithelial repair, misregulated BMP signalling may have the potential to drive epithelial cells towards a mesenchymal fate.

In summary MAECs possess a BMP pathway and are responsive to BMP2 and BMP4 stimulation. BMP4-mediated signalling resulted in downregulation of E-cadherin. This outcome may function in the initiation of repair following lung injury. However, the subsequent role of BMP signalling in complete restoration of the airway epithelium is uncertain. We hypothesised BMP pathway activation may serve to maintain the 'reparative' epithelial cells in an undifferentiated state and mediate proliferation to restore an intact epithelium. Incorrect regulation of BMP signalling resulting in prolonged de-differentiation of the airway epithelium may have implications for cancer and fibrosis following lung injury.

6.0 BMP Pathway in Human Allergic Rhinitis

6.1. Introduction

The BMP pathway is activated during lung inflammation in both murine and human adult airways (Rosendahl et al., 2002, Kariyawasam et al., 2008). The significance of this activated pathway however remains unknown. We have shown that adult airway epithelial cells express a BMP pathway, can respond to BMPs and moreover may be producing their own BMPs *in vitro*. Importantly, activated BMP signalling in response to BMP4 can inhibit E-cadherin expression in both transformed human (BEAS-2B) and normal murine airway epithelial cells (MAECs). Furthermore, BMP4 could induce a mesenchymal-like phenotype in BEAS-2B cells. While E-cadherin downregulation is necessary to permit epithelial cell repair, loss of E-cadherin mediated adhesion can trigger epithelial cell apoptosis and subsequent epithelial cell shedding in asthma (Trautmann et al., 2005). Therefore, BMP activation during inflammation may mediate repair following injury or may exasperate inflammation by promoting epithelial cell shedding and fibrosis.

Allergic rhinitis (AR) is a chronic inflammatory disease of the upper airways. Reports relating to the severity of remodelling during AR have been contradictory. Nonetheless, alterations in airway architecture associated with chronic inflammation have been observed such as epithelial cell shedding and collagen deposition (Salib and Howarth, 2003). Furthermore, TGF-β pathway expression, a pathway known to induce tissue fibrosis, is increased in individuals with AR. However, it is not known what role, if any, exists for BMP signalling during AR.

In this study, BMP pathway components were assessed in nasal biopsy sections from both non-allergic individuals and individuals with AR. Eosinophils play a major role in the late-phase inflammation seen in AR and are pivotally involved in airway damage and remodelling processes. Eosinophils elicit their response through the release of eosinophil cationic proteins namely eosinophil cationic protein (ECP), eosinophil-derived neurotoxin (EDN), eosinophil peroxidase (EPO) and major basic protein (MBP). These eosinophil-derived proteins have been shown to stimulate

airway epithelial cells to produce factors involved in remodelling processes (Pegorier et al., 2006). For this reason, primary murine airway epithelial cells (MAECs) were both cultured with eosinophils and stimulated with eosinophil-derived proteins and alterations in BMP signalling was investigated.

The aims of this study were to identify whether a BMP pathway is expressed in the airway epithelium of the upper airways and whether there was any evidence of modulation of the BMP pathway in AR. In addition, to investigate whether eosinophils and the cationic proteins they produce have the ability to modulate BMP signalling *in vitro* and possibly *in vivo*.

6.1.1. Subject Characterisation

Nasal biopsy tissue sections were a kind gift from Richard Costello, Department of Medicine, Royal College of Surgeons in Ireland, Beaumont Hospital, Ireland. Local ethical board approval for the study was obtained and all patients gave informed consent prior to taking part in the study. Subjects were recruited by local advertisement. Subjects were divided into three groups based on their symptoms and the results of cutaneous allergen tests with common aeroallergens. Subjects with perennial allergic rhinitis, (PAR), (n=6) had mild to moderate symptoms of rhinitis for most of the year and positive skin prick tests to house dust mite, PAR_1-PAR_6. In these subjects, corticosteroid therapy was withheld for a period of at least 6 weeks while antihistamines, leukotriene receptor antagonists and relief decongestant medications were discontinued for at least 24 hours prior to any testing. Subjects with seasonal allergic rhinitis, (SAR), (n=3) were asymptomatic at the time of biopsy but do exhibit mild to moderate symptoms of rhinitis in response to seasonal allergens, SAR_1-SAR_3. A control group of non- allergic individuals who were asymptomatic and had negative skin prick tests, but a positive response to a control solution, were also included, (n=4), denoted herein C_1-C_4. In addition, a small subset including one PAR individual (PAR_3) who received allergen challenge (grass) and two non-allergic individuals (C_2 and C_3) who received a test solution (the diluent used with the allergen) was included in the study.

6.1.2. Active BMP signalling in nasal epithelium of normal individuals

It is unknown whether a BMP pathway is expressed in the upper airway of non-allergic individuals. Initially we wanted to assess whether a BMP pathway is expressed in normal healthy nasal epithelium. Figure 6.1 demonstrates BMP pathway component expression in the nasal epithelium of a non-allergic control individual (C_3). BMPR-IA and BMPR-IB were expressed in the cytoplasm of airway epithelial cells (Fig. 6.1A a-b). BMPR-II was localised to the surface membrane of the airway epithelial cells and endothelial lining of blood vessels visible in the interstitial tissue

(Fig. 6.1A c). Relatively low levels of cytoplasmic Smad5 and Smad8 were evident in epithelial cells (Fig. 6.1B a, b). Phosphorylated Smad1/5/8 and Smad4 was detected in the cytoplasm of the airway epithelial cells (Fig. 6.1B c, d). In addition, Smad4 nuclear translocation was apparent (Fig. 6.1B d). These data provide the first report of BMP pathway expression in the upper airway epithelium of a non-allergic individual.

6.1.3. Altered BMP signalling in nasal epithelium during allergic rhinitis

Evidence of altered BMP signalling was investigated by comparing expression levels and localisation of BMP pathway components in the four control individuals (C_1-C_4) and six allergic individuals with perennial allergic rhinitis (PAR) (PAR_1-PAR_6). BMPR-IB appeared constitutively expressed in all tissue sections examined and the level of expression remained unchanged between normal and allergic individuals (Fig. 6.2 a-j). Similarly, BMPR-II expression did not appear altered in allergic individuals compared to non-allergic individuals (Fig. 6.3 a-j). Levels of Smad5 expression varied among normal individuals with relatively high levels detected in one individual (Fig. 6.4 a), moderate levels detected in two (Fig. 6.4 c, d) and barely detectable levels in one individual (Fig. 6.4 b). No consistent trend was observed with levels of Smad5 expression in the AR individuals. However, nuclear smad5 was detected in three out of six allergic sections examined, indicating pathway activation that was not apparent in normal individuals (Fig. 6.4 f-h). Smad8 was detected in the cytoplasm of the individuals examined with no consistent trend in level of expression or nuclear translocation observed between groups (Fig. 6.5 a-j). Phosphorylated Smad1/5/8 was predominantly localised to the cytoplasm of the epithelial cells with nuclear translocation evident in some sections (Fig. 6.6 a-j). Smad4 was localised to the cytoplasm of the epithelial cells in normal individuals. An increase in nuclear translocation was evident in allergic individuals (Fig. 6.7 a-j).

The most consistent and striking difference in BMP pathway expression involved the localisation of BMPR-IA. BMPR-IA was localised to the cytoplasm of the epithelial cells in four out of four control subjects examined, C_1-C_4 (Fig. 6.8A a-d). Membrane

localisation was apparent in tissue from one control subject (Fig. 6.8A b). In contrast, evidence of nuclear localisation was detected in all allergic (6/6) individuals, PAR_1-PAR_6 (Fig. 6.8A f-j). The level of nuclear translocation of the receptor ranged between individuals examined with on average 25% cells demonstrating nuclear BMPR-IA expression (Fig. 6.8B). Confocal microscopy confirmed nuclear localisation of BMPR-IA and revealed that the protein was distributed throughout the nucleus and not just at the nuclear membrane (Fig. 6.8C).

6.1.4. BMP pathway expression following allergen challenge

A small subset of the cohort included one PAR individual (PAR_3) who received allergen challenge (grass) and two non-allergic individuals (C_2 and C_3) who received a test solution (the diluent for the allergen). BMPR-IA expression remained localised to the cytoplasm of the epithelial cells in both normal individuals. However, in one normal individual there appeared to be a small degree of nuclear translocation (Fig. 6.9 e). In the AR individual the nuclear translocation which was evident pre allergen challenge appeared more exclusively nuclear post allergen challenge (Fig. 6.9 f). This provides evidence that nuclear BMPR-IA may be linked to inflammatory processes in the upper airway.

BMPR-IB and BMPR-II appeared relatively unaltered in both normal individuals and in the allergic individual post allergen challenge (Fig. 6.10 a-f and Fig. 6.11 a-f). Levels of expression in Smad5 and Smad8 did not appear to be altered by allergen challenge in the allergic individual examined (Fig. 6.12 a-f and Fig. 6.13 a-f). Phosphorylated Smad1/5/8 expression remained unchanged in the normal individuals (Fig. 6.14 d, e). Interestingly, there was a dramatic increased in nuclear translocation in the allergic individual post allergen challenge (Fig. 6.14 f). Smad4 was consistently increased in the nucleus in both normal individuals and in the allergic individual post allergen challenge (Fig. 6.15 a-f).

6.1.5. Evidence of tissue remodeling in individuals with seasonal and perennial allergic rhinitis

Remodeling of the airways is a common and irreversible change in airway architecture and cellular composition resulting from chronic inflammation. Remodeling has been well characterised in asthma. There persists, however, conflicting views as to the nature and extent of airway remodeling during inflammation of the upper airway such as AR. Nasal sections were assessed for overall architecture. A variation in tissue architecture was observed between normal and allergic groups. In normal individuals the epithelium uniformly lined the interstitial tissue (Fig. 6.16 a-d). In contrast in allergic individuals the epithelium and interstitium appeared altered in organization. The interstitial tissue was less even and could be seen protruding into the epithelial layer (Fig. 6.16 e-l). Although it is possible the architecture observed may be artifact arising from the tissue processing it is unlikely if we consider the allergic biopsy sections shown in Figure 6.15 photomicrographs c and f. The two sections shown represent one individual pre and post allergen challenge and yet a similar alteration in tissue architecture is seen (yellow arrows). This suggests the altered architecture is associated with the individual and not the tissue processing technique.

6.1.6. Altered BMPR-IA localisation in MAECs co-cultured with eosinophils

Eosinophil infiltration is associated with the pathology of allergic rhinitis (AR). Eosinophils can release factors which drive remodeling processes in the lung. We hypothesized that eosinophils at the site of inflammation may result in the modulation of BMPR-IA during AR. In order to determine whether BMP signalling in AECs can be modulated by eosinophils, AECs were co-cultured with eosinophils isolated from either normal or allergic individuals for time points between 20 min and 17 hours. Nuclear BMPR-IA was observed at 17 hours in AECs following co-culture with eosinophils ($3x10^5$) isolated from an allergic subject (Fig. 6.17 A d). In contrast, nuclear localisation of BMPR-IA was not detected in AECs co-cultured with

eosinophils isolated from normal individuals (Fig. 6.17 A b). BMPR-IA was not detected in the nuclei of AECs cultured in medium alone (Fig. 6.17 A a, c). BMPR-IA nuclear translocation was apparent in 18% of AECs examined (Fig. 6.17 B).

6.1.7. Altered BMPR-IA expression in MAECs exposed to eosinophil derived proteins

In our co-culture system direct contact between eosinophils and MAECs was prevented by a porous membrane which permits diffusion of soluble signals. This implicated the release of soluble signals from the eosinophils in mediating the nuclear translocation of BMPR-IA. During inflammation, eosinophils elicit their effector response in part by the release of cytotoxic proteins such as EDN, EPO and MBP. In order to examine whether these eosinophil-derived proteins can modulate BMP signalling in epithelial cells, MAECs were exposed to eosinophil-derived proteins and the effects on BMPR-IA expression were examined. Eosinophil proteins were a kind gift from Richard Costello in Beaumont Hospital. Previous work carried out in the Costello laboratory had shown MBP at a range of concentrations (0.1-10 μg/ml) was able to protect IMR32 nerve cells from apoptosis (Morgan et al., 2005). Additional work performed in the Costello laboratory had found 1 μg/ml optimal for cell signalling experiments (personal communication). Based on this two eosinophil protein concentrations were chosen for our experiments namely 0.5 μg/ml and 5 μg/ml. Culture of AECs with EDN, EPO or MBP for 17 hr resulted in nuclear localisation of BMPR-IA (Fig. 6.18 A a-g). BMPR-IA nuclear localisation was detected with a mean expression of 30% and 35%, 56% and 37%, 36% and 45% with exposure to EDN (0.5 and 5 μg/ml), EPO (0.5 and 5 μg/ml), MBP (0.5 and 5 μg/ml) respectively (Fig. 6.18 B). To investigate the effect of eosinophil-derived protein of BMPR-IA localisation over a timecourse, AECs were exposed to eosinophil proteins for 2 hr, 17 hr and 48hr and examined by immunofluorescence. At 2 hr, BMPR-IA was localised to the cytoplasm of the AECs in both untreated cells and cells exposed to eosinophil derived proteins (Fig. 6.19 a-g). Nuclear translocation was detected at 17 hr in response to EDN, EPO and MBP (Fig. 6.19 i-n). BMPR-IA nuclear localisation

appeared to be transient with relocalisation of BMPR-IA to the cytoplasm of MAECs at 48hr similar to untreated cells (Fig. 6.19 o-u).

6.1.8. Nuclear localisation of BMP2 in AECs exposed to eosinophil-derived proteins

Nuclear translocation of growth factor receptors either as receptor subunits or as intact ligand/receptor complexes has been reported (Planque, 2006). In these reports either the ligand or receptor contains a functional nuclear localisation signal (NLS). Using the PredictNLS database we identified a possible NLS sequence in BMP2 (Fig. 6.22). We investigated whether there was any evidence of BMP2 nuclear localisation in MAECs exposed to eosinophil-derived proteins. In most cases, the level of BMP2 ligand expression and localisation remained largely unaltered following exposure to EDN, EPO and MBP (Fig. 6.20). However, some nuclear translocation was apparent in response to 0.5 µg/ml EPO, 5 µg/ml EPO and 5 µg/ml MBP at 17 hr as well as in response to 0.5 µg/ml EDN following 48 hr exposure (Fig. 6.20 k, l, n, p).

6.1.9. Nuclear translocation of BMPR-IA evident in chronic inflammatory lung disease

Nuclear translocation of the EGF receptor correlates with highly proliferating tissue and increased cancer aggressiveness (Lo et al., 2006). We investigated whether nuclear BMPR-IA was apparent in chronic inflammation of the lung in sections from normal individuals and individuals with COPD. BMPR-IA was localised to the cytoplasm of airway epithelial cells in normal healthy lung (Fig. 6.21 a). In the COPD section examined nuclear BMPR-IA was apparent (Fig. 6.21 d). In normal lung, BMPR-IB and BMPR-II were detected in the cytoplasm and on the membrane of the airway epithelial cells, respectively (Fig. 6.21 b, c). BMPR-IB localisation remained cytoplasmic in the COPD section examined (Fig. 6.21 e). In the COPD section immunolocalised for BMPR-II few epithelial cells were visible with apparent

exposure of the basement membrane (Fig. 6.21 f). As a result BMPR-II localisation was difficult to discern. Nonetheless, BMPR-II localisation did appear localised to the membrane or cytoplasm in the epithelial cells visible (Fig. 6.21 f).

6.2. Discussion

When we began our study, the only report on BMP signalling in the adult lung was a study by Rosendahl et al., who identified activated BMP signalling in the inflamed airways of mice exposed to OVA allergen (Rosendahl et al., 2002). The presence of a BMP pathway in human adult airway epithelium had not been investigated. While our study was ongoing, Kariyawasam et al., reported BMP pathway activation in human patients with mild asthma following allergen challenge (Kariyawasam et al., 2008). These studies implicated a role for BMP signalling in the pathogenesis of airway inflammation. *In vitro* we identified an EMT-like response to BMP4 in the human airway epithelial cell line, BEAS-2B, where E-cadherin expression was downregulated. In addition, BMP4 had the ability to reduce E-cadherin expression in normal MAECs. We hypothesised that BMP signalling may be activated to mediate repair, however, misregulated BMP4-mediated signalling may be involved in airway remodelling by contributing to epithelial shedding and fibrosis.

Asthma and AR often occur together in a patient and are characterised by similar inflammatory processes (Jeffery et al., 2006). Remodelling during asthma is well characterised and involves both cellular and structural alterations (Chetta et al., 1997). Evidence of remodelling in AR is less apparent. It has been suggested that remodelling in the upper airways of normal individuals can occur on a continual basis in response to the constant exposure of the nasal epithelium to environmental stimuli (Togias, 2000). As a result remodelling during inflammation of the upper airways can be more difficult to discern. Basement membrane thickening has been described in the nasal airways and is associated with increased myofibroblast transformation and subsequent collagen deposition (Sanai A et al. 1999). However, other reports have contradicted these findings. In our AR study, architectural differences between nasal tissues from normal and allergic individuals were apparent. The epithelium appeared thicker in seven out of eight allergic individuals and the interstitium appeared less uniform in organisation in these individuals. Further investigation using markers for epithelial cell proliferation such as Ki-67 and PCNA as well as electron microscopy would be useful

to confirm that the apparent changes in architecture are not merely artefact resulting from the tissue processing technique.

Both Rosendahl et al., and Kariyawasam et al., identified BMP pathway components expressed on airway epithelial cells in the lower airways. Rosendahl et al., reported BMP receptor expression on the airway epithelial cells in non-inflamed airways. In addition, the study found ubiquitous expression of Smad1 but no phosphorylated Smad1/5/8 (p-Smad1/5/8) was detected in the airway epithelial cells in healthy airways. Similarly, Kariyawasam et al., also reported BMP receptor expression in airway epithelial cells of non-allergic individuals. The study did detect phosphorylated Smad1/5/8 in the airway epithelial cells but no nuclear translocation was reported. Similar to these studies, we identified BMP receptor and Smad protein expression in the nasal biopsies examined from non-allergic individuals. In our study, BMPR-IA and BMPR-IB both appeared primarily localised to the cytoplasm of the airway epithelial cells in normal individuals. TGF-β type I receptors have been reported in the cytoplasm with up to 50% residing in the ER (Koli and Arteaga, 1997, Wells et al., 1997). Receptors localised to the cytoplasm are shuttled to the surface upon pathway activation. Similarly, the intracellular signalling molecules Smad5 and Smad8 were detected in the cytoplasm of the epithelial cells as was the phosphorylated form of these proteins. The hallmark of activated BMP signalling involves Smad nuclear translocation which was not apparent in the normal tissue biopsies. Taken together, this suggests that while the BMP pathway is expressed it may not be actively signalling in healthy airways.

Some evidence of BMP pathway activation was seen in AR individuals. In our study, Smad5, but not Smad8, expression was detected in the nuclei in three out of six allergic nasal biopsies indicative of BMP pathway activity in these individuals. The apparent absence of nuclear Smad8 may indicate BMP signals in the upper airway are preferentially mediated through Smad5. In the present study p-Smad1/5/8 was predominantly detected in the cytoplasm of the epithelial cells. While nuclear translocation was apparent there was no trend that would suggest this nuclear

translocation was increased in allergic individuals. Interestingly, following allergen challenge increased nuclear translocation of p-Smad1/5/8 was observed in the PAR individual examined. In the same individuals who received allergen challenge, Smad4 expression was reproducibly increased in the nuclei of both the non-allergic and allergic individual. As Smad4 operates as a co-Smad with the ability to transduce both BMP and TGF-β signals it can represent activity of either pathway. Therefore, in non-allergic individuals nuclear Smad4 in the absence of nuclear p-Smad1/5/8 indicates increased TGF-β signalling pathway. However, in the allergic individual who received allergen challenge nuclear Smad4 and nuclear p-Smad1/5/8 indicates increased BMP signalling in place of or in addition to activated TGF-β signalling. Active BMP signalling in AR individuals has not been previously studied. However, increased TGF-β pathway activity has been reported in PAR individuals (Salib et al., 2003a).

BMPR-II was expressed on the membrane of the airway epithelial cells and this localisation was not altered in the individuals with AR or in the allergic individual who received allergen challenge. However, neither Rosendahl et al., nor Kariyawasam et al., reported an alteration in BMPR-II expression following allergen challenge despite evidence of pathway activation. BMP ligands cannot bind to a type II receptor in the absence of a type I receptor. In this way, it is likely type I BMP receptors are modulated to control BMP pathway activation where the type II receptor may be expressed constitutively on the surface membrane. In addition, it is the Type I receptor which activates the Smad signalling molecules. Therefore modulation of the type I receptor localisation and expression levels may occur to regulate pathway activation.

BMPR-IB was not altered in individuals with AR compared to non-allergic individuals nor did it appear altered following allergen challenge in our study. However, BMPR-IA did appear modulated in individuals with AR. In normal tissues, BMPR-IA appeared localised to the cytoplasm of the airway epithelial cells. In contrast, in allergic sections BMPR-IA was observed in the nuclei of the epithelial cells (Fig. 6.8). Confocal microscopy confirmed this nuclear localisation.

BMPR-IA ligand-mediated internalisation has been reported (Serrano De la Pena et al., 2005). Reshuffling of BMPR-IA between the endosome and the cell surface is required for activation of BMP signalling (Nohe et al., 2003). Furthermore BMPR-IA has been previously identified in the nucleus when it was shown to colocalise with SAP49, a splicing factor, at the inner leaflet of the nuclear membrane (Nishanian and Waldman, 2004). This suggested BMPR-IA may function inside the cell as well as at the cell membrane. However, the role of nuclear BMPR-IA remains unknown. In the asthma study the basal level of BMP pathway expression was reduced (Kariyawasam et al., 2008). However, in our study similar levels of pathway activity were seen between normal and allergic groups with moderate signs of pathway activation apparent in AR. The most striking alteration in the pathway between the normal and allergic individuals was nuclear translocation of BMPR-IA suggesting BMP signalling is modulated rather than activated during inflammation of the upper airways.

There is substantial precedence for nuclear localisation of growth factors. FGF, EGF and PDGF have been reported to translocate to the nucleus (Jans and Hassan, 1998). In addition, growth factor receptors either as fragments or intact receptor/ligand complexes have been reported in the nuclei of a number of cell types. Nuclear accumulation of the type I TGF-β receptor, as well as receptors for epidermal growth factor (EFG), fibroblast growth factor (FGF), nerve growth factor (NGF), growth hormone (GH), interleukin-1 and -5 and Notch have all been described (Marti et al., 2000, Zwaagstra et al., 2000, Stachowiak et al., 1996, Lobie et al., 1994, Jans et al., 1997, Kopan et al., 1996). Nuclear translocation of a growth factor receptor begins with binding of the ligand to the receptor and subsequent internalisation of the entire ligand-receptor complex (Jans and Hassan, 1998). In the endosomes it has been demonstrated that while most complexes are degraded and some re-shuttled to the membrane that these complexes can in fact translocate to the nucleus. Receptor nuclear translocation to date has involved tyrosine kinase receptors or so called receptor tyrosine kinases (RTKs). It has been suggested that the kinase activity possessed by the nuclear translocated RTK may augment transcription in the nucleus by increasing the phosphorylation of transcription factors (Sorkina et al., 2002).

Furthermore, it was shown the tyrosine activity of the receptor was prerequisite for nuclear translocation. This was demonstrated in cells which expressed an EGF receptor lacking the intracellular domain and therefore lacking any tyrosine kinase activity (Ullrich and Schlessinger, 1990). This non-functional receptor upon internalisation was reportedly reshuttled to membrane at a much quicker speed when compared to a tyrosine kinase active ligand/receptor complex. Nuclear translocation of a RTK therefore usually occurs following ligand binding.

Growth factor receptor signalling in the nucleus is well recognised however the mechanism by which the receptor is transported from the membrane to the nucleus and the outcome of such an event is still poorly understood. Following ligand induced internalisation the EGFR is trafficked to the endoplasmic reticulum (ER) where is associates with Sec1β, a member of the sec61 translocon, whose function is the intake of proteins from the cytosol during protein synthesis and transport of mis-folded proteins from the ER to the cytosol for ubiquitination and subsequent degradation (Sandvig and van Deurs, 2002). Abrogation of Sec1β activity resulted in abrogation of EGFR nuclear translocation (Liao and Carpenter, 2007) providing the first insight into a possible mechanism from which a membrane bound receptor can gain access to the cytosol.

Proteins expressed in the cytosol require a nuclear localisation signal (NLS) to enter the nucleus. The majority of tyrosine kinase receptors (TKRs) involved in nuclear signalling contain a NLS. NLSs have been shown to be sufficient and necessary for proteins to gain entry through the nuclear membrane (Vancurova et al., 1994). SV40 large tumour antigen (T-ag) NLS and Xenopus phosphoprotein nucleoplasmin NLS constitute the two forms of NLS identified to date (Jans and Hassan, 1998). NLSs have been identified in growth factors and cytokines such as PDGF, FGF and INF-γ through sequence homology with the putative NLSs (T-ag or nucleoplasmin). In these cases, NLS function has been confirmed through mutational analysis and/or with the ability of the NLS to target a heterologous protein, such as E-coli β-galactosidase enzyme, to the nucleus. BMPR-IA does not appear to possess a putative NLS.

However, other proteins lacking NLSs are capable of nuclear translocation. The receptor for IL-5 (IL-5R) can translocate to the nucleus although it lacks a functional NLS. Studies have shown that this is possible by means of a 'piggy back' system where the IL-5 ligand which possesses a NLS can transport the receptor to the nucleus (Jans et al., 1997). Proteins with a molecular weight of less than 45kd can diffuse through the nuclear membrane and therefore have no requirement for a NLS (Jans and Hassan, 1998). BMP4 and BMP7 do not possess a NLS sequence. However, we have identified a potential NLS in BMP2 (Figure 6.22). BMP2 and IL-5 have a molecular weight of 26 kd and 30 kd respectively. A NLS sequence in BMP2 suggests a possible role for this ligand in directing its BMP receptors to the nucleus. We detected BMP2 in the nuclei of MAEC cells by immunofluorescence implicating a possible role for BMP2 in transporting BMPR-IA to the nucleus (Figure 6.20).

BMP2, similar to BMP4, is expressed as a large inactive precursor protein which is subsequently cleaved by the substilin-like enzyme, furin. In contrast to other BMP ligands, BMP2 and BMP4 both possess two cleavage sites, site 1 (S1) and site 2 (S2). The process of cleavage at these sites has been studied for BMP4 (Figure 6.22). The BMP4 proprotein is formed as a dimer of two immature BMP4 ligands before it exits the endoplasmic reticulum (ER) (Figure 6.22). Subsequently, within the Golgi apparatus, the proBMP4 is cleaved at the first cleavage site (S1) but the excised prodomain remains noncovalently associated with the mature ligand (Figure 6.22) (Degnin et al., 2004). This cleavage at S1 is required for subsequent cleavage at S2 (Cui et al., 2001). Cleavage at S2 occurs at a lower pH and promotes the disassociation of the prodomain from the mature ligand. At present it is not known whether the small peptide, which was flanked by S1 and S2, is also liberated or remains associated with the mature ligand (Degnin et al., 2004). Cleavage at S1 and S2 regulates the biological activity of BMP4 *in vivo* (Cui et al., 2001). The proposed model surrounding this regulation involves constitutive cleavage at S1 in all tissues which releases an active ligand with a short signalling range followed by cleavage at S2 which produces a more stable ligand with long-range signalling properties (Cui et al., 2001). This is interesting considering the localisation of the putative NLS in BMP2

in relation to the two cleavage sites (Figure 6.22). The first cleavage site is contained within the NLS and so cleavage at this site would remove the NLS sequence from the mature ligand. However, cleavage at the second site may leave the NLS intact if the fragment flanked by S1 and S2 were to remain associated with the mature ligand (Figure 6.22). Alternatively, it is possible the mechanism of proteolytic cleavage of BMP2 may differ from that identified for BMP4 and BMP2 may be cleaved at S2 in the absence of cleavage at S1 (Figure 6.22). This too would yield a mature ligand containing an NLS (Figure 6.22). Therefore, differential cleavage at S1 and/or S2 of the BMP2 proprotein may either enable BMP2 to facilitate BMPR-IA nuclear translocation or may abrogate this function.

It is clear growth factors and their receptors have the ability to signal directly via nuclear translocation. However, the functional outcome of this nuclear translocation still remains largely unknown. TGF-βR1 nuclear accumulation was associated with growth arrest in A549 cells (Zwaagstra et al., 2000). However, nuclear translocation of FGFR1 in glial cells corresponded with proliferation (Stachowiak et al., 1996). EGFR been shown to bind directly to the cyclin D1 promoter, b-myb and iNOS promoters and promote proliferation (Lin et al., 2001, Hanada et al., 2006, Lo et al 2006b). In addition, nuclear EGFR has been associated with highly proliferating tissues (Lin et al., 2001). Furthermore, EGFR nuclear translocation in tissue been correlated with poor prognosis in both breast (Lo et al., 2006a) and oropharyngeal (Psyrri et al., 2005) cancer. In summary, nuclear translocation of growth factors and RTKs appear to be linked to cell cycle progression and proliferation (Planque, 2006).

In our study, BMPR-IA localisation was assessed in the chronic inflammatory lung disease, COPD (Figure 6.21). The epithelial layer in the diseased tissue appeared damaged with exposure of the basement membrane. BMPR-IA was detected in the nuclei of the epithelial cells in the diseased tissue. No nuclear localisation of BMPR-IB and BMPR-II was apparent. All receptors were localised to the cytoplasm or surface membrane in healthy lung sections. If nuclear translocation of BMPR-IA regulates proliferation of the airway epithelial cells it may serve to repair

the damaged epithelium during chronic lung inflammation. Increased TGF-β activity has been reported in asthma and perennial allergic rhinitis (Bosse and Rola-Pleszczynski, 2007, Salib et al., 2004). In our study of AR, increased Smad4 nuclear localisation in AR individuals indicates possible TGF-β activity during AR. TGF-β serves as a negative regulator of airway inflammation by inhibiting the production of proinflammatory cytokines and immune cell proliferation (Groneberg et al., 2004). Similarly, TGF-β signalling in epithelial cells has been reported to inhibit proliferation through the induction of p21 (Murakami et al., 2008, Howe et al., 1993). As a result, TGF-β signalling has the ability to inhibit full epithelial cell repair and possibly compromise epithelial barrier integrity. If BMPR-IA nuclear translocation occurs *in vivo* to promote proliferation it may serve to counteract the anti-mitogenic effects of increased TGF-β in the surrounding epithelium of an AR individual.

In our study, co-culture of MAECs with both eosinophils and eosinophil-derived proteins resulted in nuclear localisation of BMPR-IA (Figure 6.17 and Figure 6.18, respectively). Eosinophil infiltration is prominent in the pathology of allergic rhinitis (Baraniuk, 1997). Ablation of the eosinophil lineage in a mouse transgenic model exhibited a reduction in remodelling after OVA-allergen challenge (Humbles et al., 2004). The study highlighted the central role for eosinophils in airway remodelling during inflammation. Eosinophils are the primary source of TGF-β1 during inflammation (Wong et al., 2001) and have been shown to migrate toward necrotic epithelial cells *in vitro* and secrete TGF-β and FGF -2, growth factors involved in remodelling (Stenfeldt and Weneras, 2004). Eosinophils secrete PDGF-B which can induce collagen and ECM deposition as well as hyperplasia of smooth muscle cells (Ohno et al., 1995) both pivotal events in the remodelling processes. In situ hybridisation localised BMP4 mRNA to infiltrating eosinophils present in the rat uterus where they were involved in remodelling during the estrous cycle (Erickson et al., 2004). Kariyawasam et al., demonstrated eosinophils as a primary source of BMP7 during asthma. MAECs co-cultured with eosinophils from an allergic individual for 17 hr resulted in nuclear BMPR-IA. However, eosinophils from a non-allergic control individual did not modulate RIA localisation. These data suggests eosinophils can

modulate BMP signalling and eosinophils from an allergic individual may possess inherent activity necessary for this modulation. We investigated whether nuclear RIA in MAECs occurred in response to BMP4. However, after 17 hrs and up to 48hrs of recombinant BMP4 stimulation no nuclear RIA was seen (data not shown). This suggests that nuclear RIA does not occur in response to BMP4 or BMP4 alone.

Eosinophils elicit their immune response in part by the release of cytotoxic mediators' namely eosinophil derived neurotoxin (EDN), eosinophil peroxidase (EPO), and major basic protein (MBP). These cationic proteins at high concentrations are toxic to cells (Kleine et al., 1999, Hisamatsu et al., 1990, Motojima et al., 1989) by their action of membrane damage (Silberstein, 1995). In the nasal epithelium MBP was cytotoxic and caused ciliostasis (Hisamatsu et al., 1990). MBP and EPO at subcytotoxic concentrations stimulated the release of growth factors which function in remodelling processes (Pegorier et al., 2006). MAECs were exposed to the cationic proteins to investigate whether their release from eosinophils could result in nuclear translocation of BMPR-IA. MAECs exposed to EDN, EPO and MBP resulted in nuclear BMPR-IA translocation after 17 hr of exposure (Fig. 6.19). However, BMPR-IA nuclear translocation was transient with no detection of nuclear BMPR-IA at 48hr (Figure 6.19). It is likely the cytoplasmic/membrane localisation observed at this time point may represent the nuclear translocated receptor which has been exported from the nucleus but may also represent a newly synthesised receptor.

Our study has shown the BMP pathway is expressed in the nasal epithelium of non-allergic individuals. In nasal biopsy sections from individuals with AR, signs of pathway activation were observed. However, the most striking alteration was the apparent nuclear translocation of BMPR-IA. Nuclear BMPR-IA was detected in MAECs both co-cultured with eosinophils and exposed to eosinophil cationic proteins. In conclusion, BMPR-IA localisation is modulated in AR and release of cationic proteins from eosinophils infiltrating to the site of inflammation represents a possible mechanism by which this may occur *in vivo*.

CONCLUSIONS AND FUTURE DIRECTIONS

7.0 Conclusions

Bone morphogenetic protein (BMP) signalling is involved in EMT processes during development. We have identified an EMT-like response in the human adult airway epithelial cell line, BEAS-2B (Molloy et al., 2008). BMP4 inhibited E-cadherin expression and induced a mesenchymal-like phenotype in BEAS-2B cells. BMP2 also inhibited E-cadherin expression in BEAS-2B cells. In addition, BMP4 had the ability to inhibit E-cadherin expression in normal primary murine epithelial cells. This suggests a primary outcome of BMP signalling may be the inhibition of E-cadherin and implicates the BMP pathway in epithelial cell repair but also suggests this pathway may function in cancer metastasis and tissue fibrosis. The BMP pathway was modulated during allergic rhinitis with the apparent localisation of BMPR-IA to the nuclei of the airway epithelial cells. The functional significance of this localisation has yet to be determined. However, a possible mechanism surrounding this nuclear localisation was provided when MAECs co-cultured with human eosinophils or stimulated with eosinophil cationic proteins exhibited nuclear BMPR-IA.

In conclusion, BMP signalling can negatively regulate E-cadherin expression and has the ability to induce epithelial-mesenchymal transition in BEAS-2B cells. The BMP pathway is modulated during allergic rhinitis the significance of which is not known. Nonetheless this data does implicate BMP signalling in the pathogenesis of upper airway inflammation where it may be involved in remodelling processes such as airway epithelial cell shedding and fibrosis.

8.0 Future directions

This work involved the characterisation of BMP signaling in adult airway epithelial cells. All experiments were performed with AECs grown under submerged culture conditions. Future experiments are to include AECs cultured at air-liquid interface (ALI). AECs are naturally found at an air-liquid interface *in vivo*. For this reason AECs cultured at ALI provide a more physiologically relevant model compared to submerged culture. ALI culture facilitates AEC differentiation *in vitro* permitting the study of a multi-cellular epithelium. ALI allows for the formation of a polarized epithelial. In our study of BMP pathway component expression in AECs, the BMP receptors were commonly expressed in the cytoplasm. AECs grown at ALI and the formation of a fully polarized epithelium may promote membrane localisation of these receptors. In addition to cell physiology there are a number of practical advantages to using ALI culture. AECs cultured at ALI could be treated from either the basal or apical surface or both. In addition, ALI culture provides a good model to assess the effect of a given treatment on trans-epithelial integrity (TEER). However, it is important to note ALI culture is not without its caveats. In order to facilitate the full differentiation of AECs cultured at ALI, cells must be cultured at ALI for a number of weeks in which time the cultures can become increasingly susceptible to contamination. It is more expensive to maintain cells at ALI. In addition, the acquisition of bright field images can be compromised due to the porous nature of the inserts used.

The canonical BMP signalling pathway was activated in response to BMP2 and BMP4 in BEAS-2B cells, A549 cells and MAECs. Furthermore, this Smad pathway activation was sustained at day 6 in BEAS-2B cells which had undergone EMT. This suggests this pathway is involved in the induction of EMT in BEAS-2B cells. However, BMP ligands can also activate MAPK signalling. Of interest would be the investigation of MAPK signalling in lung cells in response to BMP ligands. TGF-β1 and TGF-β-induced mRNA was upregulated in BEAS-2B cells which had undergone

EMT in response to BMP4. Both TGF-β1 and TGF-β-induced are involved in EMT in other cell types. It is unclear what role TGF-β signalling had during the EMT process initiated by BMP4 in BEAS-2B cells. To investigate this further, confirmation of increased TGF-β at the protein level and determination of TGF-β pathway activation in BEAS-2B cells would be required. Subsequent to this targeted inhibition of the TGF-β pathway using a siRNA approach would be useful to gain an insight into the contribution of TGF-β signalling in BMP4-induced EMT.

In our experiments, BEAS-2B cells were characterised at day 6 for changes which had occurred in response to BMP4. Subsequent experiments are to focus on the gene targets or 'early response genes' activated by both BMP2 and BMP4 in airway epithelial cells. The identification of such target genes activated by BMPs in lung epithelial cells has not been investigated to date.

The BMP pathway is activated during inflammation. It is not clear what role BMP signalling may have during inflammation and whether this pathway activation exacerbates inflammation or as the ability to bring about resolution. Crosstalk exists between BMP and Toll-like receptor signalling suggesting BMP signalling may be involved in the production of pro-inflammatory stimuli. To gain a better insight, the role of activated BMP signalling on cytokine production by airway epithelial cells would be useful.

To date, BMP4 involvement during EMT processes in adult cells has not extended beyond *in vitro* experimentation. Of great interest would be the investigation of BMP signalling during *in vivo* tissue fibrosis. A number of mouse models exist to examine lung fibrosis such as the bleomycin injury model and the asbestos-induced pulmonary fibrosis model (Khalil and Greenberg, 1991, Brody et al., 1997). In addition, assessment of BMP signalling in human disease such as idiopathic pulmonary fibrosis (IPF) would advance our current knowledge surrounding the involvement of BMP signalling during pulmonary disease.

BMP4 had the ability to downregulate E-cadherin expression in normal MAECs. We hypothesised BMP signalling may be involved in airway epithelial cell repair. To investigate this is more detail, the BMP pathway may be assessed in MAECs grown on air-liquid interface (ALI) following mechanical injury to the epithelial monolayer. The aim would be to identify whether the BMP pathway is active in MAECs undergoing repair and to investigate the phenotype of the 'reparative cell' in terms of epithelial characteristics lost and mesenchymal characteristics gained.

During AR, the BMP pathway appeared modulated with the apparent nuclear localisation of BMPR-IA to the nucleus of the airway epithelial cells. Cell fractionation would be useful to validate BMPR-IA nuclear translocation. To gain a better insight into the functional significance of this nuclear BMPR-IA, the expression and localisation of other BMP pathway components including pathway inhibitors should be investigated. In addition, co-immunoprecipitation studies may be employed to identify BMPR-IA binding partners both at the membrane and in the nucleus.

9.0 PUBLICATIONS

Molloy EL, Adams A, Moore JB, Masterson JC, Madrigal-Estebas L, Mahon BP and O'Dea S. BMP4 induces an epithelial-mesenchymal transition-like response in adult airway epithelial cells. Growth Factors 2008; 26: 12-22.

10.0 BIBLIOGRAPHY

Alejandre-Alcazar M, Kwaspiszewska G, Reiss I, Amarie VO, Marsh LM, Sevilla-Perez J, Wygrecka M, Eul B, Kobrich S, Hesse M, Schermuly RT, Seeger W, Eickelberg O, Morty RE. Hyperoxia modulates TGF-β/BMP signalling model of bronchopulmonary dysplasia. Am J Physiol Lung Cell Mol Physiol 2006; 292:L537-L549.

Aberg N, Sundell J, Eriksson B, Hesselmar B and Aberg B. Prevalence of allergic diseases in schoolchildren in relation to family history, upper respiratory infections, and residential characteristics. Allergy 1996; 51: 232-237.

Aderem A and Ulevitch RJ. Toll-like receptors in the induction of the innate immune response. Nature 2000; 406: 782-787.

Alami J, Williams BR and Yeger H. Differential expression of E-cadherin and beta catenin in primary and metastatic Wilms's tumours. Mol Pathol 2003; 56: 218-225.

Alejandre-Alcazar MA, Shalamanov PD, Amarie OV, Sevilla-Perez J, Seeger W, Eickelberg O and Morty RE. Temporal and Sparial Regulation of Bone Morphogenetic Protein Signalling in Late Lung Development. Dev Dyn 2007; 236:2825-2835.

Allen JT and Spiteri MA. Growth factors in idiopathic pulmonary fibrosis: relative roles. Respir Res 2002; 3: 13.

Aono A, Hazama M, Notoya K, Taketomi S, Yamasaki H, Tsukuda R, Sasaki S and Fujisawa Y. Potent ectopic bone-inducing activity of bone morphogenetic protein-4/7 heterodimer. Biochem Biophys Res Commun 1995; 210: 670-677.

Bailey JM, Singh PK and Hollingsworth. Cancer Metastasis Facilitated by Developmental Pathways: Sonic Hedgehog, Notch, and Bone Morphogenetic Proteins. J Cell Biochem 2007; 102: 829-839.

Baraniuk JN. Pathogenesis of allergic rhinitis. J Allergy Clin Immunol 1997; 99: S763-772.

Batlle E, Sancho E, Franci C, Dominguez D, Monfar M, Baulida J and Garcia De

Herreros A. The transcription factor snail is a repressor of E-cadherin gene expression in epithelial tumour cells. Nat Cell Biol 2000; 2: 84-89.

Bellusci S, Henderson R, Winnier G, Oikawa T, Hogan BL. Evidence from normal expression and targeted misexpression that bone morphogenetic protein (Bmp-4) plays a role in mouse embryonic lung morphogenesis. Development 1996;122:1693-1702.

Bolos V, Peinado H, Perez-Moreno MA, Fraga MF, Esteller M, Cano A. The transcription factor Slug represses E-cadherin expression and induces epithelial mesenchymal transitions: a comparison with Snail and E47 repressors. J Cell Sci 2003; 116:499-511.

Bosse Y, Rola-Pleszczynski M. Controversy surrounding the increased expression of TGF-β1 in asthma. Respiratory Research 2007; 8:66.

Boström H, Willetts K, Pekny M, Levéen P, Lindahl P, Hedstrand H, Pekna M, Hellström M, Gebre-Medhin S, Schalling M, Nilsson M, Kurland S, Törnell J, Heath JK and Betsholtz C. PDGF-A signalling is a critical event in lung alveolar myofibroblast development and alveogenesis. Cell 1996; 85: 863-873.

Bousquet J, Jacquot W, Vignola AM, Bachert C and van Cauwenberge P. Allergic rhinitis: a disease remodeling the upper airways? J Allergy Clin Immunol 2004; 113: 43-49

Bragg AD, Moses HL and Serra R. Signalling to the epithelium is not sufficient to mediate all the effects of transforming growth factor β and bone morphogenetic protein 4 on murine embryonic lung development. Mech Dev 2001; 109: 13-26.

Braunstahl GJ, Fokkens WJ, Overbeek SE, KleinJan A, Hoogsteden HC, Prins JB. Mucosal and systemic inflammatory changes in allergic rhinitis and asthma. Clin Exp Allergy 2003; 33:579-587.

Brody AR, Liu JY, Brass D, Corti M. Analyzing the genes and peptide growth factors expressed in lung cells *in vivo* consequent to asbestos exposure and *in vitro*. Environ Health Perspect. 1997; 105 Suppl 5: 1167-1171.

Brooks SA. Appropriate glycosylation of recombinant proteins for human use: implications of choice of expression system. Mol Biotechnol 2004; 28: 241-255.

Bryant DM and Stow JL. The ins and outs of E-cadherin trafficking. Trends Cell Biol 2004; 14: 427-434

Buckley S, Shi W, Driscoll B, Ferrario A, Anderson K and Warburton D. BMP4 signalling induces senescence and modulates the oncogenic phenotype of A549 lung adenocarcinoma cells. Am J Physiol Lung Cell Mol Physiol 2004; 286: L81-L86.

Buisson AC, Gilles C, Polette M, Zahm JM, Birembaut P, Tournier JM.Wound repair-induced expression of a stromelysins is associated with the acquisition of a mesenchymal phenotype in human respiratory epithelial cells.Lab Invest 1996; 74: 658-669.

Cano A, Perez-Moreno MA, Rodrigo I, Locascio A, Blanco MJ, del Barrio MG, Portillo F, Nieto MA. The transcription snail controls epithelial-mesenchymal transitions by repressions E-cadherin expression. Nat Cell Biol 2000; 2:76-83.

Cárcamo J, Weis FM, Ventura F, Wieser R, Wrana JL, Attisano L, Massagué J. Type I receptors specify growth-inhibitory and transcriptional responses to transforming growth factor beta and activin. Mol Cell Biol 1994; 14: 3810-3821.

Cavallaro U and Christifori G. Multitasking in Tumor Progression Signalling Functions of Cell Adhesion Molecules. Ann NY Acad Sci 2004; 1014: 58-66.

Celeste AJ, Iannazzi JA, Taylor RC, Hewick RM, Rosen V, Wang EA and Wozney JM. Identification of transforming growth factor β family members present in the bone-inductive protein purified from bovine bone. Proc Natl Acad Sci 1990; 87: 9843-9847.

Centrella M, Rosen V, Wozney JM, Casinghino SR and McCarthy TL. Opposing effects by glucocorticoid and bone morphogenetic protein-2 in fetal rat bone cell cultures. J Cell Biochem 1997; 67: 528-540.

Chacko BM, Qin B, Correia JJ, Lam SS, de Caestecker MP and Lin K. The L3 loop and C-terminal phosphorylation jointly define Smad protein trimerization. Nat Struct Biol 2001; 8: 248-253.

Chagraoui J, Lepage-Noll A, Anjo A, Uzan G and Charbord P. Fetal liver stroma consists of cells in epithelial-to-mesenchymal transition. Blood 2003; 101: 2973-2982.

Chen D, Zhao M and Mundy GR. Bone Morphogenetic Proteins. Growth Factors 2004; 22:233-241.

Chetta A, Foresi A, Del Donna M, Bertorelli G, Pesci A, Oliveri D. Airways remodelling is a distinctive feature of asthma and is related to the severity of disease. Chest 1997; 111:852-857.

Chetta A, Zanini A, Foresi A, D'Ippolito R, Tipa A, Castagnaro A, Baraldos S, Neri M, Saettas M, Olivieri D. Vascular endothelial growth factor up-regulation and bronchial wall remodelling in asthma. Clin Exp Allergy 2005; 35: 1437-1442.

Chiodini I, Toriontano M, Carnevale V, Trischitta V, Scillitani A. Skeletal involvement in adult patients with endogenous hypercortisolism. J Endocrinol Invest 2008; 31: 267-276.

Cho KWY and Blitz IL. BMPs, Smads and metalloproteases: extracellular and intracellular modes of negative regulation.Curr Opin Genet Dev 1998; 8:443-449.

Chow E and Macrae F. Review of Juvenile Polyposis Syndrome. J Gastroentero Hepatol 2005; 20:1634-1640.

Chu YS, Thomas WA, Eder O, Pincet F, Perez E, Thiery JP, Dufour S. Force measurements in E-cadherin-mediated cell doublets reveal rapid adhesion strengthened by actin cytoskeleton remodeling through Rac and Cdc42.J Cell Biol 2004; 167: 1183-1194.

Clancy BM, Johnson JD, Lambert AJ, Rezvankhah S, Wong A, Resmini C, Feldman JL, Leppanen S and Pittman DD. A gene expression profile for endochondral bone formation: oligonucleotide microarrays establish novel connections between known genes and BMP-2-induced bone formation in mouse quadriceps. Bone 2003; 33: 46-63.

Come C, Arnoux V, Bibeau F and Savanger P. Roles of the Transcription Factors

Snail and Slug During Mammary Morphogenesis and Breast Carcinoma Progression. J Mammary Gland Biol Neoplasia 2004; 9: 183-193.

Comijn J, Berx G, Vermassen P, Verschueren K, van Grunsven L, Bruyneel E, Mareel M, Huylbroeck D, van Roy F. The two-handed E box binding zinc finger protein SIP1 downregulates E-cadherin and induces invasion. Mol Cell 2001; 7:1267-1278.

Constam DB and Robertson EJ. Regulation of Bone Morphogenetic Protein Activity by Pro Domians and Proprotein Convertases. J Cell Biol 1999; 144: 139-149.

Cui Y, Hackenmiller R, Berg L, Jean F, Nakayama T, Thomas G and Christian JL.The activity and signalling range of mature BMP-4 is regulated by sequential cleavage at two sites within the prodomain of the precursor. Genes Dev 2001; 15:2797-2802.

De Jong DS, Vaes BL, Dechering KJ, Feijen A, Hendriks JM, Wehrens R, Mummery CL, van Zoelen EJ, Olijve W and Steegenga WT. Identification of novel regulators associated with early-phase osteoblast differentiation. J Bone Miner Res 2004; 19: 947-958.

De la Pena LS, Billings PC, Fiori JL, Ahn J, Kaplan FS, Shore EM. Fibrodysplasia ossificans progressive (FOP), a disorder of ectopic osteogenesis, misregulates cell surface expression and trafficking of BMPR-IA. J Bone Miner Res 2005; 20: 1168-1176.

De Longh RU, Wederell E, Lovicu FJ and McAvoy JW. Transforming Growth Factor-β-Induced Epithelial-Mesenchymal Transition in the Lens: A Model for Cataract Formation. Cells Tissues Organs 2005; 179: 43-55.

Deckers M, van Dinther M, Buijs J, Que I, Lowik C, van der Pluijm G and van Dijke P. The tumor Suppressor Smad4 Is Required for Transforming Growth Factor β-Induced Epithelial to Mesenchymal Transition and Bone Metastasis of Breast Cancer Cells. Cancer Res 2006; 66: 2202-2209.

Degen WG, Weterman MA, van Groningen JJ, Cornelissen IM, Lemmers JP, Agterbos MA, Geurts van Kessel A, Swart GW and Bloemers HP. Expression of nma, a novel gene, inversely correlates with the metastatic potential of human melanoma cell lines and xenografts. Int J Cancer 1996; 65: 460-465.

Degnin C, Jean F, Thomas G and Christian JL. Cleavages within the Prodomain Direct Intracellular Trafficking and Degradation of Mature Bone Morphogenetic Protein-4. Mol Biol Cell 2004; 15: 5012-5020.

Deng H, Makizumi R, Ravikumar TS, Dong H, Yang W and Yang WL. Bone morphogenetic protein-4 is overexpressed in colonic adenocarcinomas and promotes migration and invasion of HCT116 cells.Exp Cell Res 2007; 313: 1033-1044.

Deng H, Ravikumar TS and Yang WL.Bone morphogenetic protein-4 inhibits heat-induced apoptosis by modulating MAPK pathways in human colon cancer HCT116 cells. Cancer Lett 2007; 256: 207-217.

Derynck R and Zhang YE. Smad-dependent and Smad-independent pathways in TGF-β family signalling . Nature 2003; 425: 577-584.

Dimri GP, Lee X, Basile G, Acosta M, Scott G, Roskelley C, Medrano EE, Linskens M, Rubelj I, Pereira- Smith O, Peacocke M and Campisi J. A Biomarker that identifies senescent human cells in culture and in aging sk*in vivo*. Proc Natl Acad Sci USA; 92:9363-9367.

Duong TD and Erickson CA. MMP-2 plays an essential role in producing epithelial-mesenchymal transformations in the avian embryo. Dev Dyn 2004; 229: 42-53.

Ebisawa T, Fukuchi M, Murakami G, Chiba T, Tanaka K, Imamura T and Miyazono K. Smurf1 interacts with transforming growth factor-beta type I receptor through Smad7 and induces receptor degradation. J Biol Chem 2001; 276: 12477-12480.

Eblaghie MC, Reedy M, Oliver T, Mishina Y and Hogan BLM. Evidence that autocrine signalling through Bmpr1a regulates the proliferation, survival and morphogenetic behavior of distal lung epithelial cells. Dev Biol 2006; 291: 67-82.

Erickson GF, Fugua L, Shimasaki S. Analysis of spatial and temporal expression patterns of bone morphogenetic protein family members in the rat uterus over the estrous cycle. J Endocrinol 2004; 182: 203-217.

Evans SM, Blyth DI, Wong T, Sanjar S and West MR. Decreased distribution of lung epithelial junction proteins after intratracheal antigen or lipopolysaccharide challenge: correlation with neutrophil influx and levels of BALF sE-cadherin. Am J Respir Cell Mol Biol 2002; 27: 446-454.

Feng XH and Derynck R. Specificity and Versatility in TGF-β Signalling Through Smads. Annu Rev Dev Biol 2005; 21:659-653.

Feng XH, Lin X, Derynck R. Smad2, Smad3 and Smad4 cooperate with Sp1 to induce p15 (Ink4B) transcription in response to TGF-beta. EMBO J 2000; 19: 5178-5193.

Forino M, Torregrossa R, Ceol M, Murer L, Della Vella M, Del Prete D, D'Angelo A and Anglani F. TGFβ1 induces epithelial-mesenchymal transition, but not myofibroblast transdifferentiation of human kidney tubular epithelial cells in primary culture. Int J Exp Path 2006; 87: 197-208.

Galli SJ, Mindy T and Piliponsky AM. The development of allergic inflammation. Nature 2008; 454: 445-454.

Gazzero E and Canalis E. Bone morphogenetic proteins and their antagonists. Rev Endocr Metab Disord 2006; 7: 51-65.

Gilboa L, Nohe A, Geissendorfer T, Sebald W, Henis YI and Knaus P. Bone Morphogenetic Protein Receptor Complexes on the Surface of Live Cells: A New Oligomerization Mode for Serine/Threonine Kinase Receptors. Mol Biol Cell 2002; 11: 1023-1035.

Gleich GJ, Loegering DA, Maldonado JE. Identification of a major basic protein in guinea pig eosinophil granules. J Exp Med 1973; 137: 1459-1471.

Gómez MI and Prince A. Airway epithelial cell signalling in response to bacterial pathogens. Pediatr Pulmonol 2008; 43: 11-19.

Gong Y, Krakow D, Marcelino J, Wilkin D, Chitayat D, Babul-Hirji R, Hudgins L, Cremers CW, Cremers FP, Brunner HG, Reinker K, Rimoin DL, Cohn DH, Goodman FR, Reardon W, Patton M, Francomano CA and Warman ML. Heterozygous mutations in the gene encoding noggin affect human joint morphogenesis. Nat Genet

1999; 21: 302-304.

Graziano F, Humar B and Guilford P. The role of the E-cadherin gene (CDH1) in diffuse gastric cancer susceptibility: from the laboratory to clinical practice. 2003; 14: 1705-1713.

Groneberg DA, Witt H, Adcock IM, Hansen G and Springer J. SMADS as Intracellular Mediators of Airway Inflammation. Exp Lung Res 2004; 30:223-250.

Hall A, Paterson HF, Adamson P and Ridley AJ. Cellular responses regulated by rho-related small GTP-binding proteins. Philos Trans R Soc Lond B Biol Sci 1993; 340: 267-271.

Hamada S, Satoh K, Hirota M, Kimura K, Kanno A, Masamune A, Shimosegawa T. Bone morphogenetic protein 4 induces epithelial-mesenchymal transition through MSX2 induction on pancreatic cancer cell line. J Cell Physiol 2007.

Han AC, Soler AP, Tang CK, Knudsen KA and Salazar H. Nuclear localization of E-cadherin expression in Merkel cell carcinoma. Arch Pathol Lab Med 2000; 124: 1147-1151.

Hanada N, Lo H W, Day C P, Pan Y, Nakajima Y, Hung M C: Co-Regulation of B-Myb Expression by E2F1 and EGF Receptor. Mol Carcinog 2006, 45:10-17.

Hanyu A, Ishidou Y, Ebisawa T, Shimanuki T, Imamura T and Miyazono K. The N domain of Smad7 is essential for specific inhibition of transforming growth factor-beta signalling . J Cell Biol 2001; 155: 1017-1027.

Harkema JR, Carey SA and Wagner JG. The Nose Revisited: A Brief Review of the Comparative Structure, Function, and Toxicologic Pathology of the Nasal Epithelium. Toxicologic Pathology 2006; 34: 252-269.

Hata A, Lagna G, Massagué J and Hemmati-Brivanlou A. Smad6 inhibits BMP/Smad1 signalling by specifically competing with the Smad4 tumor suppressor. Genes Dev 1998; 12: 186-197.

Helms MW, Packeisen J, Augest C, Schittek B, Boecker W, Brandt BH and Buerger.First evidence supporting a potential role for the BMP/SMAD pathway in the progression of oestrogen receptor-positive brest cancer. J Pathol 2005; 206:366-376.

Herpin A, Cunningham C. Cross-talk between the bone morphogenetic protein pathway and other major signalling pathways results in tightly regulated cell-specific outcomes. Febs J 2007; 274:2977-2985.

Hisamatsu K, Ganbo T, Nakazawa T, Murakami Y, Gleich GJ, Makiyama K, Koyama H. Cytotoxicity of human eosinophil granule major basic protein to human nasal sinus mucosa *in vitro*. J Allergy Clin Immunol 1990; 86: 52-63.

Hollnagel A, Oehlmann V, Heymer J, Ruther U and Nordheim A. Id Genes Are Direct Targets of Bone Morphogenetic Protein Induction in Embryonic Stem Cells. J Biol Chem 1999; 274:19838-19845.

Hopkins DR, Keles S and Greenspan DS. The bone morphogenetic protein 1/Tolloid-like metalloproteinases. Matrix Biol 2007; 26: 508-523.

Howe JR, Sayed MG, Ahmed AF, Ringold J, Larsen-Haidle, Merg A, Mitros FA, Vaccaro CA, Petersen GM, Giardiello, Tinley, Aaltonen LA and Lynch HT. The prevalence of MADH4 and BMPR1A mutations in juvenile polyposis and absence of BMPR2, BMPR1B, and ACVR1 mutations. J med Genet 2004; 41:484-491.

Howe PH, Dobrowolski SF, Reddy KB, Stacey DW. Release from G1 growth arrest by transforming growth factor β 1 requires cellular ras activity. J Biol Chem 1993; 268: 21448-21452.

Hullinger TG, Pan Q, Viswanathan HL and Somerman MJ. TGFbeta and BMP-2 activation of the OPN promoter: roles of smad- and hox-binding elements. Exp Cell Res 2001; 262: 69-74.

Humbles AA, Lloyd CM, McMillan SJ, Friend DS, Xanthou G, McKenna EE, Ghiran S, Gerard NP, Yu C, Orkin SH, Gerard C: A Critical Role for Eosinophils in Allergic Airways Remodelling. Science 2004, 305:1776-1779.

Ivanov DB, Philippova MP and Tkachuk VA. (2001). Structure and functions of classical cadherins. Biochemistry (Mosc) 66, 1174-86.

Iwano M, Plieth D, Danoff TM, Xue C, Okada H and Neilson EG. Evidence that fibroblasts derive from epithelium during tissue fibrosis. J Clin Invest 2002; 110: 341-350.

Iwasaki S, Iguchi M, Watanabe K, Hoshino R, Tsujimoto M and Kohno M. Specific activation of the p38 mitogen-activated protein kinase signalling pathway and induction of neurite outgrowth in PC12 cells by bone morphogenetic protein-2. J Biol Chem 1999; 274: 26503-26510.

Jamora C, DasGupta R, Kocieniewski P and Elaine Fuchs. Links between signal transduction, transcription and adhesion in epithelial bud development. Nature 2003; 422: 317-322.

Janda E, Lehmann K, Killisch I, Jechlinger M, Herzig M, Downward J, Beug H and Grunert. Ras and TGFβ cooperatively regulate epithelial cell plasticity and metastasis: dissection of Ras signalling pathways. J Cell Biol 2002; 156: 299-313.

Janda E, Nevolo M, Lehmann K, Downward J, Beug H and Grieco M. Raf plus TGF-β-dependent EMT is initiated by endocytosis and lysosomal degradation of E-cadherin. Oncogene 2006; 25: 7117-7130.

Jans DA, Briggs LJ, Gustin SE, Jans P, Ford S, Young IG: The cytokine interleukin-5 (IL-5) effects cotransport of its receptor subunits to the nucleus *in vitro*. FEBS Letters 1997, 410:368-372.

Jans DA, Hassan G. Nuclear targeting by growth factors, cytokines, and their receptors: a role in signalling? BioEssays 1998; 20: 400-411.

Jeffery PK and Haahtela T. Allergic rhinitis and asthma: inflammation in a one-airway condition. BMC pulmonary medicine 2006; 6(Suppl 1):S5.

Kaiser S, Schirmacher P, Philipp A, Protschka M, Moll I, Nicol K, Blessing M.Induction of bone morphogenetic protein-6 in skin wounds. Delayed reepitheliazation and scar formation in BMP-6 overexpressing transgenic mice. J Invest Dermatol 1998; 111: 1145-1152.

Kallurin R and Neilson EG. Epithelial-mesenchymal transiton and its implications for fibrosis. J Clin Invest 2003; 112: 1776-1784.

Karaulanov E, Knochel W and Niehrs C. Transcriptional regulation of BMP4 synexpression in transgenic Xenopus. EMBO J 2004; 23: 844-856.

Kariyawasam HH and Robinson DS. The role of eosinophils in airway tissue remodelling in asthma . Curr Opin Immunol 2007; 19: 681-686.

Kariyawassam HH, Xanthou G, Barkans J, Aizen M, Kay AB, Robinson DS. Basal expression of bone morphogenetic protein receptor is reduced in mild asthma. Am J Respir Crit Care Med 2008; 177: 1074-1081.

Karkema JR, Carey SA and Wagner JG. The Nose Revisited: A Brief Review of the Comparative Structure, Function, and Toxicologic Pathology of the Nasal Epithelium. Toxicologic Pathology 2006; 34: 252-269.

Kasai H, Allen JT, Mason RM, Kamimura and Zhang Z. TGF-β1 induces human alveolar epithelial to mesenchymal cell transition (EMT). Respir Res 2005; 6: 56.

Katoh M and Katoh M. Cross-talk of WNT and FGF Signalling Pathways at GSK3β to Regulate β-Catenin and SNAIL Signalling Cascades. Cancer Biol Ther 2006; 5: 1059-1064.

Khalil N, Greenberg AH. The role of TGF-beta in pulmonary fibrosis. Ciba Found Symp 1991; 157: 194-211.

Kim K, Lu Z and Hay ED. Direct evidence for a role of β-catenin/LEF-1 signalling pathway in induction of EMT. Cell Biol Int 2002; 26: 463-476.

Kimura N, Matsuo R, Shibuya H, Nakashima K and Taga T. BMP2-induced apoptosis is mediated by activation of the TAK1-p38 kinase pathway that is negatively regulated by Smad6. J Biol Chem 2000; 275: 17647-17652.

Kishigami S and Mishina Y. BMP signalling and early embryonic pattering. Cytokine Growth Factors Rev 2005;16:265-278.

Kleine TJ, Gleich GJ, Lewis SA. Eosinophil major basic protein increases membrane

permeability in mammalian urinary bladder epithelium. Am J Physiol 1998; 275 (1 Pt 1): C93-103.

Koli K, Myllarniemi M, Vuorinen K, Salmenkivi K, Ryynanen MJ, Kinnula VL, Keski-Oja J. Bone morphogenetic protein-4 inhibitor gremlin is overexpressed in idiopathic pulmonary fibrosis. Am J Pathol 2006; 169:61-71.

Koli KM, Arteaga CL. Predominant cytosolic localization of type II transforming growth factor receptors in human breast carcinoma cells. Cancer Res 1997; 57: 970-977.

Kopan R, Schroeter EH, Weintraub H, Nye JS: Signal transduction by activated mNotch: Importance of proteolytic processing and its regulation by the extracellular domain. Proc Natl Acad Sci 1996, 93:1683-1688.

Kratochwil K, DuU M, Farinas I, Galceran J and Grosschedl R. Lef1 expression is activated by BMP-4 and regulates inductive tissue interactions in tooth and hair development. Genes Dev 1996; 10: 1382-1394.

Kraunz KS, Nelson HH, Liu M, Wiencke JK and Kelsey KT. Interaction between the bone morphogenetic proteins and Ras/MAP-kinase signalling pathways in lung cancer. Br J Cancer 2005; 93: 949-952.

Langenfeld EM and Langenfeld J. Bone Morphogenetic Protein-2 Stimulates Angiogenesis in Developing Tumors. Mol Cancer Res 2004; 2: 141-149.

Langenfeld EM, Calvano SE, Abou-Nukta F, Lowry SF, Amenta P, Langenfeld J. The mature bone morphogenetic protein-2 is aberrantly expressed in non-small cell lung carcinomas and stimulates tumor growth of A549 cells. Carcinogenesis 2003; 24:1445-1454.

Langenfeld EM, Kong Y, Langenfeld J. Bone morphogenetic protein 2 stimulation of tumor growth involves the activation of Smad-1/5. Oncogene 2006;25:685-692.

Larue L and Bellacosa A. Epithelial-mesenchymal transition in development and cancer: role of phosphatidylinositol 3' kinase/AKT pathways.Oncogene 2005; 24: 7443-7475.

Lee JM, Dedhar S, Kalluri R and Thompson EW. The epithelial-mesenchymal transition: new insights in signalling , development, and disease. J Cell Biol 2006; 973-981.

Liao HJ, Carpenter G. Role of the Sec61 translocon in EGF receptor trafficking to the nucleus and gene expression.Mol Biol Cell 2007; 18: 1064-1072.

Lieber M, Smith B, Szakal A, Nelson-Rees W and Todaro G. A continuous tumor-cell line from a human lung carcinoma with properties of type II alveolar epithelial cells.Int J Cancer 1976; 17: 62-70.

Liebner S, Cattelino A, Gallini R, Rudini N, Iurlaro M, Piccolo S and Dejana E. Beta-catenin is required for endothelial-mesenchymal transformation during heart cushion development in the mouse. J Cell Biol 2004; 166: 359-367.

Lin SY, Makino K, Xia W, Matin A, Wen Y, Kwong KY, Bourguignon L, Hung MC: Nuclear localization of EGF receptor and its potential new role as a transcription factor. Nat Cell Biol 2001, 3:802-808.

Liu JH, Wei S, Burnette PK, Gamero AM, Hutton M and Djeu JY. Function association of TGF-β receptor II with cyclin B. Oncogene 1999; 18:269-275.

Liu X, Sun Y, Weinberg RA and Lodish HF. Ski/Sno and TGF-beta signalling . Cytokine Growth Factor Rev 2001; 12: 1-8.

Lo HW, Hsu SC, Hung MC. EGFR signalling pathway in breast cancers: from traditional signal transduction to direct nuclear translocalization. Breast cancer research and treatment 2006a; 95: 211-218.

Lo HW and Hung MC. Nuclear EGFR signalling network in cancers: linking EGFR pathway to cell cycle progression, nitric oxide pathway and patient survival. British Journal of Cancer 2006b; 94: 184-188.

Lo RS, Chen YG, Shi Y, Pavletich NP and Massagué J. The L3 loop: a structural motif determining specific interactions between SMAD proteins and TGF-beta

receptors. EMBO J 1998; 17: 996-1005.

Lobie PE, Wood TJJ, Chen CM, Waters MJ, Norstedt G: Nuclear translocation and anchorage of the growth hormone receptor. J Biol Chem 1994, 296:31735-31746.

Logeart-Avramoglou D, Bourguignon M, Oudina K, Ten Dijke P and Petite H. An assay for the determination of biologically active bone morphogenetic proteins using cells transfected with an inhibitor of differentiation promoter-luciferase construct. Anal Biochem 2006; 349: 78-86.

Lories RJU and Luyten FP. Bone Morphogenetic Protein signalling in joint homeostasis and disease. Cytokine Growth Factor Rev 2005; 16: 287-298.

Luo K. Negative regulation of BMP signalling by the ski oncoprotein. J Bone Joint Surg Am 2003; 85-A Suppl 3: 39-43.

Luyten FP, Cunningham NS, Ma S, Muthukumaran N, Hammonds RG, Nevins WB, Woods WI, Reddi AH. Purification and partial amino acid sequence of osteogenin, a protein initiating bone differentiation. J Biol Chem 1989; 264: 13377-13380.

Ma L, Lu MF, Schwartz RJ and Martin JF. Bmp2 is essential for cardiac cushion epithelial-mesenchymal transition and myocardial patterning. Development 2005; 132: 5601-5611.

Marcelino J, Sciortino CM, Romero MF, Ulatowski LM, Ballock RT, Economides AN, Eimon PM, Harland RM and Warman ML. Human disease-causing NOG missense mutations: effects on noggin secretion, dimer formation, and bone morphogenetic protein binding. Proc Natl Acad Sci U S A 2001; 98: 11353-11358.

Maric I, Poljak L, Zoricic S, Bobinac D, Bosukonda D, Sampath KT and Vukicevic S. Bone Morphogenetic Protein-7 Reduces the Severity of Colon Tissue Damage and Accelerates the Healing of Inflammation Bowel Disease in Rats. J Cell Physiol 2003; 196: 258-264.

Marti U, Wells A: The Nuclear Accumulation of a Variant Epidermal Growth Factor Receptor (EGFR) Lacking the Transmembrane Domain Requires Coexpression of a Full-length EGFR. Mol Cell Biol Res Comm 2000, 3:8-14.

Maschler S, Grunert S, Danielopol A, Beug H, Wirl G.Enhanced tenascin-C expression and matrix deposition during Ras/TGF-beta-induced progression of mammary tumor cells.Oncogene. 2002; 23: 3622-3633.

Masterson JC and O'Dea S. 5-Bromo-2-deoxyuridine activates DNA damage signalling responses and induces a senescence-like phenotype in p16-null lung cancer cells. Anticancer Drugs 2007; 18: 1053-1068.

McBride S, Tatrai E, Blundall R, Kovacikova Z, Cardozo L, Adamis Z,Smith T and Harrison. Characterisation of lectin binding patterns of mouse bronchiolar and rat alveolar epithelial cells in culture. The Histochemical Journal 2000; 32:33-40.

McDougall CM, Blaylock MG, Douglas JG, Brooker RJ, Helms PJ and Walsh GM. Nasal epithelial cells as surrogates for bronchial epithelial cells in airway inflammation studies. Am J Respir Cell Mol Biol. 2008; 39: 560-568.

Michiels F and Collard JG. Rho-like GTPases: their role in cell adhesion and invasion. Biochem Soc Symp 1999; 65: 125-146.

Mishina Y, Hanks MC, Miura S, Tallquist MD and Behringer RR. Generation of Bmpr/Alk3 conditional knockout mice. Genesis 2002; 32: 69-72.

Miyazono K, Maeda S and Imamura T. BMP receptor signalling : Transcriptional targets, regulation of signals, and signalling cross-talk. Cytokine Growth Factor Rev 2005; 16: 251-263.

Molloy EL, Adams A, Moore JB, Masterson JC, Madrigal-Estebas L, Mahon BP and O'Dea S. BMP4 induces an epithelial-mesenchymal transition-like response in adult airway epithelial cells. Growth Factors 2008; 26: 12-22.

Montesano R. Bone morphogenetic protein-4 abrogates lumen formation by mammary epithelial cells and promotes invasive growth. Biochem Biophys Res Commun 2007; 353: 817-822.

Morgan RK, Costello RW, Durcan N, Kingham PJ, Gleich GJ, McLean WG and Walsh MT. Diverse effects of eosinophil cationic granule proteins on IMR-32 nerve

cell signaling and survival. Am J Respir Cell Mol Biol; 2005 33: 169-177.

Motojima S, Frigas E, Loegering DA, Gleich GJ: Toxicity of eosinophil cationic proteins for guinea pig tracheal epithelium *in vitro*. Am Rev Respir Dis 1989, 139:801-805.

Moustakas A and Heldin CH. Ecsit-ement on the crossroads of Toll and BMP signal transduction. Genes Dev 2003; 17: 2855-2859.

Murakami M, Ohkuma M, Nakamura M. Molecular mechanism of transforming growth factor-β-mediated inhibition of growth arrest and differentiation in a myoblast cell line. Dev Growth Differ 2008; 50: 121-130.

Nakajima Y, Yamagishi T, Hokari S and Nakamura H. Mechanisms Involved in Valvuloseptal Endocardial Cushion Formation in Early Cardiogenesis: Roles of Transforming Growth Factor (TGF)-β and Bone Morphogenetic Protein (BMP). Anat Rec 2000; 258: 119-127.

Nakayama T, Cui Y and Christian JL. Regulation of BMP/Dpp signaling during embyronic development. Cell Mol Life Sci 2000; 57: 943-956.

Nishanian TG, Waldman T: Interction of the BMPR-IA tumor suppressor with a developmentally relevant splicing factor. Biochemical and Biophysical Research Communications 2004, 323:91-97.

Nishita M, Ueno N and Shibuya H. Smad8B splice variant lacking the SSXS site that inhibits Smad8-mediated signalling. Genes Cells 1999; 4:583-591.

Nobes CD and Hall A. Rho, rac, and cdc42 GTPases regulate the assembly of multimolecular focal complexes associated with actin stress fibers, lamellipodia, and filopodia. Cell 1995; 81: 53-62.

Noë V, Fingleton B, Jacobs K, Crawford HC, Vermeulen S, Steelant W, Bruyneel E, Matrisian LM and Mareel M. Release of an invasion promoter E-cadherin fragment by matrilysin and stromelysin-1. J Cell Sci 2001; 114: 111-118.

Nohe A, Hassel S, Ehrlich M, Neubauer F, Sebald W, Henis YI, Knaus P. The mode

of bone morphogenetic protein (BMP) receptor oligomerization determines different BMP-2 signalling pathways. J Biol Chem 2002; 277:5330-5338.

Nohe A, Keating E, Underhill TM, Knaus P, Peterson NQ: Effect of the distribution and clustering of the type IA BMP receptor (ALK3) with the type II BMP receptor on the activation of signalling pathways. J Cell Sci 2003; 116: 3277-3284.

Nusrat A, Parkos CA, Bacarra AE, Godowski PJ, Delp-Archer C, Rosen EM and Madara JL. Hepatocyte growth factor/scatter factor effects on epithelia. Regulation of intercellular junctions in transformed and nontransformed cell lines, basolateral polarization of c-met receptor in transformed and natural intestinal epithelia, and induction of rapid wound repair in a transformed model epithelium. J Clin Invest 1994; 93: 2056-2065.

Ohno I, Nitta Y, Yamauchi K, Hoshi H, Honma M, Woolley K, O'Byrne P, Dolovich J, Jordana M, Tamura G. Eosinophils as a potential source of platelet-derived growth factor B-chain (PDGF-B) in nasal polyposis and bronchial asthma. Am J Respir Cell Mol Biol 1995; 13: 639-647.

Okada H, Danoff TM, Kalluri R and Neilson EC. Early role of FSP1 in epithelial-mesenchymal transformation. Am J Physiol 1997; 273: F563-574.

Okagawa H, Markwald RR, Sugi Y. Functional BMP receptor in endocardial cells in required in atrioventricular cushion mesenchymal cell formation in chick. Dev Biol 2007; 306: 179-192.

Olver RE, Schneeberger EE, Walters DV. Epithelial solute permeability, ion transport and tight junction morphology in the developing lung of the fetal lamb. J Physiol 1981; 315: 395-412.

Onichtchouk D, Chen YG, Dosch R, Gawantka V, Delius H, Massagué J and Niehrs C. Silencing of TGF-beta signalling by the pseudoreceptor BAMBI. Nature 1999; 401: 480-485.

Park KS, Wells JM, Zorn AM, Wert SE, Laubach VE, Fernandez LG, Whitsett JA.Transdifferentiation of ciliated cells during repair of the respiratory epithelium. Am J Respir Cell Mol Biol 2006; 34: 151-157.

Pawankar R, Lee KH, Nonaka M and Takizawa R.Role of mast cells and basophils in chronic rhinosinusitis. Clin Allergy Immunol 2007; 20: 93-101.

Pegorier S, Wagner LA, Gleich GJ, Pretolani M: Eosinophil-Derived Cationic Proteins Activate the Synthesis of Remodeling Factors by Airway Epithelial Cells. J Immunol 2006, 177: 4861-4869.

Peinado H, Ballestar E, Esteller M, Cano A. Snail mediates E-cadherin repression repression by the recruitment of the Sin3A/histone deacetylase 1 (HDAC1)/HDAC2 complex. Mol Cell Biol 2004a; 24:306-319.

Peinado H, Marin F, Cubillo E, Stark HJ, Fusenig N, Nieto MA and Cano A. Snail and E47 repressors of E-cadherin induces distinct invasive and angiogenic properties *in vivo*. J Cell Sci 2004b; 117; 2827-2839.

Peinado H, Portillo F, Cano A. Transcriptional regulation of cadherins during development and carcinogenesis. Int J Dev Biol 2004c; 48: 365-375.

Pereira RC, Delany AM and Canalis E. Effects of Cortisol and Bone Morphogenetic Protein-2 on Stromal Cell Differentiation: Correlation With CCAAT-enhancer Binding Protein Expression. Bone 2002; 30: 685-691.

Perk J, Iavarone A and Benezra R. Id Family of Helix-Loop-Helix Proteins in Cancer.Nat Rev 2005; 5:603-614.

Planque N. Nuclear trafficking of secreted factors and cell-surface receptors: new pathways to regulate cell proliferation and differentiation, and involvement in cancers. Cell communication and signalling 2006; 4:7.

Pouliot F, Blais A and Labrie C. Overexpression of a dominant negative type II bone morphogenetic protein receptor inhibits the growth of human breast cancer cells. Cancer Res 2003; 63: 277-281.

Psyrri A, Yu Z, Weinberger PM, Saskai C, Haffty B, Camp R, Rimm D, Burtness BA. Quantitative determination of nuclear and cytoplasmic epidermal growth factor receptor expression in oropharyngeal squamous cell cancer by using automated quantitative analysis. Clin Cancer Res 2005; 11: 5856-5862.

Puchelle E, Zahm JM, Tournier JM and Coraux C. Airways Epithelial Repair, Regeneration, and Remodeling after Injury in Chronic Obstructive Pulmonary Disease. Proc Am Thorac Soc 2006; 3:726-733.

Qing J, Zhang Y, Derynck R. Structural and functional characterization of the transforming growth factor-beta -induced Smad3/c-Jun transcriptional cooperativity. J Biol Chem 2000; 275: 38802-38812.

Raferty LA and Sutherland DJ. TGF-β Family Signal Transduction in Drosophila Development: From Mad to Smads. Dev Biol 1999; 210: 251-268.

Rawlins EL and Hogan LM. Epithelial stem cells of the lung: privileged few or opportunities for many. Development 2006; 133:2455-2465.

Reddel RR, Yang K, Gerwin BI, McMenamin MG, Lechner JF, Su RT, Brash DE, Park J-B, Rhim JS, Harris CC. Transformation of human bronchial epithelial cells by infection with SV40 or adenovirus-12 SV40 hybrid virus, or transfection via strontium phosphate coprecipitation with a plasmid containing SV40 early region genes. Cancer Res 1988; 48:1904-1909.

Ribeiro-Filho LA, Franks J, Sasaki M, Shiina H, Li LC, Nojima D, Arap S, Carroll P, Enokida H, Nakagawa M, Yonezawa S and Dahiya R. CpG hypermethylation of promoter region and inactivation of E-cadherin gene in human bladder cancer. Mol Carcinog 2002; 34: 187-198.

Robert B. Bone morphogenetic protein signalling in limb outgrowth and patterning. Develop Growth Differ 2007; 49: 455-468.

Rommel C and Hafen E. Ras - a versatile cellular switch. Curr Opin Genet Dev 1998; 8: 412-418.

Rose MC. Mucins: structure, function, and role in pulmonary diseases.Am J Physiol 1992; 263: L413-429.

Rosendahl A, Pardali E, Speletas M, Ten Dijke P, Heldin CH: Activation of bone morphogenetic protein/smad signalling in bronchial epithelial cells during airway inflammation. Am J Respir Cell Mol Biol 2002, 27:160-169.

Rothhammer T, Poser I, Soncin F, Bataille F, Moser M and Bosserhoff AJ. Bone Morphogenic Proteins Are Overexpressed in Malignant Melanoma and Promote Cell Invasion and Migration. Caner Res 2005; 65:448-456.

Saito T, Oda Y, Itakura E, Shiratsuchi H, Kinoshita Y, Oshiro Y, Tamiya S, Hachitanda Y, Iwamoto Y and Tsuneyoshi M. Expression of intercellular adhesion molecules in epithelioid sarcoma and malignant rhabdoid tumor. Pathol Int 2001; 51: 532-542.

Sakai D, Suzuki T, Osumi N and Wakamatsu Y. Cooperative action of Sox9, Snail2 and PKA signalling in early neural crest development. Development 2006; 133: 1323-1333.

Salib RJ, Drake-Lee A, Howarth PH. Allergic rhinitis: past, present and the future. Clin Otolaryngol 2003a; 28: 291-303.

Salib RJ, Howarth PH. Remodelling of the upper airways in allergic rhinitis: is it a feature of the disease? Clin Exp Allergy 2003b; 33: 1629-1633.

Salib RJ, Kumar S, Wilson SJ, Howarth PH. Nasal mucosal immunoexpression of the mast cell chemoattractants TGF-β, eotaxin, and stem cell factor and their expression in allergic rhinitis. J Allergy Clin Immunol 2004; 114: 799-806.

Samad TA, Rebbapragada A, Bell E, Zhang Y, Sidis Y, Jeong SJ, Campagna JA, Perusini S, Fabrizio DA, Schneyer AL, Lin HY, Brivanlou AH, Attisano L and Woolf CJ. DRAGON, a bone morphogenetic protein co-receptor. J Biol Chem 2005; 280: 14122-14129.

Sanai A, Nagata H, Konna A. Extensive interstitial collagen deposition on the basement membrane zone in allergic nasal mucosa. Acta Otolaryngol 1999; 119: 473-478.

Sandvig K, van Deurs B. Membrane traffic exploited by protein toxins. Annu Rev Cell Dev Biol 2002; 18: 1-24.

Sapkota G, Alarcon C, Spagnoli FM, Brivanlou AH and Massague. Balancing BMP Signalling through Integrated Inputs into the Smad1 Linker. Mol Cell 2007; 25: 441-454.

Sauer T, Boudjema G, Jebsen PW and Naess O. Immunocytochemical expression of E-cadherin on fine-needle aspirates from breast carcinomas correlate with the cell dissociation pattern seen on smears. Diagn Cytopathol 2001; 25: 382-388.

Savanger P. Leaving the neighborhood: molecular mechanisms involved during epithelial-mesenchymal transition. BioEssays 2001; 23: 912-923.

Segditsas S and Tomlinson I. Colorectal cancer and genetic alterations in the Wnt pathway. Oncogene 2006; 25: 7531-7537.

Sekiya T, Adachi S, Kohu K, Yamada T, Higuchi O, Furukawa Y, Nakamura Y, Nakamura T, Tashiro K, Kuhara S, Ohwada S and Akiyama T. Identification of BMP and activin membrane-bound inhibitor (BAMBI), an inhibitor of transforming growth factor-beta signalling , as a target of the beta-catenin pathway in colorectal tumor cells. J Biol Chem 2004; 279: 6840-6846.

Settle SH Jr, Rountree RB, Sinha A, Thacker A, Higgins K and Kingsley DM. Multiple joint and skeletal patterning defects caused by single and double mutations in the mouse Gdf6 and Gdf5 genes. Dev Biol. 2003; 254: 116-130.

Shannon JM and Hyatt BA. Epithelial-Mesenchymal Interactions in the Developing Lung. Annu Rev Physiol 2004; 66: 625-645.

Shi W, Bellusci S and Warburton D. Lung development and adult lung diseases. Chest 2007; 132: 651-656.

Shi Y and Massague J. Mechanisms of TGF-β Signalling from Cell Membrane to the Nucleus. Cell 2003; 113: 685:700.

Shibuya H, Iwata H, Masuyama N, Gotoh Y, Yamaguchi K, Irie K, Matsumoto K, Nishida E and Ueno N. Role of TAK1 and TAB1 in BMP signalling in early Xenopus development. EMBO J 1998; 17: 1019-1028.

Shih JY, Tsai MF, Chang TH, Chang YL, Yuan A, Yu CJ, Lin SB, Liou GY, Lee ML, Chen JJ, Hong TM, Yang SC, Su JL, Lee YC and Yang PC. Transcription repressor slug promotes carcinoma invasion and predicts outcome of patients with lung adenocarcinoma. Clin Cancer Res 2005; 11: 8070-8078.

Shook D, Keller R. Mechanisms, mechanics and function of epithelial-mesenchymal transitions in early development. Mech Dev 2003; 120:1351-1383.

Shu W, Guttentag S, Wang Z, Andl T, Ballard P, Lu MM, Piccola S, Birchmeier W, Whitsett JA, Millar SE and Morrisey EE. Wnt/β-catenin signalling acts upstream of N-myc, BMP4, and FGF signalling to regulate proximal-distal patterning in the lung. Dev Biol 2005; 283: 226-239.

Sibbald B. Epidemiology of allergic rhinitis. Monogr Allergy 1993; 31: 61-79.

Silberstein DS. Eosinophil function in health and disease. Critical Reviews in Oncology/Hematology 1995, 19: 47-77.

Simic P and Vukicevic S. Bone morphogenetic in development and homeostasis of kidney. Cytokine Growth Factors 2005; 16:199-308.

Song L, Fassler R, Mishina Y, Jiao K and Baldwin HS. Essential functions of Alk3 during AV cushion morphogenesis in mouse embryonic hearts. Dev Biol 2007; 301: 276-286.

Sorkina T, Huang F, Beguinot L, Sorkin A. Effect of tyrosine kinase inhibitors on clathrin-coated pit recruitment and internalization of epidermal growth factor receptor. J Biol Chem 2002; 277: 27433-27441.

Stachowiak MK, Maher PA, Joy A, Mordechai E, Stachowiak EK: Nuclear localization of functional FGF receptor 1 in human astrocytes suggests a novel mechanism for growth action. Mol Brain Res 1996, 38:61-165.

Stelnicki EJ, Longaker MT, Holmes D, Vanderwall K, Harrison MR, Largman C and Hoffman WY. Bone morphogenetic protein-2 induces scar formation and skin maturation in the second trimester fetus. Plast Reconstr Surg 1998; 101: 12-19.

Stenfeldt AL, Wennerås C. Danger signals derived from stressed and necrotic epithelial cells activate human eosinophils. Immunology 2004; 112: 605-614.

Stripp BR and Reynolds SD. Clara Cells. Encyclopedia of respiratory medicene 2006, 1: 471-478.

Stripp BR and Reynolds SD. Maintenance and Repair of the Bronchiolar Epithelium. Proc Am Thomac Soc 2008; 5:328-333.

Strutz F, Zeisberg M, Ziyadeh FN, Yang QC, Kalluri R, Muller GA and Neilson EG. Role of basic fibroblast growth factor-2 in epithelial-mesenchymal transformation. Kidney Int 2002; 61: 1714-1728.

Sun J, Chen H, Chen C, Whitsett JA, Mishina Y, Bringas P, Ma JC, Warburton D and Shi W. Prenatal Lung Epithelial Cell-Specific Abrogation of Alk3-Bone Morphogenetic Protein Signalling Causes Neonatal Respiratory Distress by Disrupting Distal Airway Formation. Am J Pathol 2008; 172: 571-582.

Suzawa M, Takeuchi Y, Fukumoto S, Kato S, Ueno N, Miyazono K, Matsumoto T and Fujita T. Extracellular matrix-associated bone morphogenetic proteins are essential for differentiation of murine osteoblastic cells *in vitro*.Endocrinology 1999; 140: 2125-2133.

Takizawa H. Bronchial Epithelial Cells in Allergic Reactions. Curr Drug Targets Inflamm Allergy 2005; 4: 305-311.

Theriault BL, Shepherd TG, Mujoomdar ML, Nachtigal MW. BMP4 induces EMT and Rho GTPase activation in human ovarian cancer cells. Carcinogenesis 2007; 28:1153-1162.

Thiery JP. Epithelial-mesenchymal transitions in development and pathologies. Curr Opin Cell Biol 2003; 15: 740-746.

Thiery JP. Epithelial-mesenchymal transitions in tumour progression. Nat Rev Cancer 2002; 2: 442-454.

Thompson EW and Newgreen DF. Carcinoma Invasion and Metastasis: A Role for Epithelial-Mesenchymal Transition? Cancer Res 2005; 65:5991-5994.

Togias A. Unique mechanistic features of allergic rhinitis. J Allergy Clin Immunol 2000; 105:s599-604.

Trautmann A, Kruger K, Akdis M, Muller-Wening D, Akkaya A, Brocker EB, Blaser K and Akdis CA. Apoptosis and loss of adhesion of bronchial epithelial cells in asthma. Int Arch Allergy Immunol 2005; 138: 142-150.

Trautmann A, Schmid-Grendelmeier P, Krüger K, Crameri R, Akdis M, Akkaya A, Bröcker EB, Blaser K, Akdis CA. T cells and eosinophils cooperate in the induction of bronchial epithelial cell apoptosis in asthma. J Allergy Clin Immunol 2002; 109: 329-337.

Trivedi SG and Lloyd CM. Eosinophils in the pathogenesis of allergic airways disease. Cell Mol Life Sci 2007; 64: 1269-1289.

Ullrich A, Schlessinger J. Signal transduction by receptors with tyrosine kinase activity. Cell 1990; 61: 203-213.

Urist MR. Bone: formation by autoinduction. Science 1965; 150: 893-899.

Valcourt U, Kowanetz M, Niimi H, Heldin CH and Moustakas A. TGF-β and the Smad Signalling Pathway Support Transcriptional Reprogramming during Epithelial-Mesenchymal Cell Transition. Mol Biol Cell 2005; 16: 1987-2002.

Vancurova I, Jochova J, Lou W, Paine PL. An NLS is sufficient to engage facilitated translocation by the nuclear pore complex and subsequent intranuclear binding. Biochem Biophys Res Commun 1994; 205: 529-536.

Vaporidi K, Tsatsanis C, Georgopoulos D and Tsichlis PN. Effects of hypoxia and hypercapnia on surfactant protein expression proliferation and apoptosis in A549 alveolar epithelial cells. Life Sci 2005; 78: 284-293.

Varga AC and Wrana JL. The disparate role of BMP in stem cell biology. Oncogene 2005; 24: 5713-5721.

VonBubnoff A and Cho KWY. Intracellular BMP Signalling Regulation in Vertebrates: Pathway or Network? Dev Biol 2001; 239: 1-14.

Walsh GM. Eosinophil granule proteins and their role in disease. Curr Opin Hematol 2001; 8: 28-33.

Warburton D, Schwarz M, Tefft D, Flores-Delgado G, Anderson KD and Cardoso WV. The molecular basis of lung morphogenesis. Mech Dev 2000; 92:55-81.

Weaver M, Dunn NR and Hogan BLM. Bmp4 and Fgf10 play opposing roles during lung bud morphogenesis. Development 2000; 127: 2695-2704.

Weaver M, Yingling JM, Dunn NR, Bellusci S, Hogan BL. Bmp signalling regulates proximal-distal differentiation of endoderm in mouse lung development. Development 1999; 126:4005-4015.

Wells RG, Yankelev H, Lin HY, Lodish HF. Biosynthesis of the type I and type II TGF-β receptors. Implications for complex formation. J Bio Chem 1997; 272: 11444-11451.

Willis BC, Lieber JM, Luby-Phieps K, Nicholson AG, Crandall ED, du Bois RM and Borok Z. Induction of Epithelial-Mesenchymal Transition in Alveolar Epithelial cells by Transforming Growth Factor-β1. Am J Pathol 2005; 166: 1321-1332.

Wilson JW and Bamford TL. Assessing the evidence for remodelling of the airway in asthma. Pulm Pharmacol Ther 2001; 14: 229-247.

Winnier G, Blessing M, Labosky PA, Hogan BL. Bone morphogenetic protein-4 is required for mesoderm formation and patterning in the mouse. Genes Dev 1995; 9:2105-2116.

Wong CK, Wang CB, Li MLY, Ip WK, Tian YP and Lam CWK. Induction of adhesion molecules upon the interaction between eosinophils and bronchial epithelial cells: Involvement of p38 MAPK and NF-κB. Int Immunopharmacol 2006; 6: 1859-

1871.

Wong DT, Elovic A, Matossian K, Nagura N, McBride J, Chou MY, Gordon JR, Rand TH, Galli SJ, Weller PF. Eosinophils from patients with blood eosinophilia express transforming growth factor β 1. Blood 1991; 78: 2702-2707.

Wozney JM, Rosen V, Byrne M, Celeste AJ, Moutsatsos I and Wang EA. Growth factors influencing bone development. J Cell Sci Suppl 1990; 13: 149-156.

Wozney JM, Rosen V, Celeste AJ, Mitsock LM, Whitters MJ, Kriz RW, Hewick RM, Wang EA. Novel regulators of bone formation: molecular clones and activities. Science 1988; 242: 1528-1534.

Xiao C, Shim J, Kluppel M, Zhang SS, Dong C, Flavell RA, Fu XY, Wrana JL, Hogan BLM and Ghosh S. Ecsit is required for Bmp signalling and mesoderm formation during embryogenesis. Genes Dev 2003; 17: 2933-2949.

Xiao Z, Watson N, Rodriquez C and Lodish HF. Nucleocytoplasmic Shuttling of Smad1 Conferred by Its Nuclear Localization and Nuclear Export Signals. J Biol Chem 2001; 276: 39404-39410.

Yamashita H, ten Dijke P, Heldin CH and Miyazono K. Bone Morphogenetic Protein Receptors. Bone 1996; 19:569-574.

Yang J, Mani SA, Donaher JL, Ramaswamy S, Itzykson RA, Come C, Savagner P, Gitelman I, Richardson A and Weinberg RA. Twist, a master regulator of morphogenesis, plays an essential role in tumor metastasis. Cell 2004; 117: 927-939.

Yang S, Du Y, Wang Z, Yuan W, Qiao Y, Zhang M, Zhang J, Gao S, Yin J, Sun B and Zhu T. BMP-6 promotes E-cadherin expression through repressing δEF1 in breast cancer cells. BMC Cancer 2007; 7: 211.

Yoshida Y, Tanaka S, Umemori H, Minowa O, Usui M, Ikematsu N, Hosoda E, Imamura T, Kuno J, Yamashita T, Miyazono K, Noda M, Noda T and Yamamoto T. Negative regulation of BMP/Smad signalling by Tob in osteoblasts. Cell 2000; 103: 1085-1097.

Yoshida Y, von Bubnoff A, Ikematsu N, Blitz IL, Tsuzuku JK, Yoshida EH, Umemori H, Miyazona K, Yamamoto T and Cho KW. Tob proteins enhance inhibitory Smad-receptor interactions to repress BMP signalling . Mech Dev 2003; 120: 629-637.

Yoshikawa H, Nakase T, Myoui A and Ueda T. Bone morphogenetic proteins in bone tumors. J Orthop Sci 2004; 9: 334-340.

Zavadil J and Bottinger EP. TGF-β and epithelial-to-mesenchymal transitions. Oncogene 2005; 24: 5764-5774.

Zeisberg EM, Tarnavaski O, Zeisberg M, Dorfman AL, McMullen JR, Gustafsson E, Chandraker A, Yuan X, Pu WT, Roberts AB, Neilson EG, Sayegh MH, Izumo S and Kalluri R. Endothelial-to-mesenchymal transtion contributes to cardiac fibrosis. Nat Med 2007; 13: 952-961.

Zeisberg M, Hanai J, Sugimoto H, Mammoto T, Charytan D, Strutz F and Kalluri R. BMP-7 counteracts TGF-beta1-induced epithelial-to-mesenchymal transition and reverses chronic renal injury. Nat Med 2003; 9: 964-968.
Zhu H, Kavsak P, Abdollah S, Wrana JL and Thomsen GH. A SMAD ubiquitin ligase targets the BMP pathway and affects embryonic pattern formation. Nature 400; 687-693.

Zwaagstra JC, Guimond A, O'Connor-McCourt MD: Predominant Intracellular Localization of the type I Transforming Growth Factor-β Receptor and Increased Nuclear Accumulation after Growth Arrest. Exp Cell 2000, Res 258:121-134.

Zwaagstra JC, Kassam Z and O'Connor-McCourt MD. Down-regulation of Transforming Growth Factor-β Receptors: Cooperatively between the Types I, II, and III Receptors and Modulation at the Cell Surface. Exp Cell Res 1999; 252: 352-362.

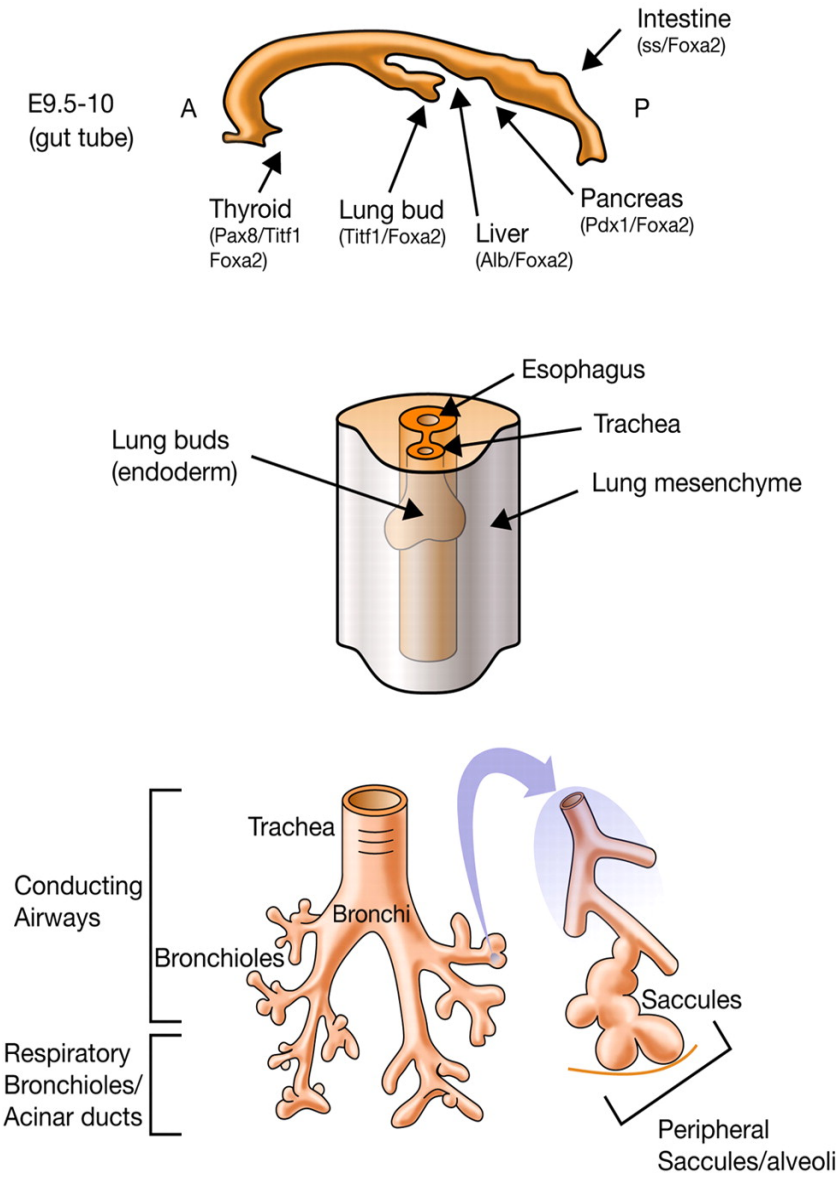

Figure 1.1 Patterning of the foregut endoderm: lung bud formation and branching morphogenesis (Maeda et al., 2007)

Mouse endoderm at approximately E9.5-10. *Top*: TTF-1 (Titf-1 gene) is expressed at sites of lung and thyroid formation along the anterior-posterior (A-P) axis. *Middle*: Lung buds as they evaginate into the surrounding mesenchyme. *Bottom*: conducting and peripheral regions of the lung at approximately E12. Later in morphogenesis (E17-18) peripheral saccules are formed (*bottom right insert*). Alveolarisation occurs postnatally.

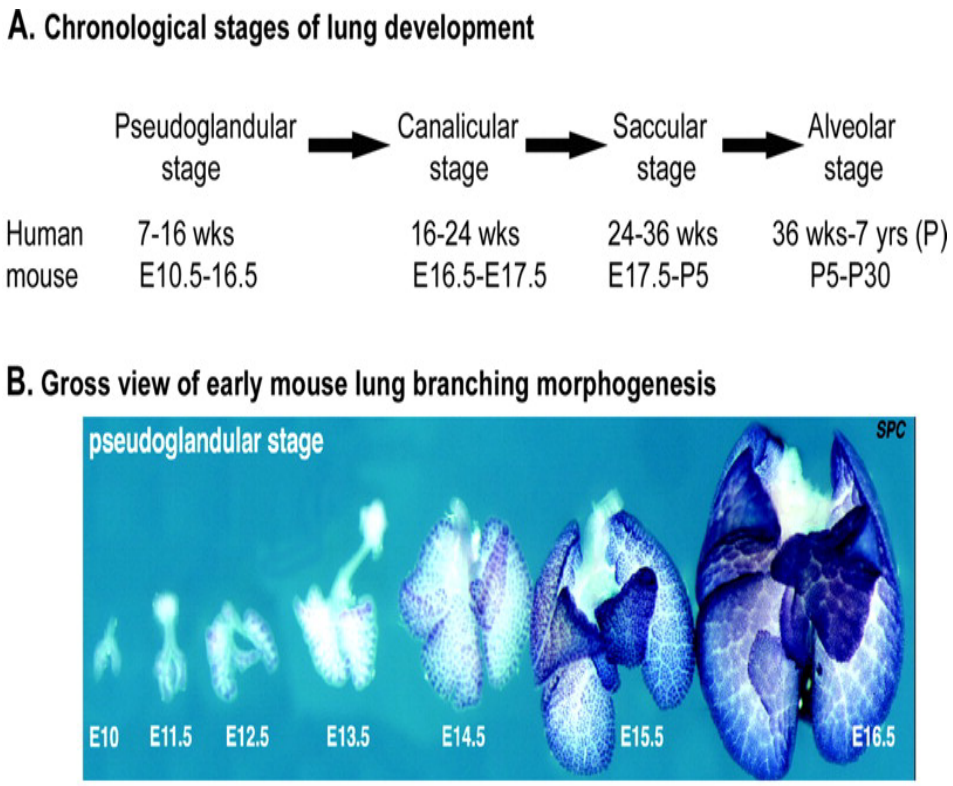

Figure 1.2 Lung developmental chronology (Shi et al., 2007)

(A) Chronological stages of lung development in human and mouse. (B) Gross view of mouse lung development. The adult mouse lung develops as a unilobar left and quadrilobed right lung.

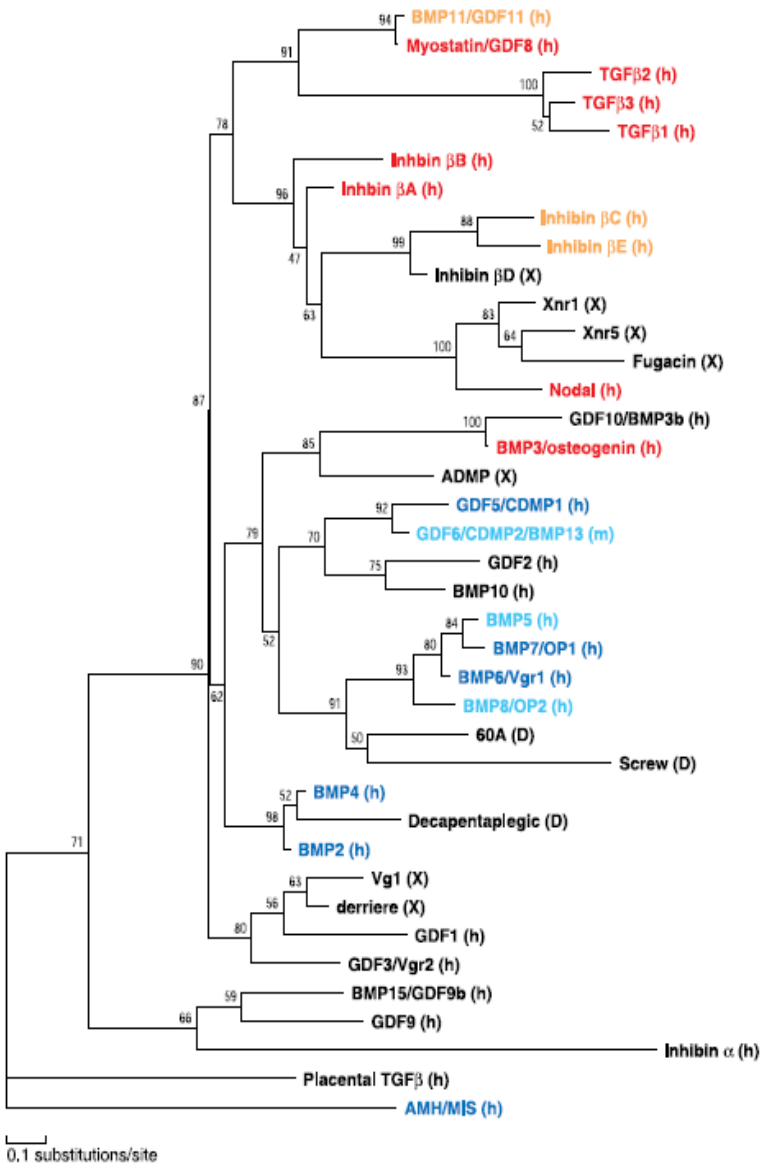

Figure 1.3 Phylogenetic tree of the TGF-β superfamily (Miyazawa et al., 2002)

Tree depicts evolutionary related ligands in human (h), mouse (m), Xenopus (X) and Drosophila (D). Ligands that activate the Activin/TGF-β pathway through Smad2 and Smad3 are shown in red. Ligands that activate the BMP pathway through Smad1, 5, 8 are shown in dark blue. Ligands that may activate the Activin/TGF-β pathway or the BMP pathway, but whose receptors and downstream signalling pathways have not been fully determined, are shown in orange and light blue respectively.

Figure 1.4

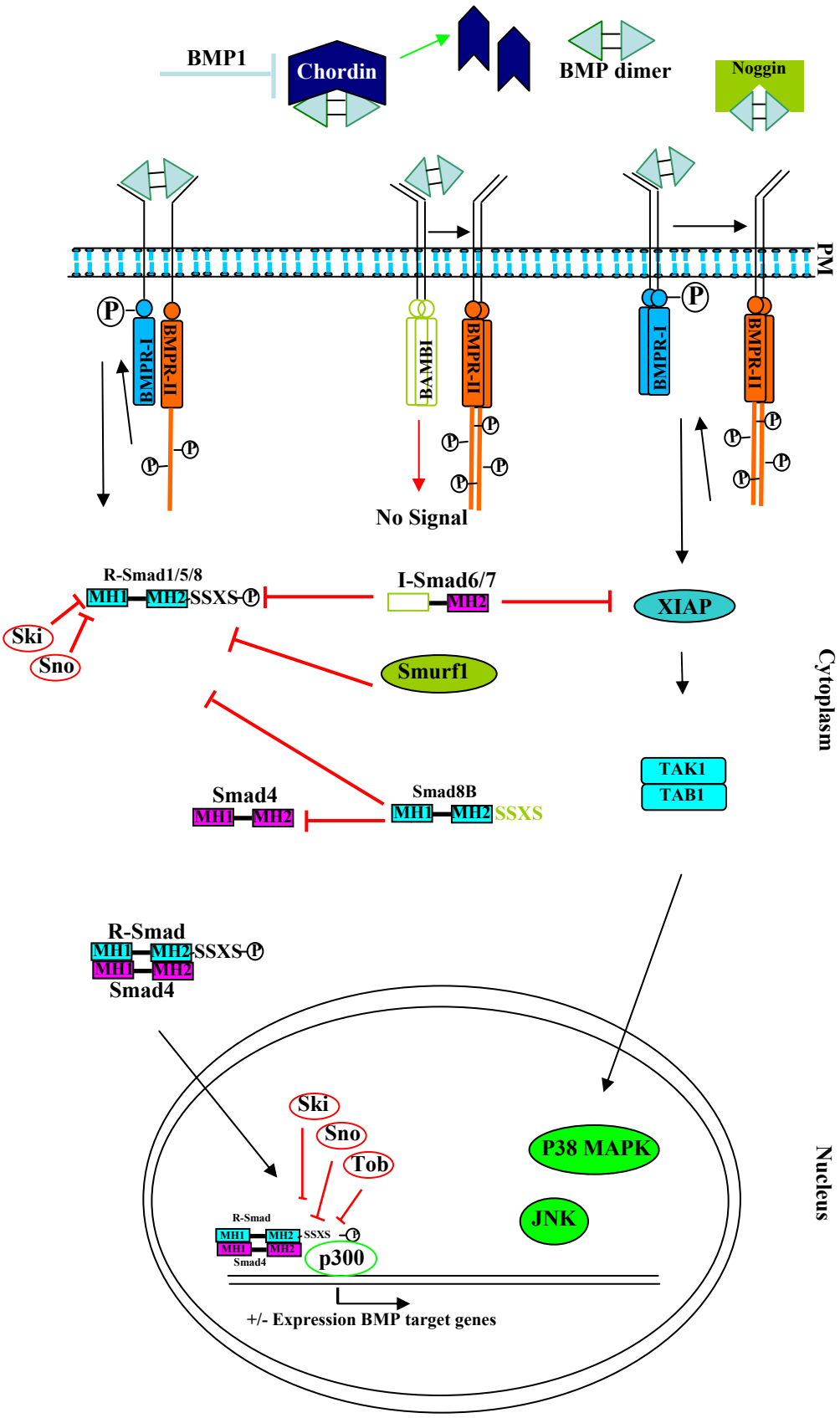
BMP1
Chordin
BMP dimer
Noggin
PM
BMPR-I
BMPR-II
BAMBI
No Signal
R-Smad1/5/8
MH1
MH2
SSXS
I-Smad6/7
XIAP
Ski
Sno
Smurf1
Cytoplasm
TAK1
TAB1
Smad4
Smad8B
R-Smad
Smad4
Tob
P38 MAPK
JNK
p300
+/- Expression BMP target genes
Nucleus

Figure 1.4 The 'canonical' BMP-Smad pathway and the BMP-MAPK pathway.

In the BMP-Smad pathway BMP2 and BMP4 bind to BMPR-IA or -IB and BMPR-II preformed complexes. This leads to phosphorylation of the type I receptor (BMPR-I) by the type II receptor (BMPR-II) which in turn leads to the phosphorylation of the R-Smad (Smad1/5/8) on the SSXS phosphorylation sequence. Activated R-Smads bind to the co-Smad, Smad4, through their MH2 protein binding domain. R-Smad/Smad4 complexes enter the nucleus and bind DNA via their MHI DNA-binding domain. This serves to activate or repress target gene expression following the recruitment of coactivators (p300) or corepressors, respectively (Ski, Sno, Tob). Extracellular inhibitors (chordin, noggin) bind BMP ligands outside the cell and prevent ligand-receptor binding. BAMBI inhibits BMP signalling through its action as a pseudoreceptor. Smad6, Smad7, Smad8B, Smurf as well as Ski and Sno all inhibit BMP signalling in the cytoplasm. Smad6/Smad7 lack the MH1 DNA binding domain. Smad8B is structurally similar to the R-Smads but lacks the SSXS phosphorylation sequence. In the BMP-MAPK pathway, BMP2 binds BMPR-IA homomeric receptor complex and subsequently recruits the Type II receptor complex. In this form the receptors may interact with XIAP which in turn activates TAK1 through its interaction with TAB1. TAK1 activity promotes activation of p38 MAPK and JNK. Smad6 can inhibit the BMP-MAPK pathway as well the canonical Smad pathway. Red indicates inhibition.

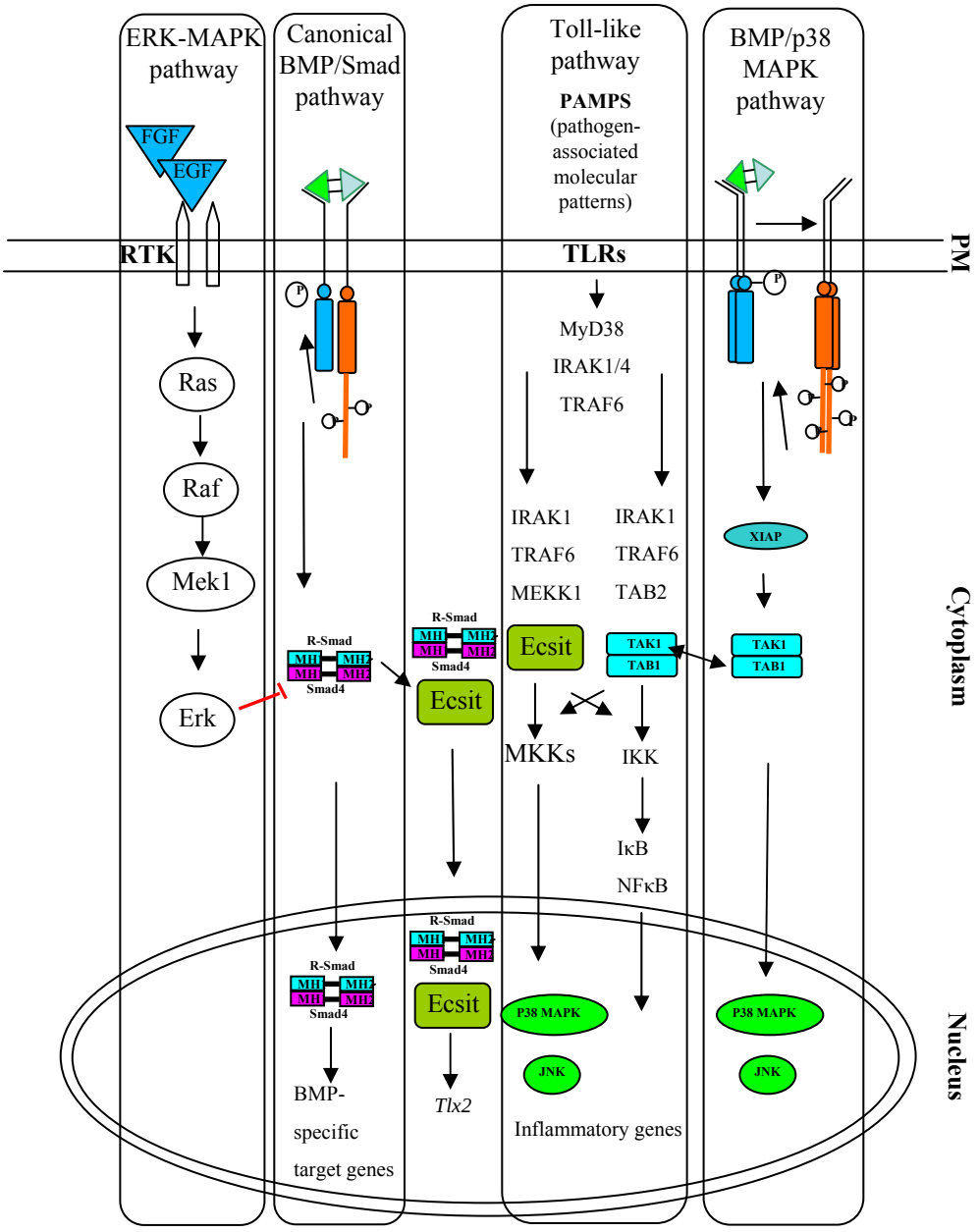

Figure 1.5 Crosstalk between the BMP pathway and other signal transduction pathways: the ERK-MAPK and TLR signalling pathways.

ERK-MAPK signalling is activated by growth factors such as EGF and FGF and is mediated through Ras family members which activate ERK. ERK can phosphorylate the linker region in R-Smad1 and target the protein for ubiquitination inhibiting BMP signalling. Both BMP-Smad and BMP-MAPK signalling can converge with TLR signalling. Activated Toll-like receptor recruits MyD88 which activates IRAK and TRAF6. The IRAK1/TRAF6 complex then associates with TAB1 and TAK1. Activated TAK1 leads to phosphorylation of IκB and its subsequent degradation leading to NFκB nuclear import. Alternatively, the IRAK1/TRAF6 complex can associate with Ecsit which can recruit Mekk1, activate MAPK kinases leading to JNK and p38 MAPK activation. Both outcomes regulate inflammatory gene expression. Ecsit can interact with the BMP-Smad pathway to regulate the BMP target gene, *Tlx2*. In addition, it is possible the BMP-MAPK pathway may lead to the activation of inflammatory genes through the TLR pathway via the TAB1-TAK1 complex. However, no experimental data has been generated to support this.

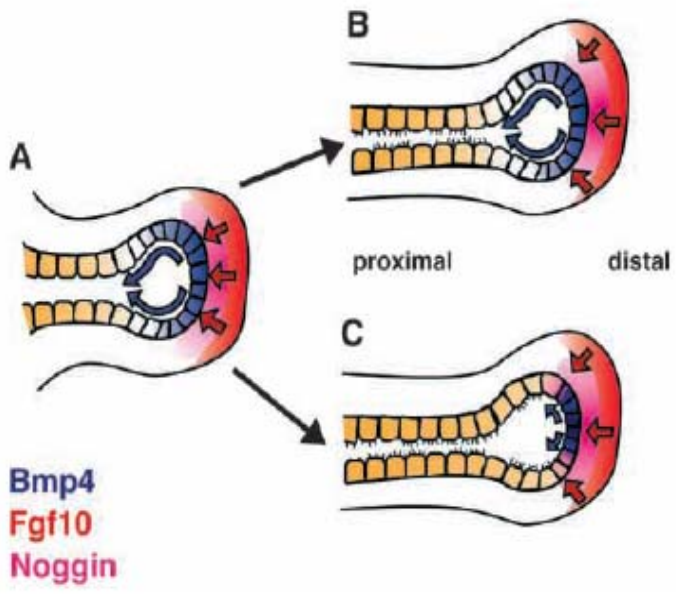

Figure 1.6 BMP4-mediated signalling regulates proximal-distal patterning of the lung epithelium (Weaver et al., 1999).

An extending bud is shown schematically during normal lung development and in mice in which noggin (the BMP antagonist) is overexpressed (*Sp-C-Noggin*). Blue, red and pink denote BMP4, FGF10 and Noggin gene expression, respectively. (A) Cells present at the lung branch tip receive a combination of BMP4 and FGF10 and are maintained as distal progenitor cells. (B) As the lung bud extends, cells which become more distant to the lung branch tip leave the region of high BMP4 and FGF10 and initiate proximal differentiation. (C) In *Sp-C-Noggin* transgenic lungs, BMP4 signalling is inhibited, this leads to cells which adopt a proximal phenotype closer to the lung branch tip.

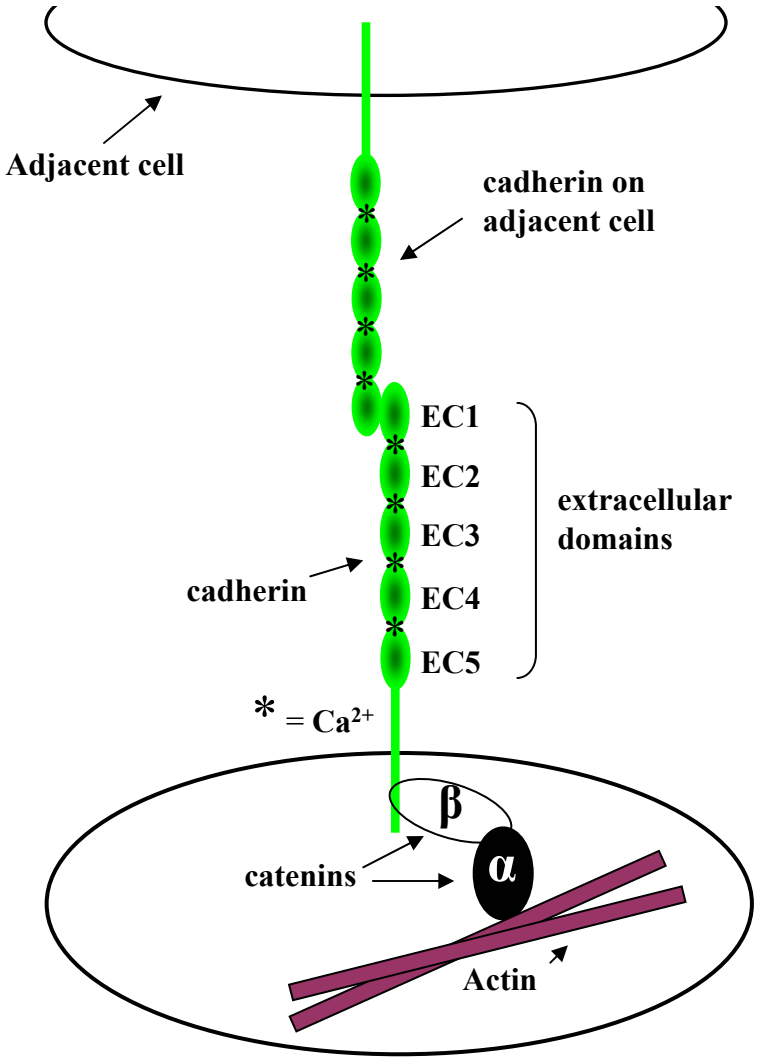

Figure 1.7 The *zonula* adherens junction

The classical cadherins possess five extracellular domains (EC1-5) which bind cadherins on the adjacent cell. The conformation of the cadherin molecule is only stable in the presence of calcium (Ca^{2+}). The intracellular domain of classical cadherins is associated with α-catenin and β-catenin. α-catenin connects to the actin cytoskeleton and stabilizes the adherens junction complex.

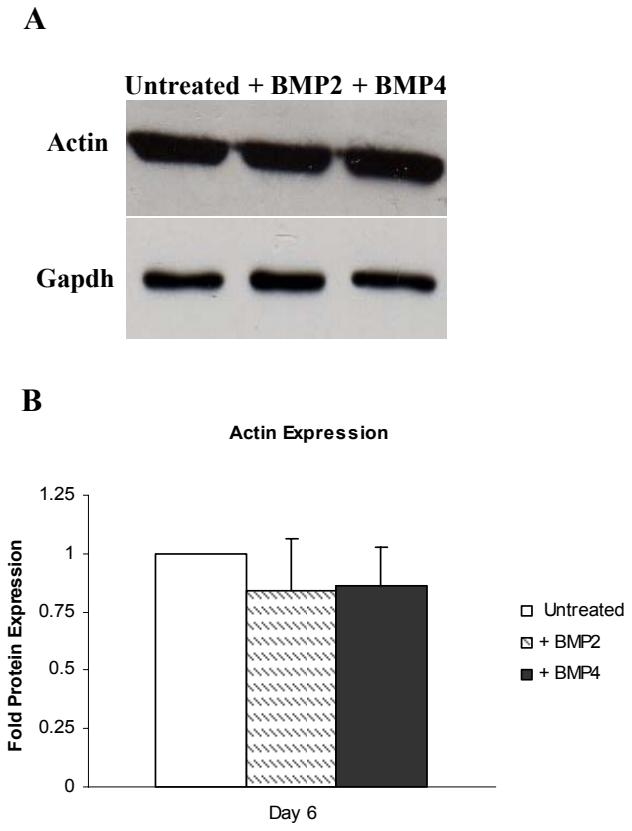

Figure 3.1 Actin expression in BMP2- and BMP4-treated cells

Western blot analysis of actin expression in BMP2- and BMP4-treated BEAS-2B cells at day 6. (A) Representative western images. (B) Densitometric quantification of actin expression. Values were normalised to GAPDH. Each bar represents the mean ± SEM of at least three independent experiments. No significant change in actin expression was observed in BEAS-2B cells following 6 days BMP2 and BMP4 treatment. Actin was therefore deemed a suitable housekeeper protein for subsequent BMP experiments.

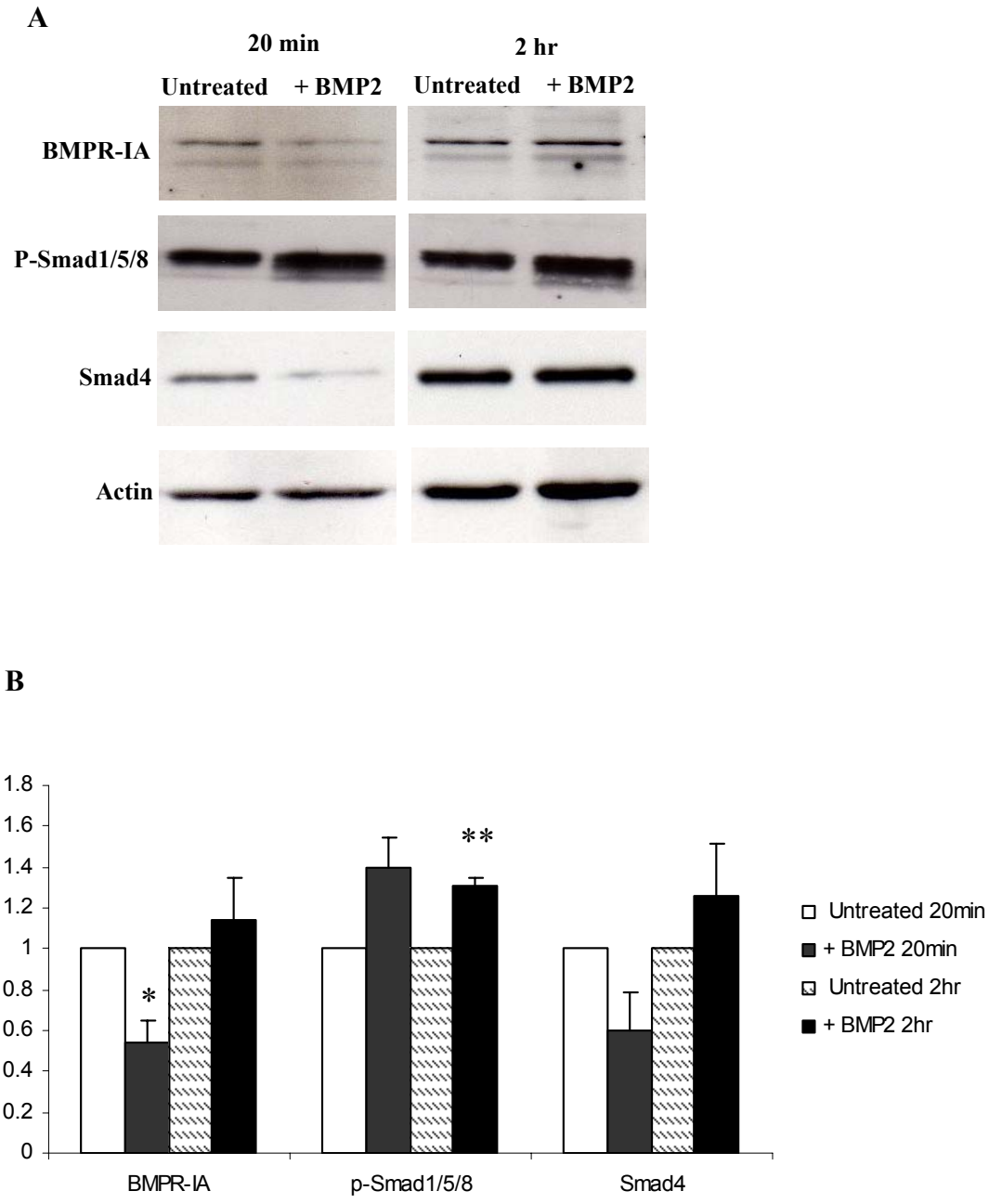

Figure 3.2 BMP pathway expression in BEAS-2B cells following 20 min and 2 hr BMP2 stimulation

Western blot analysis of BMP receptor IA (BMPR-IA), phosphorylated Smad1/5/8 (p-Smad1/5/8) and Smad4 in BEAS-2B cells following 20 min and 2 hr BMP2 stimulation. (A) Representative western images (B) Densitometric quantification presented as fold change compared to untreated cells. Values obtained were normalised to actin. Each bar represents the mean ± SEM of at least three independent experiments. Significance was determined using a student *t*-test where *=P<0.05 and **=P<0.01.

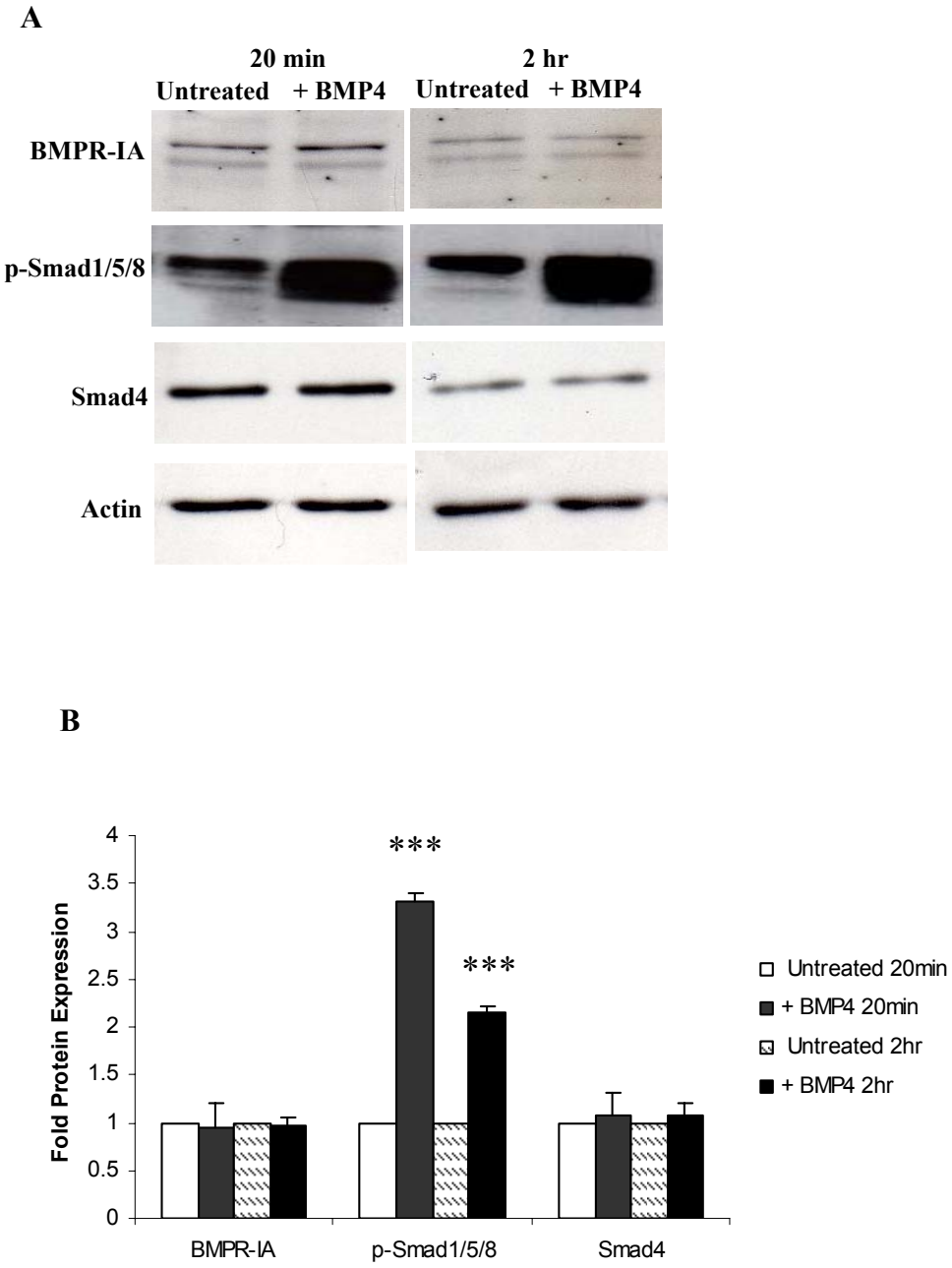

Figure 3.3 BMP pathway expression in BEAS-2B cells following 20 min and 2 hr BMP4 stimulation

Western blot analysis of BMP receptor IA (BMPR-IA), phosphorylated Smad1/5/8 (p-Smad1/5/8) and Smad4 in BEAS-2B cells following 20 min and 2 hr BMP4 stimulation. (A) Representative western images (B) Densitometric quantification presented as fold change compared to untreated cells. Values obtained were normalised to actin. Each bar represents the mean ± SEM of at least three independent experiments. Significance was determined using a student *t*-test where *** =P<0.001.

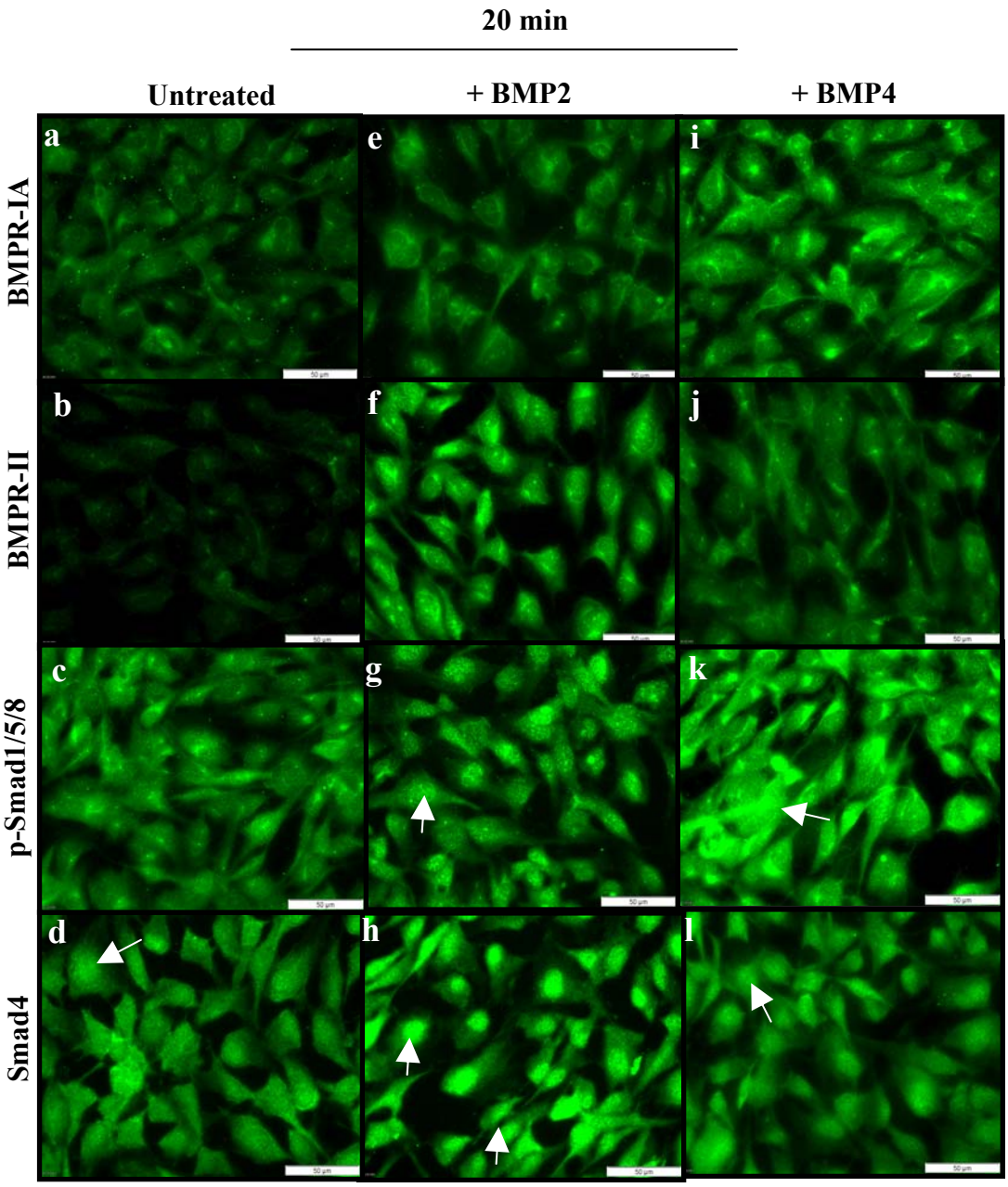

Figure 3.4 Localisation of BMP pathway components in BEAS-2B cells following 20 min BMP2 and BMP4 stimulation

Representative immunofluorescence images of BMP pathway components in untreated BEAS-2B cells (a-d) and following 20 min BMP2 (e-h) or BMP4 stimulation (i-l). BMPR-IA expression remained unchanged in response to BMP2 and BMP4 (e, i). BMPR-II expression appeared induced with BMP2 and BMP4 treatment (f, j). Increased nuclear p-Smad1/5/8 expression was detected in BMP2-treated cells (g) where an increase in cytoplasmic localisation was detected following BMP4 treatment (k). Nuclear Smad4 was detected in response to both BMP2 and BMP4 (h, l). Increased expression and/or nuclear localisation is denoted by arrows. Scale bars represent 50 µm. Negative antibody controls shown in Fig.3.21.

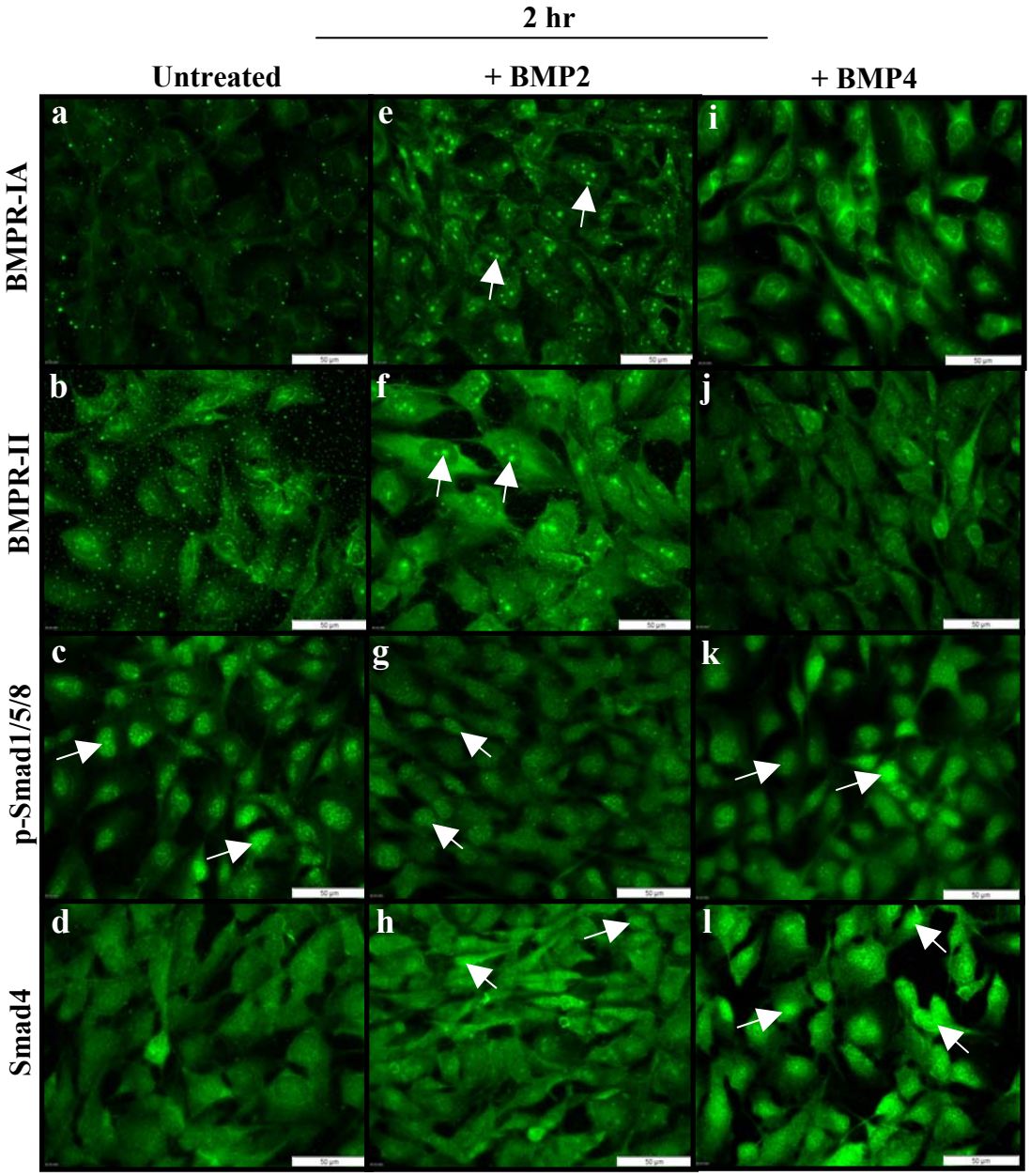

Figure 3.5 Localisation of BMP pathway components in BEAS-2B cells following 2hr BMP2 and BMP4 stimulation

Representative immunofluorescence images of BMP pathway components in untreated BEAS-2B cells (a-d) and following 2hr BMP2 (e-h) or BMP4 stimulation (i-l). BMPR-IA expression appeared increased on BMP2- and BMP4-treated cells (e, i). BMPR-II expression was unchanged following BMP2 and BMP4 treatment (f, j). Of note were BMPR-IA and BMPR-II aggregates on the cell membrane or inside the cell following BMP2 treatment (e and f, denoted by arrows). Nuclear p-Smad1/5/8 was evident in BMP2- and BMP4-treated cells (g, k). Smad4 was predominantly localised to the cytoplasm in BMP2-treated cells (h). Increased nuclear Smad4 was detected in response to BMP4 (l). Increased expression and/or nuclear localisation is denoted by arrows. Scale bars represent 50 µm. Negative antibody controls shown in Fig.3.21.

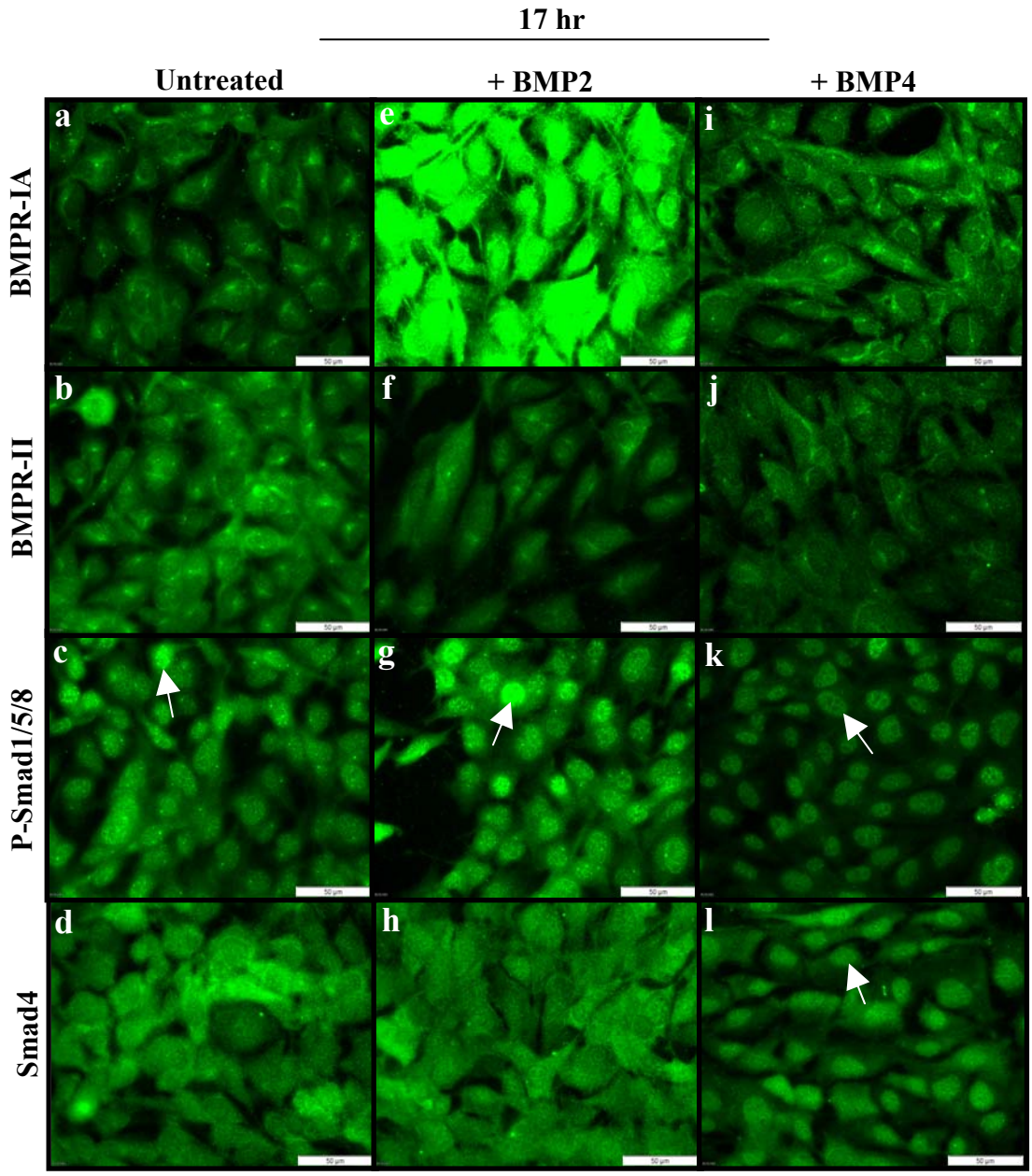

Figure 3.6 Localisation of BMP pathway components in BEAS-2B cells following 17hr BMP2 and BMP4 stimulation

Representative immunofluorescence images of BMP pathway components in untreated BEAS-2B cells (a-d) and following 17hr BMP2 (e-h) or BMP4 stimulation (i-l). BMPR-IA expression was upregulated at 17hr following BMP2 stimulation (e) but appeared relatively unchanged in response to BMP4 (i). BMPR-II expression appeared unchanged in response to BMP2 and BMP4 (f, j). Nuclear localisation was observed with p-Smad1/5/8 in BMP2- and BMP4-treated cells (g, k). Smad4 was predominantly localised to the cytoplasm in untreated and BMP2-treated cells (h). Smad4 nuclear localisation was apparent following BMP4 treatment (l). Increased expression and/or nuclear localisation is denoted by arrows. Scale bars represent 50 µm. Negative antibody controls shown in Fig.3.21.

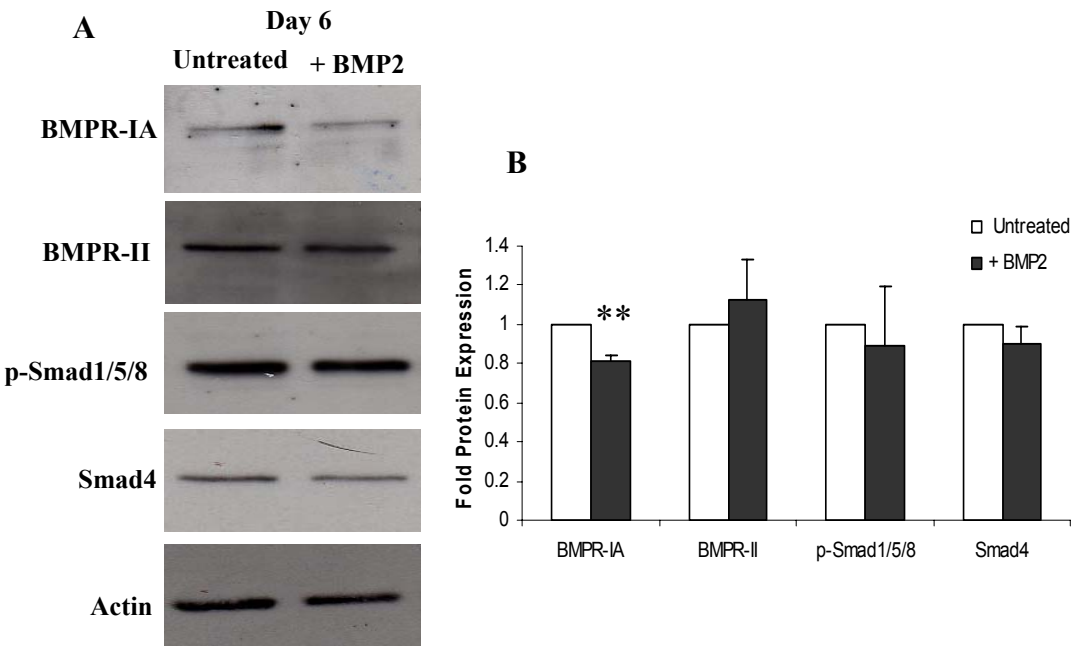

Figure 3.7 BMP pathway expression in BEAS-2B cells at day 6 following BMP2 stimulation

Western blot analysis of BMPR-IA, BMPR-II, phosphorylated Smad1/5/8 and Smad4 at day 6 in BEAS-2B cells cultured in the presence of BMP2. (A) Representative western images (B) Densitometric quantification presented as fold change compared to untreated cells. Values obtained were normalised to actin. Each bar represents the mean ± SEM of at least three independent experiments. Significance was determined using a student *t*-test where ** = $P<0.01$.

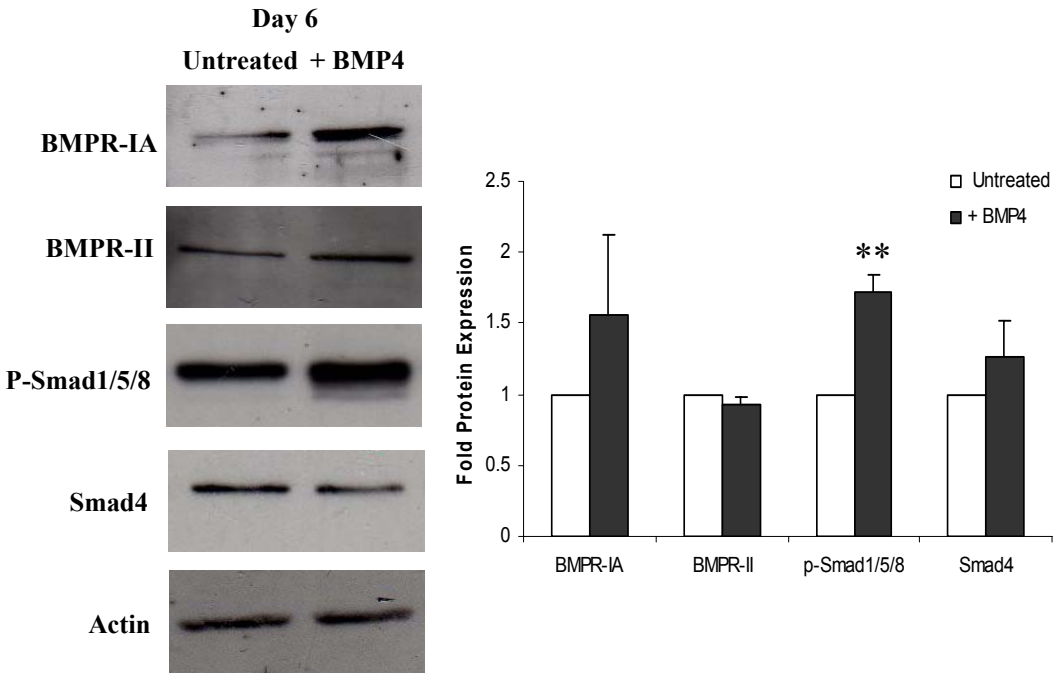

Figure 3.8 BMP pathway expression in BEAS-2B cells at day 6 following BMP4 stimulation

Western blot analysis of BMPR-IA, BMPR-II, phosphorylated Smad1/5/8 and Smad4 at day 6 in BEAS-2B cells cultured in the presence of BMP4. (A) Representative western images (B) Densitometric quantification presented as fold change compared to untreated cells. Values obtained were normalised to actin. Each bar represents the mean ± SEM of at least three independent experiments. Significance was determined using a student *t*-test where ** = $P<0.01$.

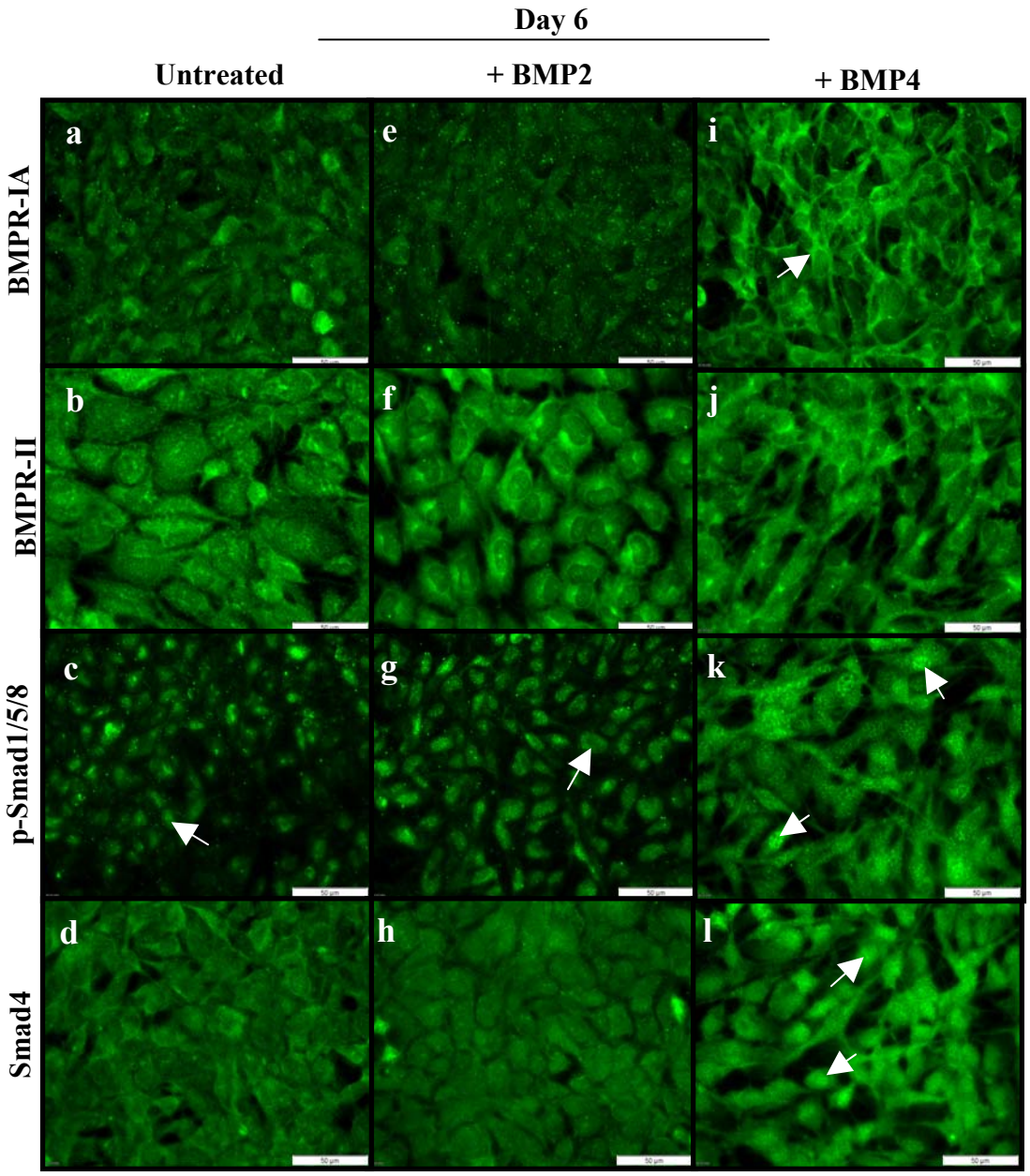

Figure 3.9 Localisation of BMP pathway components in BEAS-2B cells at day 6 following BMP2 and BMP4 stimulation

Representative immunofluorescence images of BMP pathway components in untreated BEAS-2B cells (a-d) and at day 6 following BMP2 (e-h) or BMP4 stimulation (i-l). BMPR-IA, BMPR-II, p-Smad1/5/8 and Smad4 expression was comparable between untreated and BMP2-treated cells suggesting no pathway activation was ongoing in these cells at day 6. Pathway activation was observed in BMP4-treated cells at day 6. Increased BMPR-IA was observed where BMPR-II appeared largely unaltered. Increased p-Smad1/5/8 cytoplasmic expression and nuclear translocation was evident. In addition, nuclear localisation of Smad4 was apparent in BMP4-treated cells at day 6. Increased expression and/or nuclear localisation is denoted by arrows. Scale bars represent 50 µm. Negative antibody controls shown in Fig.3.21.

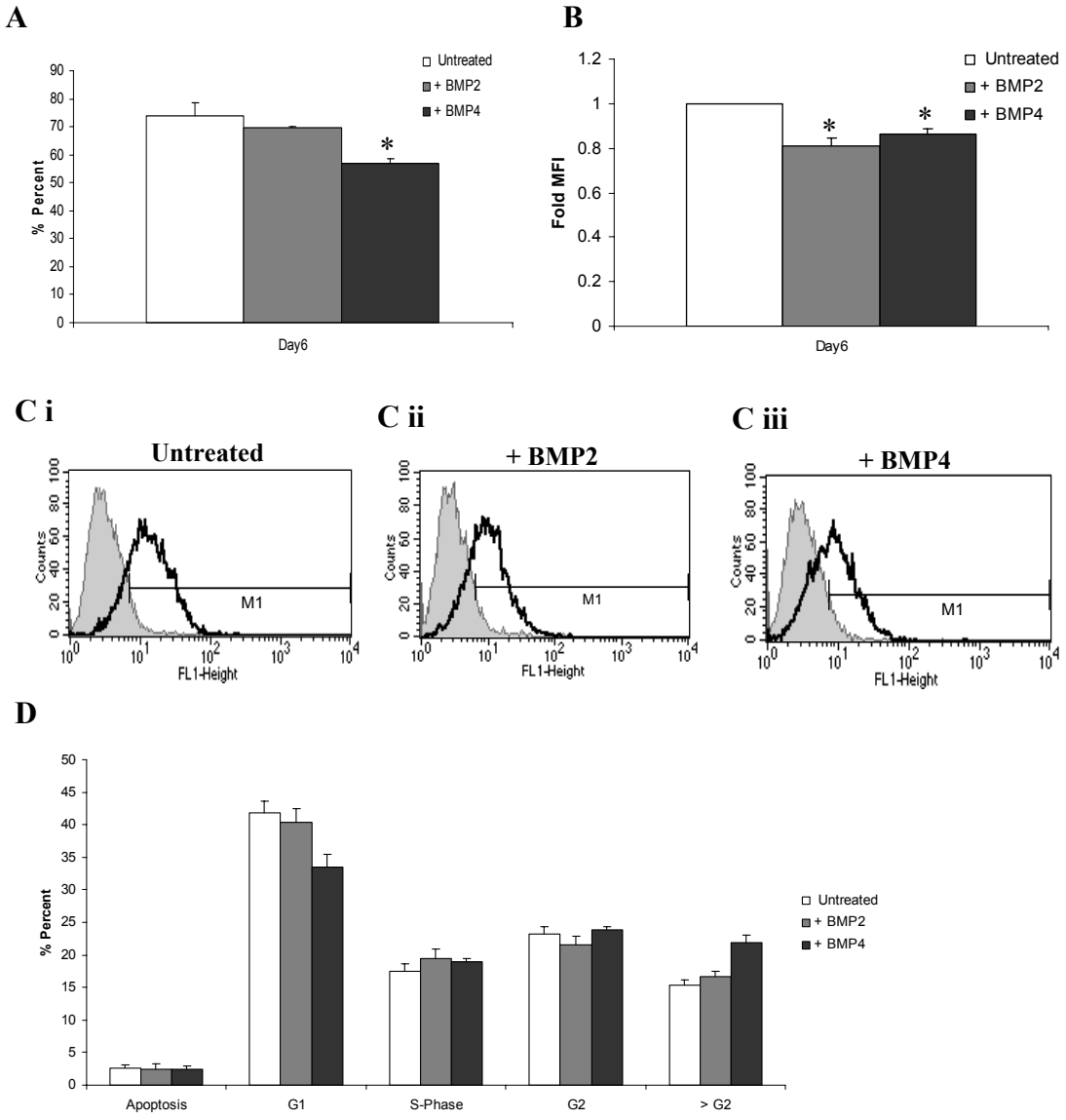

Figure 3.10 Analysis of senescence associated β-galactosidase (SA-β-gal) expression and cell cycle distribution in BMP2- and BMP4-treated BEAS-2B cells

(A) Graph depicting percent cells positive for SA-β-gal in untreated and in BMP2- and BMP4-treated cells at day 6. BMP2 treatment did not significantly alter the number of cells expressing SA-β-gal where BMP4 treatment significantly reduced the number of cells expressing SA-β-gal at day 6. (B) The mean fluorescence intensity (MFI) of the SA-β-gal-positive population was significantly decreased in the presence of BMP2 (* = $P<0.05$) and BMP4 (* = $P<0.05$). Data is presented as fold change compared to untreated. (C) Representative histograms of SA-β-gal expression in untreated (i), BMP2- (ii) and BMP4-treated (iii) cells at day 6. Endogenous β-galactosidase (β-gal) activity was inhibited and SA-β-gal was determined using the fluorescent substrate C_{12}FDG. Cells incubated with inhibitor only (grey fill) and inhibitor plus C_{12}FDG (black line) were used to determine percentage SA-β-gal positive cells and mean fluorescence intensity (MFI). (D) Propidium iodide analysis of cell cycle progression revealed no alteration in cell cycle distribution in response to BMP2 or BMP4. Values represent the mean ± SEM obtained from at least three independent experiments. Significance as compared to untreated cells was calculated using a one-way ANOVA corrected using the Bonferroni multiple comparison test, where * = $P<0.05$.

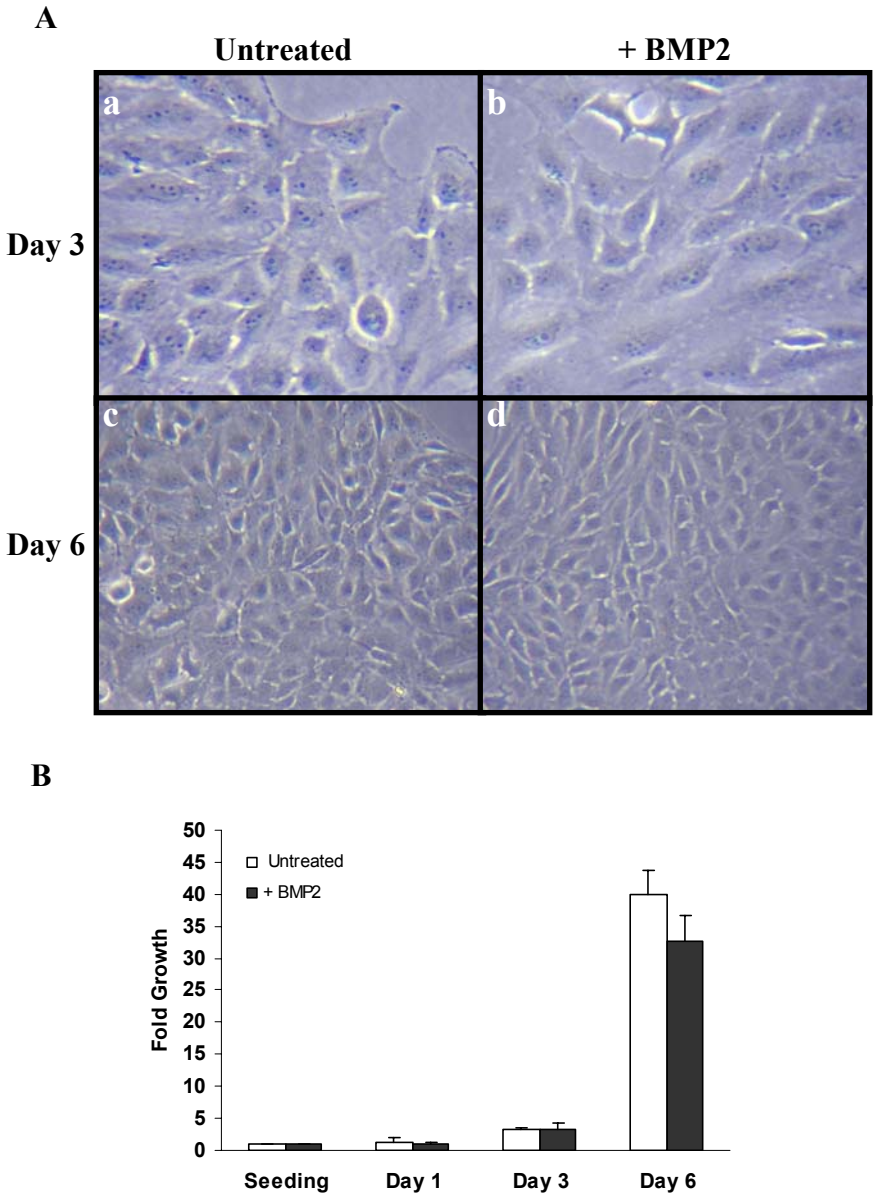

Figure 3.11 BEAS-2B morphology and cell proliferation in the presence of BMP2

(A) Phase contrast photomicrographs of BEAS-2B cells cultured in serum-free medium (untreated) or in serum free medium containing 100 ng/ml BMP2 (+BMP2) for 3 days (a and b) or 6 days (c and d). At day 3 and up to day 6 no alteration in morphology was observed. (B) Cell counts were determined at day 1, day 3 and day 6 in BEAS-2B cells cultured in serum-free medium (untreated) or in serum-free medium containing 100 ng/ml BMP2 (+ BMP2). BMP2 had no significant effect on BEAS-2B proliferation. Proliferation is presented as fold relative to seeding density. Each bar represents the mean ± SEM of three independent experiments.

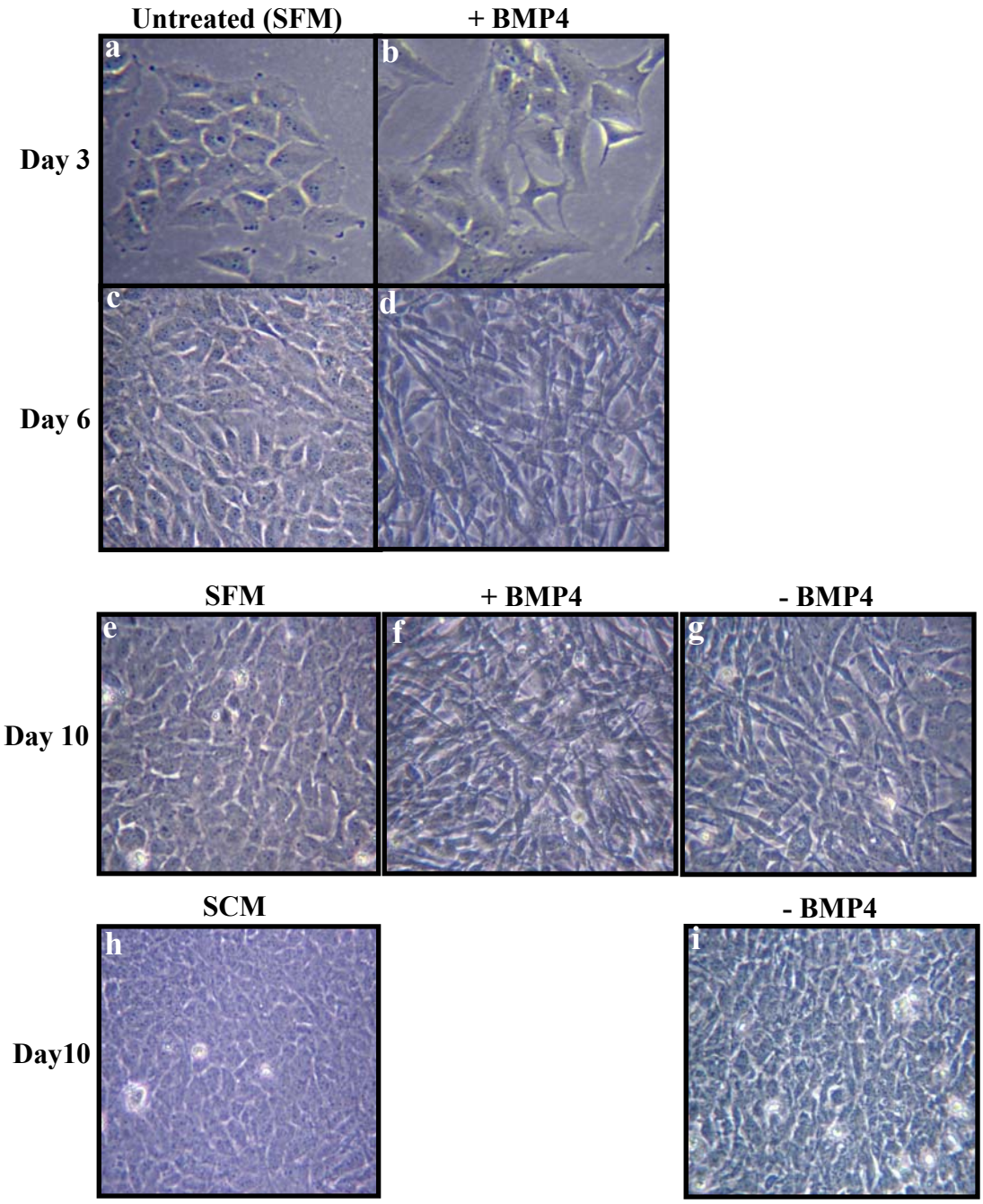

Figure 3.12 BMP4 induces a mesenchymal-like change in morphology

Phase contrast photomicrographs of BEAS-2B cells cultured in serum-free medium (untreated SFM) or in serum-free medium containing 100 ng/ml BMP4 (+BMP4) for 3 days (a and b) or 6 days (c and d). At day 3, a change in morphology is apparent in the presence of BMP4 (b). At day 6, untreated cells display typical epithelial cell morphology (c). In contrast, BMP4-treated cells appear more fibroblast-like with loss of cell-cell contact (d). At day 6, medium was replaced on untreated cells with either fresh serum-free medium (SFM) or 10% serum containing medium (SCM) (e and h, respectively). Similarly at day 6, medium on BMP4 treated cells was replaced with either serum-free medium alone (-BMP4) (g) or containing BMP4 (+BMP4) (f) or serum containing medium alone (-BMP4) (i). Phase contrast images were taken 4 days later. Untreated cells at day 10 in either SFM or SCM retained an epithelial-like morphology (e and h). BMP4-treated cells which were re-stimulated at day 6 displayed an enhanced fibroblast-like morphology (f). Cells which had BMP4 withdrawn retained their fibroblast-like morphology (g) although this was reduced compared to their day 6 counterpart (d). Similarly, BMP4-treated cells placed in SCM medium at day 6 had greatly lost their fibroblast-like morphology (i). However, they did appear more angular compared to untreated cells in SCM (i compared to h).

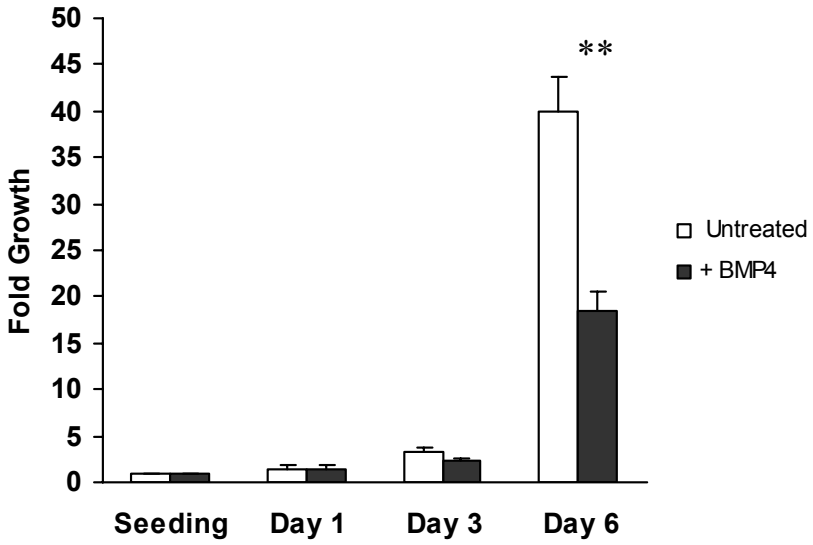

Figure 3.13 BEAS-2B proliferation in the presence of BMP4

Cell counts were determined at day 1, day 3 and day 6 in BEAS-2B cells cultured in serum-free medium (untreated) or in serum-free medium containing 100 ng/ml BMP4 (+ BMP4). BMP4 significantly inhibited cell proliferation at day 6. Proliferation is presented as fold relative to seeding density. Each bar represents the mean ± SEM of three independent experiments. Significance was obtained using the students *t*-test where **=P<0.001.

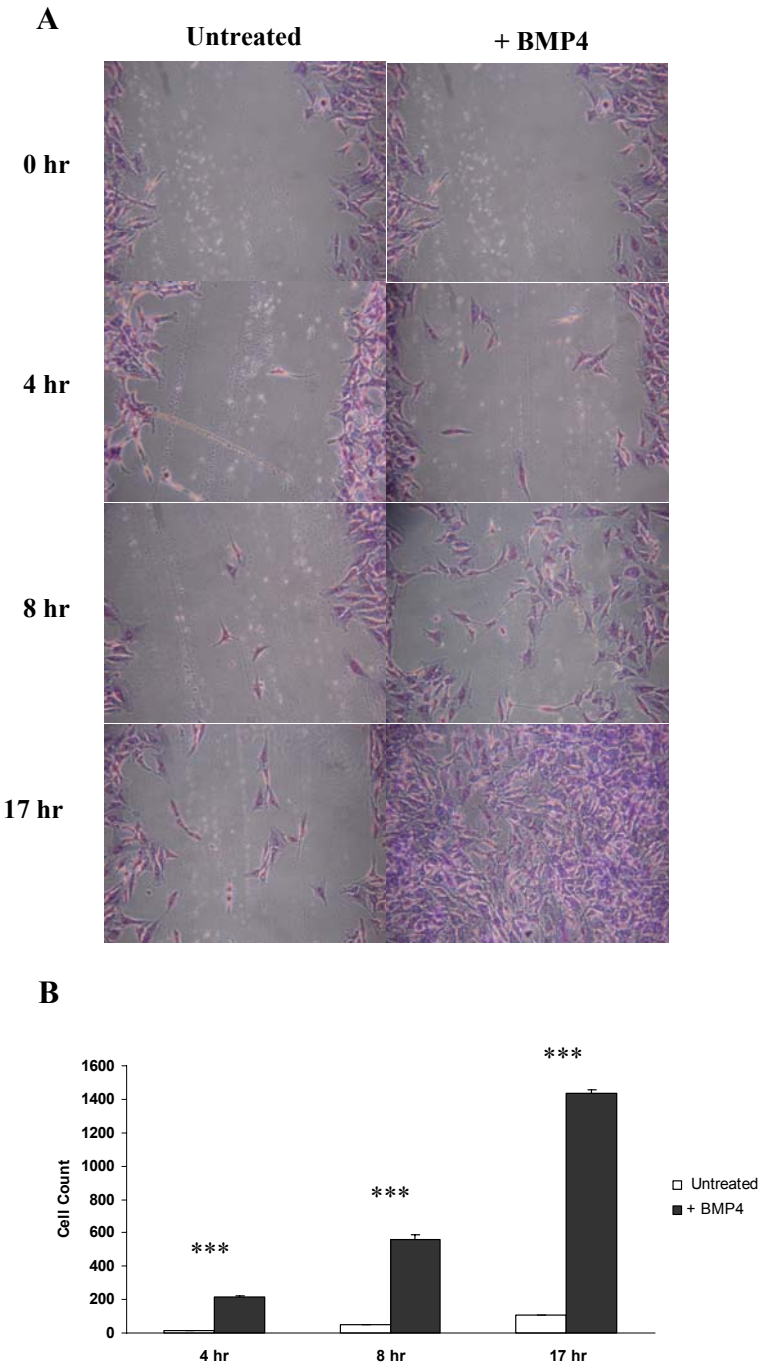

Figure 3.14 BMP4 increases BEAS-2B cell migration (Molloy et al., 2008)

(A) A wound assay was performed (by A Adams in Shirley O'Dea Laboratory) to assess the effect of BMP4 on cell migration. Cells in the presence of BMP4 began to migrate after 4hr and at 17hr the denuded area was entirely repopulated. (C) Graph illustrates number of cells migrated at each time point. Bars represent the mean ± SEM of three independent experiments. Student *t*-test was used to determine significance, where *** $P<0.0001$.

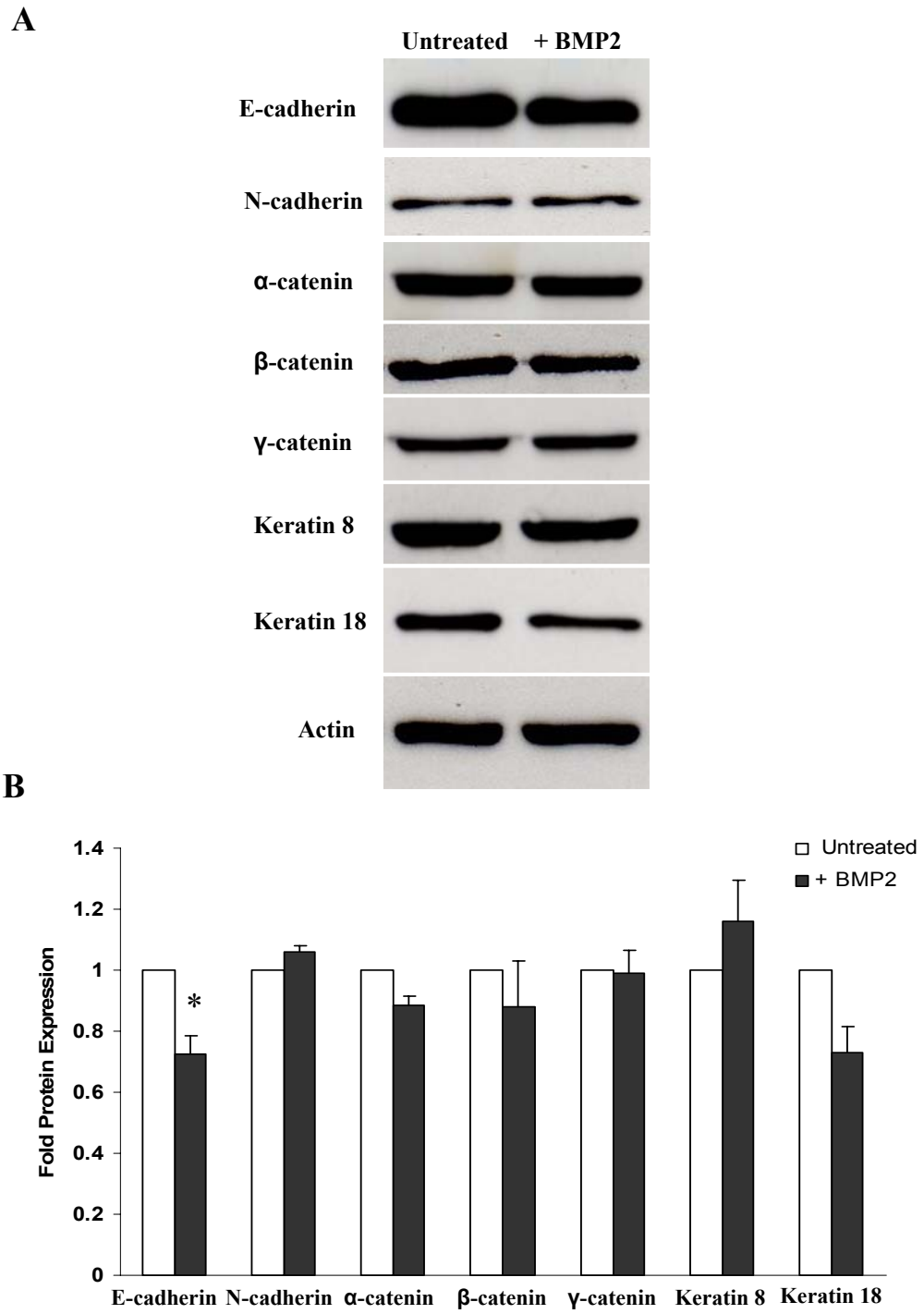

Figure 3.15 Expression of adherens junction proteins and cytokeratin proteins in BMP2-treated cells

(A) Western blot analysis of adherens junction protein and cytokeratin protein expression in cells cultured in serum-free medium alone (untreated) and in serum-free medium containing 100 ng/ml BMP2 (+BMP2) for 6 days. (B) Densitometric quantification presented as fold change compared to untreated cells. BMP2 treatment resulted in significant downregulation of E-cadherin expression. Values obtained were normalised to actin. Each bar represents the mean ± SEM of at least three independent experiments. Significance was determined using a student *t*-test where *=P<0.05.

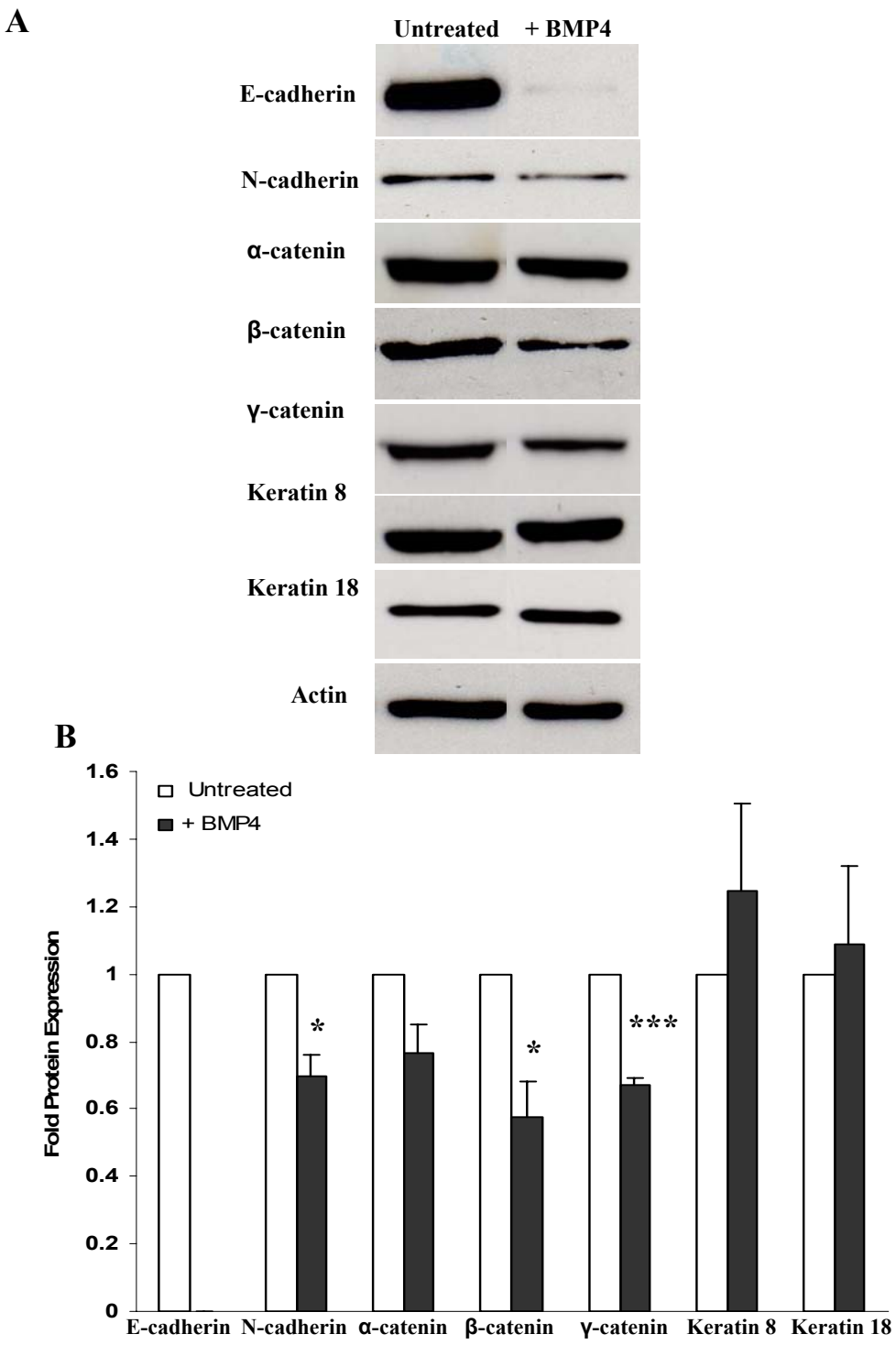

Figure 3.16 Expression of adherens junction proteins and cytokeratin proteins in BMP4-treated cells

(A) Western blot analysis of adherens junction and cytokeratin protein expression in cells cultured in serum-free medium (untreated) and in serum-free medium containing 100 ng/ml BMP4 (+BMP4) for 6 days. (B) Densitometric quantification presented as fold change compared to untreated cells. BMP4 treatment resulted in almost complete abrogation of E-cadherin expression and significantly reduced expression of β- and γ-catenin at day 6. No change in α-catenin or cytokeratin expression was detected. Values were normalised to actin. Each bar represents the mean ± SEM of at least three independent experiments. Significance was obtained using a students *t*-test where * = $P<0.05$ and *** = $P<0.001$.

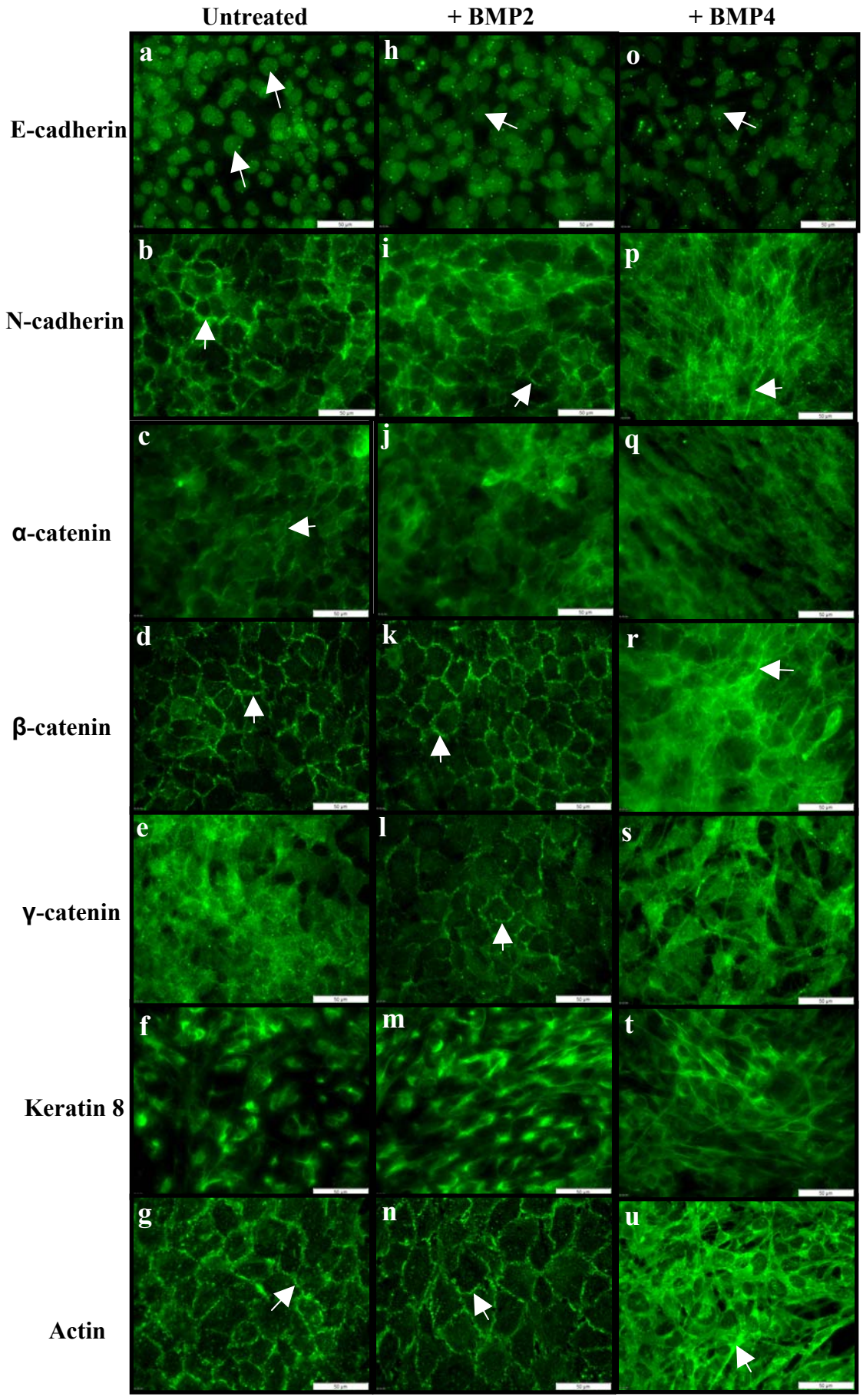
Untreated
+ BMP2
+ BMP4
E-cadherin
N-cadherin
α-catenin
β-catenin
γ-catenin
Keratin 8
Actin
a
h
o
b
i
p
c
j
q
d
k
r
e
l
s
f
m
t
g
n
u

Figure 3.17 Localisation of adherens junction and cytoskeletal proteins in BMP2- and BMP4-treated cells

Representative immunofluorescence images of adherens junction and cytoskeletal protein expression in untreated BEAS-2B cells (a-g) and at day 6 following BMP2 (h-n) and BMP4 stimulation (o-u). E-cadherin was localised to the nuclei (denoted with arrows) in untreated BEAS-2B cells and the localisation was not changed following BMP2 or BMP4 treatment (a, h, 0). N-cadherin was localised to the membrane in untreated BEAS-2B cells (b). This localisation was not changed in BMP2-treated cells at day 6 (i). However, following BMP4 treatment N-cadherin localisation appeared more cytoplasmic (p). α-catenin localisation remained largely unchanged in response to either ligand (c, j, q). β-catenin was localised to the membrane in untreated BEAS-2B cells and remained unaltered in response to BMP2 (d, k). However, β-catenin did appear increasingly cytoplasmic following BMP4 treatment (r). γ-catenin was localised to the cytoplasm in untreated cells (e) and appeared more membranous in BMP2-treated cells (l) but was largely unaltered in BMP4-treated cells (s). Keratin 8 appeared unchanged in BMP2- and BMP4-treated cells (f, m, t). Actin was polarised in untreated and BMP2-treated cells (g, n). However, this polarised actin localisation was lost in BMP4-treated cells at day 6 (u). Scale bars represent 50 μm. Membrane/cytoplasmic localisation denoted with arrows. Negative antibody controls shown in Fig.3.21.

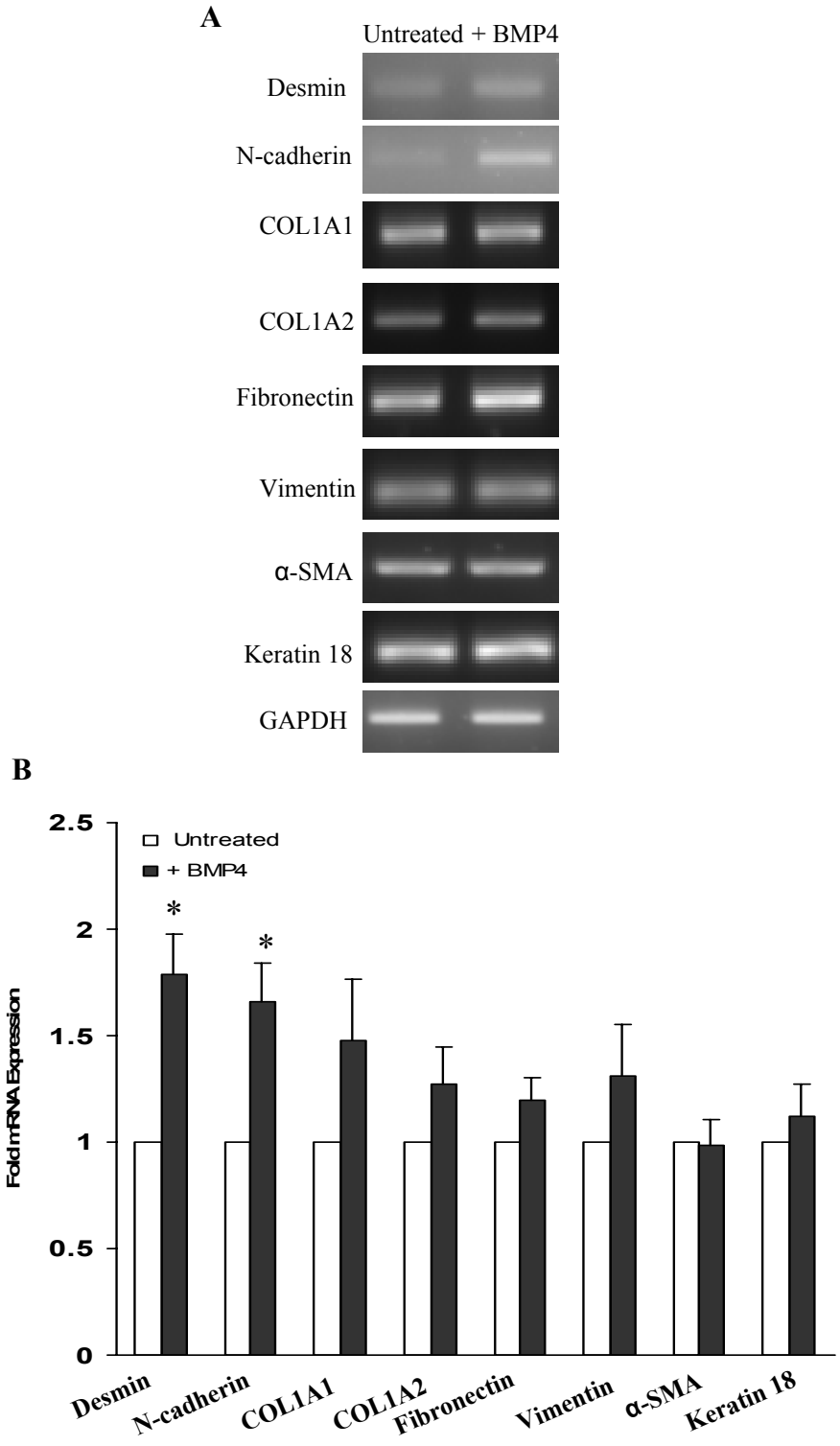

Figure 3.18 BMP4 modulates expression of cytoskeletal and ECM-related genes

(A) RT-PCR analysis demonstrates upregulation of cytoskeletal and ECM-related gene expression following BMP4 treatment for 6 days (RT-PCR preformed by EM Molloy and JC Masterson in Shirley O'Dea Laboratory). (B) Densitometric quantification was carried out and normalised to glyceraldehyde-3-phosphate (GAPDH). Data is presented as fold change compared to untreated cells. Bars represent the mean ± SEM of at least three independent experiments. Significance compared to untreated cells was determined using a students t-test where * = $P<0.05$.

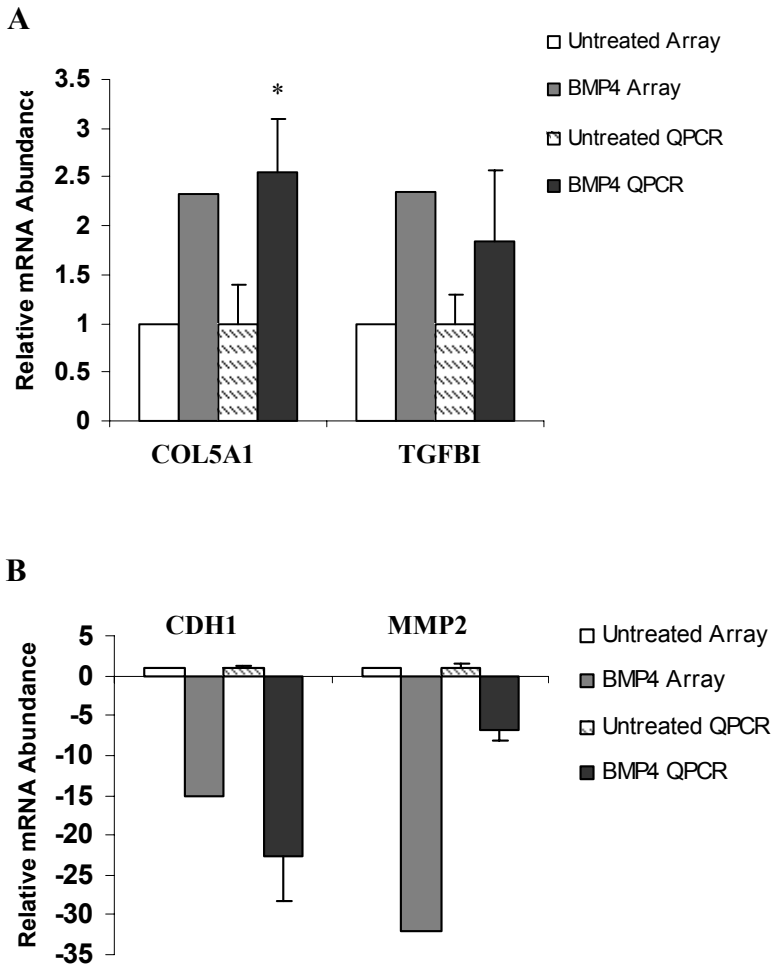

Figure 3.19 Genes validated by independent QPCR (Molloy et al., 2008)

Comparison of the relative expression of two (A) upregulated (COL5A1 and TGFBI) and two (B) downregulated (CDH1 and MMP2) genes identified by PCR array analysis and verified by independent quantitative PCR (QPCR) (QPCR preformed by JB Moore in Shirley O'Dea Laboratory). QPCR was done using total RNA isolated from three independent passages and using independent primers to those used in the array experiments. Relative abundance was normalised to GAPDH. QPCR values are mean ± SEM of n=3 (CDH1: n=2) and expressed a fold relative to untreated cells. Significance compared to untreated cells was determined using a students *t*-test where * = $P<0.05$.

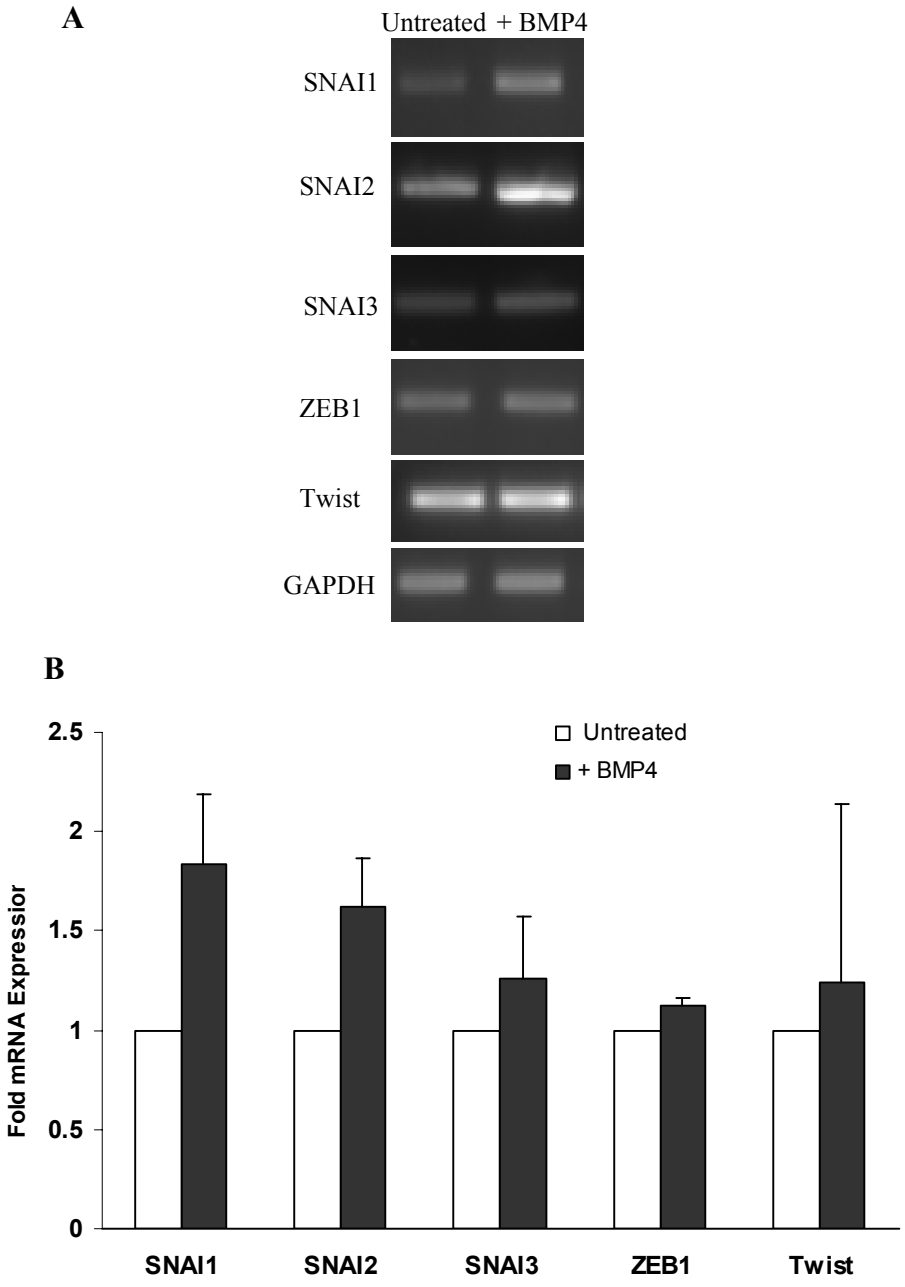

Figure 3.20 BMP4 modulates transcriptional repressors of E-cadherin

(A) RT-PCR analysis demonstrates upregulation of several transcriptional repressors of E-cadherin expression at day 6 after BMP4 treatment (RT-PCR preformed by EM Molloy and JC Masterson in Shirley O'Dea Laboratory). (B) Densitometric quantification was carried out and normalised to glyceraldehyde-3-phosphate (GAPDH). Data is presented as fold change compared to untreated cells. Bars represent the mean ± SEM of at least three independent experiments. The level of upregulation observed with BMP4 treatment was not deemed significant using a students *t*-test.

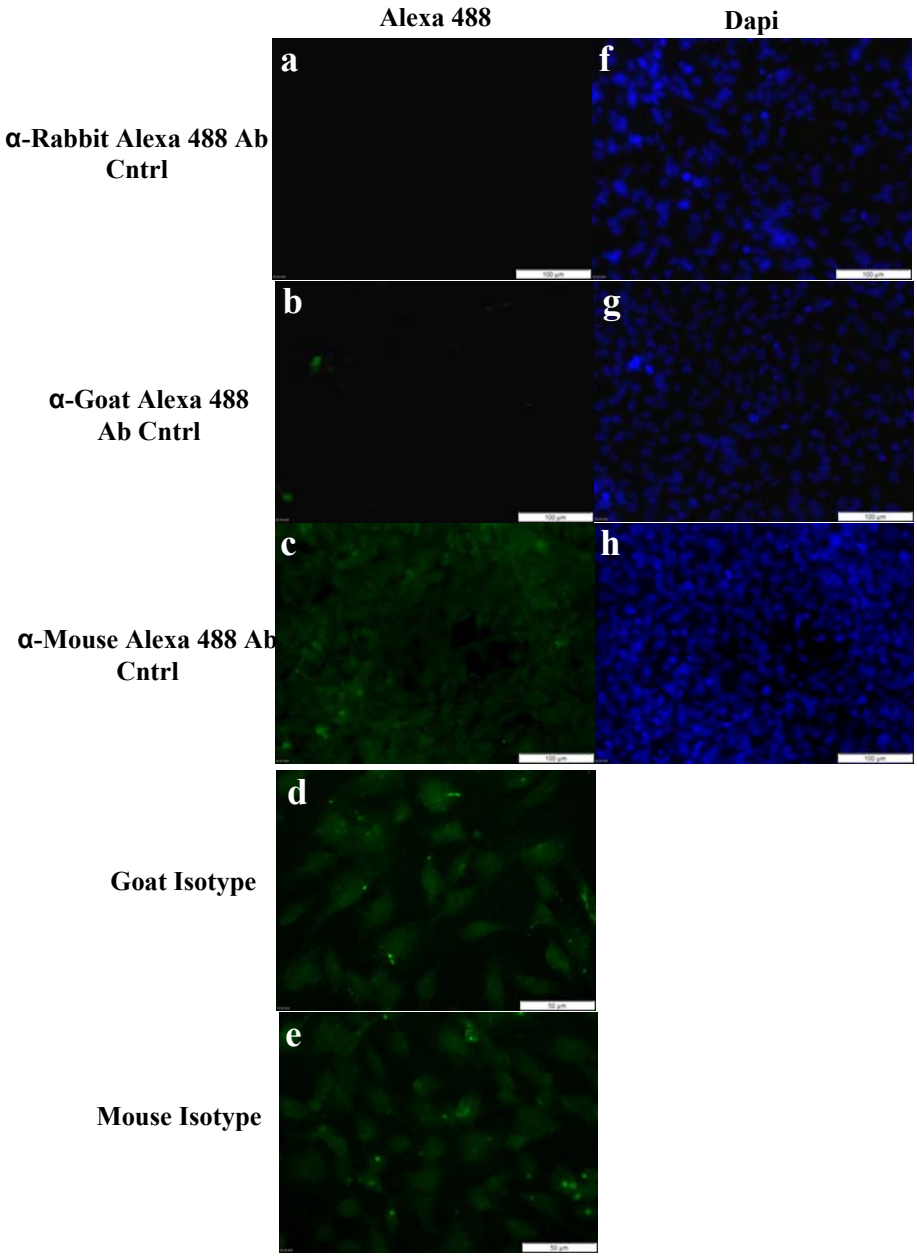

Figure 3.21 Immunofluorescence antibody controls

Photomicrographs represent immunofluorescence antibody controls on BEAS-2B cells. Secondary antibody control (Ab Cntrl) omitted primary antibody where cells were incubated in either α-rabbit (a), α-goat (b) or α- mouse (c) alexa488-conjugated secondary antibody (a-c). Isotype control cells were incubated with irrelevant goat IgG (d) or mouse IgG (e). Dapi counterstained nuclei shown right of image (f-h). Scale bars represent 100 µm (a-c and f-g) and 50 µm (e, f).

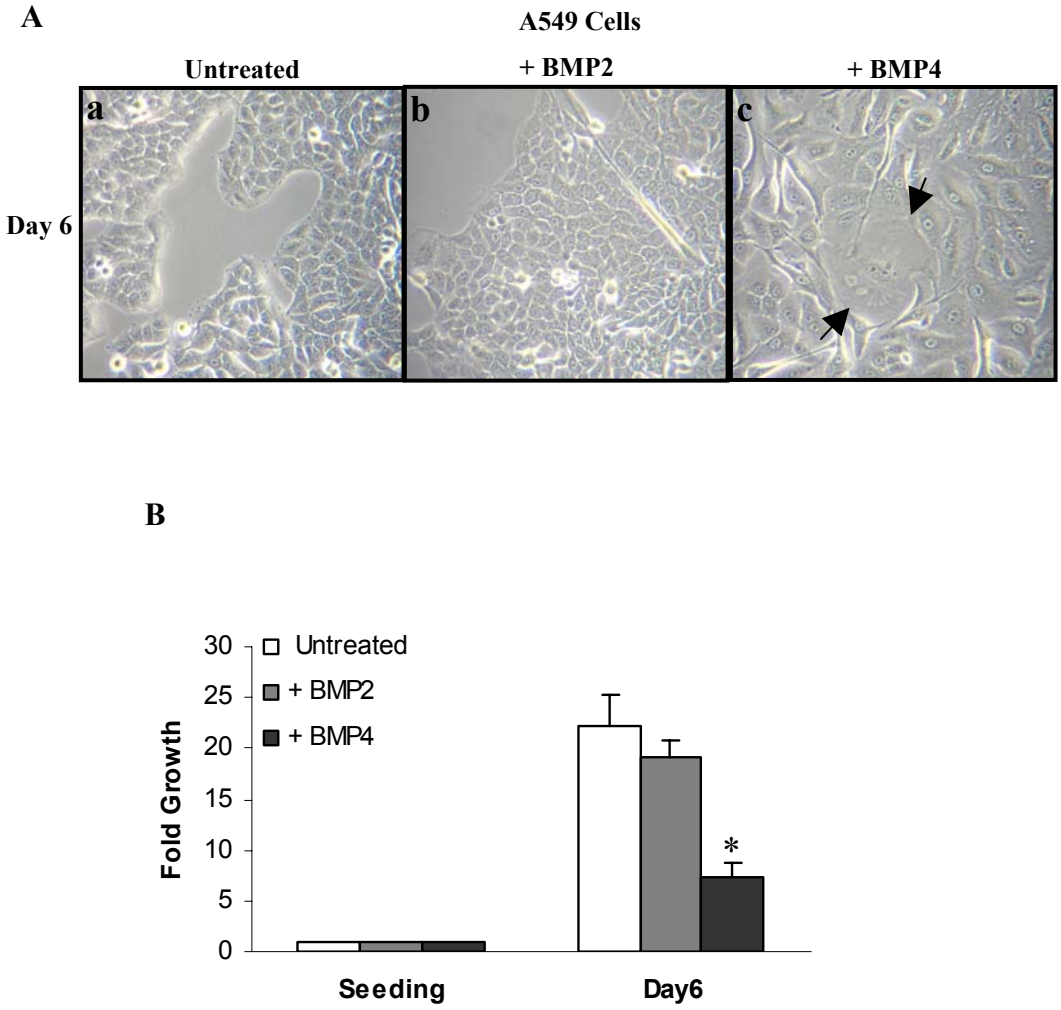

Figure 4.1 BMP2- and BMP4-mediated effects on A549 cell morphology and proliferation

(A) Phase contrast photomicrographs of A549 cells cultured in serum-free medium (untreated) or in serum-free medium containing 100 ng/ml BMP2 (+ BMP2) or 100 ng/ml BMP4 (+ BMP4) for 6 days (a-c). Untreated A549 cells displayed characteristic epithelial morphology (a) which remained largely unaltered in the presence of BMP2 (b). BMP4-treated cells appeared enlarged by day 6, enlarged cell denoted by arrows (c). (B) Cell counts were determined at day 6 in A549 cells cultured in serum-free medium (untreated) or in serum-free medium containing 100 ng/ml BMP2 (+ BMP2) or 100 ng/ml BMP4 (+BMP4). BMP2 had no significant effect on BEAS-2B proliferation. However, BMP4 significantly inhibited A549 cell proliferation by day 6. Cell counts are presented as fold relative to seeding density. Each bar represents the mean ± SEM of three independent experiments. Significance was obtained using the Students *t*-test where * = $P < 0.05$.

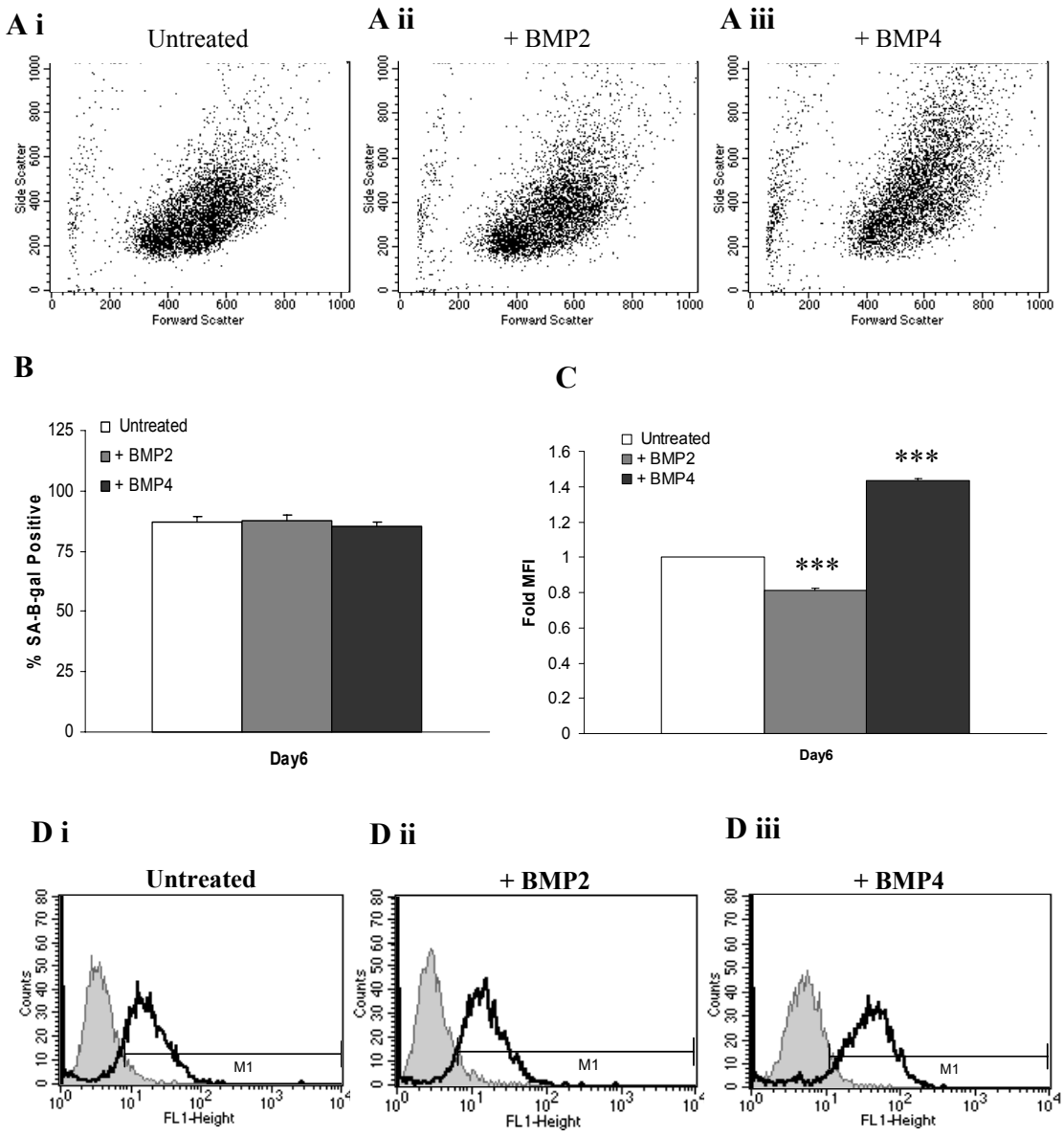

Figure 4.2 Analysis of senescence associated β-galactosidase (SA-β-gal) expression in BMP2- and BMP4-treated A549 cells at day 6

(A) Representative dot plots demonstrating cell size and cell granularity as determined by forward scatter (FSC) and side scatter (SSC), respectively, in untreated (i), BMP2- (ii) and BMP4-treated (iii) cells at day 6. (B) Graph depicting percent cells positive for SA-β-gal in untreated and in BMP2- and BMP4-treated cells at day 6. Neither BMP2 nor BMP4 treatment significantly altered the number of cells expressing SA-β-gal. (C) The mean fluorescence intensity (MFI) of the SA-β-gal-positive population was significantly decreased in the presence of BMP2. However, an increase in SA-β-gal expression was detected in response to BMP4 at day 6. Data is presented as fold change compared to untreated cells. Values represent the mean ± SEM obtained from at least three independent experiments. Significance as compared to untreated cells was calculated using a one-way ANOVA corrected using the Bonferroni multiple comparison test, where *** = $P<0.001$. (D) Representative histograms of SA-β-gal expression in untreated (i), BMP2- (ii) and BMP4-treated (iii) cells at day 6. Endogenous β-galactosidase (β-gal) activity was inhibited and SA-β-gal was determined using the fluorescent substrate C_{12}FDG. Cells incubated with inhibitor only (grey fill) and inhibitor plus C_{12}FDG (black line) were used to determine percentage SA-β-gal positive cells and mean fluorescence intensity (MFI).

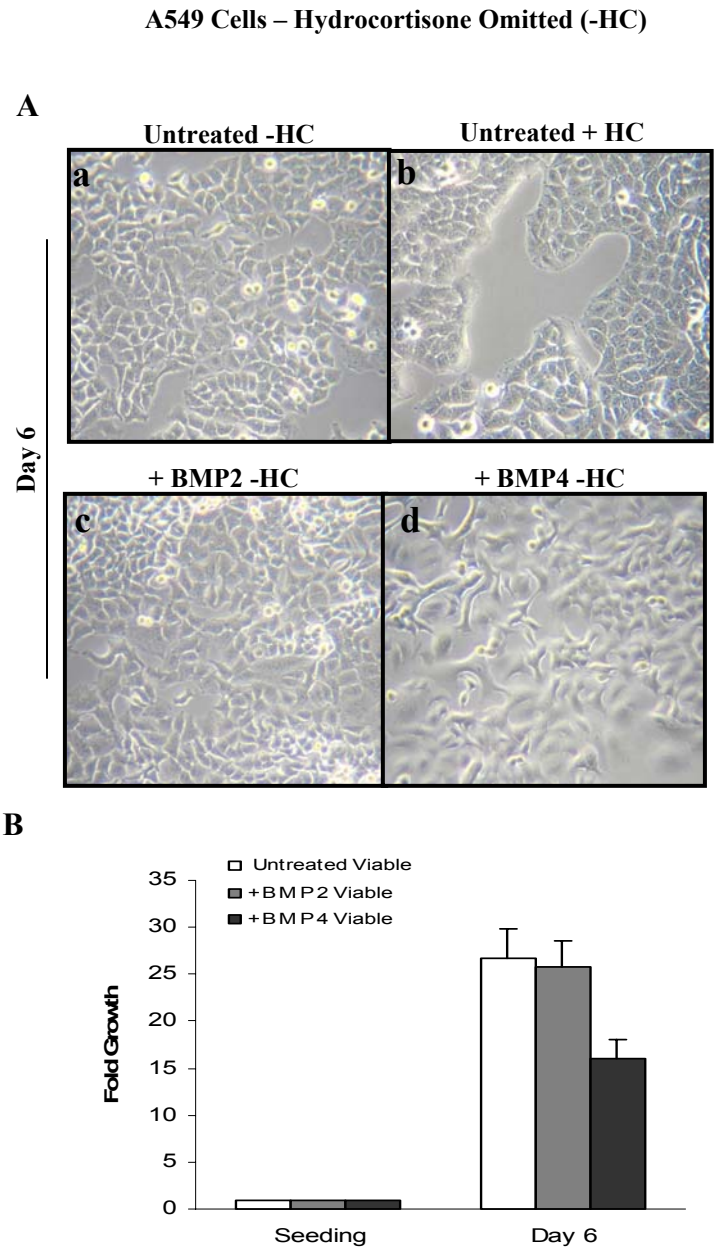

Figure 4.3 BMP2- and BMP4-mediated effects on A549 cell morphology and proliferation in the absence of hydrocortisone (-HC)

(A) Phase contrast photomicrographs of A549 cells cultured in serum-free medium (-HC) (untreated) or in serum free medium (-HC) containing 100 ng/ml BMP2 (+BMP2) or 100 ng/ml BMP4 (+ BMP4) for 6 days (a, c, d). Untreated A549 cells displayed characteristic epithelial morphology (a). However, untreated A549 cells in the absence of HC (a) did appear more flattened compared to A549 cells grown in HC containing medium (b). BMP2 did not affect A549 cell morphology (c compared to a). BMP4-treated cells appeared angular in shape and exhibited a loss in cell-cell contact (d compared to a). (B) Cell counts were determined at day 6 in A549 cells cultured in serum-free medium (-HC) (untreated) or in serum-free medium (-HC) containing 100 ng/ml BMP2 (+ BMP2) or 100 ng/ml BMP4 (+BMP4). Cell counts are presented as fold relative to seeding density. BMP2 had no significant effect on BEAS-2B proliferation. BMP4 weakly inhibited A549 cell proliferation where the level of inhibition was not found to be significant. Each bar represents the mean ± SEM of three independent experiments.

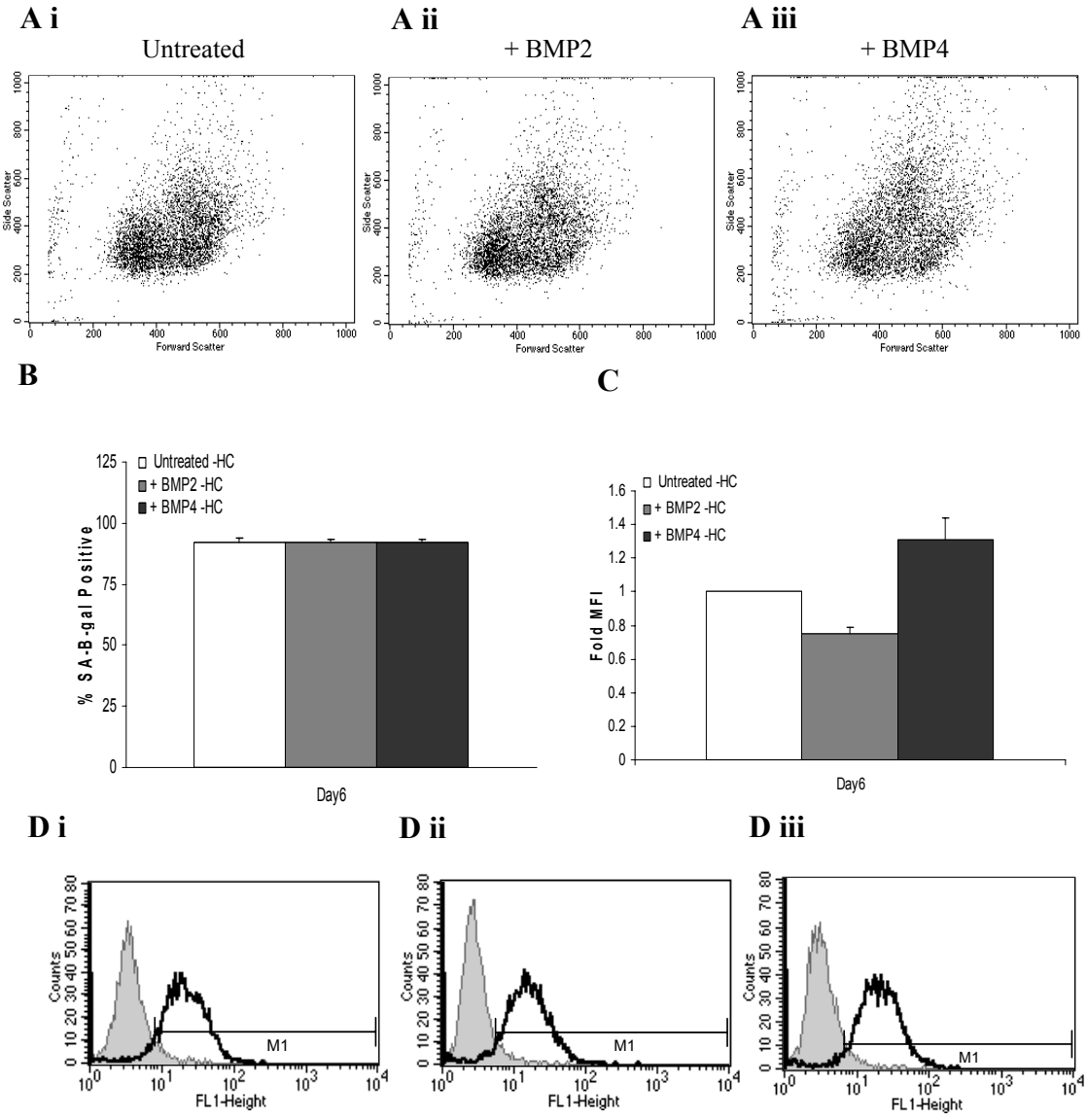

Figure 4.4 Analysis of senescence associated β-galactosidase (SA-β-gal) expression in BMP2- and BMP4-treated A549 cells at day 6 in the absence of hydrocortisone (-HC)

(A) Representative dot plots demonstrating cell size and cell granularity as determined by forward scatter (FSC) and side scatter (SSC), respectively, in untreated (i), BMP2- (ii) and BMP4-treated (iii) cells at day 6.(B) Graph depicting percent cells positive for SA-β-gal in untreated and in BMP2- and BMP4-treated cells at day 6 cultured in serum-free medium omitting hydrocortisone (-HC). Neither BMP2 nor BMP4 treatment significantly altered the number of cells expressing SA-β-gal. (C) The mean fluorescence intensity (MFI) of the SA-β-gal-positive population was decreased in the presence of BMP2. BMP4 did not significantly alter SA-β-gal expression under these cell culture conditions (-HC). Data is presented as fold change compared to untreated cells. Values represent the mean ± SEM obtained from at least three independent experiments. No significance was obtained using a one-way ANOVA corrected using the Bonferroni multiple comparison test. (D) Representative histograms of SA-β-gal expression in untreated (i), BMP2- (ii) and BMP4-treated (iii) cells at day 6. Endogenous β-galactosidase (β-gal) activity was inhibited and SA-β-gal was determined using the fluorescent substrate C_{12}FDG. Cells incubated with inhibitor only (grey fill) and inhibitor plus C_{12}FDG (black line) were used to determine percentage SA-β-gal positive cells and mean fluorescence intensity (MFI).

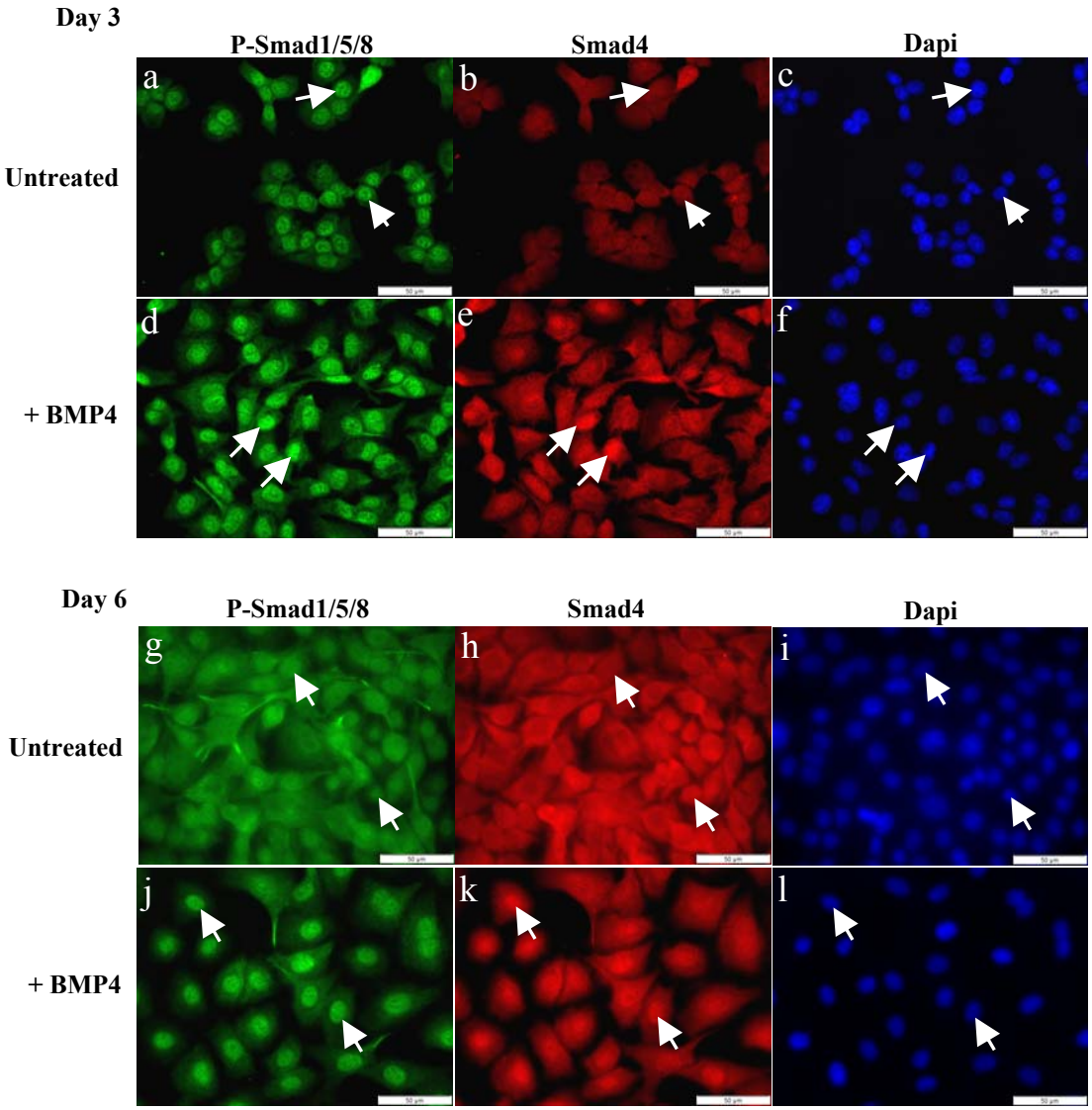

Figure 4.5 Phosphorylated Smad1/5/8 and Smad4 localisation in A549 cells cultured in the presence of BMP4

Immunofluorescence photomicrographs of p-Smad1/5/8 and Smad4 in untreated A549 cells (Untreated) cultured in serum-free medium omitting hydrocortisone (-HC) at day 3 (a, b) and day 6 (g, h) and in medium (-HC) containing 100 ng/ml BMP4 (+BMP4) at day 3 (d, e) and day 6 (j, k). At day 3, nuclear p-Smad1/5/8 and nuclear Smad4 were detected in untreated A549 cells (a-c). Nuclear p-Smad1/5/8 and nuclear Smad4 were increased in BMP4-treated cells at day 3 (d-f). At day 6, weak nuclear p-Smad1/5/8 was observed with no nuclear Smad4 seen in untreated cells (g-i). Nuclear p-Smad1/5/8 and nuclear Smad4 was evident in BMP4-treated cells at day 6 (j-l). Dapi nuclear counterstain shown left of each image (c, f, i, l). Arrows denote nuclear translocation. Scale bars represent 50 µm. Images shown are representative of two independent experiments. Negative antibody controls shown in Fig. 3.21.

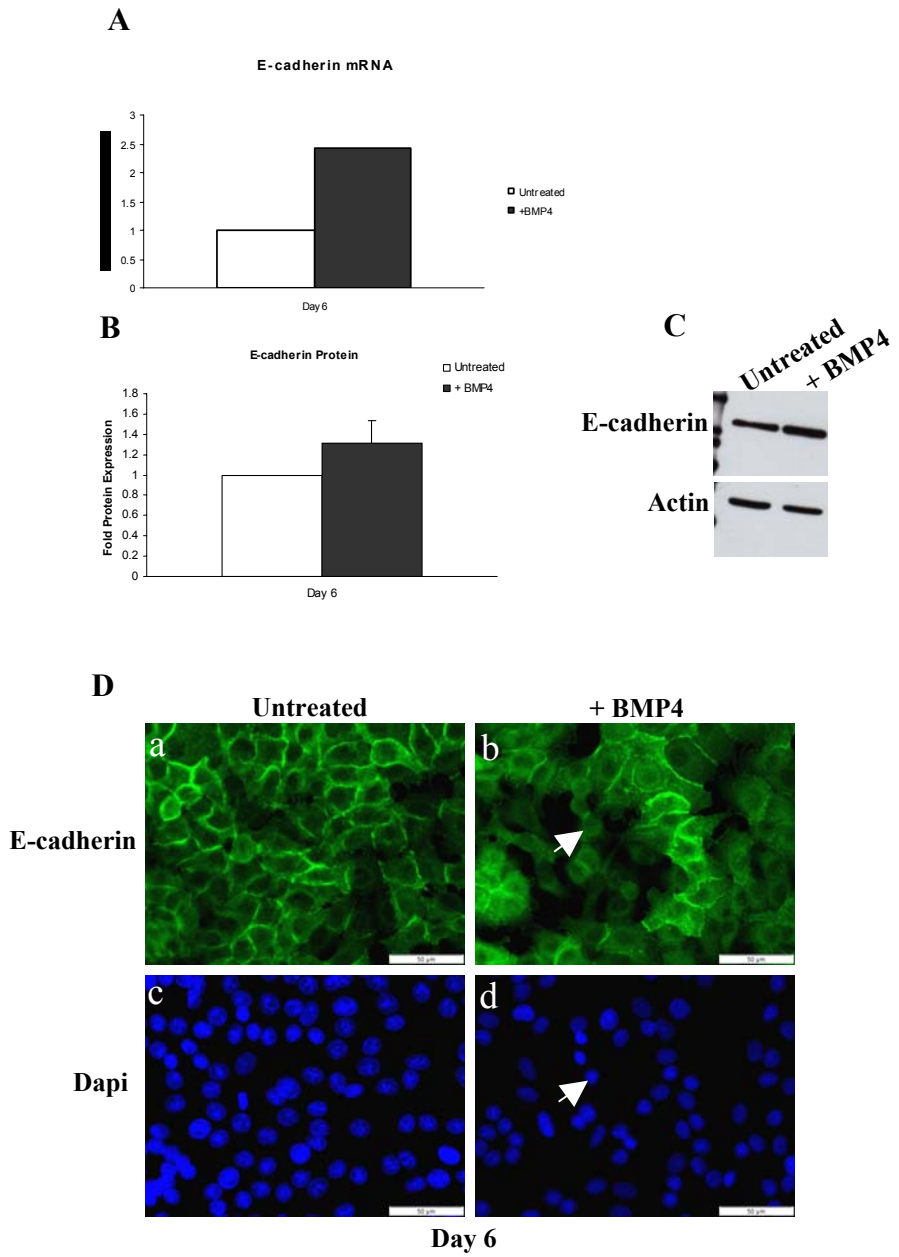

Figure 4.6 E-cadherin expression and localisation in BMP4-treated A549 cells at day 6.

(A) QPCR data shown for E-cadherin gene (CDH1) (Data generated by A Adams and JB Moore in Shirley O'Dea Laboratory). Data also presented in Table 4.1 (B) Densitometric quantification of E-cadherin protein expression revealed no significant alteration in E-cadherin expression in response to BMP4 by day 6. Values obtained for E-cadherin were normalised to actin. Data is presented as fold relative to untreated cells where the bar represents mean of three independent experiments ± SEM. (C) Representative western blot image of E-cadherin expression in untreated A549 cells (Untreated) cultured in serum free medium omitting hydrocortisone (-HC) and in serum-free medium (-HC) containing 100 ng/ml BMP4 (+BMP4) at day 6. (D) Immunofluorescence photomicrographs of E-cadherin in untreated A549 cells (Untreated) cultured in serum-free medium omitting hydrocortisone (-HC) day 6 (a) and in medium (-HC) containing 100 ng/ml BMP4 (+BMP4) at day 6 (b). Corresponding Dapi counterstain shown below (c, d). Arrows denote membrane E-cadherin localisation or cells lacking membrane staining. Scale bars represent 50 µm. Images shown are representative of two independent experiments. Negative antibody controls shown in Fig. 3.21.

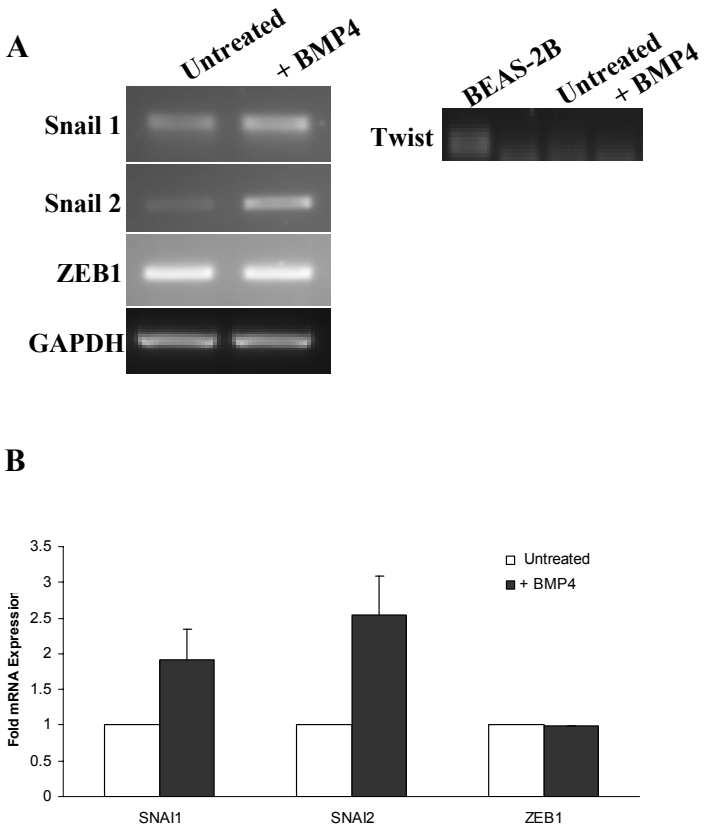

Figure 4.7 BMP4 modulates transcriptional repressors of E-cadherin in A549 cells

(A) RT-PCR analysis demonstrates upregulation of the transcriptional repressors of E-cadherin, Snail 1 (SNAI1) and Snail2 (SNAI2), at day 6 after BMP4 treatment. No change in ZEB1 expression was seen in response to BMP4. Twist was not expressed by A549 cells cultured in serum-free medium alone (untreated) or in response to BMP4 (+BMP4) (B) Densitometric quantification was carried out and normalised to glyceraldehyde-3-phosphate (GAPDH). Data is presented as fold change compared to untreated cells. Bars represent the mean ± SEM of at least three independent experiments. The level of upregulation observed with BMP4 treatment was not deemed significant using a students *t*-test.

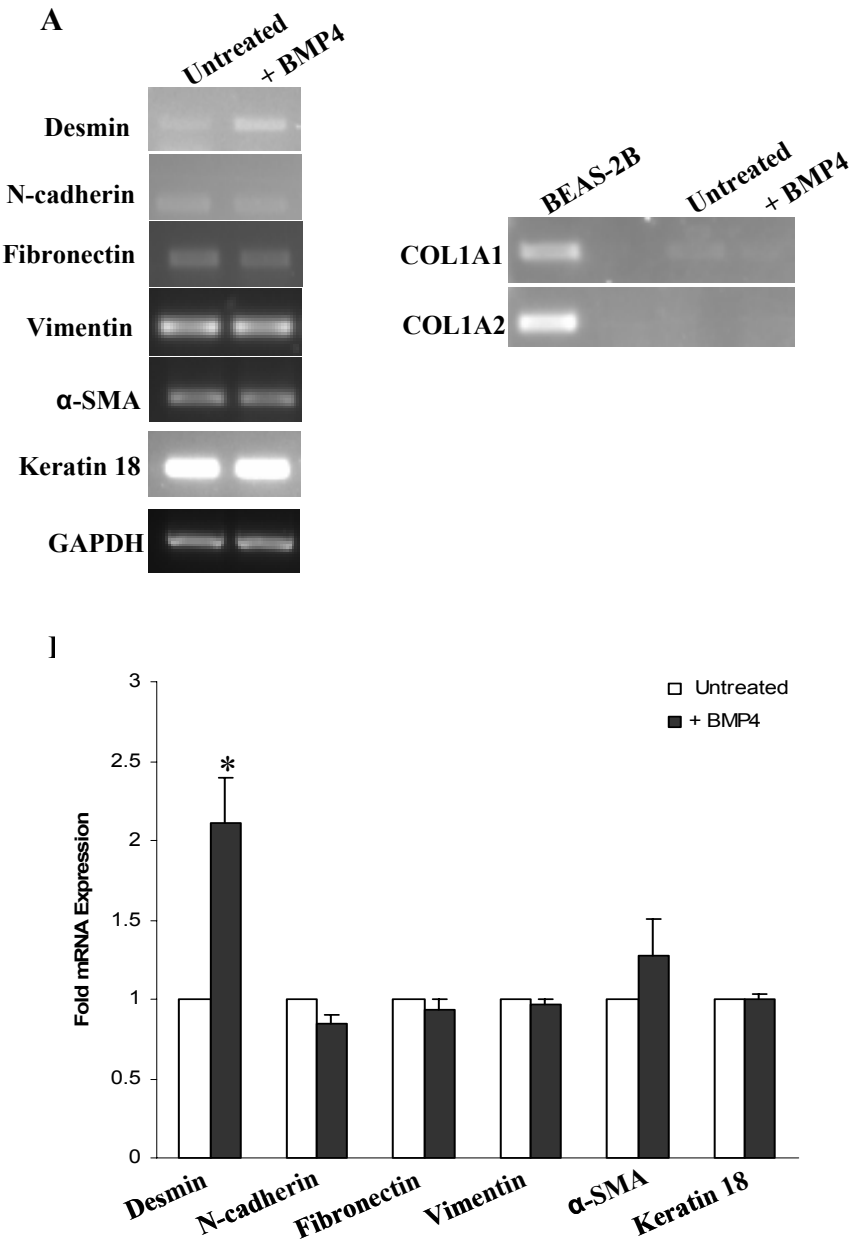

Figure 4.8 BMP4 modulates expression of cytoskeletal and ECM-related genes in A549 cells

(A) RT-PCR analysis demonstrates upregulation of cytoskeletal and ECM-related gene expression following BMP4 treatment for 6 days. (B) Densitometric quantification was carried out and normalised to glyceraldehyde-3-phosphate (GAPDH). Data is presented as fold change compared to untreated cells. Bars represent the mean ± SEM of at least three independent experiments. Significance compared to untreated cells was determined using a students *t*-test where * = $P<0.05$.

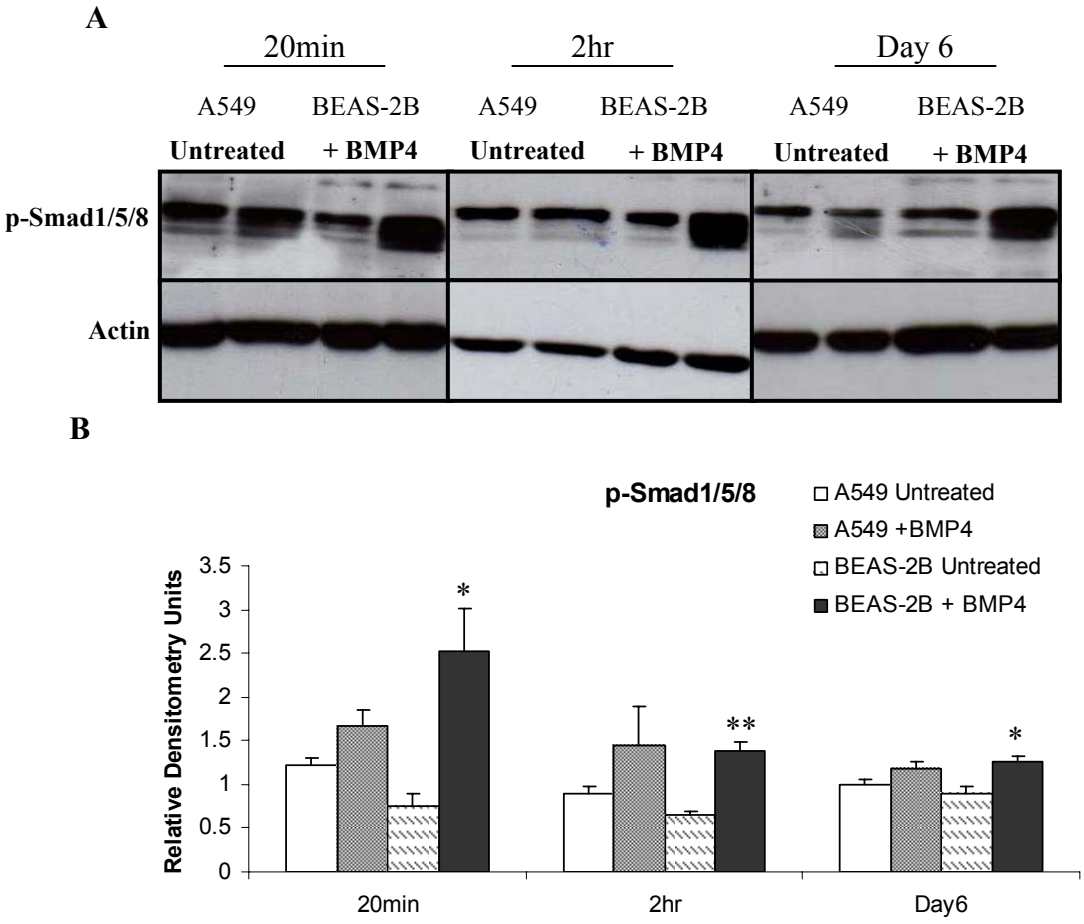

Figure 4.9 Phosphorylated Smad1/5/8 expression in A549 and BEAS-2B cells following 20 min, 2 hr and 6 days BMP4 stimulation

(A) Western blot analysis of relative p-Smad1/5/8 levels in A549 cells and BEAS-2B cells cultured in serum-free medium alone (untreated) and in serum-free medium containing 100 ng/ml BMP4 (+BMP4) for 20 min, 2 hr and 6 days. (B) Densitometric quantification of p-Smad1/5/8 levels. Values are presented as raw densitometric units normalised to actin. Bars represent the mean ± SEM of three independent experiments. Students *t*-test was used to calculate significance compared to untreated where * = $P < 0.05$ and ** = $P < 0.01$.

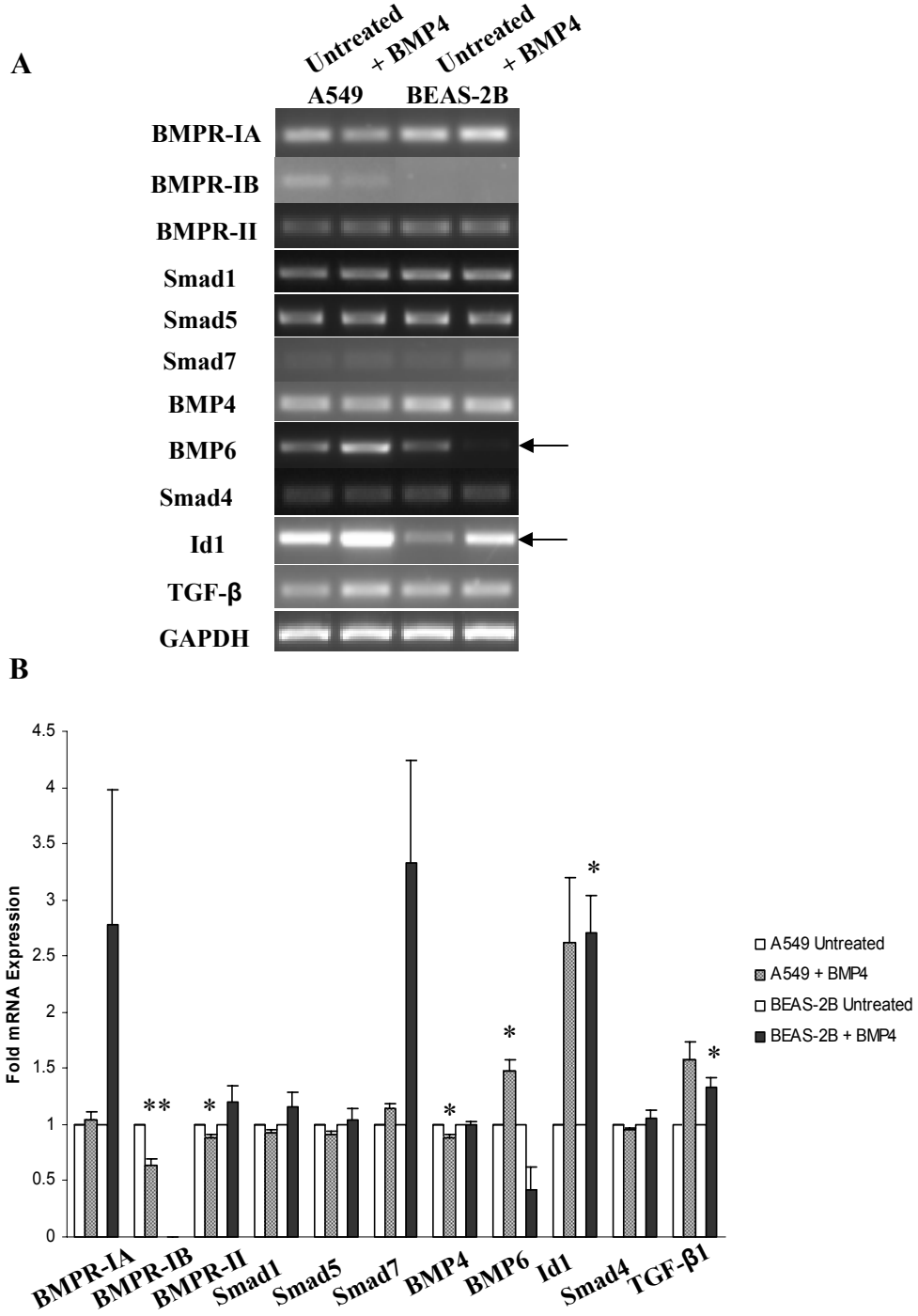

Figure 4.10 BMP pathway modulation in BMP4-treated A549 and BEAS-2B cells at day6

(A) RT-PCR analysis of BMP pathway components in A549 and BEAS-2B cells cultured in serum-free medium (untreated) and in serum-free medium containing 100 ng/ml BMP4 (+BMP4) for 6 days. (B) Densitometric quantification was carried out on each pathway component and normalised to glyceraldehyde-3-phosphate (GAPDH). Data is presented as fold change compared to untreated cells. Bars represent the mean ± SEM of at least three independent experiments. Significance was determined using the students *t*-test where * = $P<0.05$.

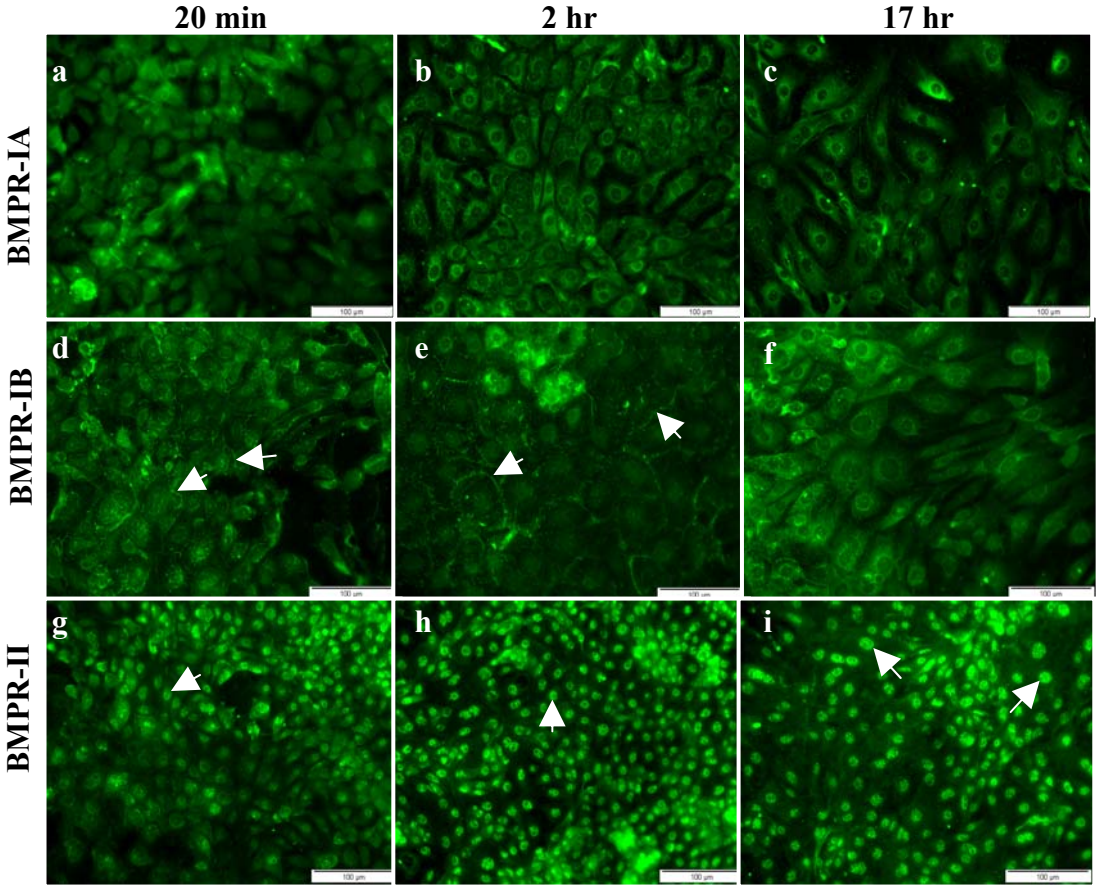

Figure 5.1 BMP receptor expression in MAECs in the absence of exogenous BMP stimulation

Representative photomicrographs of BMPR-IA, BMPR-IB and BMPR-II localisation in untreated MAECs cultured in serum-free medium for 20 min, 2 hr and 17 hr. BMPR-IA appeared localised to the cytoplasm of MAECs at 20 min, 2 hr and 17 hr (a-c). BMPR-IB localisation was apparent at the membrane and in the cytoplasm of MAECs cultured in serum-free medium for 20 min and 2 hr (d, e). However, BMPR-IB membrane localisation was not visible at 17 hr where only cytoplasmic localisation was evident (f). BMPR-II was localised to the nuclei of untreated MAECs and this localisation was not altered at 20 min, 2 hr and 17 hr (g-i). Scale bars represent 100 µm. Arrows denoted nuclear or membrane localisation. Negative immunofluorescence antibody controls (Ab Cntrl) shown in Fig. 5.17.

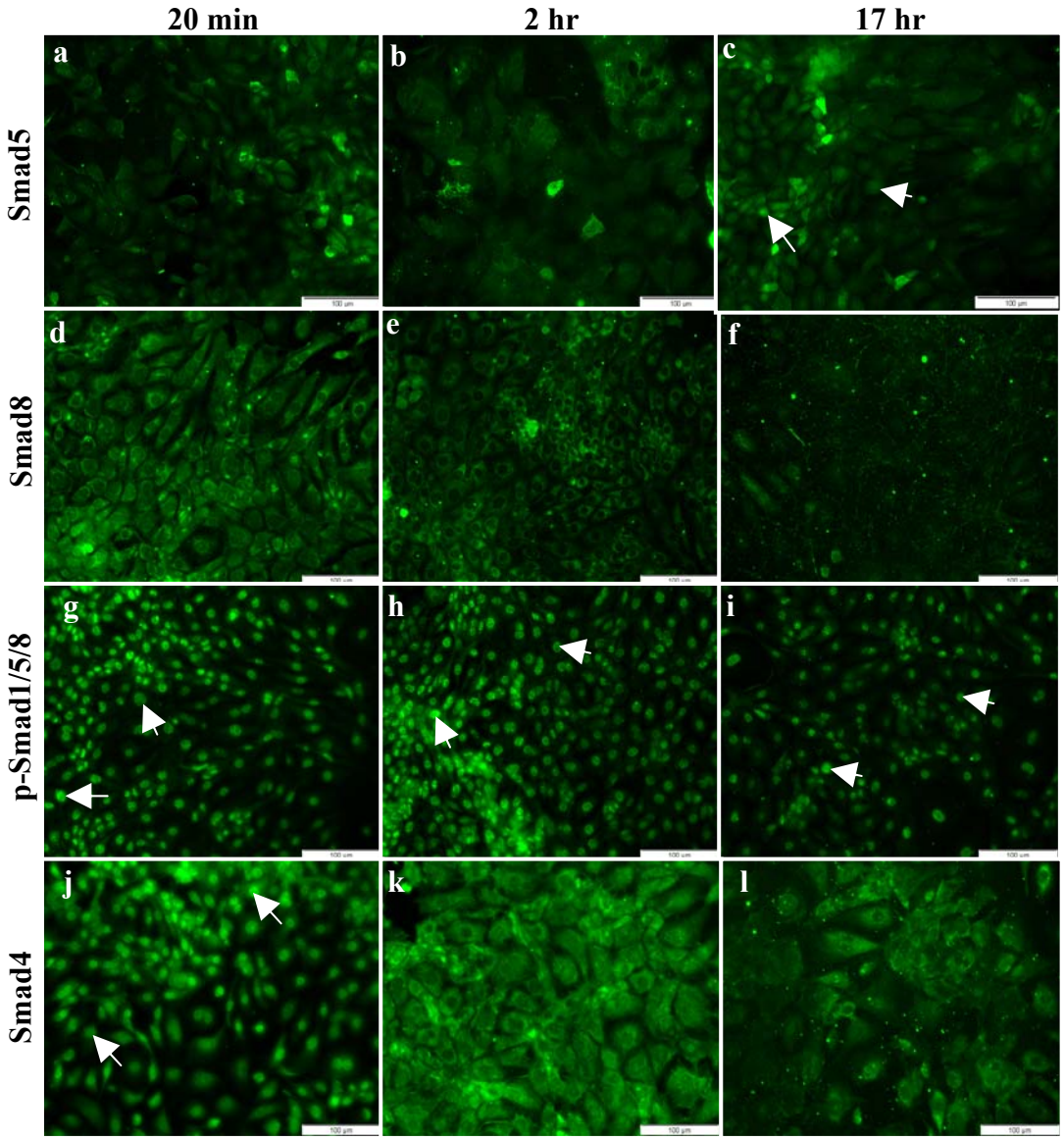

Figure 5.2 Smad protein expression in MAECs in the absence of exogenous BMP stimulation

Representative photomicrographs of Smad5, Smad8, phosphorylated Smad1/5/8 (p-Smad1/5/8) and Smad 4 localisation in untreated MAECs cultured in serum-free medium for 20 min, 2 hr and 17 hr. Smad5 was detected at low levels in the cytoplasm of untreated MAECs at 20 min and 2 hr (a, b). Weak Smad5 nuclear localisation was visible at 17 hr (c). Smad8 was detected in the cytoplasm at 20 min (d) and the levels of expression appeared reduced at 2 hr (e) and 17 hr (f). P-Smad1/5/8 was observed in the nuclei of MAECs at 20 min, 2 hr and 17 hr in serum-free medium (g-i). Smad4 was detected in the nuclei of MAECs at 20 min (j). Smad4 was visible in the cytoplasm of MAECs at 2 hr and 17 hr (k, l). Scale bars represent 100 μm. Arrows denoted nuclear localisation. Negative immunofluorescence antibody controls (Ab Cntrl) shown in Fig. 5.17.

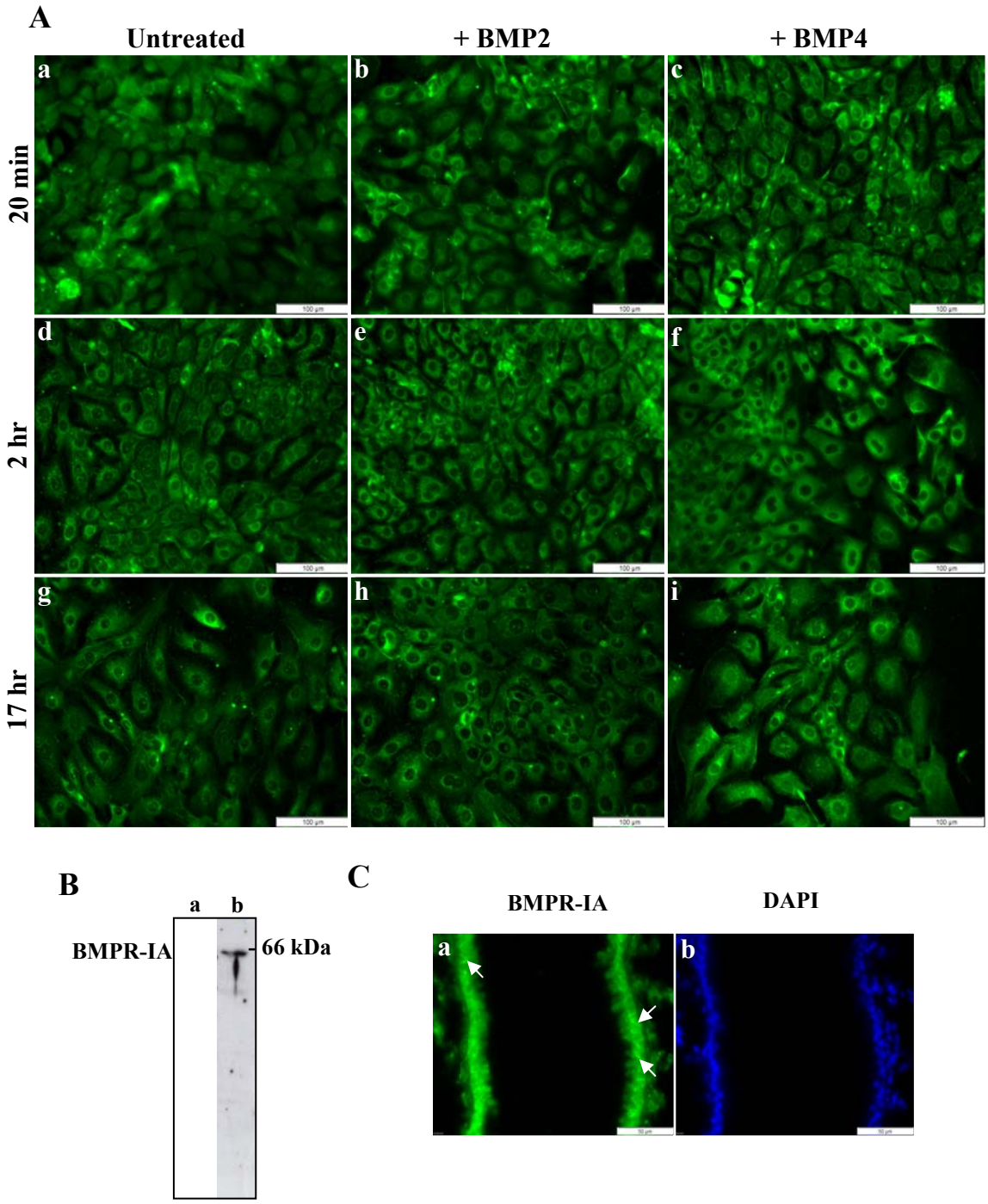

Figure 5.3 BMPR-IA localisation in MAECs in response to BMP2 and BMP4 stimulation

(A) Representative photomicrographs of BMPR-IA localisation in untreated MAECs cultured in serum-free medium (a, d, g) and in serum-free medium containing 100 ng/ml BMP2 (b, e, h) or 100 ng/ml BMP4 stimulation (c, f, i) for 20 min, 2 hr and 17 hr. BMPR-IA appeared localised to the cytoplasm of MAECs and the level of expression did not appear changed in response to BMP2 or BMP4. Scale bars represent 100 µm (B) Western blot validation of BMPR-IA antibody on mouse lung whole cell lysate (20 µg/lane) (a) and MLE mouse lung cell line whole cell lysate (10 µg/lane) (b). (C) Immunofluorescence images of BMPR-IA localised to basolateral and apical membrane of airway lung epithelial cells denoted with arrows (a). Dapi nuclear counterstain (b). Negative immunofluorescence antibody control image (Ab Cntrl) shown in Fig. 5.17 a.

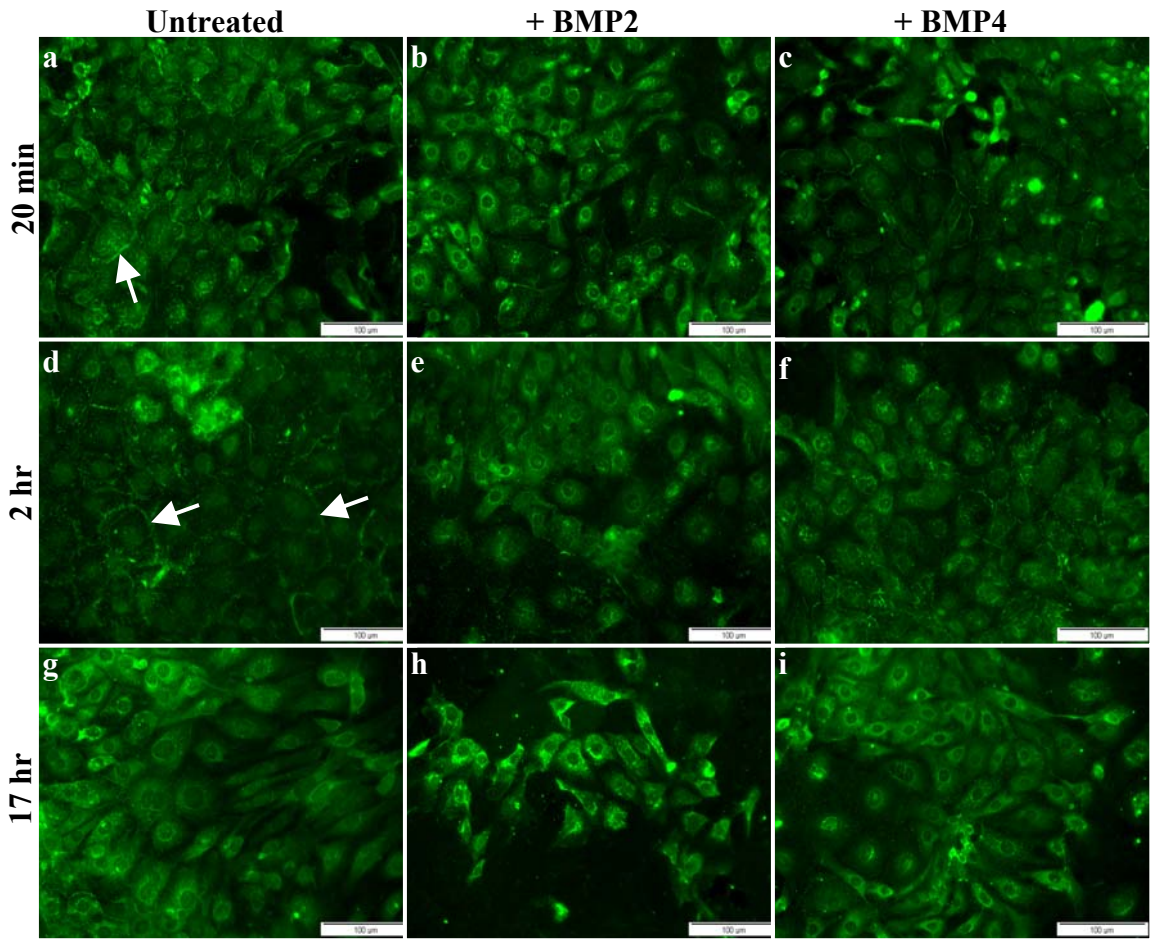

Figure 5.4 BMPR-IB localisation in MAECs in response to BMP2 and BMP4 stimulation

Representative photomicrographs of BMPR-IB localisation in untreated MAECs cultured in serum-free medium (a, d, g) and in serum-free medium containing 100 ng/ml BMP2 (b, e, h) or 100 ng/ml BMP4 stimulation (c, f, i) for 20 min, 2 hr and 17 hr. BMPR-IB appeared localised to the cytoplasm and membrane in untreated MAECs at 20 min and 2 hr (a, d). BMPR-IB appeared cytoplasmic in BMP2- and BMP4-treated cells with the level of expression comparable to untreated cells at 20 min (a-c), 2 hr (d-f) and 17 hr (g-i). Scale bars represent 100 µm. Arrows denote membrane localisation. Negative immunofluorescence antibody control image (Ab Cntrl) shown in Fig. 5.17 c.

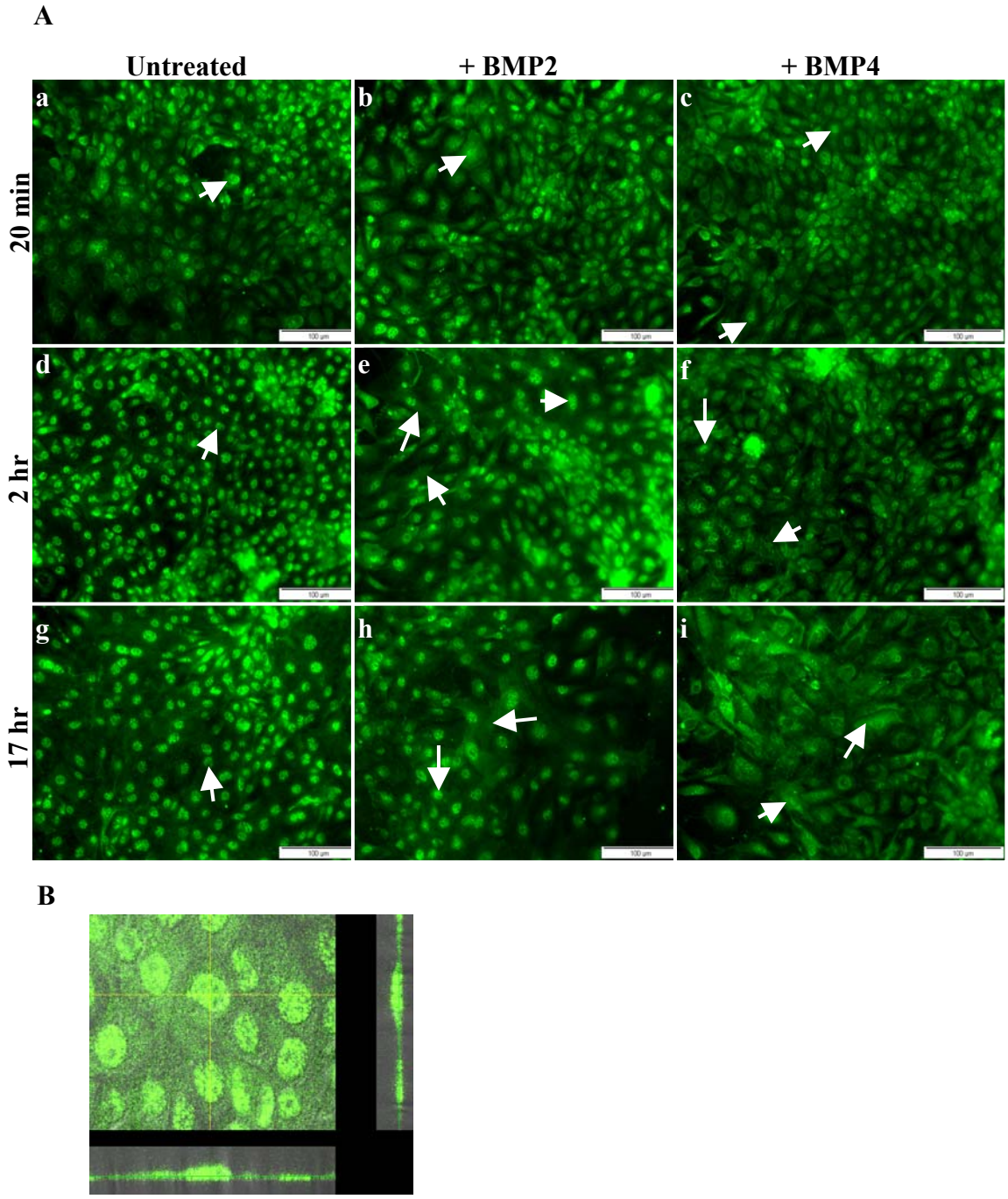

Figure 5.5 BMPR-II localisation in MAECs in response to BMP2 and BMP4 stimulation

(A) Representative photomicrographs of BMPR-II localisation in untreated MAECs cultured in serum-free medium (a, d, g) and in serum-free medium containing 100 ng/ml BMP2 (b, e, h) or 100 ng/ml BMP4 stimulation (c, f, i) for 20 min, 2 hr and 17 hr. BMPR-II appeared localised to the nuclei of untreated MAECs over the time course experiment (a, d, g). BMP2 treatment resulted in an increase in cytoplasmic localisation at 20 min and 2 hr (b, e). However, nuclear localisation remained at 17 hr (h). BMP4 treatment resulted in increased BMPR-II cytoplasmic localisation at 2 hr (f). At 17 hr, BMPR-II appeared entirely localised to the cytoplasm in BMP4-treated cells (i). Scale bars represent 100 µm. Arrows denote cytoplasmic or nuclear localisation. (B) Confocal microscopy confirmed BMPR-II nuclear localisation. Negative immunofluorescence antibody control image (Ab Cntrl) shown in Fig. 5.17 c.

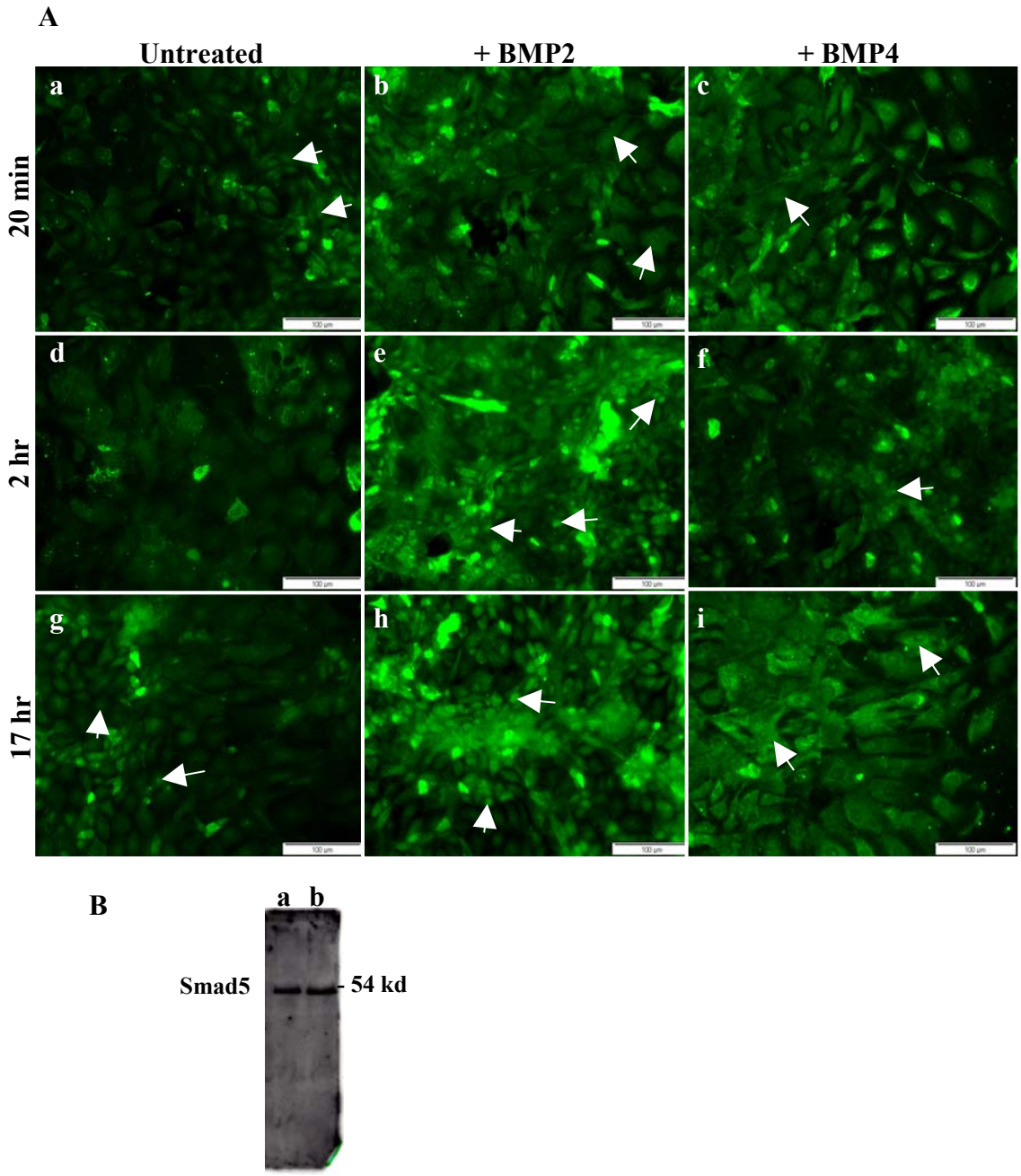

Figure 5.6 Smad5 localisation in MAECs in response to BMP2 and BMP4 stimulation

(A) Representative photomicrographs of Smad5 localisation in untreated MAECs cultured in serum-free medium (a, d, g) and in serum-free medium containing 100 ng/ml BMP2 (b, e, h) or 100 ng/ml BMP4 stimulation (c, f, i) for 20 min, 2 hr and 17 hr. Smad5 was expressed at low levels in untreated MAECs (a, d, g) with nuclear localisation apparent at 17 hr (g). BMP2 treatment resulted in an increase in cytoplasmic expression at 20 min, 2 hr and 17 hr (b, e, h) with Smad5 nuclear translocation apparent at 2 hr and 17 hr (e, h). BMP4 treatment resulted in increased cytoplasmic expression at 20 min, 2hr and 17hr (c, f, i). Scale bars represent 100 µm. Arrows denote increased cytoplasmic expression and/or nuclear localisation. (B) Western blot validation of Smad5 antibody on mouse lung whole cell lysate (20 µg/lane) (a) and MLE mouse lung cell line whole cell lysate (20 µg/lane) (b). Negative immunofluorescence antibody control (Ab Cntrl) shown in Fig. 5.17 c

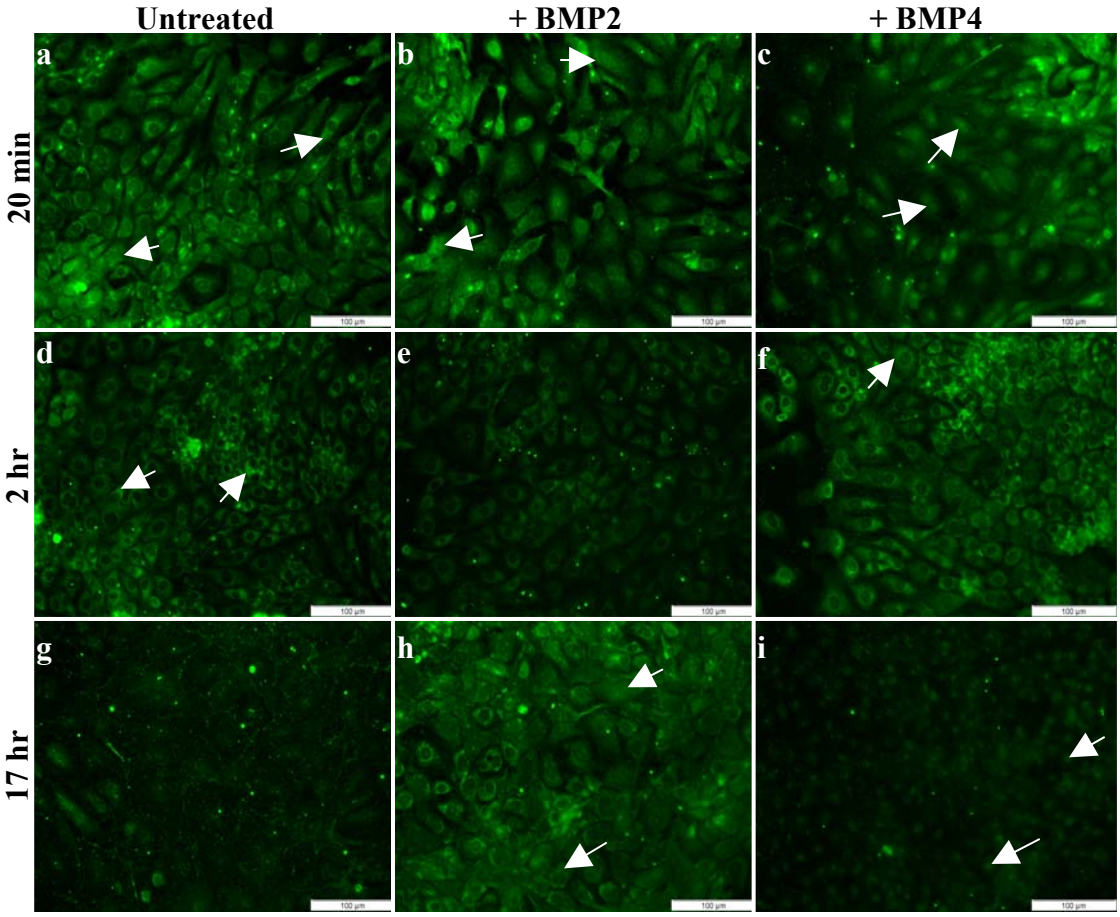

Figure 5.7 Smad8 localisation in MAECs in response to BMP2 and BMP4 stimulation

Representative photomicrographs of Smad8 localisation in untreated MAECs cultured in serum-free medium (a, d, g) and in serum-free medium containing 100 ng/ml BMP2 (b, e, h) or 100 ng/ml BMP4 stimulation (c, f, i) for 20 min, 2 hr and 17 hr. Smad8 was expressed at low levels in untreated MAECs (a, d, g). BMP2 treatment resulted in an increase in cytoplasmic expression at 20 min (b) which appeared reduced at 2 hr (e) and increased again at 17 hr (h). BMP4 treatment resulted in nuclear translocation of Smad8 at 20min (c) which was not sustained at 2 hr (f). Smad8 level of expression in BMP4-treated cells appeared comparable to untreated at 17 hr (i). However, weak Smad8 nuclear localisation was apparent in BMP4-treated cells at 17 hr (i). Scale bars represent 100 µm. Arrows denote increased expression and/or nuclear localisation. Negative immunofluorescence antibody control (Ab Cntrl) shown in Fig. 5.17 c.

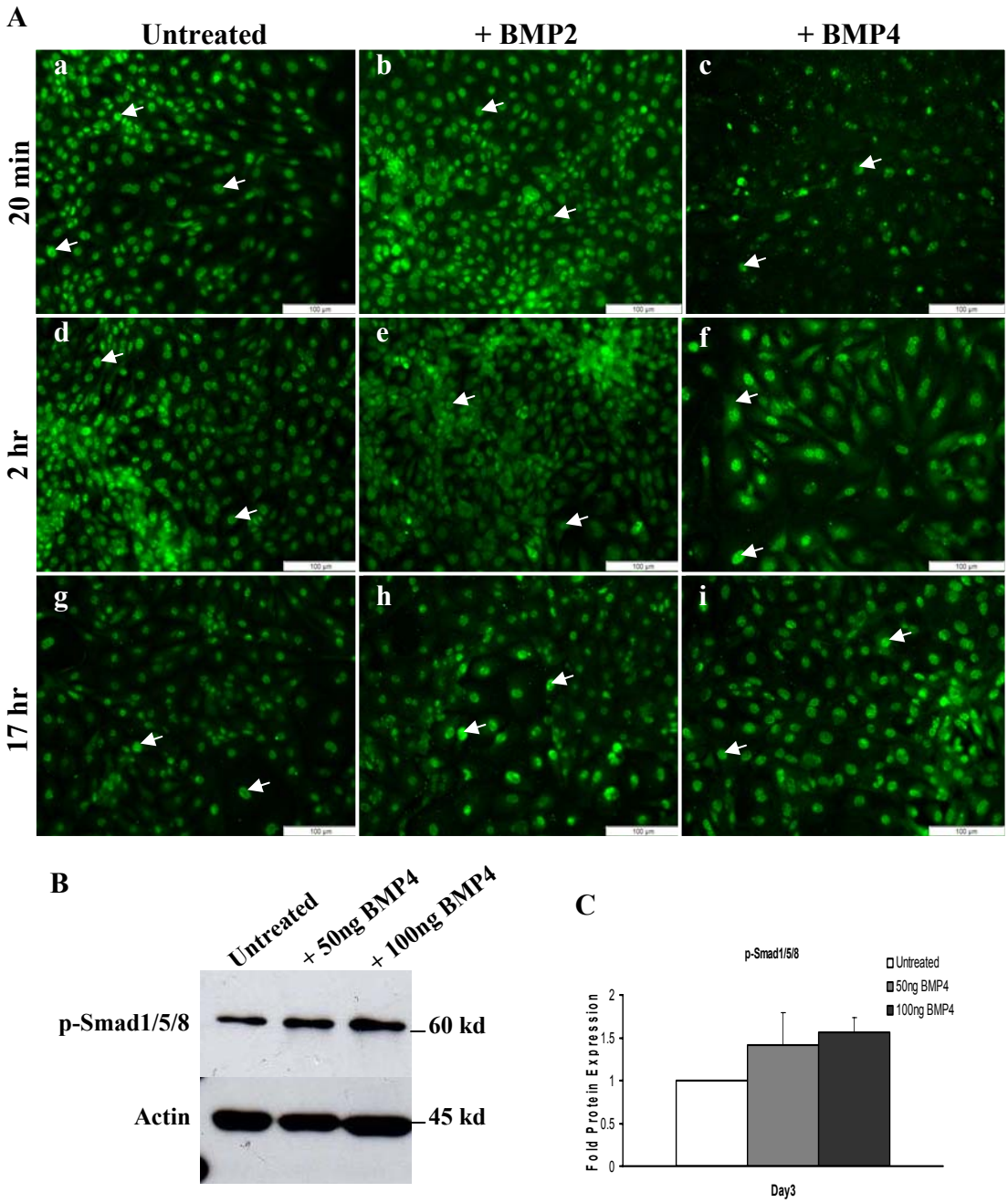

Figure 5.8 p-Smad1/5/8 localisation in MAECs in response to BMP2 and BMP4 stimulation

(a) Representative photomicrographs of phosphorylated Smad1/5/8 (p-Smad1/5/8) localisation in untreated MAECs cultured in serum-free medium (a, d, g) and in serum-free medium containing 100 ng/ml BMP2 (b, e, h) or 100 ng/ml BMP4 stimulation (c, f, i) for 20 min, 2 hr and 17 hr. P-Smad1/5/8 was expressed in the nuclei of untreated MAECs at 20 min, 2 hr and 17 hr in serum-free medium (a, d, g). At 20 min, p-Smad1/5/8 localisation was unchanged in response to BMP2 and BMP4 (b, c, respectively). At 2 hr, some increase in cytoplasmic expression was seen in BMP2- and BMP4-treated cells (e, f, respectively). At 17 hr, a slight increase in nuclear localisation was seen in response to BMP2 and BMP4 (h, i, respectively). Scale bars represent 100 µm. Arrows denote increased expression and/or nuclear localisation. (B) Representative western blot of MAECs cultured in serum-free medium alone (Untreated) or serum-free medium containing 50 ng/ml or 100 ng/ml BMP4 (+BMP4). (C) Densitometric quantification of p-Smad1/5/8 revealed increased p-Smad1/5/8 at day 3 in response to 100 ng/ml BMP4. Values obtained were normalised to actin and presented as fold compared to untreated cells. Bars represent the mean ± StDev of two independent experiments. Negative immunofluorescence antibody control (Ab Cntrl) shown in Fig. 5.17 a.

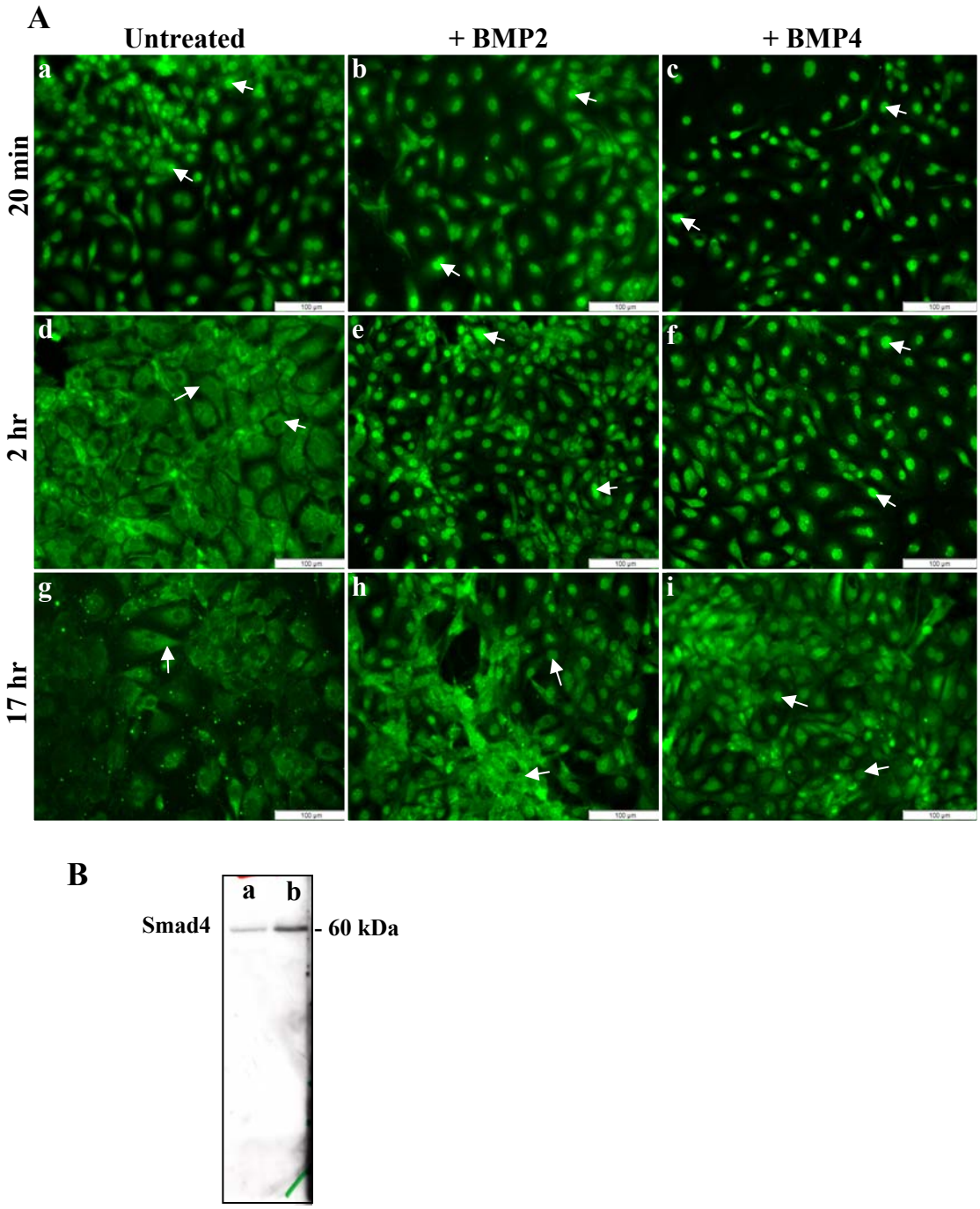

Figure 5.9 Smad4 localisation in MAECs in response to BMP2 and BMP4 stimulation

(A) Representative photomicrographs of Smad4 localisation in untreated MAECs cultured in serum-free medium (a, d, g) and in serum-free medium containing 100 ng/ml BMP2 (b, e, h) or 100 ng/ml BMP4 stimulation (c, f, i) for 20 min, 2 hr and 17 hr. Smad4 was expressed in the nuclei of untreated MAECs at 20 min (a) but appeared cytoplasmic at 2 hr (d) and 17 hr (g). BMP2 treatment resulted in increased nuclear translocation compared to untreated at 20 min, 2 hr and 17 hr (b, e, h). Similarly, BMP4 treatment resulted in increased nuclear translocation compared to untreated at 20 min, 2 hr and 17 hr (c, f, i). Scale bars represent 100 µm. Arrows denote increased expression and/or nuclear localisation. (B) Western blot validation of Smad4 antibody on mouse lung whole cell lysate (20 µg/lane) (a) and MLE mouse lung cell line whole cell lysate (20 µg/lane) (b). Negative immunofluorescence antibody control (Ab Cntrl) shown in Fig. 5.17 e.

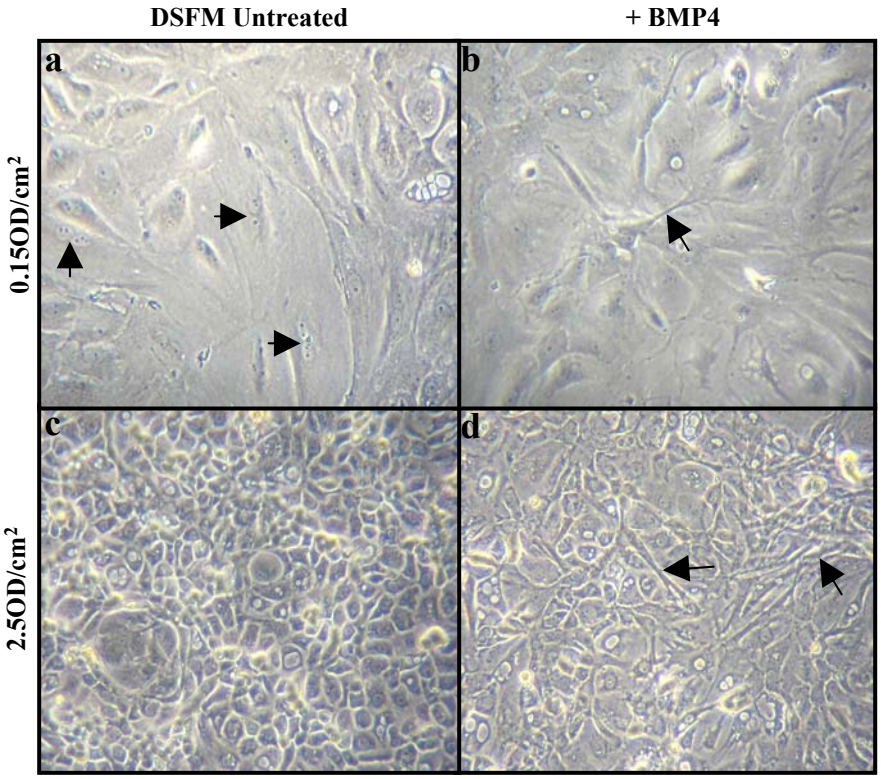

Figure 5.10

Comparison of morphology in MAECs seeded at either low or high seeding density

Representative images of MAECs at day 3 seeded at either low density (0.15 OD/cm^2) (a) or high density (2.5 OD/cm^2) (c) in defined serum-free medium alone (DSFM Untreated) or defined serum-free medium containing 100 ng/ml BMP4 (+ BMP4) (b, d). An increase in senescent-like cells were visible when cells were seeded at low density (a, arrows) whereas MAECs maintained a characteristic epithelial cobblestone morphology at high density (c). Cells treated with 100 ng/ml BMP4 did appear more angular at low seeding density (b, arrows) but this morphology effect was more pronounced at high density with cells which looked elongated and fibroblast-like (d, arrows).

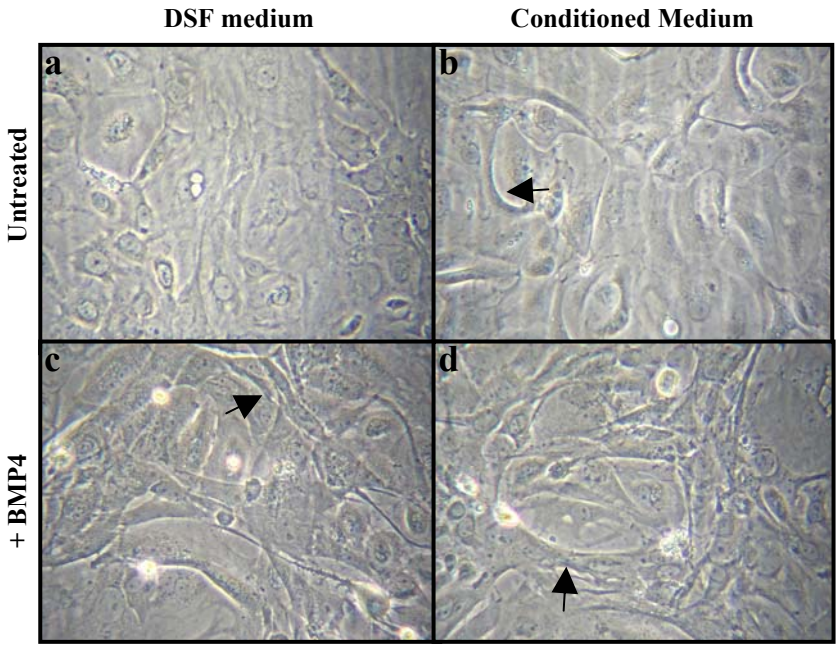

Figure 5.11 MAEC morphology in conditioned media from BEAS-2B cells

MAECs cultured in conditioned medium from BEAS-2B cells (CM) were morphologically different from MAECs cultured in defined serum-free medium (DSFM). At day 6, cells grown in DSFM had characteristic epithelial morphology (a). In response to 100 ng/ml BMP4 an increase in elongated fibroblast-like cells was visible (c, arrows). Cells grown in conditioned medium (b) appeared more angular compared to DSFM (a). BMP4-treatment in CM medium did result in an increase in similar fibroblast-like cells (d).

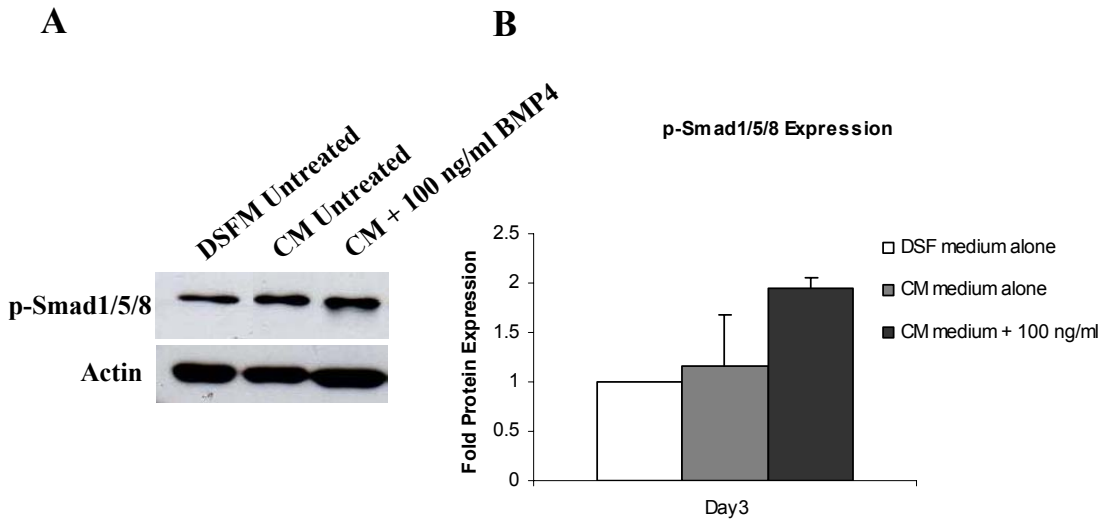

Figure 5.12 BMP4 increases p-Smad1/5/8 expression in MAECs cultured in conditioned medium

(A) Representative western blot image of p-Smad1/5/8 expression in MAECs cultured in serum-free medium alone (DSF medium alone), in conditioned medium (CM) or conditioned medium + 100 ng/ml BMP4 (CM + 100 ng/ml BMP4) for 3 days. Increased p-Smad1/5/8 was evident in CM + BMP4 cells compared to CM untreated. (B) Densitometric analysis of p-Smad1/5/8 expression in MAECs cultured in CM medium alone and CM medium containing 100 ng/ml BMP4 represented as fold compared to cells grown in serum-free medium (DSF medium alone). No increase in p-Smad1/5/8 levels was detected in MAECs cultured in CM medium compared cells cultured in DSF medium. Increased levels of p-Smad1/5/8 was detected in CM + 100 ng/ml BMP4 compared to CM alone but this was not found to be significant. A significant increased in p-Smad1/5/8 was detected in MAECs cultured in CM + 100 ng/ml BMP4 compared to DSF cells. Values obtained were normalised to actin. Bars represent mean ± StDev of two independent experiments.

Figure 5.13

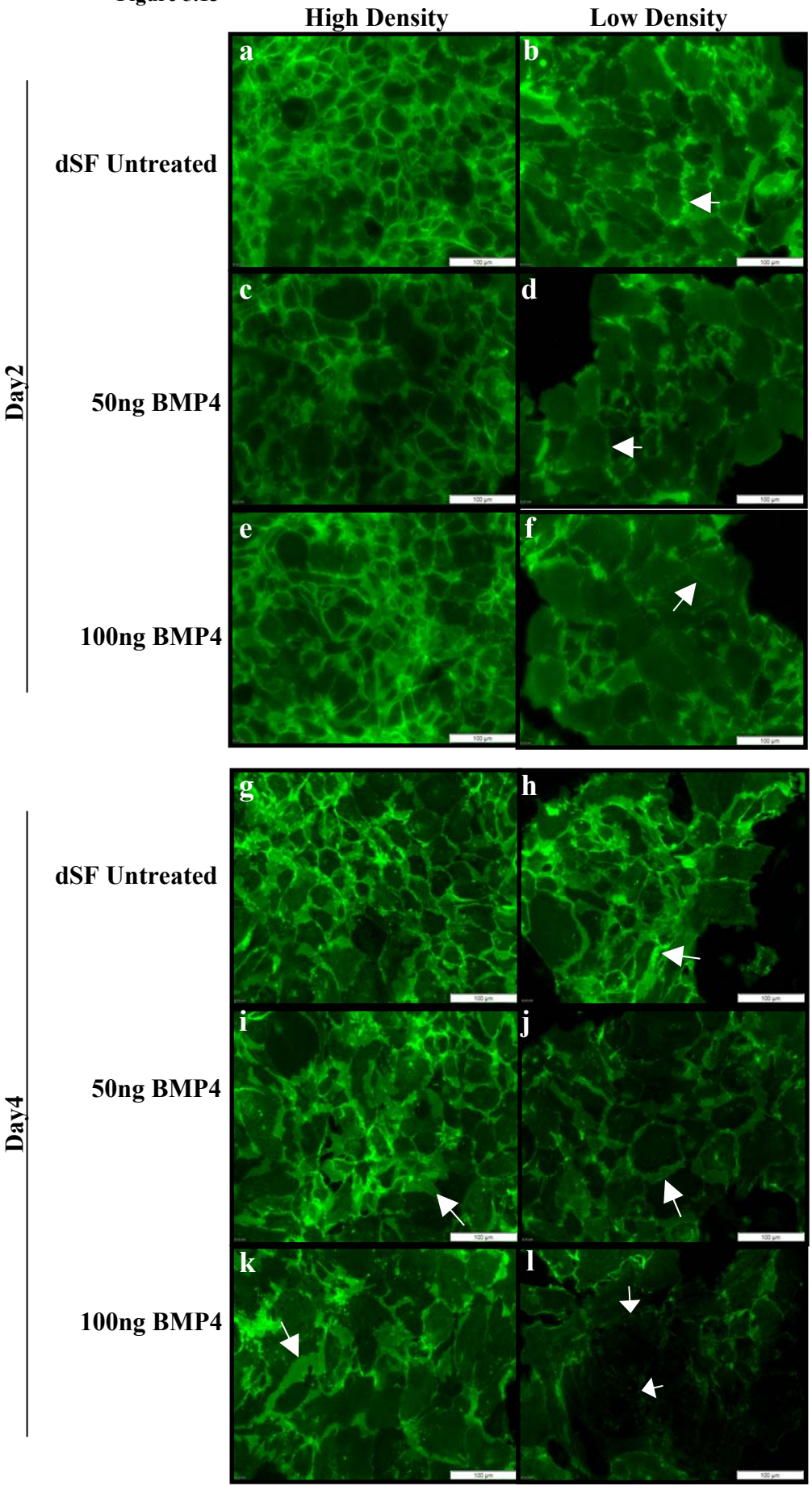
High Density
Low Density
Day2
dSF Untreated
50ng BMP4
100ng BMP4
Day4
dSF Untreated
50ng BMP4
100ng BMP4
a
b
c
d
e
f
g
h
i
j
k
l

Figure 5.13 Analysis of E-cadherin localisation MAECs cultured in dSF medium following BMP4 treatment

Representative immunofluorescence photomicrographs of E-cadherin localisation in MAECs cultured in defined serum-free medium alone (DSF Untreated) and defined serum-free medium containing either 50 ng/ml (50 ng BMP4) or 100 ng/ml BMP4 (100 ng BMP4) at day 2 (a-f) and day 4 (g-l). MAECs at high and low density are shown. Membrane E-cadherin localisation was visible on all cells. At day 2, on MAECs at high density E-cadherin expression and localisation was comparable between untreated cells and BMP4-treated cells (a, c, e). At low density, a slight reduction in the level of expression was apparent in response to 50 ng/ml and 100 ng/ml BMP4 (b, d, f, denoted with arrows). At day 4, BMP4-treated MAECs at high density had increasingly cytoplasmic E-cadherin localisation (g, I, k, arrows). At low density, a decrease in E-cadherin expression was apparent on both 50 ng/ml and 100 ng/ml BMP4-treated cells (j, l, arrows). Scale bar represents 100 μm. Negative immunofluorescence antibody controls (Ab Cntrl) shown in Fig. 5.17 e.

Figure 5.14

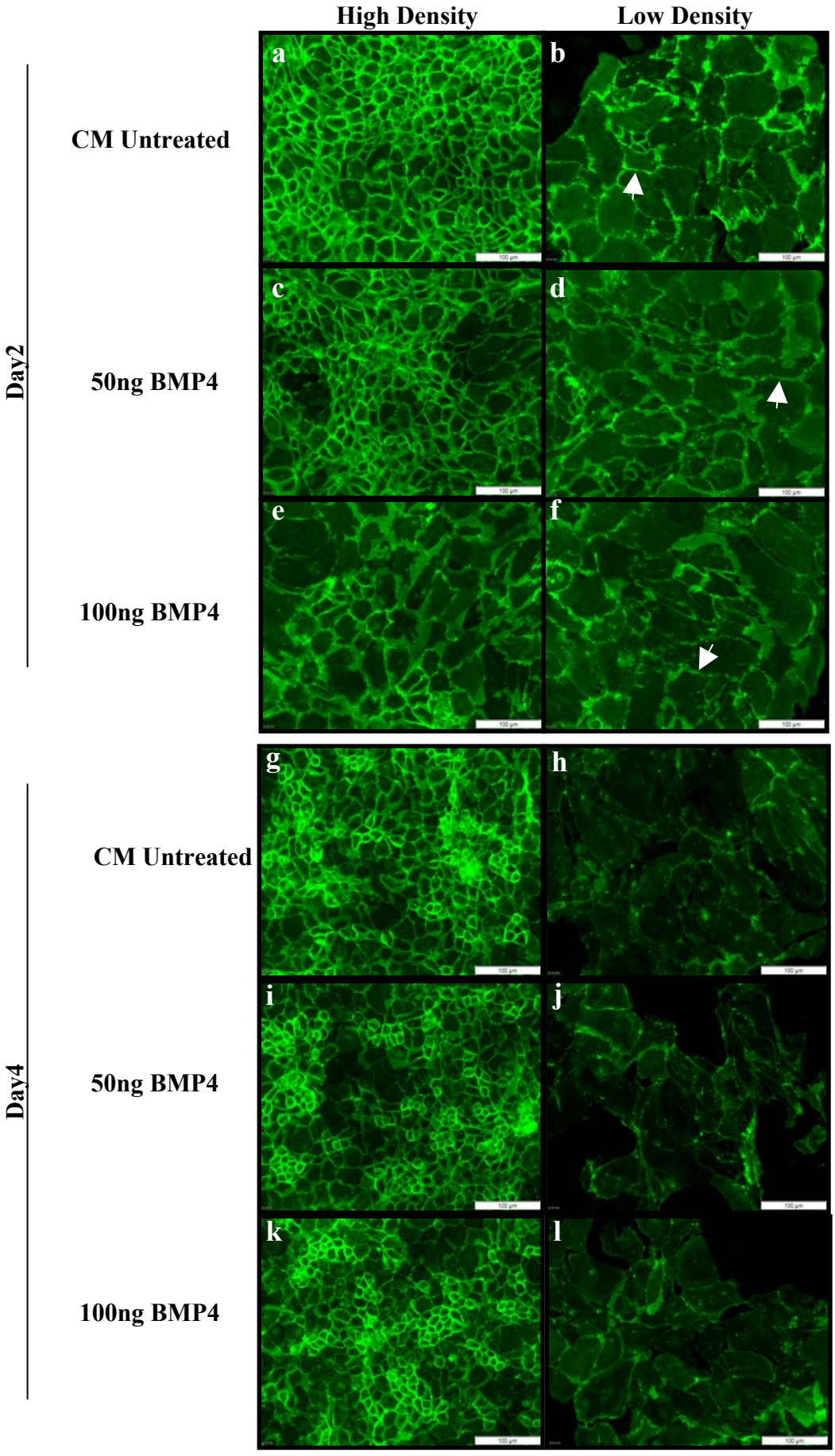
High Density
Low Density
Day2
CM Untreated
50ng BMP4
100ng BMP4
Day4
CM Untreated
50ng BMP4
100ng BMP4
a
b
c
d
e
f
g
h
i
j
k
l

Figure 5.14 Analysis of E-cadherin localisation MAECs cultured in CM medium following BMP4 treatment

Representative immunofluorescence photomicrographs of E-cadherin localisation in MAECs cultured in conditioned medium alone (CM Untreated) and conditioned medium containing either 50 ng/ml (50 ng BMP4) or 100 ng/ml BMP4 (100 ng BMP4) at day 2 (a-f) and day 4 (g-l). MAECs at high and low density are shown. Membrane E-cadherin localisation was visible on all cells. At day 2, on MAECs at high density E-cadherin expression and localisation was comparable between untreated cells and BMP4-treated cells (a, c, e). At low density, a slight reduction in the level of expression was apparent in response to 50 ng/ml and 100 ng/ml BMP4 on MAECs (b, d, f, arrows). At day 4, E-cadherin expression and localisation was comparable between BMP4-treated and untreated cells (g, I, k). At low density, a decrease in E-cadherin expression was apparent compared to day 2 (h, j, l compared to b, d, f). No further reduction in E-cadherin was apparent in response to 50 ng/ml or 100 ng/ml BMP4 (j, l). Scale bar represents 100 μm. Negative immunofluorescence antibody controls (Ab Cntrl) shown in Fig. 5.17 e.

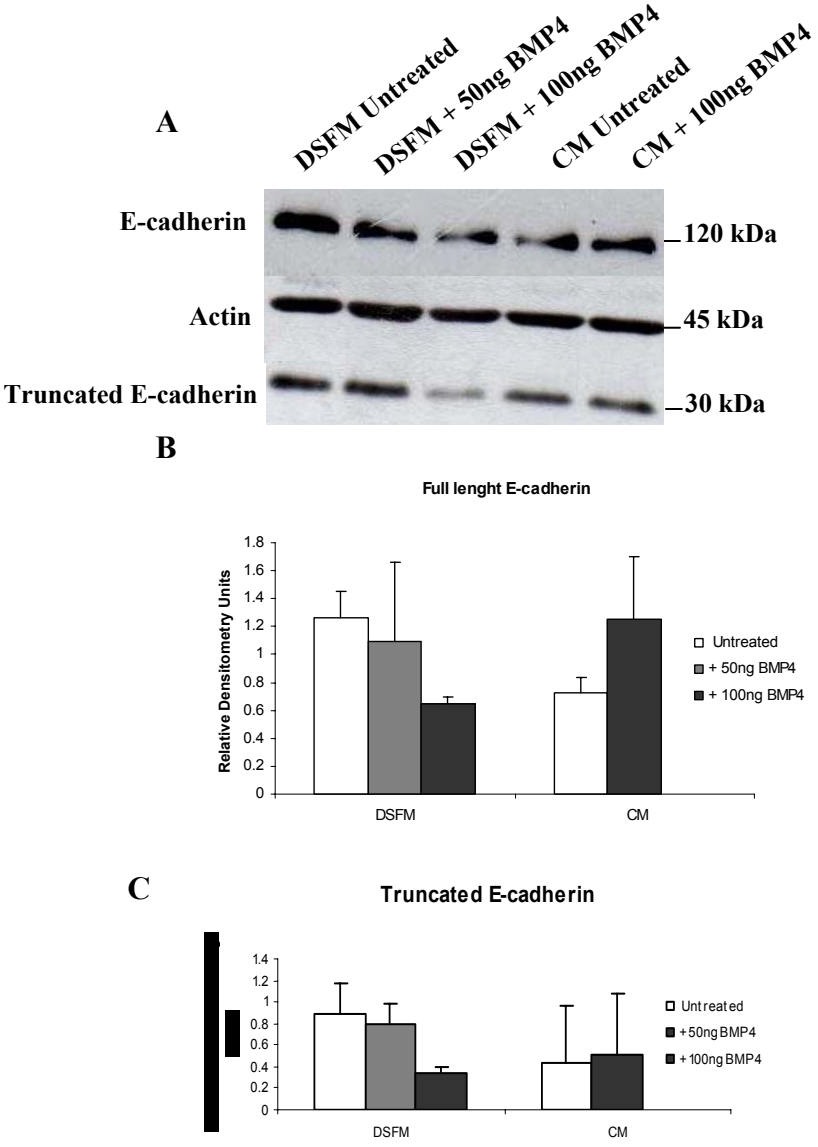

Figure 5.15 E-cadherin protein expression is reduced in MAECs with BMP4 treatment

(A) Western blot analysis of E-cadherin expression at day 3 in MAECs cultured in both defined serum free medium (DSF medium) and conditioned medium (CM medium) alone or containing either 50 ng/ml (DSFM only) or 100 ng/ml BMP4. The E-cadherin antibody used detects both full length E-cadherin (120 kDa) and truncated E-cadherin (30 kDa). (B) Densitometric quantification demonstrated reduced expression of both full length E-cadherin (120 kDa) and truncated E-cadherin (30 kDa) in response to 100 ng/ml BMP4 in DSFM only. E-cadherin expression was not significantly altered in CM medium in response to 100 ng/ml BMP4. All values were normalised to actin. Bars represent mean ± StDev of two independent experiments.

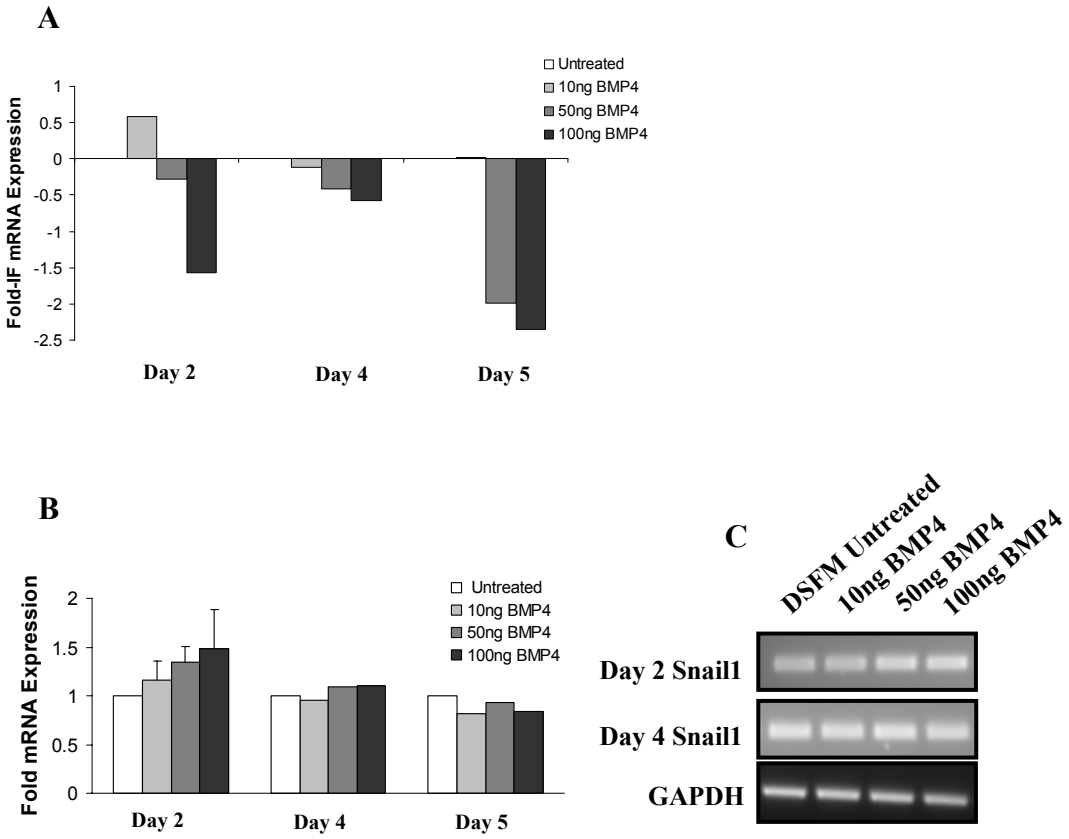

Figure 5.16 Analysis of E-cadherin mRNA and Snail1 mRNA in BMP4-treated MAECs

(A) Quantitative PCR (QPCR) analysis of E-cadherin mRNA expression in MAECs cultured in defined serum-free medium (DSFM) at day 2, day 4 and day 5 in response to 10 ng/ml, 50 ng/ml and 100 ng/ml BMP4. Values were normalised to GAPDH. Data is represented as fold relative to untreated cells. Bars represent mean of two independent experiments. E-cadherin mRNA was reduced in BMP4-treated cells at day 2 and up to day 4 in response to 50 ng/ml and 100 ng/ml BMP4. E-cadherin inhibition was not apparent in response to 10 ng/ml BMP4 at day 4. (B) Semi-quantitative PCR (RT-PCR) analysis of Snail1 mRNA expression in MAECs cultured in defined serum-free medium (DSFM) at day 2, day 4 and day 5 in response to 10 ng/ml, 50 ng/ml and 100 ng/ml BMP4. Values were normalised to GAPDH. Data is represented as fold relative to untreated cells. Bars represent mean ± StDev of two independent experiments (day 2 only). Increased Snail1 mRNA was detected in response to 100 ng/ml and 50 ng/ml BMP4 at day 2. No significant alteration in Snail1 expression was seen in response to 10 ng/ml BMP4. Snail1 levels were not elevated at day 4 or day 5. (C) Representative Snail1 RT-PCR gel image.

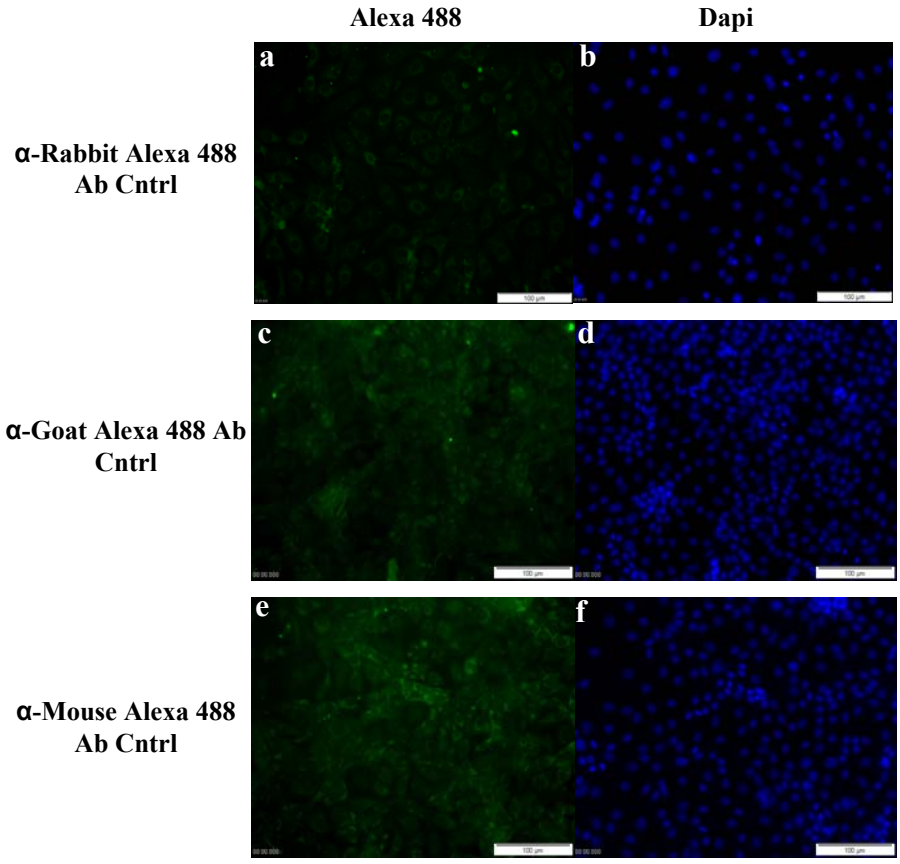

Figure 5.17 Immunofluorescence antibody controls

Photomicrographs represent immunofluorescence antibody controls on MAECs. Secondary antibody control (Ab Cntrl) omitted primary antibody where cells were incubated in either α-rabbit (a), α-goat (b) or α- mouse (c) alexa488-conjugated secondary antibody (a-c). Dapi counterstained nuclei shown right of image (d-f). Scale bars represent 100 μm.

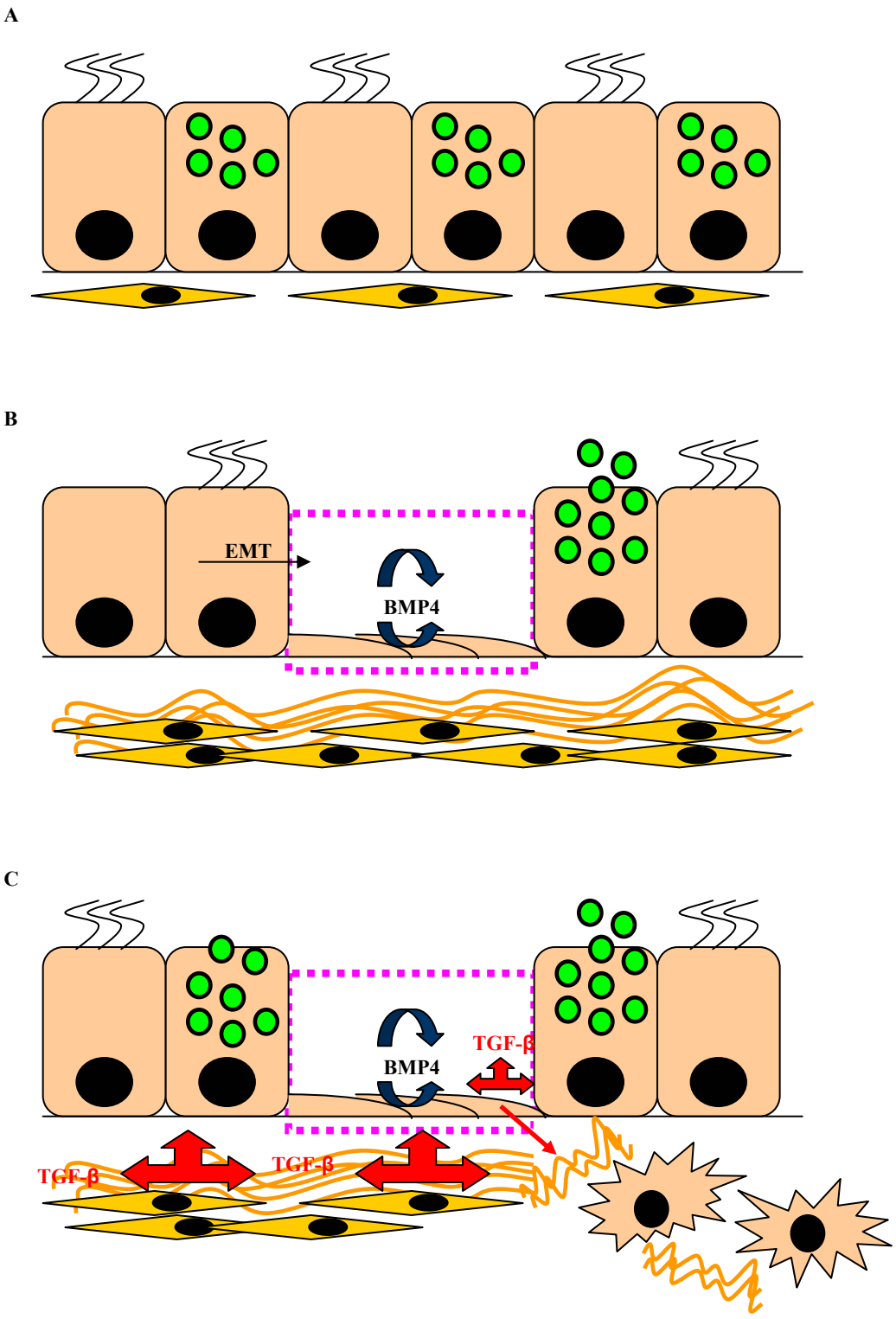

Figure 5.18 Diagram depicting injury and repair in the airway epithelium

(A) Diagram depicts the cell types which populate a healthy airway epithelium. (B) Following injury, epithelial cells are shed and myofibroblast transformation can lead to collagen deposition. In this state, epithelial cells which are adjacent to the denuded area spread out and proliferate to protect the exposed basement membrane. We hypothesise BMP signalling may be active in these 'reparative' cells. (C) In the event of sustained inflammation, epithelial-mesenchymal transition (EMT) may occur in response to profibrotic stimuli, such as TGF-β or BMP4 or both.

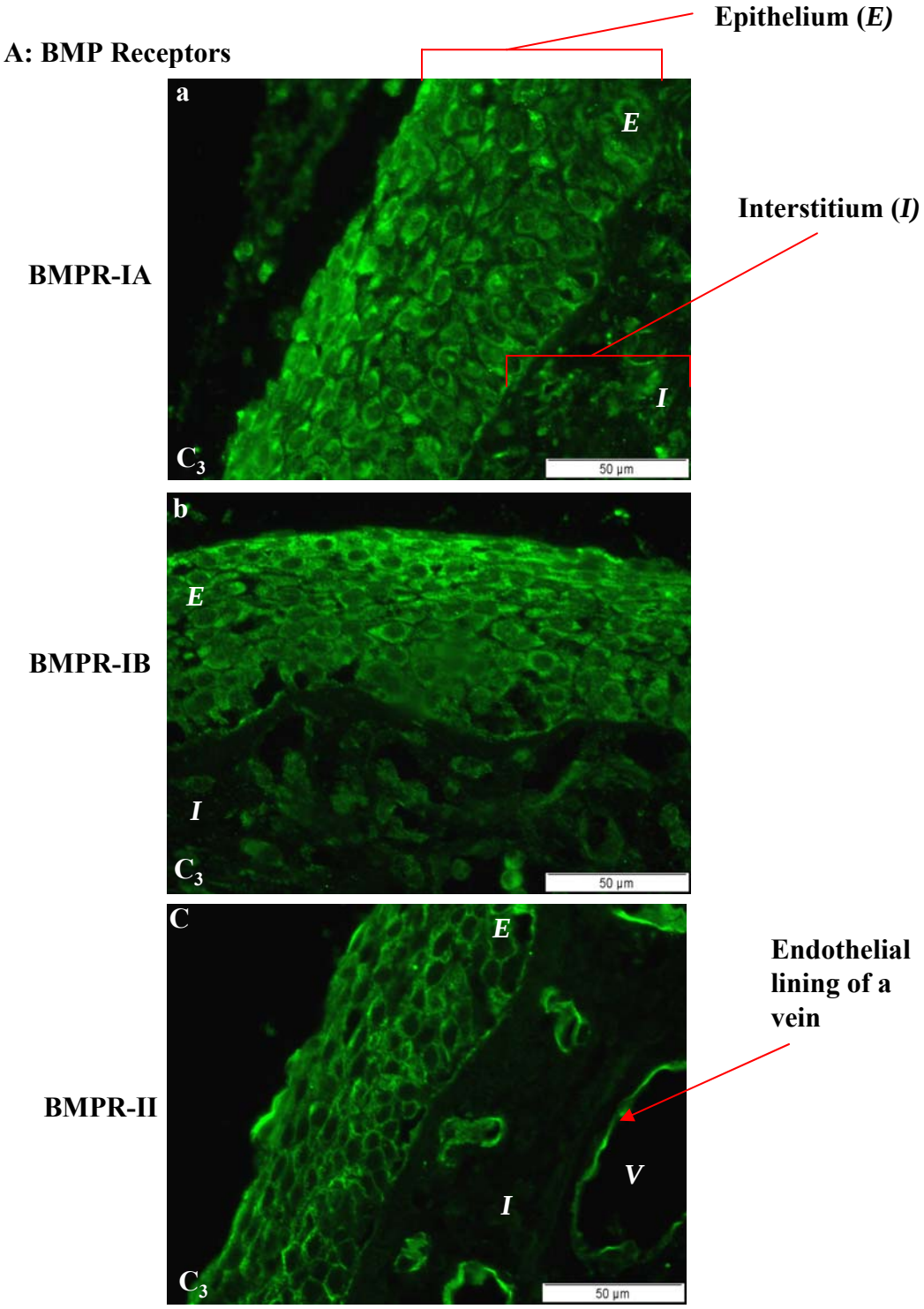

Figure 6.1 A: Localisation of BMP pathway receptors in the nasal epithelium of a normal individual

Photomicrographs represents nasal tissue immunolocalised for BMP pathway receptors from one normal individual (C_3) (a-c). BMP receptors BMPR-IA, BMPR-IB and BMPR-II were localised to the cytoplasm and/or surface membrane of airway epithelial cells (a-c). E = epithelial layer, I= interstitial tissue containing V = veins. Scale bar represents 50 µm.

B: Intracellular signalling molecules, Smads

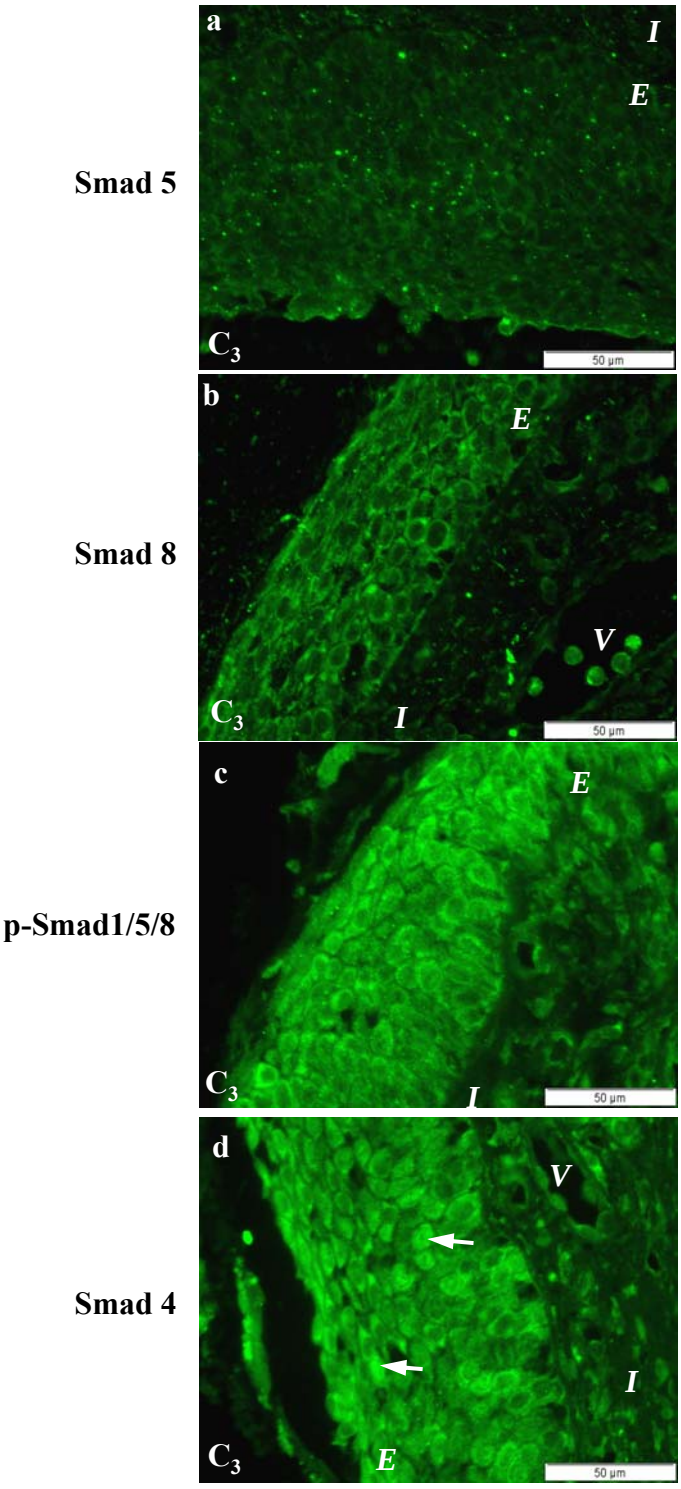

Figure 6.1 B: Localisation of Smad proteins in the nasal epithelium of a normal individual

Photomicrographs represents nasal tissue immunolocalised for the intracellular signalling molecules, Smads, from one normal individual (a-d). Smad proteins Smad5, Smad8, phosphorylated Smad1/5/8 (p-Smad1/5/8) and Smad4 were localised to the cytoplasm of airway epithelial cells (a-d). Smad4 nuclear localisation was evident denoted by arrows (d). E = epithelial layer, I= interstitial tissue containing V = veins. Scale bar represents 50 µm.

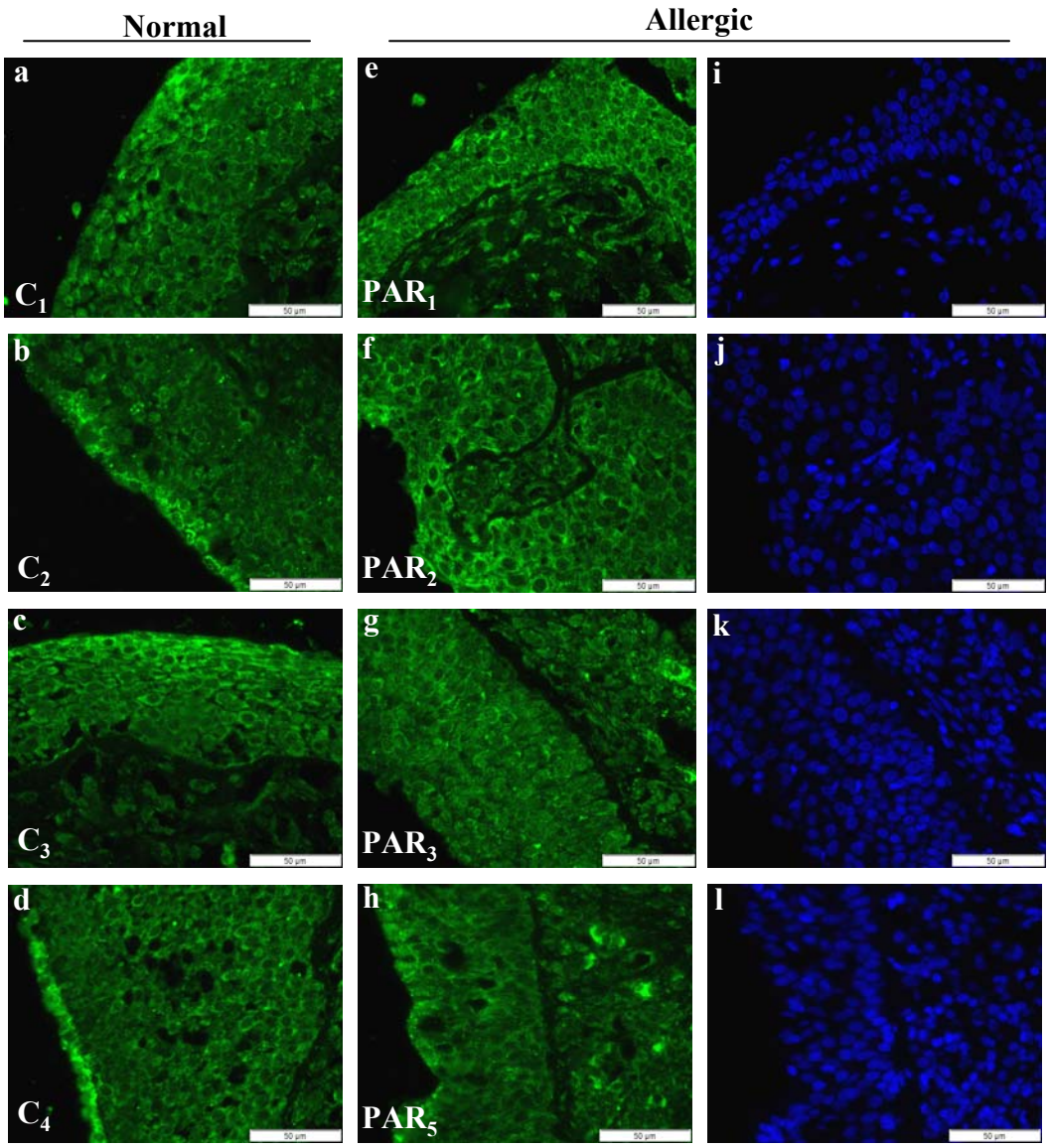

Figure 6.2: BMPR-IB localisation in normal and allergic individuals

Photomicrographs represent nasal tissue from four out of four normal individuals (a-d, C_1-C_4) and four out of six allergic individuals (e-h, PAR_1-PAR_3, PAR_5) immunolocalised for BMPR-IB. BMPR-IB was visible in the cytoplasm of the airway epithelial cells in normal individuals (a-d). Expression levels were similar in airway epithelial cells of allergic sections (e-h). Corresponding dapi image for allergic sections shown right (i-l). Scale bar represents 50 µm. Antibody control (Ab Cntrl) omitted primary antibody shown in Figure 6.3 (e).

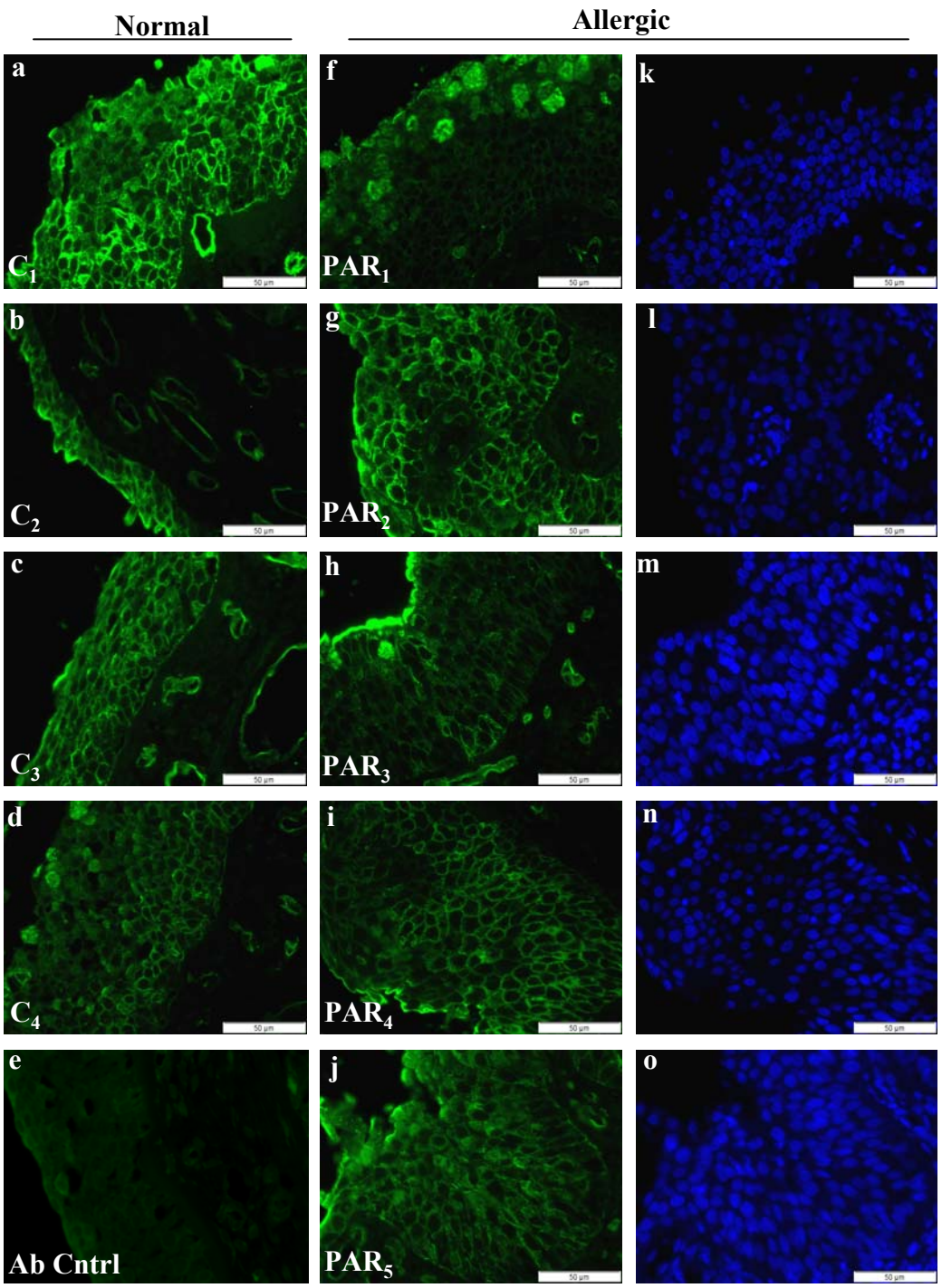

Figure 6.3: BMPR-II localisation in normal and allergic individuals

Photomicrographs represent nasal tissue from four out of four normal individuals (a-d, C_1-C_4) and five out of six allergic individuals (f-j, PAR_1-PAR_5) immunolocalised for BMPR-II. BMPR-II was expressed on the surface of epithelial cells in normal individuals (a-d). Expression levels were similar on epithelial cells of allergic sections (f-j). Corresponding dapi image for allergic sections shown right (k-o). Scale bar represents 50 µm. Antibody control (Ab Cntrl) omitted primary antibody (e).

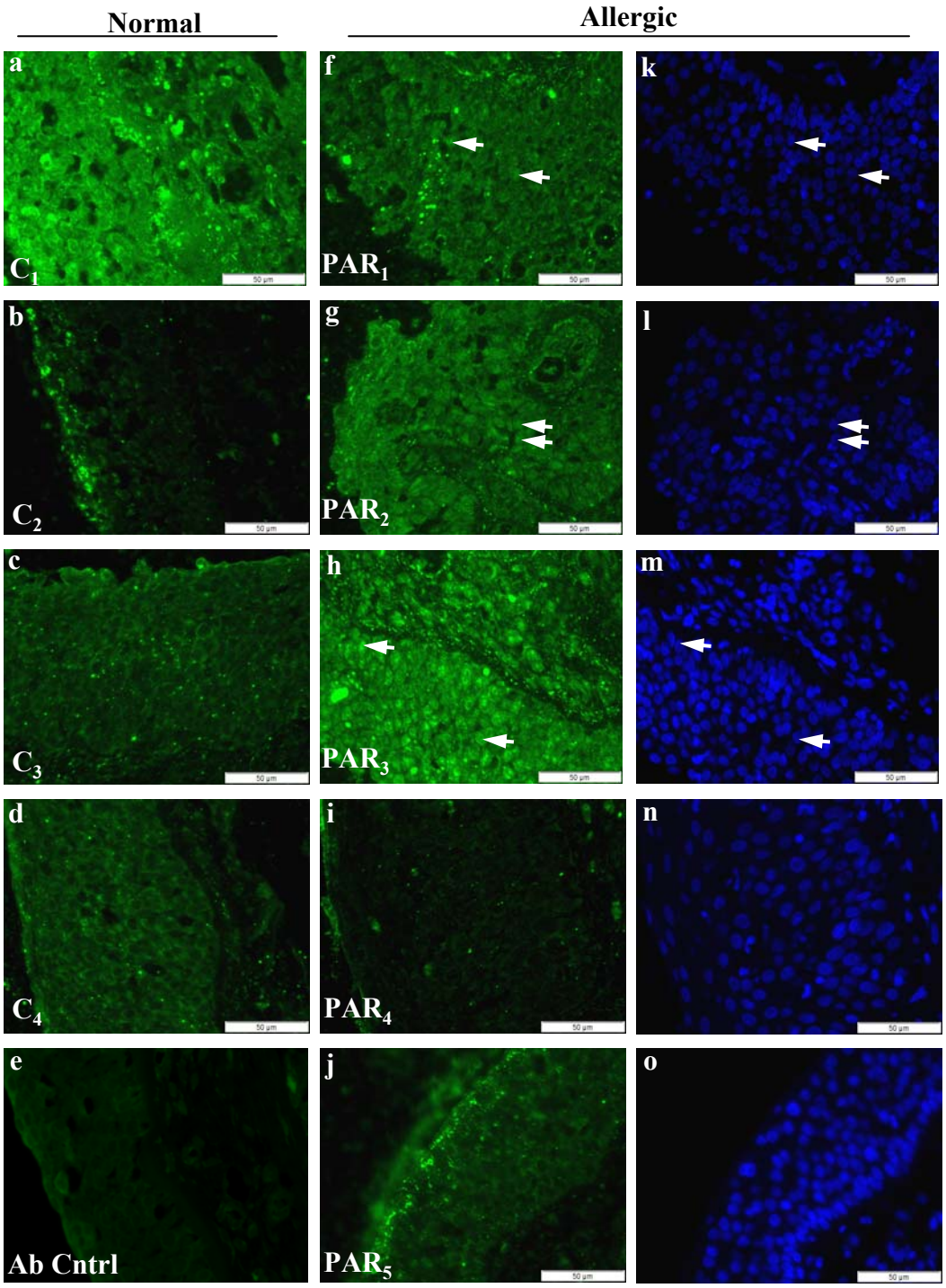

Figure 6.4: Smad5 localisation in normal and allergic individuals

Photomicrographs represent nasal tissue from four out of four normal individuals (a-d, C_1-C_4) and five out of six allergic individuals (f-j, PAR_1-PAR_5) immunolocalised for Smad5. Smad5 was expressed in the cytoplasm of epithelial cells in normal individuals (a-d). No trend to suggest increased levels was detected in allergic sections (f-j). However, nuclear translocation was observed in some sections denoted by arrows (f-h). Corresponding dapi image for allergic sections shown right (k-o). Scale bar represents 50 µm. Antibody control (Ab Cntrl) omitted primary antibody (e).

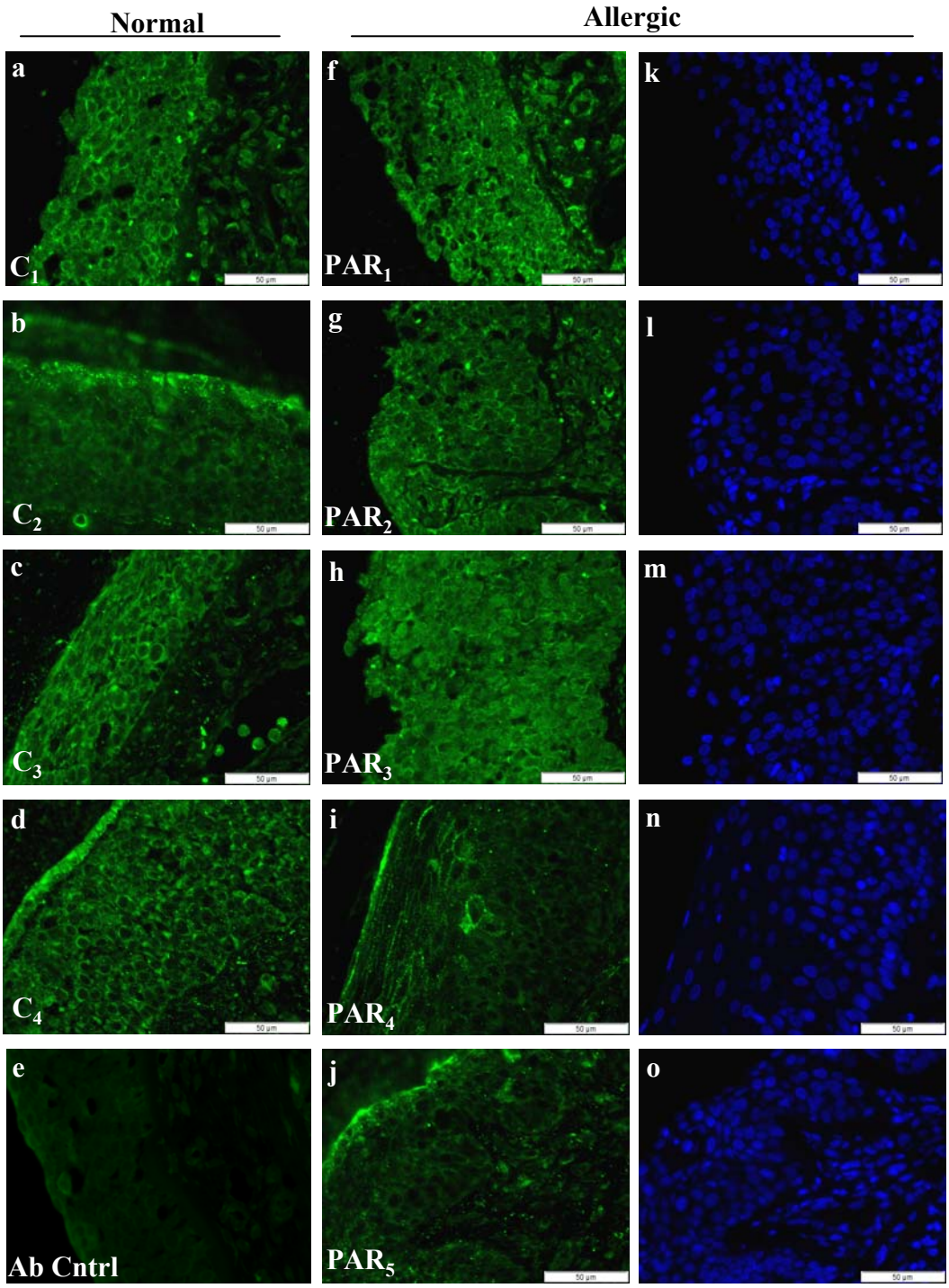

Figure 6.5: Smad8 localisation in normal and allergic individuals

Photomicrographs represent nasal tissue from four out of four normal individuals (a-d, C_1-C_4) and five out of six allergic individuals (f-j, PAR_1-PAR_5) immunolocalised for Smad8. Smad8 was expressed in the cytoplasm of epithelial cells in normal individuals (a-d). No trend to suggest increased levels was observed in allergic sections (f-j). Corresponding dapi image for allergic sections shown right (k-o). Scale bar represents 50 µm. Antibody control (Ab Cntrl) omitted primary antibody (e).

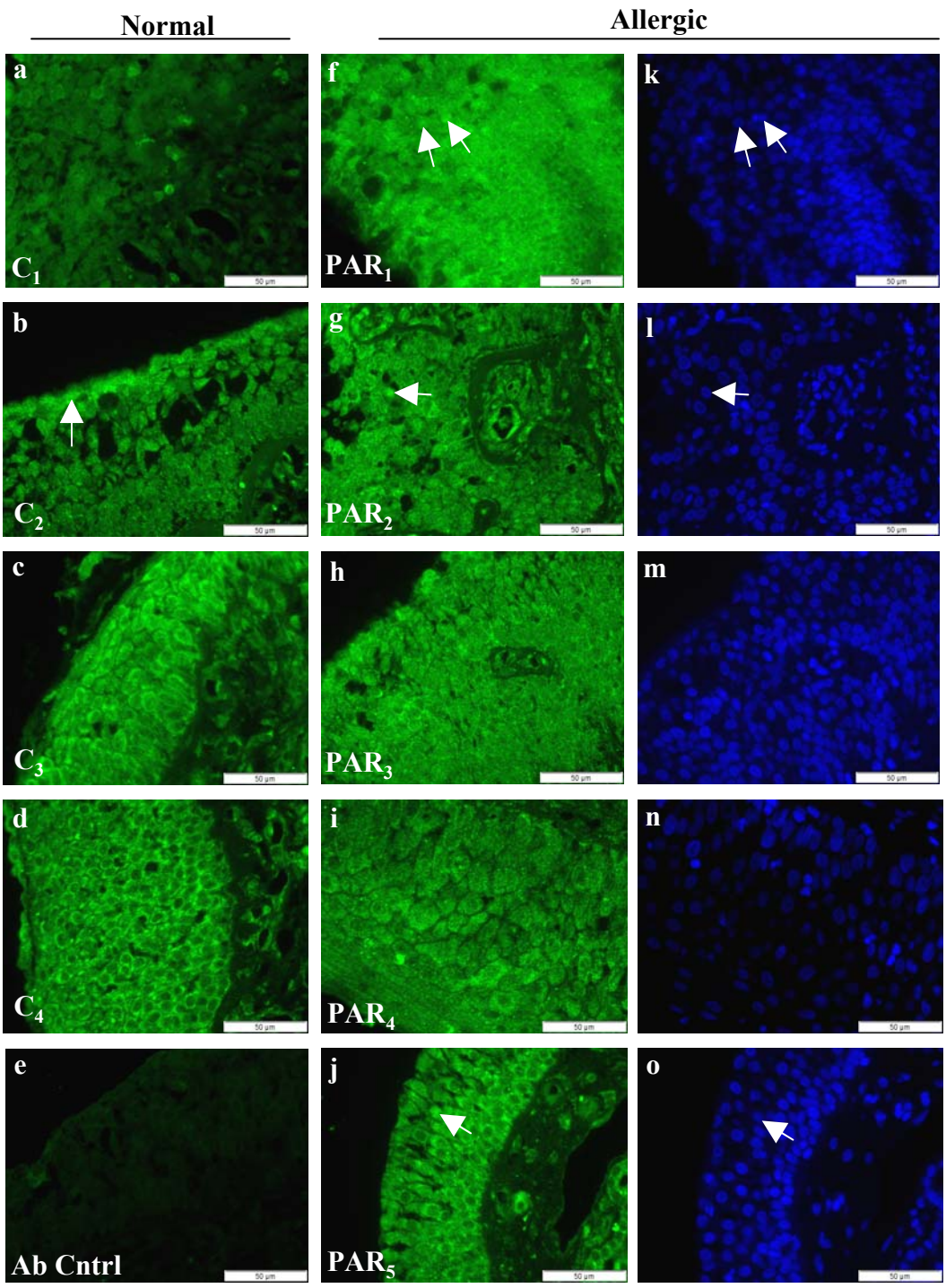

Figure 6.6: Phosphorylated Smad1/5/8 localisation in normal and allergic individuals

Photomicrographs represent nasal tissue from four out of four normal individuals (a-d, C_1-C_4) and five out of six allergic individuals (f-j, PAR_1-PAR_5) immunolocalised for the phosphorylated form of Smad1, 5 and 8. P-Smad1/5/8 was expressed in the cytoplasm of epithelial cells in normal individuals (a-d). Nuclear localisation was observed in one normal section (b). Similar levels of p-Smad1/5/8 was detected in allergic sections with nuclear translocation observed in some sections (f, g, j). Corresponding dapi image for allergic sections shown right (k-o). Arrows denote nuclear translocation. Scale bar represents 50 µm. Antibody control (Ab Cntrl) omitted primary antibody (e).

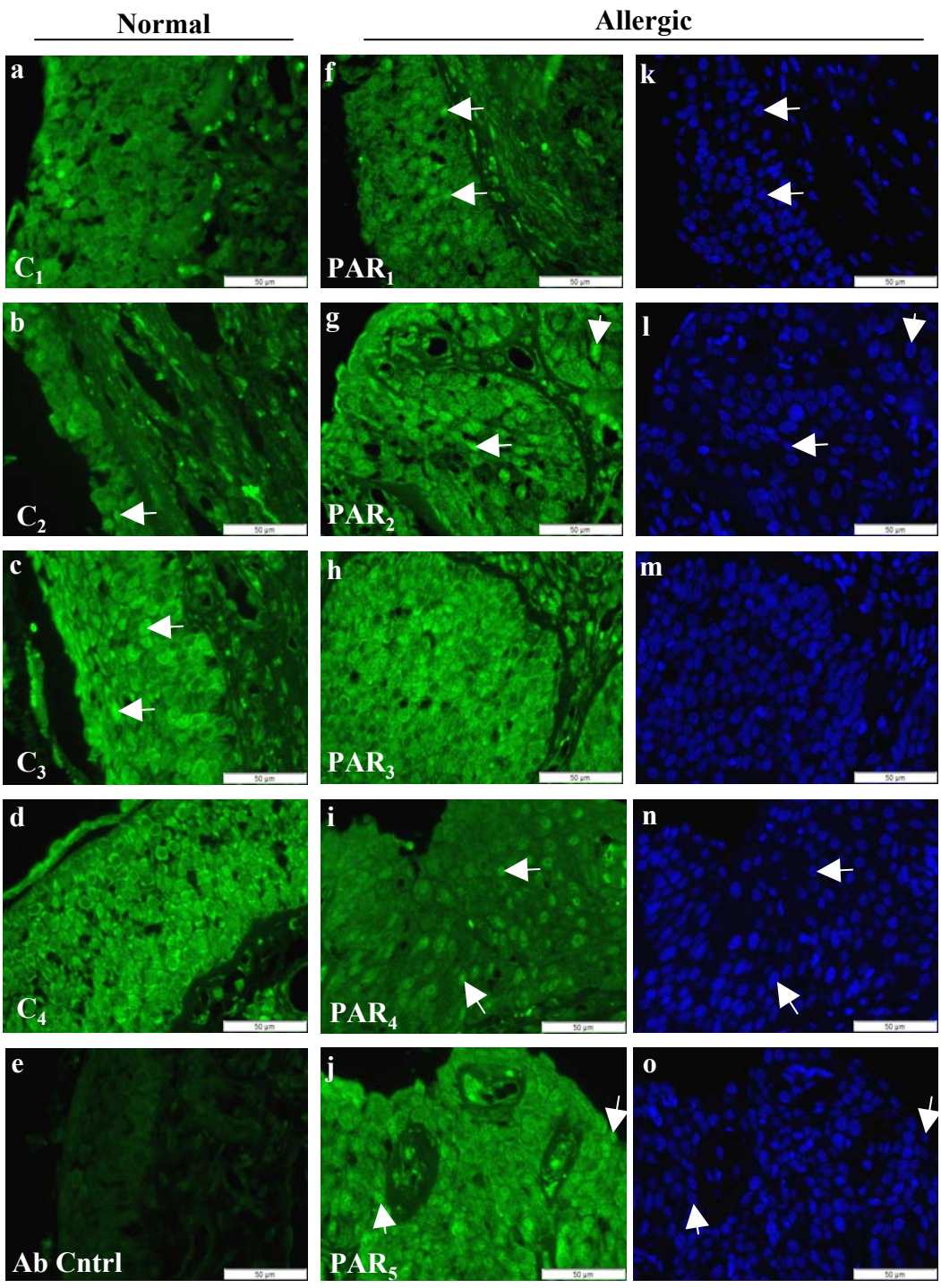

Figure 6.7: Smad4 localisation in normal and allergic individuals

Photomicrographs represent nasal tissue from four out of four normal individuals (a-d, C_1-C_4) and five out of six allergic individuals (f-j, PAR_1-PAR_5) immunolocalised for the co-Smad, Smad4. Smad4 was expressed in the cytoplasm of epithelial cells in normal individuals with occasional nuclear translocation evident (b, c). Similar levels of Smad4 was detected in the cytoplasm in allergic sections. However, an increase in Smad4 nuclear translocation was observed (f-j). Corresponding dapi image for allergic sections shown right (k-o). Arrows denote nuclear translocation. Scale bar represents 50 µm. Antibody control (Ab Cntrl) omitted primary antibody (e).

Figure 6.8 A

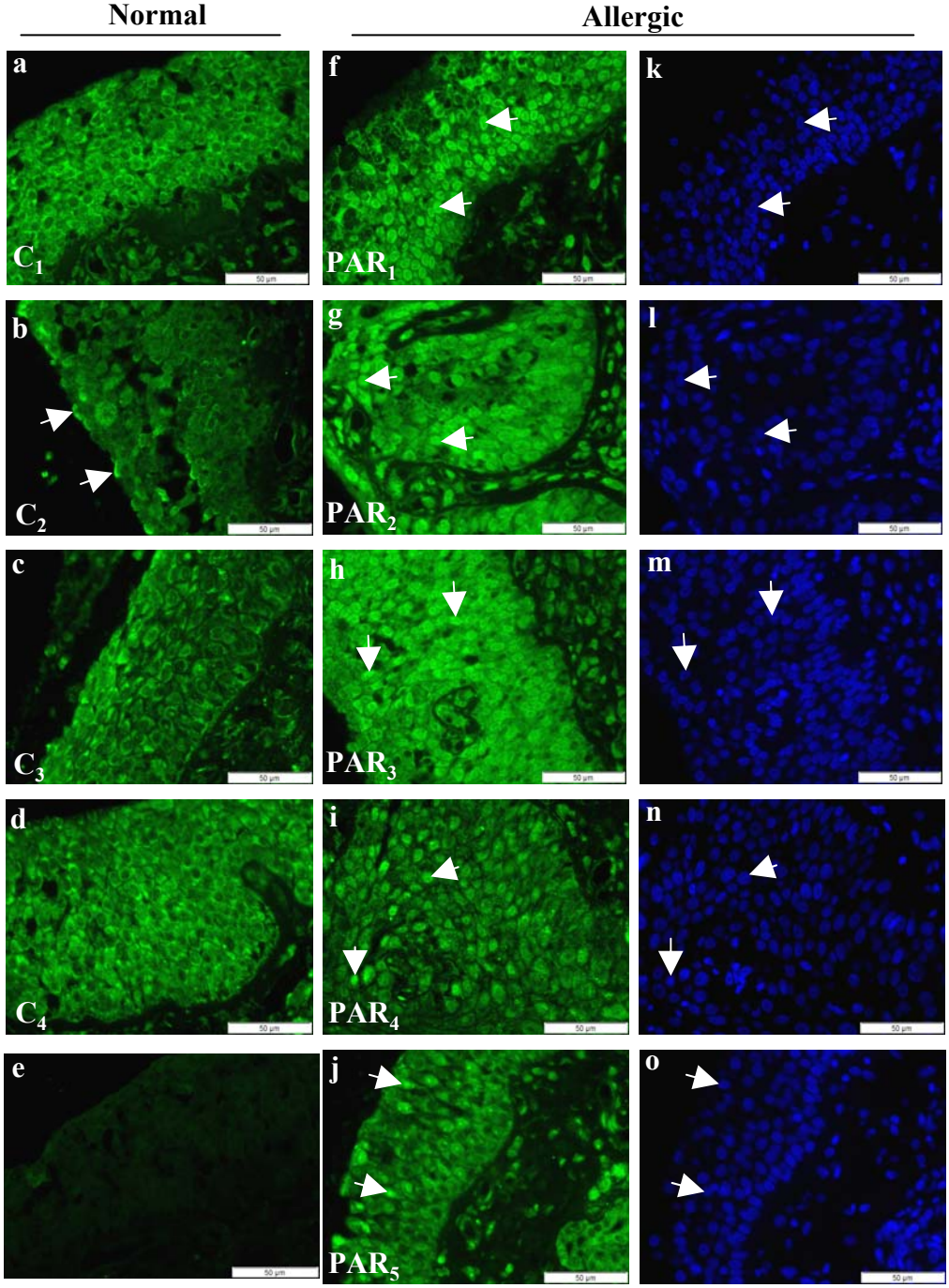
Normal
Allergic
a
f
k
C1
PAR1
b
g
l
C2
PAR2
c
h
m
C3
PAR3
d
i
n
C4
PAR4
e
j
o
PAR5

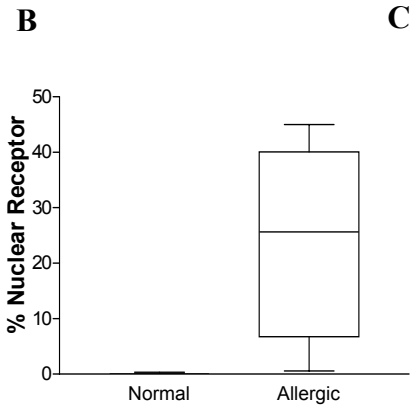
B
% Nuclear Receptor
50
40
30
20
10
0
Normal
Allergic

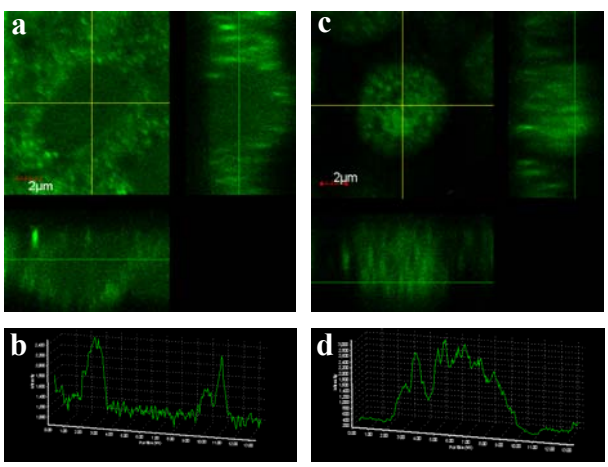
C
a
c
2µm
2µm
b
d

Figure 6.8: BMPR-IA localisation in normal and allergic individuals

(A) Photomicrographs represent nasal tissue from four out of four normal individuals (a-d, C_1-C_4) and five out of six allergic individuals (f-j, PAR_1-PAR_5) immunolocalised for BMPR-IA. BMPR-IA was expressed in the cytoplasm of epithelial cells in normal individuals (a-d). Membrane localisation was apparent on one normal individual (b). Nuclear translocation of the receptor was apparent in all allergic individuals shown (5/6) (f-j). Corresponding dapi image for allergic sections shown right (k-o). Arrows indicate membrane or nuclear localisation. Scale bar represents 50 μm. Antibody control (Ab Cntrl) omitted primary antibody (e). (B) In normal nasal biopsies, less than 1% epithelial cells contained nuclear BMPR-IA (n=4). In AR biopsies, on average 25% epithelial cells demonstrated nuclear BMPR-IA (n=6). (C) Confocal microscopy and z-stacking analysis was carried out as indicated on normal (a) and AR (c) nasal tissue and revealed that BMPR-IA was distributed throughout the nucleus and was not just localised to the nuclear membrane. BMPR-IA was localised to the cytoplasm of the airway epithelial cells from normal biopsies (b). Scale bar represents 2 μm.

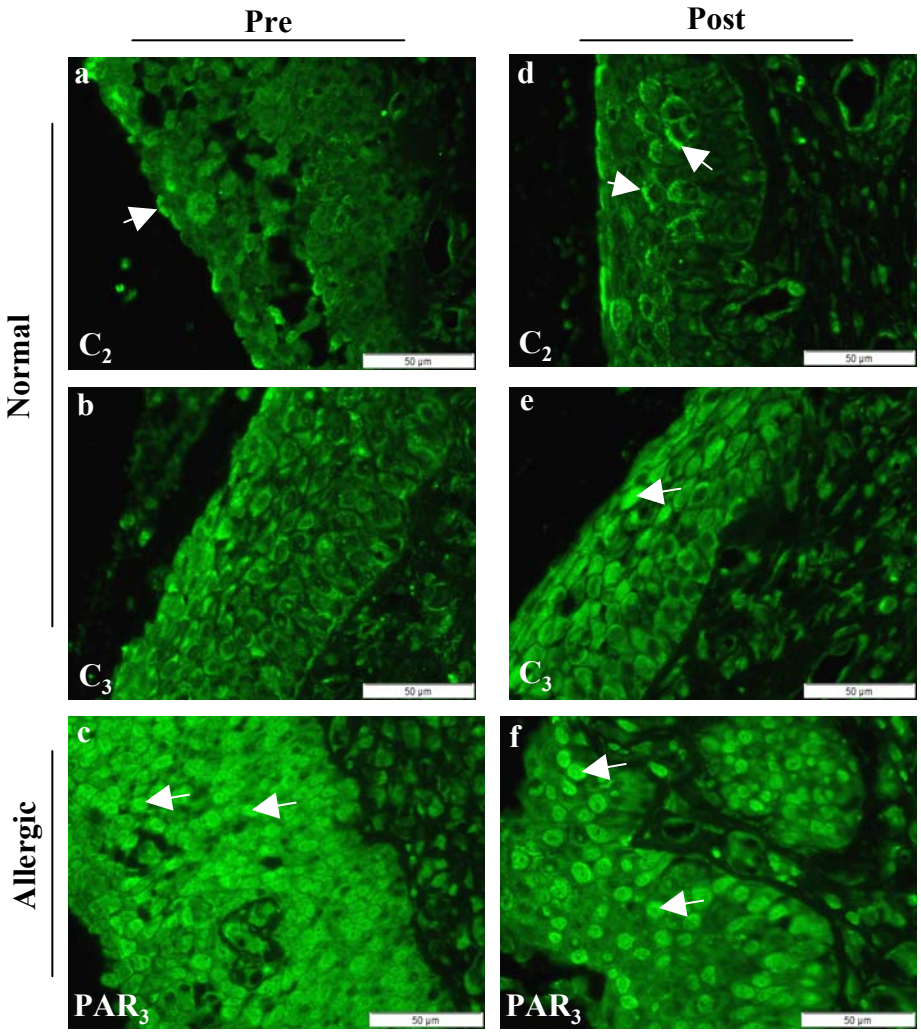

Figure 6.9: BMPR-IA following allergen challenge

Photomicrographs represent two normal (a, b) individuals and one allergic (c) individual pre (a-c) and 48 hr post allergen challenge (d-f). Tissues were immunolocalised for BMPR-IA. BMPR-IA was localised to the cytoplasm of normal individuals (a, b) with membrane BMPR-IA apparent denoted with arrows (a) as previously shown in Fig.6.8A. BMPR-IA nuclear localisation was observed in the allergic tissue section shown (c) as presented in Fig.6.8A. Following allergen challenge, BMPR-IA was largely unaltered in the two normal individuals (d, e). However, a possible increase in membrane localisation was apparent (d) as well as nuclear BMPR-IA apparent in one normal individual (e). Increased nuclear BMPR-IA was apparent in the allergic individual following allergen challenge (f). Arrows denote membrane or nuclear localisation. Scale bars represent 50 µm.

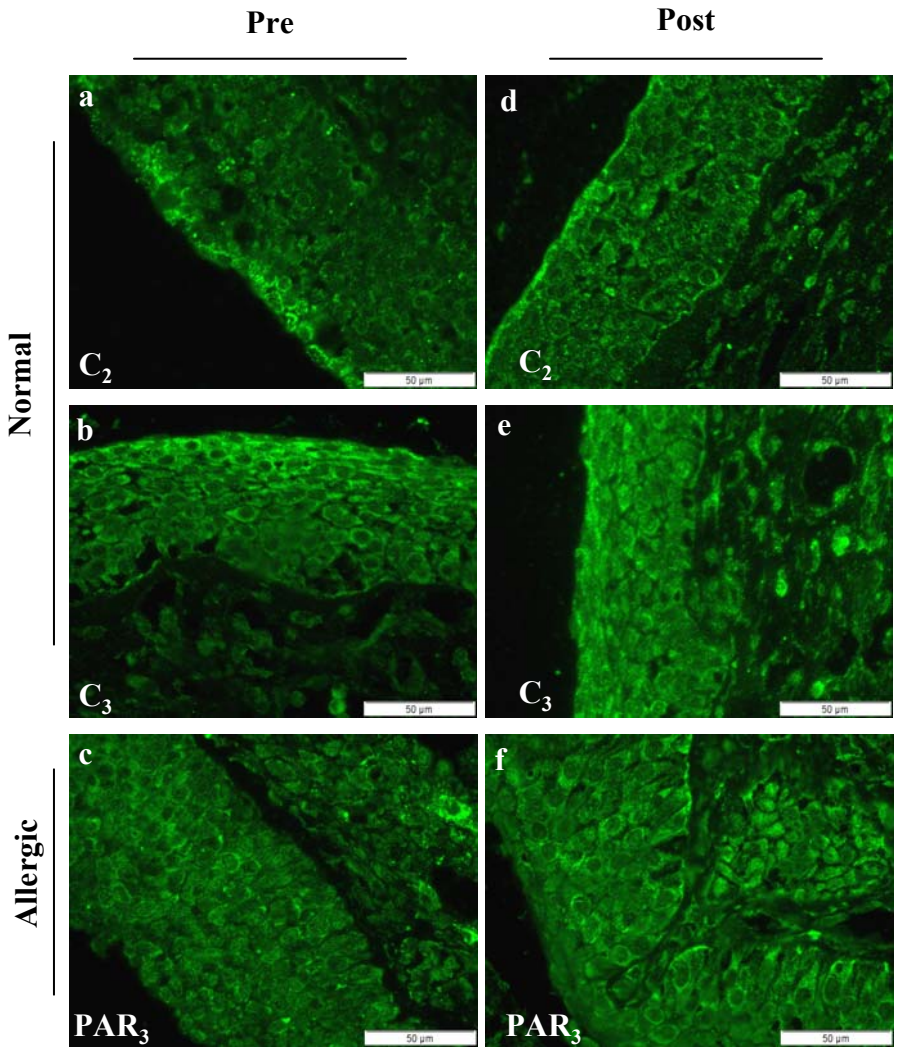

Figure 6.10: BMPR-IB following allergen challenge

Photomicrographs represent two normal (a, b) individuals and one allergic (c) individual pre and 48 hr post allergen challenge (d-f). Tissues were immunolocalised for BMPR-IB. BMPR-IB was localised to the cytoplasm of the two normal individuals and one allergic individual (a-c) as previously shown Fig.6.2. BMPR-IB localisation did not appear altered following allergen challenge (d-f). Scale bars represent 50 µm.

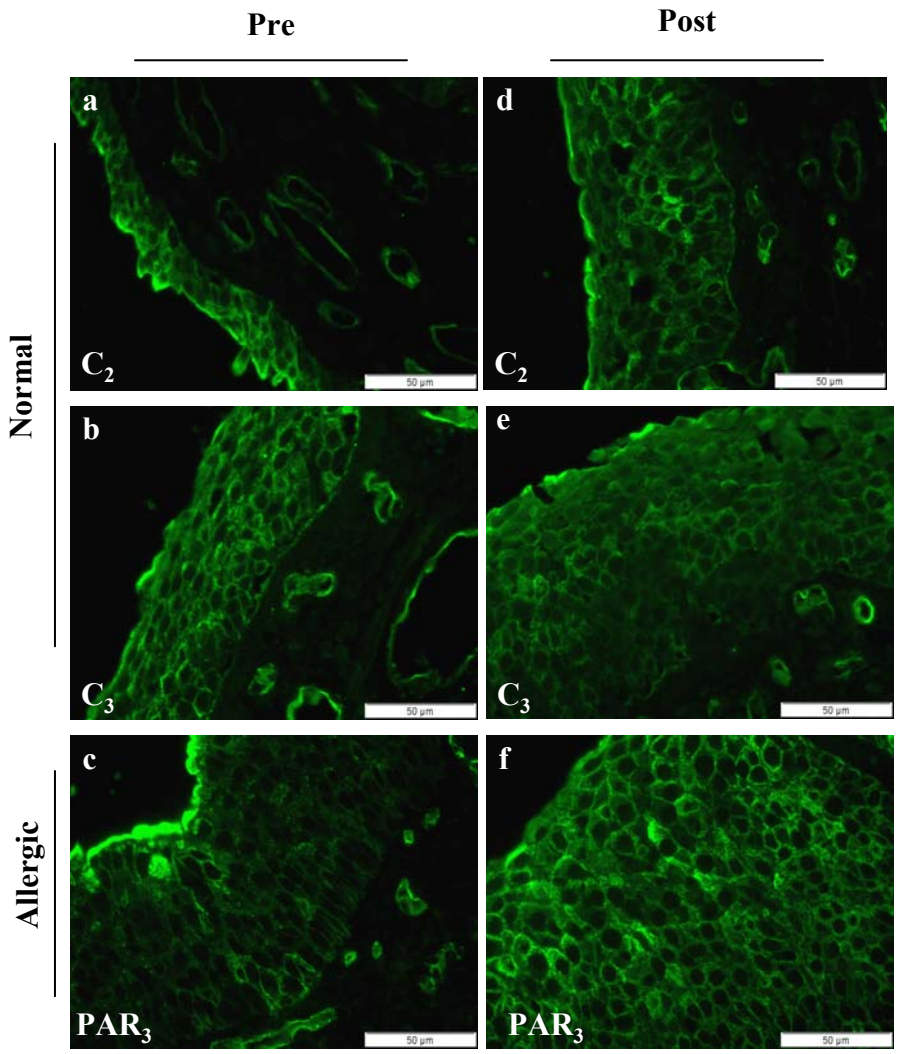

Figure 6.11: BMPR-II following allergen challenge

Photomicrographs represent two normal (a, b) individuals and one allergic (c) individual pre and 48 hr post allergen challenge (d-f). Tissues were immunolocalised for BMPR-II. BMPR-II was localised to the surface membrane of the two normal individuals and one allergic individual (a-c) as previously shown in Fig.6.3. BMPR-II localisation did not appear altered following allergen challenge (d-f). Scale bars represent 50 µm.

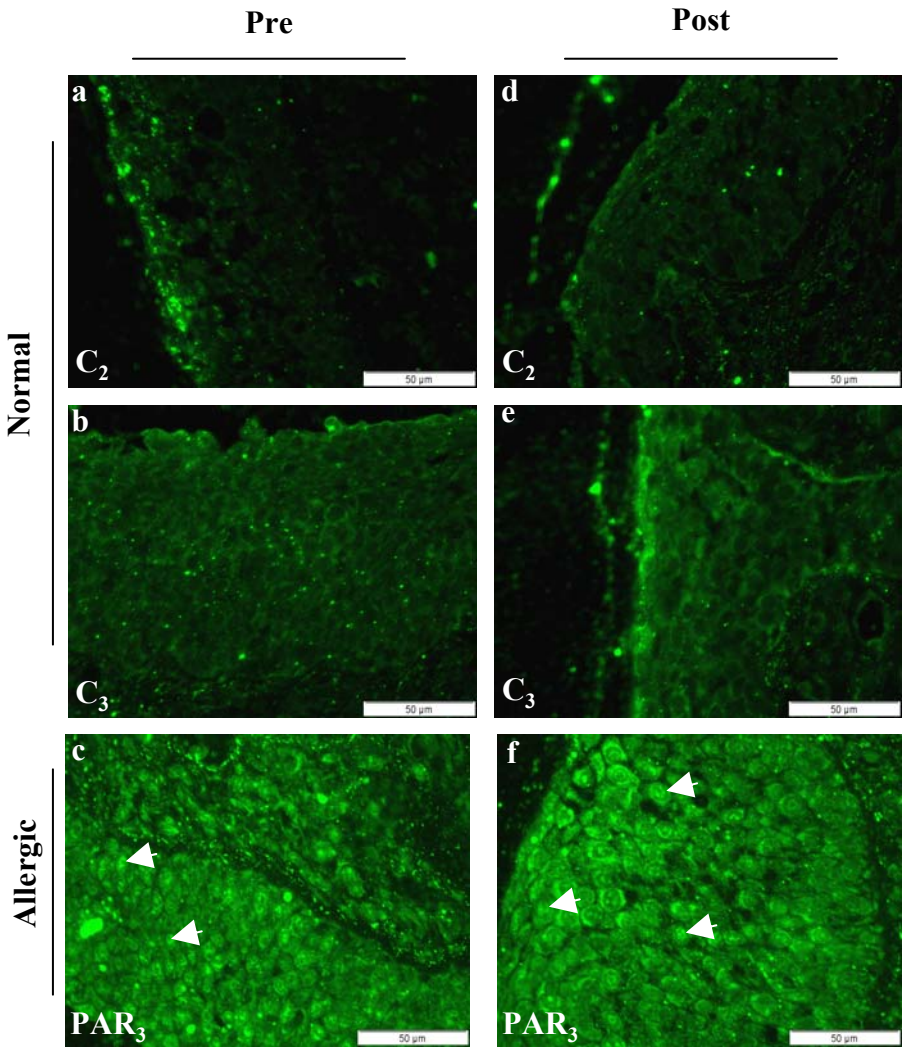

Figure 6.12: Smad5 following allergen challenge

Photomicrographs represent two normal (a, b) individuals and one allergic (c) individual pre and 48 hr post allergen challenge (d-f). Tissues were immunolocalised for Smad5. Smad5 was localised to the cytoplasm at low levels of normal individuals (a, b) as previously shown in Fig.6.4. Smad5 nuclear localisation was observed in the allergic individual (c) as previously shown in Fig.6.4. Following allergen challenge, Smad5 was unaltered in the two normal individuals (d, e). Similar levels of cytoplasmic and nuclear Smad5 was apparent in the allergic individual following allergen challenge (f). Arrows denote nuclear localisation. Scale bars represent 50 µm.

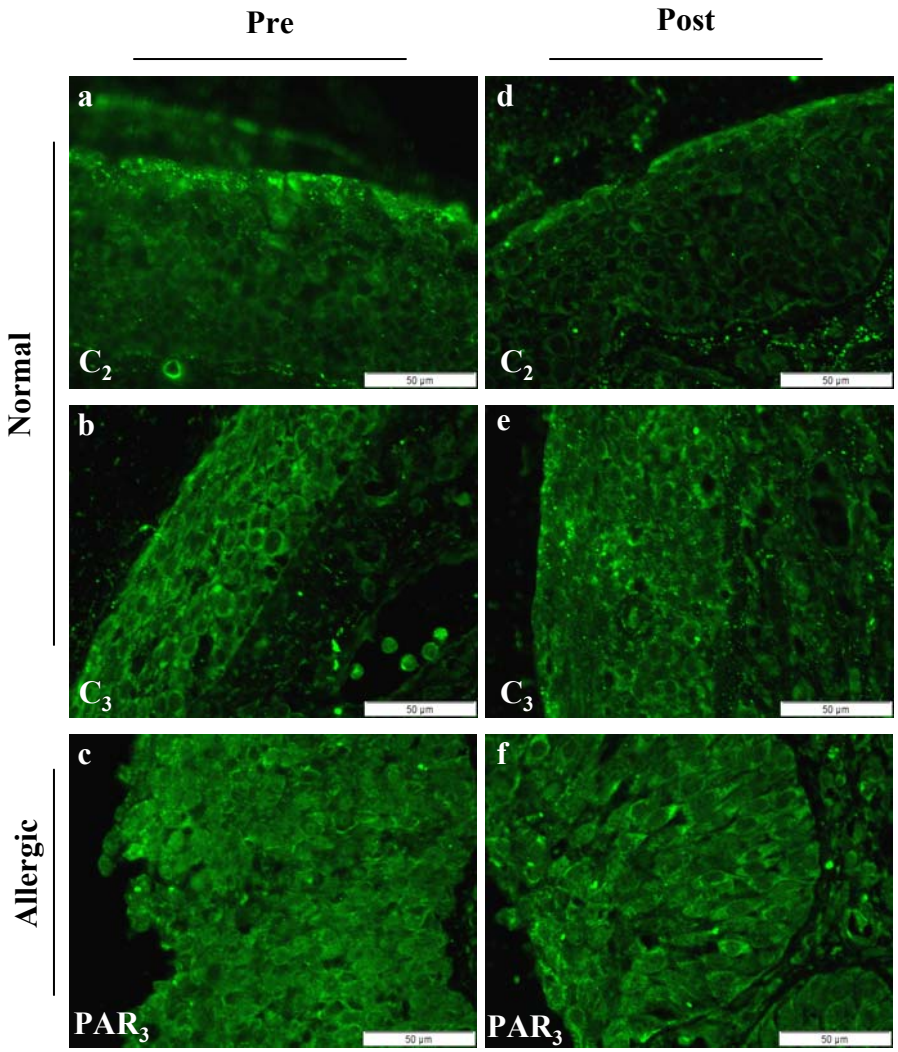

Figure 6.13: Smad8 following allergen challenge

Photomicrographs represent two normal (a, b) individuals and one allergic (c) individual pre and 48 hr post allergen challenge (d-f). Tissues were immunolocalised for Smad8. Smad8 was localised to the cytoplasm of the two normal individuals and one allergic individual (a-c) as previously shown in Fig.6.5. Smad8 localisation did not appear altered following allergen challenge (d-f). Scale bars represent 50 µm.

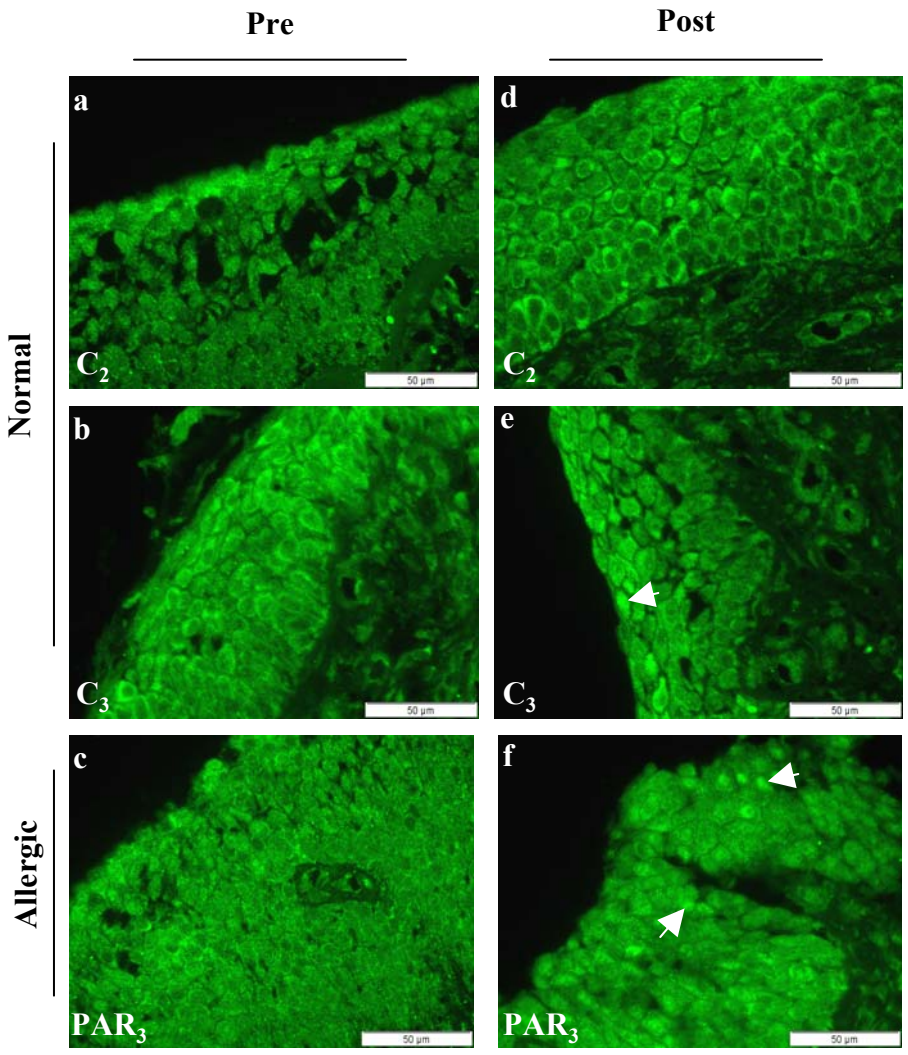

Figure 6.14: Phosphorylated Smad1/5/8 following allergen challenge

Photomicrographs represent two normal (a, b) individuals and one allergic (c) individual pre and 48 hr post allergen challenge (d-f). Tissues were immunolocalised for p-Smad1/5/8. P-Smad1/5/8 was localised to the cytoplasm of the two normal individuals and one allergic individual (a-c) as previously shown in Fig.6.6. Following allergen challenge, p-Smad1/5/8 was largely unaltered in the two normal individuals (d, e) with some nuclear localisation of p-Smad1/5/8 detected (e). Increased nuclear p-Smad1/5/8 was observed in the allergic individual following allergen challenge (f). Arrows denote nuclear localisation. Scale bars represent 50 µm.

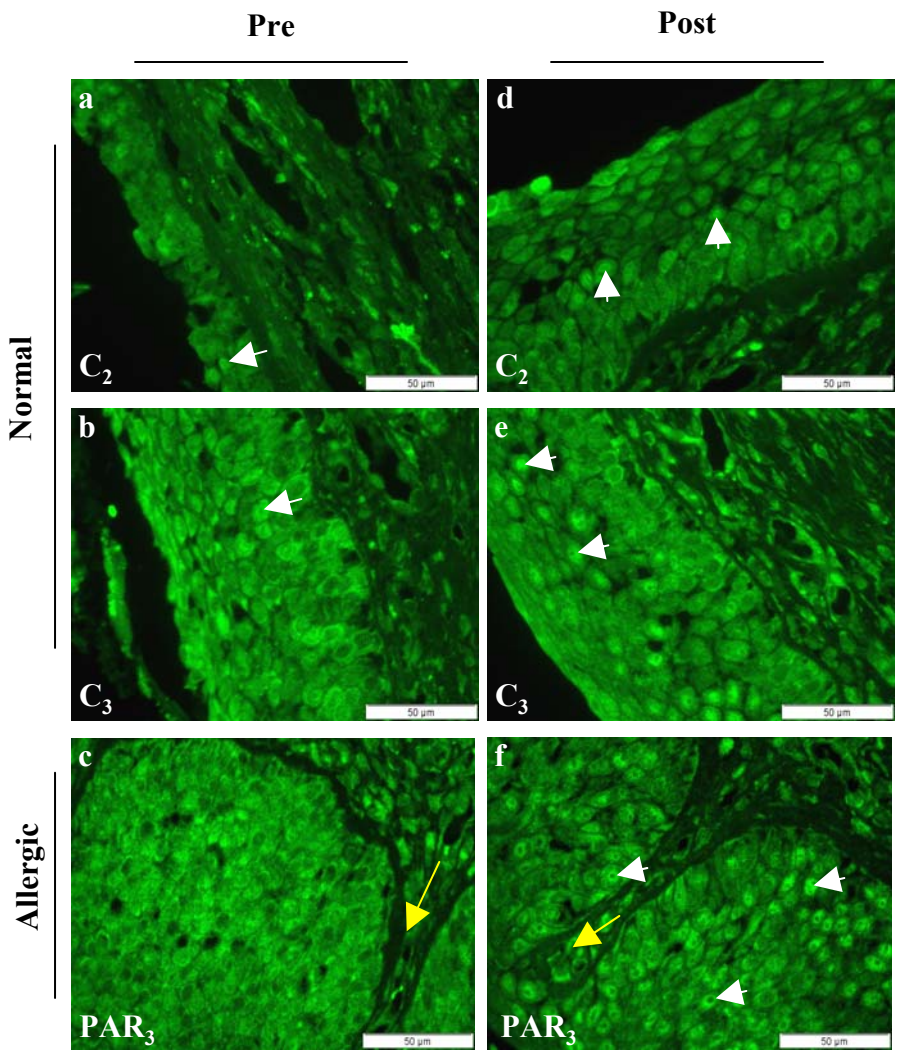

Figure 6.15: Smad4 following allergen challenge

Photomicrographs represent two normal (a, b) individuals and one allergic (c) individual pre and 48 hr post allergen challenge (d-f). Tissues were immunolocalised for Smad4. Smad4 was localised to the cytoplasm of the two normal individuals and one allergic individual (a-c) as previously shown in Fig.6.7. Nuclear Smad4 was seen in the two normal individuals (a, b). Following allergen challenge, nuclear Smad4 was increased in the two normal individuals (d, e) and in the allergic individual following allergen challenge (f). White arrows denote nuclear localisation. Yellow arrows denote interstitial tissue which appears to be protruding into the epithelium. Scale bars represent 50 µm.

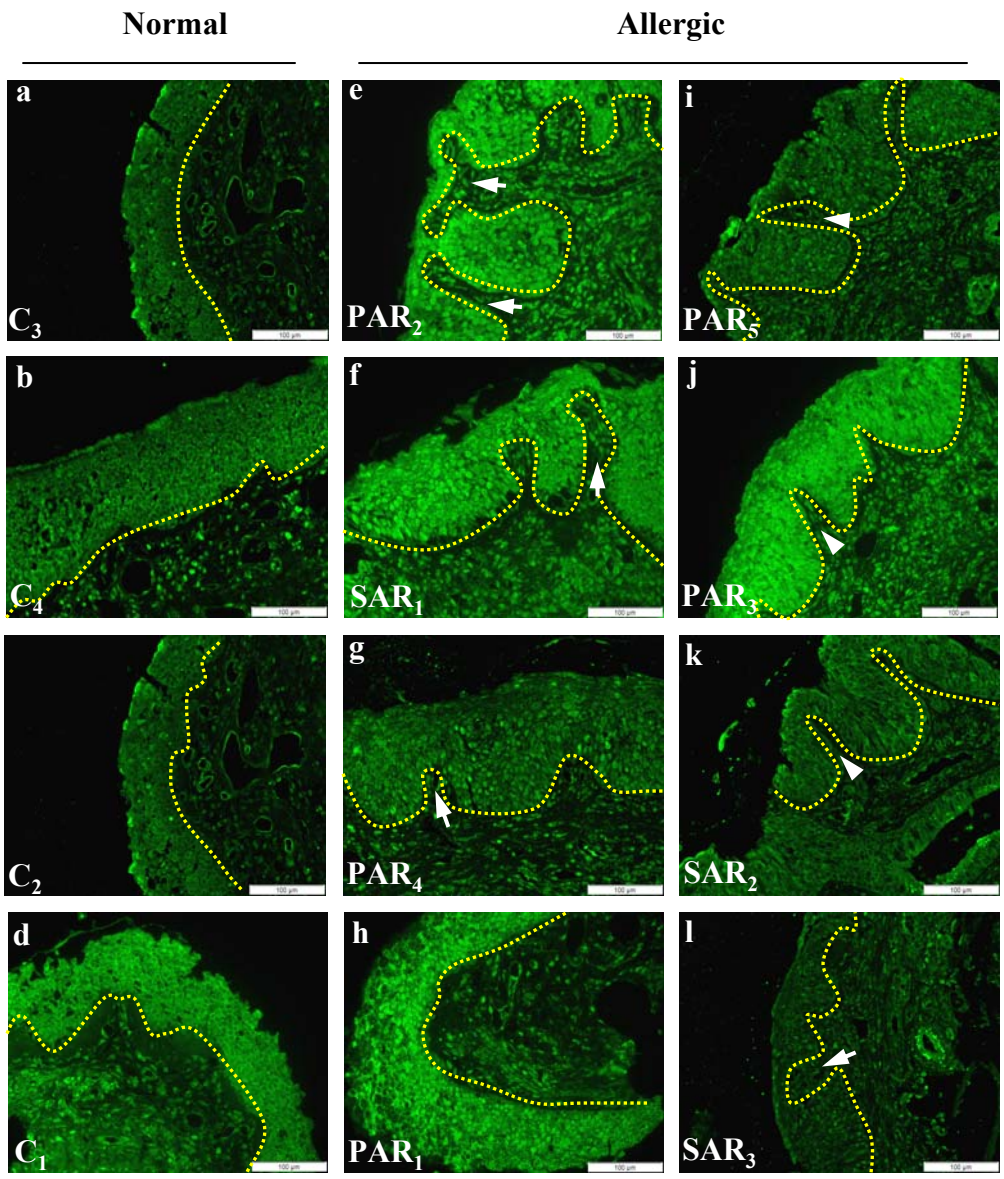

Figure 6.16: Evidence of tissue remodeling in individuals with seasonal and perennial allergic rhinitis

Photomicrographs represent images taken of four normal sections (a-d) and eight allergic sections (e-l) consisting of both perennial (PAR) (e, g, h-j) and seasonal (SAR) allergic individuals (f, k, l). In normal individuals the epithelium uniformly lined the interstitial tissue (a-d). In allergic individuals, the interstitial layer appeared altered with protrusion into the epithelium denoted by arrows (e-l). Tissues were immunolocalised for BMPR-IA. Yellow dashed line separates epithelium from the interstitial tissue. Scale bars represent 100 µm.

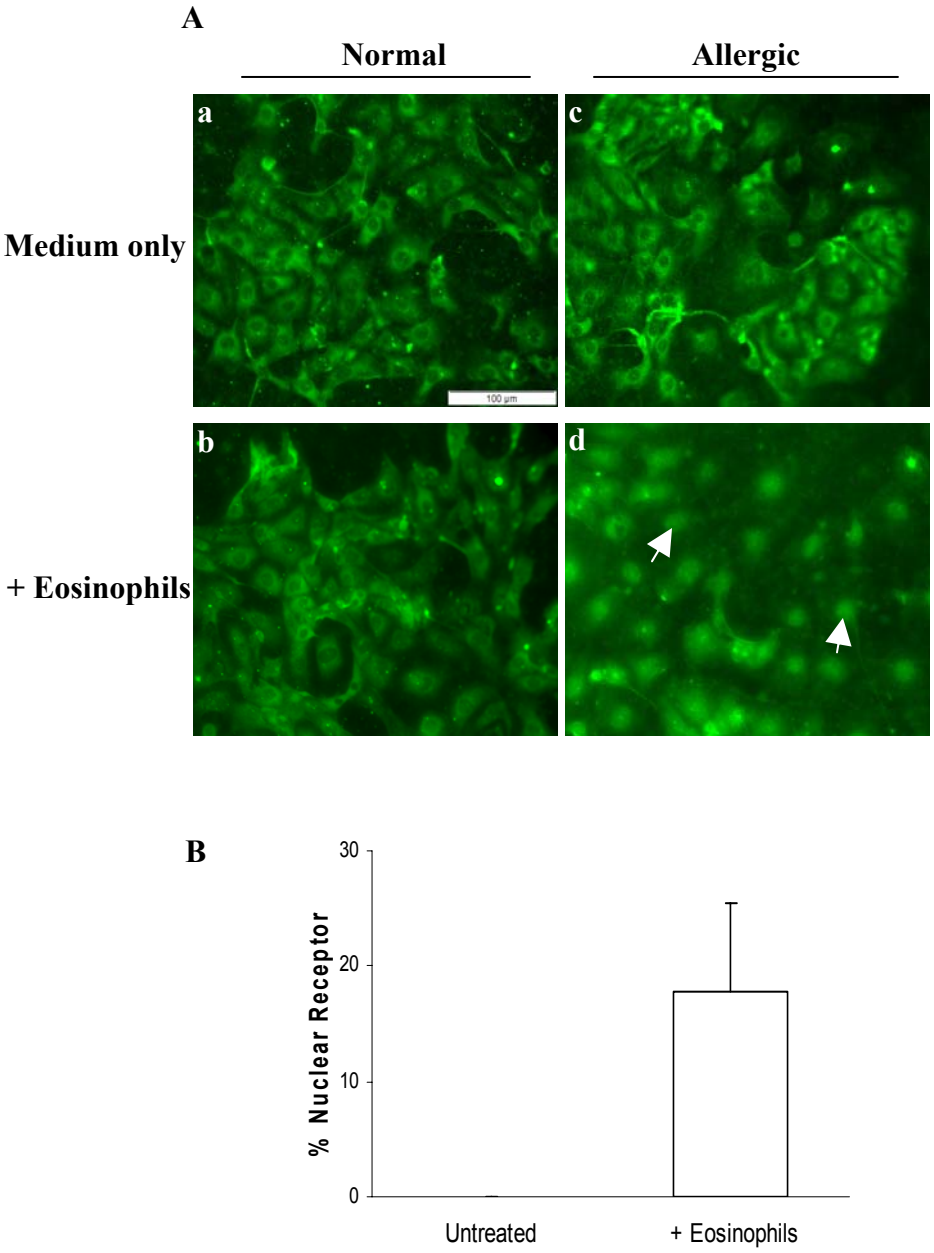

Figure 6.17: Altered BMPR-IA expression in MAECs co-cultured with eosinophils

(A) MAECs were co-cultured with eosinophils from both a non-allergic individual and an allergic individual. BMPR-IA localisation was assessed by immunofluorescence. BMPR-IA was localised to the cytoplasm in untreated MAECs (a, c). BMPR-IA cytoplasmic localisation remained in MAECs co-cultured with eosinophils from a normal individual (b). However, BMPR-IA nuclear localisation was evident in MAECs co-cultured with eosinophils from an allergic individual (d). Scale bar represents 100 µm. (B) The percentage of MAECs with nuclear localisation was quantified and found to be 17.8 % of cells counted. Approximately 500 cells were counted in three fields of view.

Figure 6.18 A

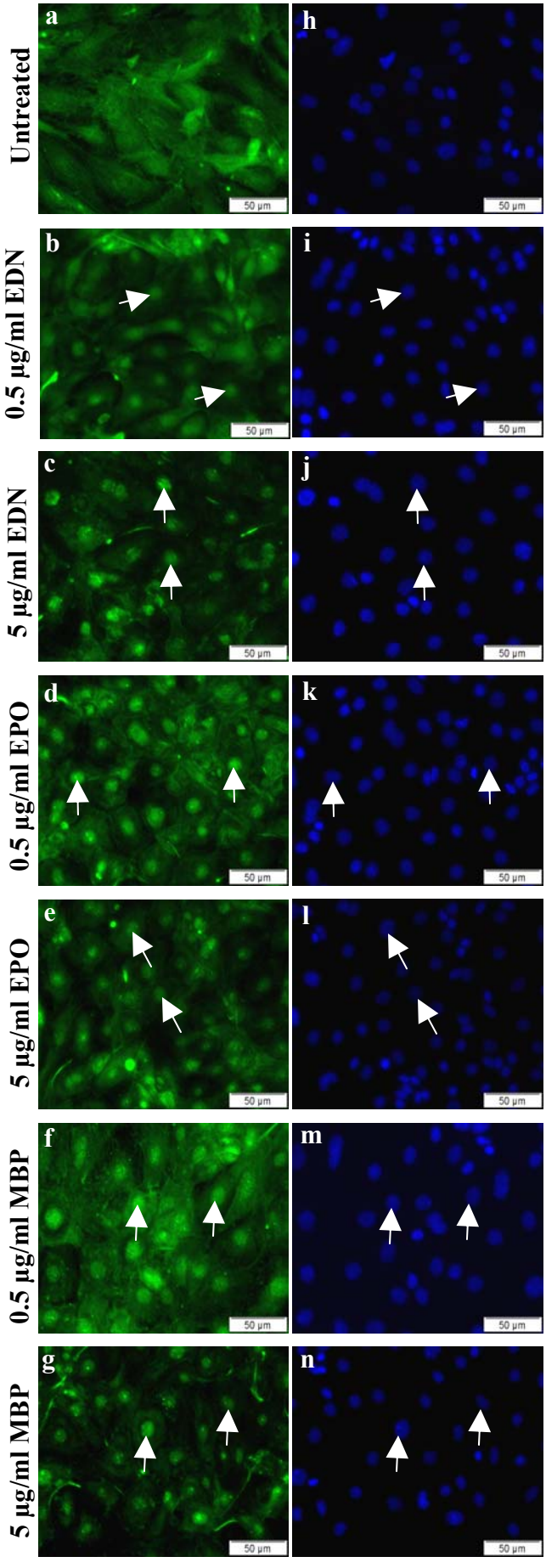

B

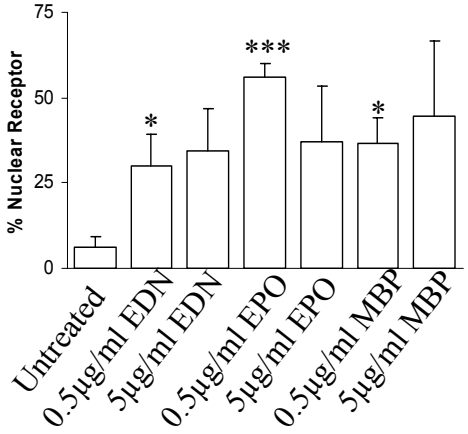

Figure 6.18: Nuclear BMPR-IA in MAECs exposed to eosinophil-derived proteins

(A) Primary normal murine airway epithelial cells (MAECs) were exposed to human eosinophil-derived proteins. Photomicrographs represent BMPR-IA localisation in MAECs cultured in control serum-free medium (Untreated) and MAECs exposed to 0.5 µg/ml or 5 µg/ml EDN for 17hr (+EDN), 0.5 µg/ml or 5 µg/ml EPO for 17hr (+EPO) or 0.5 µg/ml or 5 µg/ml MBP for 17hr (+MBP). Arrows indicate nuclear localisation of BMPR-IA. Scale bars represent 50 µm. (B) BMPR-IA nuclear localisation was quantified by counting positively immunolocalised nuclei. Graph illustrates mean expression of BMPR-IA in 30% and 35%, 56% and 37%, 36% and 45% of MAECs with exposure to 0.5 µg/ml and 5 µg/ml EDN, 0.5 µg/ml and 5 µg/ml EPO or 0.5 µg/ml and 5 µg/ml MBP, respectively. Results are representative of counts obtained from three separate experiments. Approximately 800 cells were counted in at least three fields of view. Significance where * = $P < 0.05$ or *** = $P < 0.001$ was obtained using the Student's *t*-test.

Figure 6.19 A

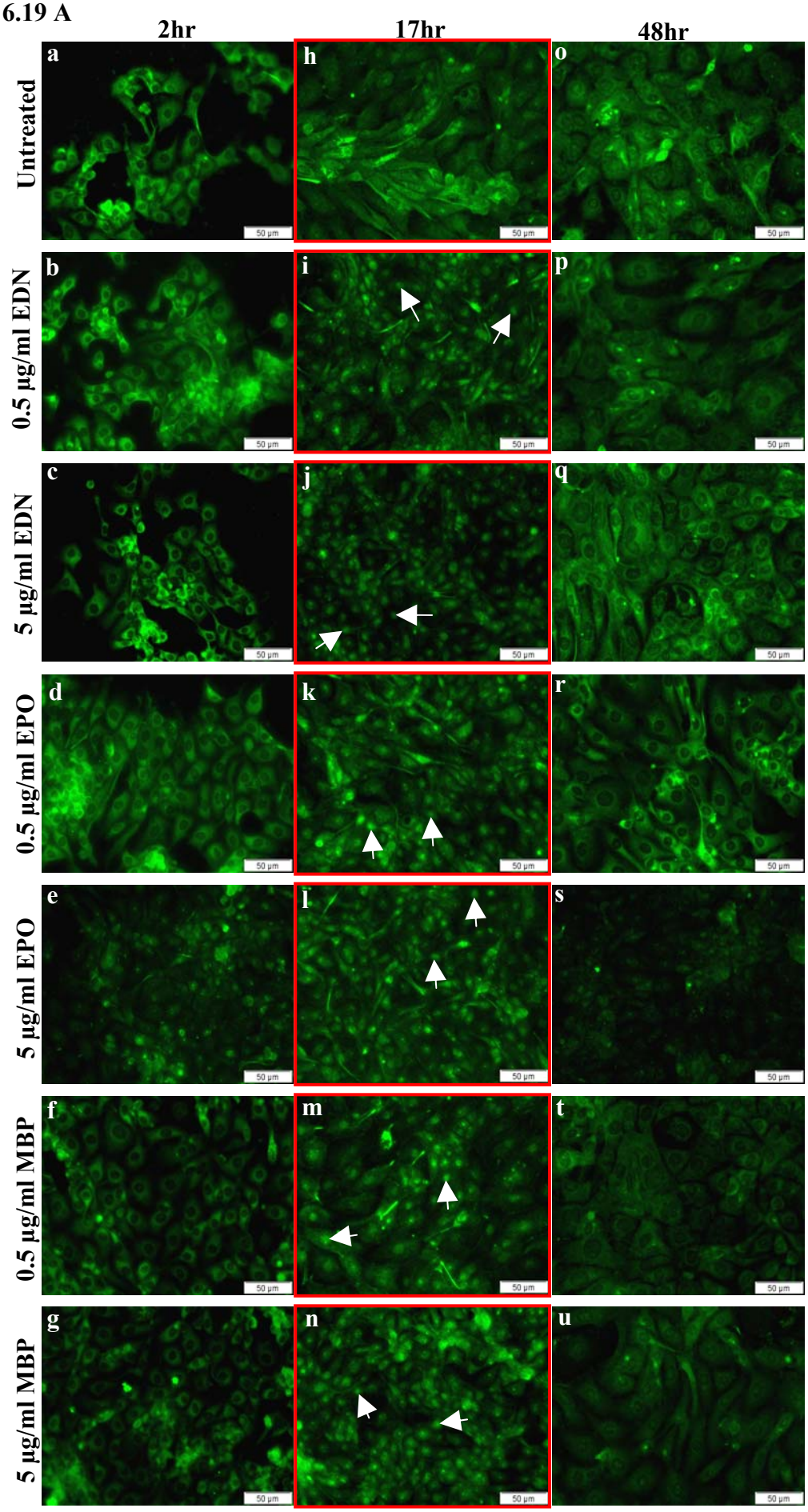
2hr
17hr
48hr
Untreated
0.5 µg/ml EDN
5 µg/ml EDN
0.5 µg/ml EPO
5 µg/ml EPO
0.5 µg/ml MBP
5 µg/ml MBP
a
h
o
b
i
p
c
j
q
d
k
r
e
l
s
f
m
t
g
n
u
50 µm

Figure 6.19 B

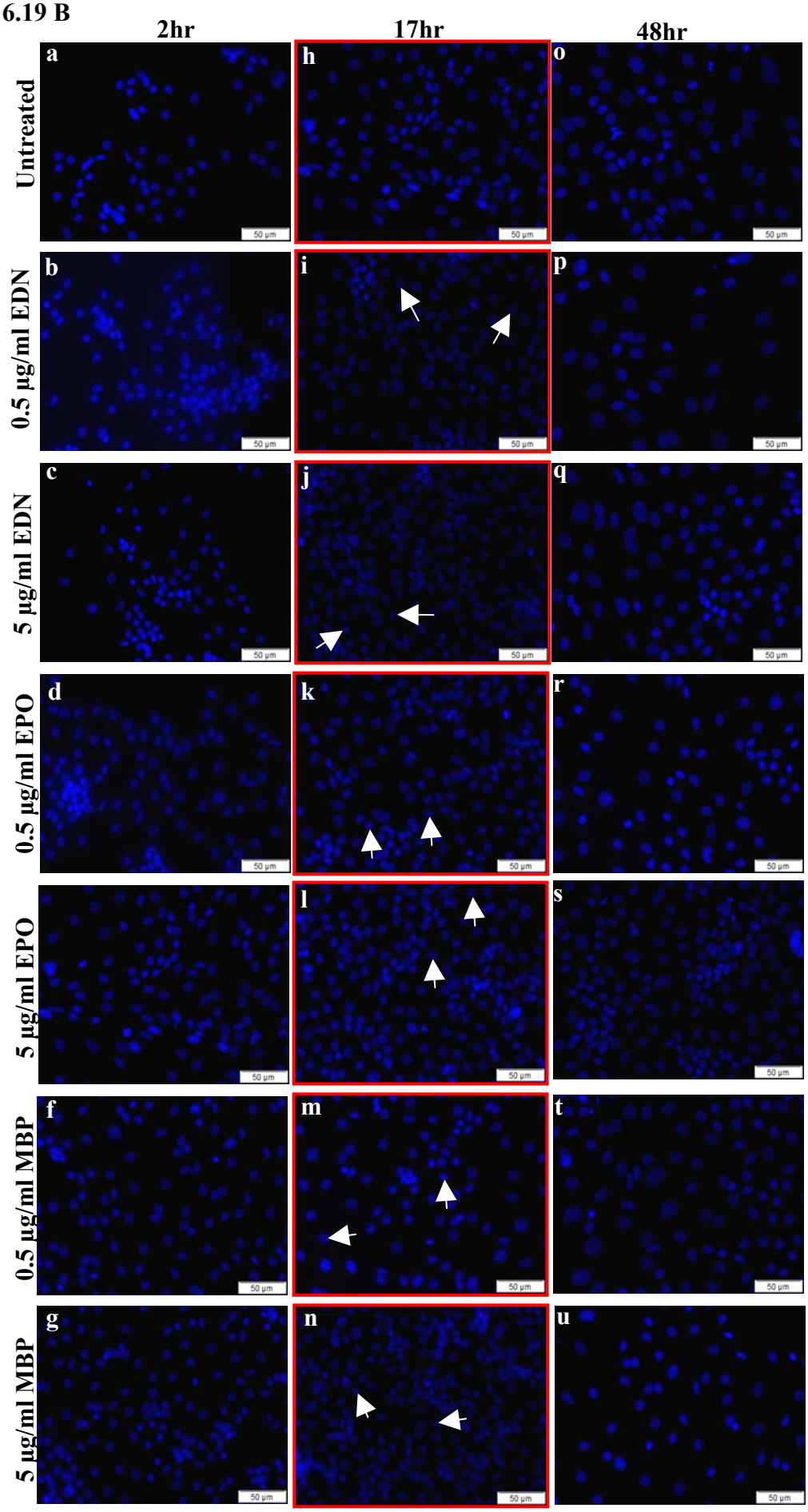
2hr
17hr
48hr
Untreated
0.5 µg/ml EDN
5 µg/ml EDN
0.5 µg/ml EPO
5 µg/ml EPO
0.5 µg/ml MBP
5 µg/ml MBP
a
h
o
b
i
p
c
j
q
d
k
r
l
s
f
m
t
g
n
u
50 µm

Figure 6.19: Assessment of nuclear BMPR-IA over timecourse exposure to eosinophil derived proteins

(A) Primary normal murine airway epithelial cells (MAECs) were exposed to human eosinophil-derived proteins over a timecourse of 2 hr, 17 hr and 48 hr (a-u). BMPR-IA appeared localised to the cytoplasm of untreated cells at 2 hr, 17 hr and 48 hr (a, h, o). At 2hr, BMPR-IA was localised to the cytoplasm of MAECs exposed to EDN, EPO and MBP (b-g) at either concentration (0.5 μg/ml and 5 μg/ml). At 17hr, BMPR-IA appeared localised to the nuclei of cells exposed to EDN, EPO and MBP at both concentrations (0.5 μg/ml and 5 μg/ml) to varying degrees (i-n). BMPR-IA was relocalised to the cytoplasm with no nuclear localisation apparent following 48 hr exposure to EDN, EPO and MBP (p-u). Arrows denote BMPR-IA nuclear localisation. Scale bars represent 50 μm. (B) Corresponding dapi counterstain. Arrows confirm BMPR-IA is localised to the nuclei of MAECs.

Figure 6.20 A

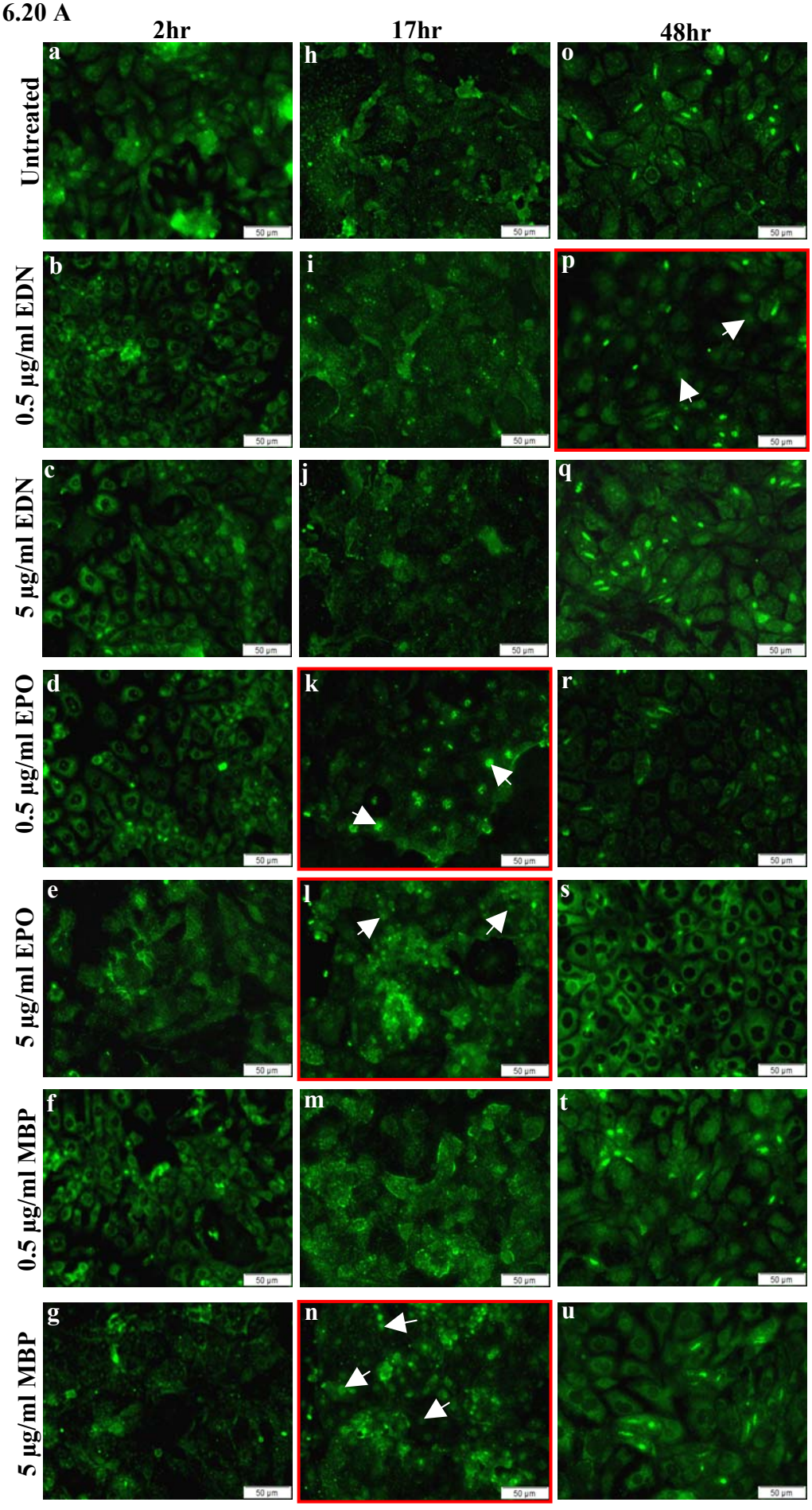
2hr
17hr
48hr
Untreated
0.5 µg/ml EDN
5 µg/ml EDN
0.5 µg/ml EPO
5 µg/ml EPO
0.5 µg/ml MBP
5 µg/ml MBP
a
h
o
b
i
p
c
j
q
d
k
r
e
l
s
f
m
t
g
n
u
50 µm

Figure 6.20 B

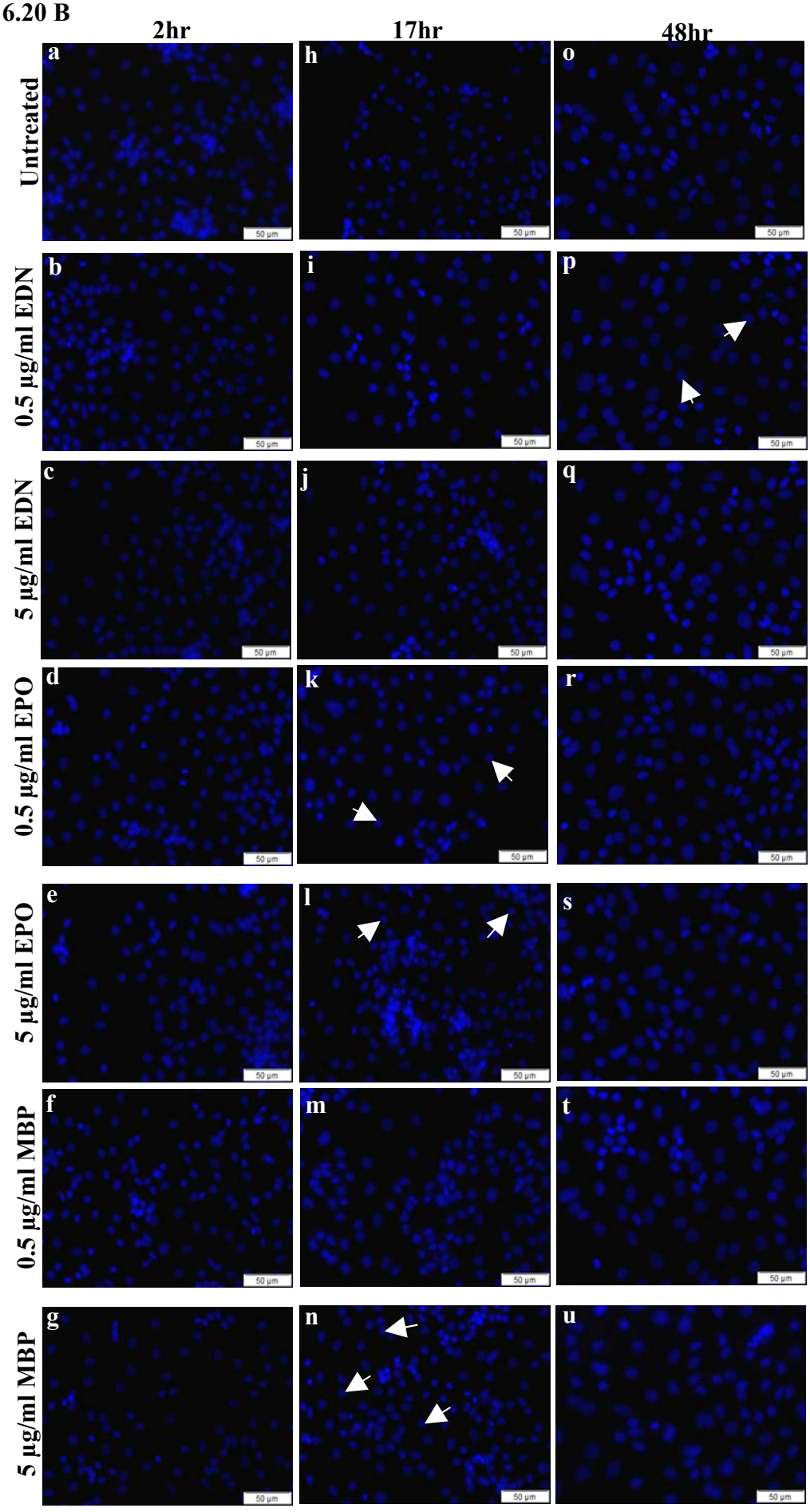
2hr
17hr
48hr
Untreated
0.5 µg/ml EDN
5 µg/ml EDN
0.5 µg/ml EPO
5 µg/ml EPO
0.5 µg/ml MBP
5 µg/ml MBP
a
h
o
b
i
p
c
j
q
d
k
r
e
l
s
f
m
t
g
n
u
50 µm

Figure 6.20: Assessment of BMP2 ligand in MAECs exposed to eosinophil-derived proteins

(A) Primary normal murine airway epithelial cells (MAECs) were exposed to human eosinophil-derived proteins over a timecourse of 2 hr, 17 hr and 48 hr (a-u). BMP2 appeared localised to the cytoplasm of untreated cells at 2 hr, 17 hr and 48 hr (a, h, o). In most cases, the level of BMP2 expression and localisation remained largely unaltered following exposure to EDN, EPO and MBP. However, some nuclear translocation was apparent at 17 hr in response to 0.5 μg/ml and 5 μg/ml EPO and 5 μg/ml MBP and at 48 hr in response to 0.5 μg/ml EDN (k, l, n, p). Arrows denote BMP2 ligand nuclear localisation. Scale bars represent 50 μm. (B) Corresponding dapi counterstain images. Arrows confirm BMP2 staining is localised to the nuclei of MAECs.

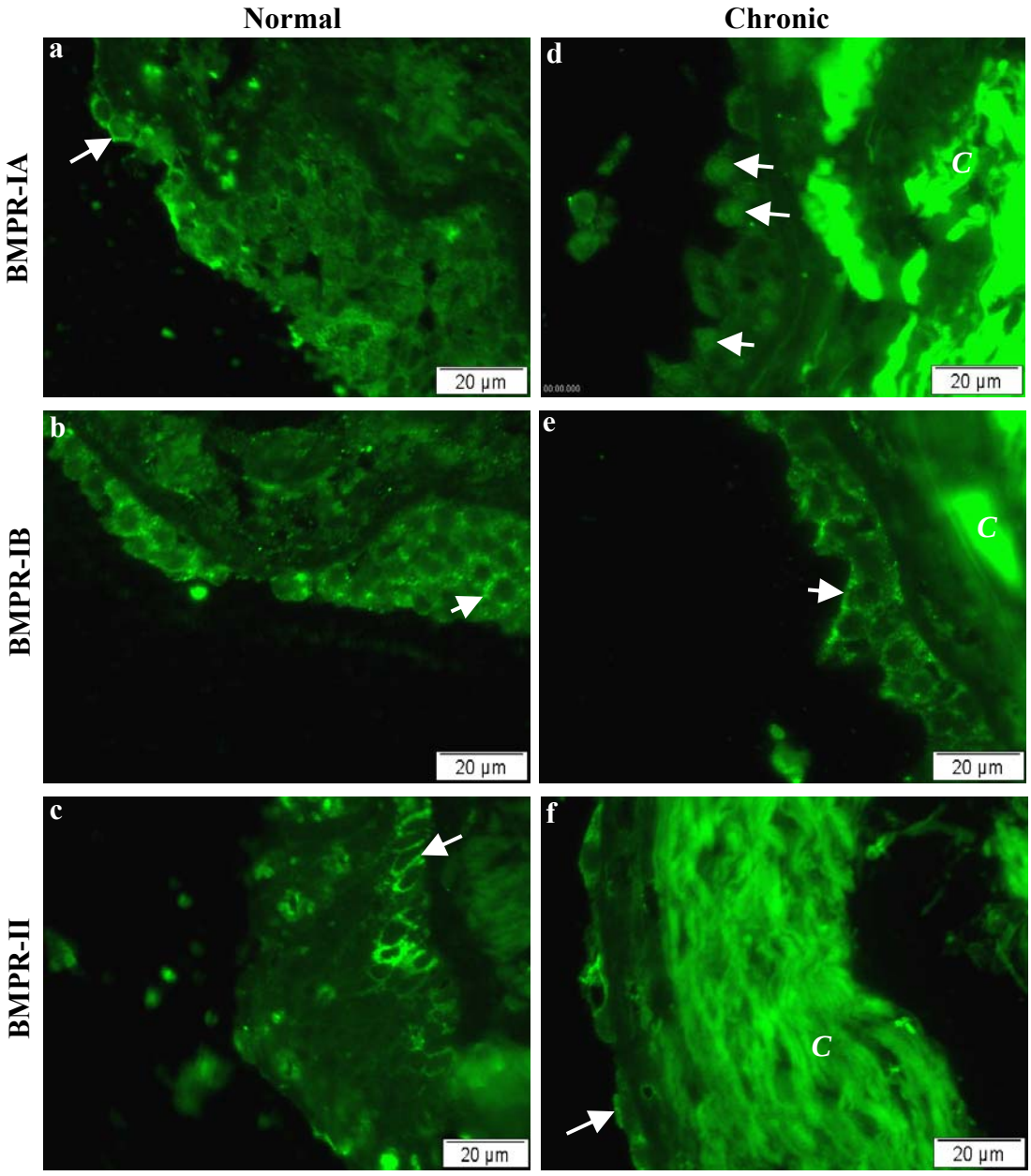

Figure 6.21 BMP Receptors in Lung Inflammation

Photomicrographs represent BMPR-IA, BMPR-IB and BMPR-II immunolocalised in normal healthy lung and chronic inflammatory lung (COPD) sections. BMPR-IA, BMPR-IB and BMPR-II appeared localised to the cytoplasm and/or membrane of the airway epithelial cells in normal sections (a-c). BMPR-IA appeared nuclear in the COPD lung section examined (d). BMPR-IB remained localised to the cytoplasm in diseased tissue (e). Few epithelial cells remained in the COPD section immunolocalised for BMPR-II (f). However, some membrane BMPR-II localisation was apparent (f). Arrows denote receptor localisation. Scale bars represent 20 µm. Extensive collagen deposition evident in disease sections (*C*).

A

MVAGTRCLLALLLPQVLLGGAAGLVPELGRRKFAAASSGRPSSQPSDEVLSEFELRLLS
MFGLKQRPTPSRDAVVPPYMLDLYRRHSGQPGSPAPDHRLERAASRANTVRSFHEESL
EELPETSGKTTRRFFFNLSSIPTEEFITSAELQVFREQMQDALGNNSSFHHRINIYEIIKPA
TANSKFPVTRLLDTRLVNQNASRWESFDVTPAVMRWTAQGHANHGFVVEVAHLEEKQ
GVSKRHVRISRSLHQDEHSWSQIRPLLVTFGHDGKGHPLHKREKRQAKHKQRKRLKSS
CKRHPLYVDFSDVGWNDWIVAPPGYHAFYCHGECPFPLADHLNSTNHAIVQTLVNSVN
SKIPKACCVPTELSAISMLYLDENEKVVLKNYQDMVVEGCGCR

B

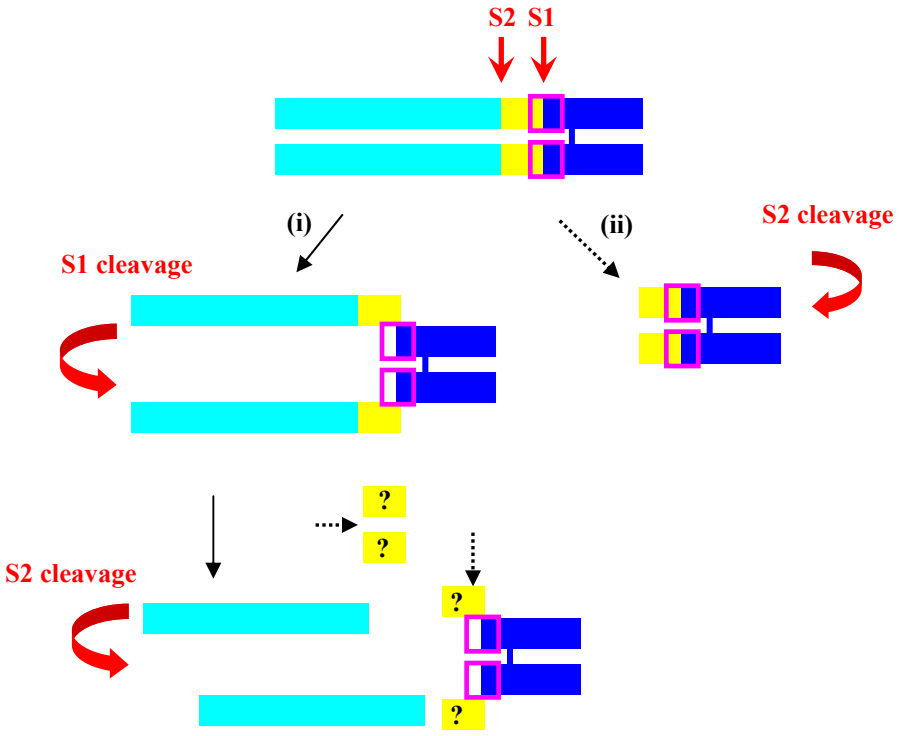

Figure 6.22 Identification of a potential nuclear localisation signal (NLS) in BMP2 ligand

(A) A potential NLS was identified in the amino acid sequence for the BMP2 proprotein using the PredictNLS online alignment programme. Mature protein denoted with dark blue text. Proprotein denoted with light blue text. Sequence between the first (S1) and second (S2) cleavage site is denoted with yellow text. S1 (R-E-K-R) and S2 (R-I-S-R) are underlined. NLS amino acid sequence highlighted with pink box. (B i) Proposed model for sequential cleavage of the BMP4 proprotein. BMP4 proprotein (light blue) is cleaved at S1 but the excised prodomain remains noncovalently associated with the mature ligand. At a lower pH the ligand is cleaved at the second site (S2) which releases the prodomain fragments from the mature ligand (dark blue). It is not known what happens to the small peptide which is liberated following cleavage at S2 (yellow). If this peptide was to remain bound to the mature ligand the putative NLS may remain intact (denoted by pink box). (B ii) Alternatively, BMP2 may be cleaved at S2 only. The mechanisms of proteolytic cleavage which have been previously demonstrated are shown with solid black arrows. The mechanisms of proteolytic cleavage which have not been previously demonstrated are shown with dashed arrows.